



**HAL**  
open science

# Mechanics of human macrophages phagocytosis : cytoskeleton dynamics and force measurement

Claire Bigot

► **To cite this version:**

Claire Bigot. Mechanics of human macrophages phagocytosis : cytoskeleton dynamics and force measurement. Human health and pathology. Université Paul Sabatier - Toulouse III, 2023. English. NNT : 2023TOU30396 . tel-04699971

**HAL Id: tel-04699971**

**<https://theses.hal.science/tel-04699971v1>**

Submitted on 17 Sep 2024

**HAL** is a multi-disciplinary open access archive for the deposit and dissemination of scientific research documents, whether they are published or not. The documents may come from teaching and research institutions in France or abroad, or from public or private research centers.

L'archive ouverte pluridisciplinaire **HAL**, est destinée au dépôt et à la diffusion de documents scientifiques de niveau recherche, publiés ou non, émanant des établissements d'enseignement et de recherche français ou étrangers, des laboratoires publics ou privés.



# THÈSE

En vue de l'obtention du  
**DOCTORAT DE L'UNIVERSITÉ DE TOULOUSE**  
Délivré par l'Université Toulouse 3 - Paul Sabatier

---

Présentée et soutenue par  
**Claire BIGOT**

Le 30 juin 2023

**Mécanique de la phagocytose chez les macrophages humains:  
dynamique du cytosquelette et mesure de forces**

---

Ecole doctorale : **BSB - Biologie, Santé, Biotechnologies**

Spécialité : **IMMUNOLOGIE**

Unité de recherche :

**IPBS - Institut de Pharmacologie et Biologie Structurale**

Thèse dirigée par

**Renaud POINCLOUX et Laurent MALAQUIN**

Jury

Mme Sophie Féréol, Rapporteur

Mme Emmanuelle Helfer, Rapporteur

M. Jacques Fattaccioli, Examineur

M. Christophe VIEU, Examineur

M. Renaud POINCLOUX, Co-directeur de thèse

M. Laurent MALAQUIN, Co-directeur de thèse

## RESUME

La phagocytose est un processus clé de notre immunité et homéostasie, consistant à détecter et capturer de larges particules ( $> 0,5 \mu\text{m}$ ). Ce mécanisme est notamment mis en œuvre par des cellules immunitaires spécialisées comme les macrophages, des phagocytes professionnels responsables de l'élimination des cellules apoptotiques, débris et micro-organismes. Les macrophages interagissent continuellement avec leur environnement, et adaptent leur comportement en réaction aux propriétés mécaniques de ce dernier, un phénomène appelé mécanosensibilité. Chez les macrophages, les acteurs majeurs de cette fonction sont les podosomes, des structures d'adhérence qui permettent de sonder l'environnement extracellulaire en appliquant des forces protrusives. La phagocytose a été décrite comme un processus mécanosensible. En effet, il semble que plus les particules cibles sont rigides, plus elles seront capturées efficacement. Dès lors, l'étude des podosomes au niveau des phagosomes est une voie privilégiée pour la compréhension du processus global de phagocytose.

Une première partie de ce travail a d'abord visé à étudier la présence de structures de types podosomes au niveau des phagosomes. Des essais de phagocytose ont été réalisés sur des billes de polystyrène et du Zymosan opsonisés par des IgG (phagocytose Fc) ou non opsonisés. Lors de la phagocytose Fc, des structures punctiformes d'actine apparaissent au niveau des coupes phagocytaires et des phagosomes clos. La caractérisation par microscopie de fluorescence super-résolue de ces points d'actine a révélé une structure similaire à celle des podosomes en termes de taille, durée de vie et de composition protéique. Nous les avons ainsi dénommés PAPs pour Podosomes Associés aux Phagosomes. Comme dans le cas des podosomes, qui sont ciblés par des vésicules contenant des protéases, la présence de PAPs est corrélée à la maturation des phagosomes en phagolysosomes.

Une deuxième partie concerne le développement d'une méthode permettant l'étude des mécanismes moléculaires impliqués dans la génération de forces au cours de la phagocytose. En effet, ces mécanismes sont encore mal documentés, principalement à cause de l'absence de méthode simple d'évaluation de ces forces sur un grand nombre de cellules vivantes. La méthode ici proposée combine des mesures de compression à des mesures de traction. Cette méthode repose sur l'analyse des forces appliquées par les macrophages phagocytant des micro piliers de polyacrylamide de taille et de rigidité contrôlées. Les déviations et variations de rayons des piliers au cours de la phagocytose sont mesurés en routine avec une précision

## RESUME

nanométrique. Des simulations mécaniques ont ensuite permis d'estimer l'amplitude et la direction des forces de compression et de traction impliquées. Nous avons ensuite montré que la contractilité de l'actomyosine est responsable de la contraction du pilier. Enfin, ce modèle de phagocytose frustrée a permis d'analyser la dynamique des forces générées sur plusieurs heures et sur un grand nombre de cellules en parallèle, et a révélé que les forces de traction et de compression ne sont pas nécessairement couplées et que l'énergie totale de déformation des piliers diminue avec le nombre d'événements de phagocytose, ce qui suggère que les macrophages sont plus efficaces pour phagocyter une seule particule à la fois.

Ce travail a donc permis de mettre en évidence la présence de podosomes au niveau des phagosomes clos dans la phagocytose médiée par les récepteurs Fc, et leur corrélation avec la maturation du phagosome. Il propose également une méthode originale qui devrait permettre de mettre en évidence quels sont les acteurs moléculaires impliqués dans la génération de force au cours de la phagocytose.

## ABSTRACT

Phagocytosis is a key process of our immunity and homeostasis, consisting in detecting and capturing large particles ( $> 0.5 \mu\text{m}$ ). This mechanism is performed by specialized immune cells such as macrophages, professional phagocytes responsible for eliminating apoptotic cells, debris and microorganisms. They continuously interact with their tissue environment to probe and adapt their behaviour in response to perceived mechanical changes, a phenomenon called mechanosensing. In macrophages, the major players in this function are the podosomes, adhesion structures that probe the extracellular environment by applying protrusive forces. Phagocytosis is a mechanosensitive process: the greater the rigidity of the target particles, the more efficiently they are captured. Investigating podosomes at the level of phagosomes is a privileged and novel way to study the global process of phagocytosis.

The first part of this work describes the presence of podosome-like structures at the level of phagosomes. Phagocytosis experiments were carried out on polystyrene beads and Zymosan, opsonized by IgG (phagocytosis FcR) or not. During FcR phagocytosis, punctiform actin structures appear at the level of phagocytic cups and closed phagosomes. Characterization by fluorescence super-resolution microscopy of these actin dots revealed a structure similar to that of podosomes in terms of size, lifespan and protein composition. We have named them PAPs, standing for Phagosome-Associated Podosomes. The presence of PAPs is correlated with the maturation of phagosomes into phagolysosomes.

The second part describes a novel method for studying the molecular mechanisms involved in the generation of forces exerted by macrophages during phagocytosis. Prior to this work, such mechanisms were insufficiently documented, mainly due to a lack of a simple method for evaluating these forces on a large number of living cells. The method hereby presented combines measurements of compression and traction forces, and consists in analysing the forces applied by human macrophages phagocytosing polyacrylamide micropillars of controlled size and rigidity. Using an automated procedure, the variations in radii and displacements of the pillars during phagocytosis are measured with nanometric precision. Finite element-based mechanical simulations were used to estimate the magnitude and direction of the compressive and tensile forces generated. The results issued from these simulations support that actomyosin contractility is responsible for pillar contraction. Finally, this model of frustrated phagocytosis,

## ABSTRACT

allows to analyse the dynamics of the forces generated over several hours and on a large number of cells, revealing that traction and compression forces are not necessarily coupled and that the pillar strain energy decreases with the number of phagocytosis events, suggesting that macrophages are more efficient at phagocytizing one particle at a time.

To conclude, this work has investigated the presence of podosomes at the level of closed phagosomes in Fc $\gamma$ - mediated phagocytosis, and their correlation with phagosome maturation. It also proposes a simple method to screen molecular actors for studying the forces generated during phagocytosis.

“[I]n a question like this truth is only to be had by laying together many varieties of error.”

— Virginia Woolf, *A Room of One's Own*



## ACKNOWLEDGMENTS

### *Au Jury*

Je tiens à exprimer ma profonde gratitude aux membres du jury de ma thèse pour leur temps, leur expertise et leur soutien.

Tout d'abord, je remercie chaleureusement **Sophie Féréol** et **Emmanuèle Helfer** pour leur relecture attentive du manuscrit. Vos commentaires et vos suggestions constructives ont grandement contribué à l'amélioration de ce travail.

Je remercie également **Jacques Fattacioli** pour sa participation et ses précieuses remarques qui ont permis de nourrir la réflexion autour de cette thèse.

Je souhaite également exprimer ma reconnaissance à **Christophe Vieu**, président de ce jury, pour son rôle central dans le déroulement de ma soutenance. Ta bienveillance, et tes conseils avisés ont été précieux en cette fin de projet.

### *Aux membres de mon comité de thèse :*

**Juliette Fittreman** et **François Cannone Hergaux** pour leur écoute et leurs recommandations.

À vous tous, je suis extrêmement reconnaissante pour l'attention et le soin que vous avez portés à l'évaluation de mon travail. Merci de m'avoir accompagnée dans cette étape cruciale de mon parcours académique.

### *A mes directeurs de thèse*

**Isabelle Maridonneau-Parini**, qui m'a ouvert les portes de son laboratoire en misant sur mon parcours « atypique », initié au monde fascinant de l'immunologie et partagé sa passion pour la recherche académique. J'ai énormément appris à tes côtés. Merci pour l'énergie que tu as insufflé à ce projet et pour avoir su me pousser à dépasser mes limites. J'ai un immense respect pour ta carrière et suis honorée d'avoir été ta dernière doctorante.

**Renaud Poincloux**, merci d'avoir repris la direction de la thèse et d'avoir su l'emmener vers mes appétences de développement technologique. Ta perspective unique et tes suggestions créatives ont enrichi cette recherche de façon significative.

**Laurent Malaquin**, merci de m'avoir guidée avec tant de dévouement et de bienveillance. Ton encadrement attentif et tes encouragements m'ont aidé à surmonter les nombreux défis posés par cette thèse interdisciplinaire. La biologiste que j'étais au début de cette thèse ne soupçonnait pas qu'elle découvrirait l'univers de la salle blanche et des simulations par éléments finis ; tu as toujours su me donner les éléments essentiels pour m'y lancer. Tes contributions intellectuelles et humaines ont enrichi non seulement ce travail, mais également mon développement personnel et professionnel. Un immense merci.

## ACKNOWLEDGEMENTS

### *A mes équipes d'accueil*

#### **A l'IPBS**

Je remercie tous les membres permanents de l'équipe « Architecture des phagocytes » de m'avoir transmis leur passion pour les macrophages, ainsi que leur savoir-faire technique unique : Arnaud Labrousse, Véronique Le Cabec, Christel Verollet, Brigitte Raynaud Messina.

Un remerciement tout particulier à Arnaud Métails qui m'a rejoint sur le projet alors dans le creux de la vague et qui a su, par sa grande rigueur et sa bonne humeur, me permettre de garder le cap.

Je tiens également à remercier du fond du cœur les post-doc Margot Tertrais, Javier Rey-Barroso et Zoï Vahlas.

Zoï, ton énergie optimiste nous a toujours poussé à aller de l'avant.

Margot, je n'oublierai jamais la grande solidarité qui nous a unies au moment de la passation des manips phagocytose, en plein Covid. Merci du recul dont tu fais preuve en toute circonstance.

Enfin, Javier, merci d'avoir été d'une patience exemplaire et d'avoir joint tes forces et ton grain de folie au projet.

Je remercie également les stagiaires qui ont apporté leur enthousiasme à ce projet : Maureen Verdier, Margaux Cortès, et Marjolaine Malgeri, je vous souhaite pleine réussite quelque soit la voie que vous suivrez ensuite.

Je ne peux terminer ces remerciements que par ceux sans qui tout ce cheminement aurait semblé insurmontable : Perrine Verdys, Ophélie Dufrançais, Rémi Mascarau, Thibaut Sanchez, (et Sarah Monard qui nous a rejoint en cours de route), notre club des cinq, contre vents et tempêtes. Je ne crois pas qu'il existe des personnalités plus différentes que les nôtres, qui pourtant forment un groupe aussi soudé. Nous avons grandi scientifiquement et personnellement ensemble, et je suis reconnaissante aujourd'hui de pouvoir vous appeler des amis.

#### **Au LAAS**

Merci aux membres permanents Christophe Vieu, Christophe Thibaut, Etienne Dagues, Bastien Venzac de faire de l'équipe EliA un lieu d'échanges et de liberté intellectuelle où chaque voix est entendue.

Merci à mes co-thésards Ophélie Thomas Chemin, Ianis Drobecq, Matthieu Sagot et notamment mes co-bureaux Victor Fabre, Victor Fournier, Elise Rigot et Anne Sophie Bajeot pour la création de « Zinzinland ». Nos recherches, d'une grande diversité disciplinaire, se sont enrichies au contact les unes des autres, et ont, je crois, développé encore davantage notre avide curiosité scientifique.

### *Aux plateformes*

Ce travail n'aurait pu voir le jour sans l'accompagnement des plateformes technologiques. Je tiens à remercier à la plateforme Micro et Nano technologie Renatech Pierre François Calmon, Aurélie Lecestre, Laurent Bouscayrol, Benjamin Reig et Adrian Laborde. A la plateforme

## ACKNOWLEDGEMENTS

caractérisation du LAAS, merci à Charline Blatché, Sandrine Assie Souleille et Julie Foncy. A la plateforme CMAEB, merci à Isabelle Fourqueaux.

### *Aux collaborateurs*

Frédéric Lagarrigue, merci pour les conversations tardives qui m'ont beaucoup éclairé sur l'environnement de la recherche académique, merci aussi pour ton partage d'expertise autour des intégrines.

Catherine Astarie Dequeker: merci d'avoir révisé avec bienveillance une partie du manuscrit. Merci à « l'équipe cryo EM » : Stéphanie Balor et Marion Jasnin , j'ai hâte de voir les résultats. Merci enfin à Daan Vorselen, dont les travaux ont grandement inspiré les miens et pour les riches échanges en congrès.

### *A l'équipe enseignante du service Physiologie de la faculté des Sciences Pharmaceutiques*

Lise Cirioni, Cendrine Cabou, Daniel Cussac, Lise Lefevre, et tout particulièrement Yannis Sainte-Marie et Victorine Douin avec qui j'ai eu l'immense plaisir de dispenser les TD et TP à mes futurs condisciples. La petite graine de l'enseignement est plantée, je ne sais encore sous quelle forme elle germera, mais la suite de ma vie professionnelle comportera sans aucun doute une composante de transmission des savoirs.

### *Aux donateurs de sang, et à l'Établissement Français du Sang*

qui grâce à leur engagement, nous permettent d'avoir accès à des poches de sang et d'en extraire des macrophages humains, modèle d'étude au plus proche de la « vraie vie » particulièrement pertinent lorsqu'on s'efforce de comprendre des process physiologiques .

### *A mes amis*

Si les quelques années passées au sein de mes deux laboratoires auront été riches en belles rencontres, j'ai aussi la chance d'être entourée de personnes exceptionnelles qui m'ont soutenue, chacune à leur manière, tout au long de cette aventure.

D'abord, un grand merci à mes colocataires, Thalia et Sébastien, pour leur douceur de vivre et les projets improbables (de la construction d'une paillote à l'apprentissage du skate sur la Garonne). Cet espace de vie que nous avons créé ensemble fut bien souvent mon phare dans la tempête.

A mes amis de toujours : Inès, Matthieu, Bastien et Coline. Pour m'avoir sorti du laboratoire et embarqué dans un trek au Piton des Neiges, pour ne pas se prendre trop au sérieux, et plus généralement pour être des amis en or, merci.

Alors que je construisais des théories, certains ont commencé à bâtir leur famille. Pour tous les EVJF, les mariages, et les petits nouveaux à accueillir, merci à Karen, Quentin, Morgane, Fabien, bébé Ariane, Marie Elisabeth, Nicolas, bébé Quentin, Marina, Benjamin, bébé Louis, Cyrielle, Laurie, Antoine, Nathalie, Quentin, Matthieu et Yu. Partager votre bonheur, mais aussi vos doutes et vos découvertes est une source continue d'inspiration.

A ceux qui sont apparus sur le chemin : Jérôme et Manon. Merci pour les discussions jusqu'au petit matin, les cellules de crise quand c'était nécessaire et surtout, votre immense générosité.

## ACKNOWLEDGEMENTS

A ceux qui sont loin mais qui n'en sont pas moins des soutiens essentiels : Daniela, Erwan, Fleur, Julien. Merci de votre écoute toujours sincère et de vous être déplacés de si loin pour assister à la soutenance.

Enfin, merci aux Drs Upadhyay, El Shikha, Shayan, Arabaciyan, pour avoir ouvert la voie, et montré que tout était possible à qui le veut vraiment. C'est en accompagnant vos parcours que j'ai pu commencer à esquisser le mien, et pour cela, je vous remercie de tout mon cœur.

*A Jorge*

Il est de coutume de remercier son partenaire pour le soutien moral apporté tout au long de ce process de doctorat, ô combien ardu. Non seulement tu as assuré ce support avec un calme olympien, mais tu as également été un de mes meilleurs soutien scientifique. Je ne te remercierai jamais assez pour les soirées entières à m'expliquer la modélisation par éléments finis, et les week-ends à griffonner des théories sur des post-its. Toi qui en connais à présent autant sur la phagocytose que moi sur la physique mécanique, cette thèse est en partie la tienne.

*A l'ensemble de ma famille, notamment mes parents et mes frères*

qui m'assurent depuis toujours un soutien indéfectible sur lequel je sais que je peux toujours compter. Maman, ta thèse n'a jamais pu être finalisée, car tu avais un autre projet ancré au ventre, et tu as choisi de donner naissance à une petite fille plutôt qu'à un manuscrit. Aujourd'hui, elle te dédit le sien.

## PREFACE

## Context

The present study spanned a duration of 3.5 years and was conducted across two distinct laboratory settings: namely, the Institute of Pharmacology and Structural Biology (IPBS) within the group focusing on the *Architecture and Dynamics of Phagocytes*, and the Laboratory for Analysis and Architecture of Systems (LAAS) within the group specializing in *Engineering in Life Science Application* (ELiA). The enduring collaboration between these two research entities facilitated the execution of interdisciplinary endeavours, exemplified by the present thesis, wherein navigation of disparate scientific paradigms proved essential. The initial segment of this thesis endeavour was jointly overseen by Laurent Malaquin (LAAS) and Isabelle Maridonneau-Parini (IPBS), who retired at the commencement of the third year. Subsequently, the latter part of the thesis received co-supervision from Laurent Malaquin and Renaud Poincloux (IPBS).

## Scientific communications

### Publications

This thesis work has led to **two journal publications** as first co-author, which are described in this dissertation:

- **Tertrais, M. Bigot, C et al.** (2021) ‘Phagocytosis is coupled to the formation of phagosome-associated podosomes and a transient disruption of podosomes in human macrophages’, *European Journal of Cell Biology*, 100(4), p. 151161. Available at: <https://doi.org/10.1016/j.ejcb.2021.151161>.
- **Bigot, C. et al.** (2023) ‘Compression Force Microscopy: a simple method to evaluate phagocytic forces’.

The first article, published in 2021 in the *European Journal of Cell Biology*, discusses the presence and characterisation of podosome-like structures during phagocytosis of human

macrophages. In this work, Margot Tertrais and I presented phagocytic targets to human macrophages to study how their phagocytosis affected the podosomes, typical rich-actin structures involved in adherence, mechanosensing and extra-cellular matrix degradation. During phagocytosis mediated by the Fc receptors, we correlated the disappearance of podosomes with the apparition of actin-rich *foci* at the phagocytic site and further characterization showed both structures shared similar features. We thus called these *foci* “Phagosome Associated Podosomes” (PAPs) and hypothesized their role.

The second article is about to be submitted and introduces a method that allows the evaluation of forces applied by macrophages during phagocytosis. I developed here a novel method to estimate compression and traction forces exerted by the cells, by measuring the deformation of hydrogel micropillars used as phagocytic targets. Simulations using finite elements allowed me to correlate the rate of deformation with the strain energy and then compared the effect of the target stiffness, and cytoskeleton inhibitors on that calculated energy. Dynamic live videos also showed the effect of the number of phagocytic targets per cell on the outcome of phagocytosis.

Previous work at the University of Florida has led to one publication as a co-author:

- Akbar, M.A. *et al.* (2017) ‘ $\alpha$ -1 Antitrypsin Inhibits RANKL-induced Osteoclast Formation and Functions’, *Molecular Medicine*, 23(1), pp. 57–69. Available at: <https://doi.org/10.2119/molmed.2016.00170>.

This work studies the effect of the protein  $\alpha$ -antitrypsin (AAT) on osteoclast formation and function *in vitro*. It reveals AAT inhibits the expression of the main receptor (RANK) involved in osteoclast differentiation and supports a potential therapeutic effect of this protein for the treatment of osteoporosis. This work is mentioned here because I actively participated in experiments leading to its publication, which was my first introduction to research and myeloid cells.

## Conferences

I have contributed to several international congresses, with either oral talks or poster presentations:

- **Quantitative Approach of the Living** (2022, online): Virtual poster presentation
- **Microphysiological systems** (2022, Cargèse): Poster presentation

- **8<sup>th</sup> edition of the Invadosomes consortium** (2022, Sète): Poster presentation, for which I received the best poster presentation award.
- **Immunobiophysics EMBO workshop** (2023, Les Houches Physics School): Oral presentation, awarded by a prize for best oral talk.

### Scientific mediation

The research journey also included scientific mediation events such as “My thesis in 180sec”, in which I reached the regional finale in 2021. The presentation is available online: <https://youtu.be/QfwRXn6M9oU>.

### Grants

Along with the thesis, I wrote and successfully obtained two grants. The first was a mobility grant for Canada, called the “PhD joint program” between CNRS and Toronto University. The sanitary conditions unfortunately did not allow me to use this grant.

The second is a grant awarded by the FRM (Fondation pour la Recherche Médicale) for the end of the thesis. I thus obtained 6 months of additional financing to complete this work.

### Teaching and student supervision

#### Teaching

In addition to my experimental work, I had the opportunity to teach Physiology and Histology at the Faculty of Pharmacy, Paul Sabatier University. Over the course of three years, I managed a comprehensive teaching load of 64 hours per year, which included conducting tutorials and practical sessions for classes ranging from 12 to 60 students. Furthermore, I supervised the bibliographical projects of six third-year pharmacy students and actively participated in organizing the final exams

## **Student supervision**

This work has received the help of three students I had the chance to supervise in the laboratory:

- Margaux Cortes, a 2<sup>d</sup> year bachelor student in biology, who quantified phagocytosis assays;
- Maureen Verdier, a 3<sup>rd</sup> year bachelor student in biology, who developed the automation of the image analysis for the force quantification method;
- Marjolaine Malgeri, a 4<sup>th</sup> year engineer student at INSA, who built the simulation strategy on Comsol<sup>®</sup> software.

## LIST OF ABBREVIATIONS

### LIST OF ABBREVIATIONS

AFM	Atomic Force Microscopy
APC	Antigen Presenting Cell
BMDM	Bone Marrow Derived Macrophages
CR	Complement Receptor
DRF	Diaphanous-Related Formins
ECM	Extracellular Matrix
EEA1	Early Endosome Antigen 1
ERM	Ezrin/Radixin/Moesin
Fc	Fragment crystallin
FcR	Fc Receptor
GEF	Guanine nucleotide Exchange Factor
hMDM	human Monocytes Derived Macrophages
IgG	Immunoglobulin
iPALM	interferometric PhotoActivated Localization Microscopy
ITAM	Immunoreceptor Tyrosine-based Activation Motif
ITIM	Immunoreceptor Tyrosine-based Inhibition Motif
LAMP	Lysosomal-Associated Membrane Proteins
LAT	Linker for Activation of T cells
LSP-1	Lymphocyte Specific Protein-1
MGC	MultiGiant Cell
MLCK	Myosin Light-Chain Kinase
MMP	Matrix MetalloProteinases
MPA	MicroPipette Aspiration
MP-TFM	Microparticle Force Microscopy
MTOC	MicroTubule Organization Center
NK	Natural Killer
PAA	Polyacrylamide
PAPA	Pyogenic sterile Arthritis, Pyoderma gangrenosum, and Acne syndrome
PAMP	Pathogen Associated Molecular Pattern
PIP3	Phosphatidylinositol-3,4,5-trisphosphate

## LIST OF ABBREVIATIONS

PIP2	PhosphatidyInositol-4,5-bisphosphate
PI 3-K	Phosphatidylinositol 3-kinase
PFM	Protrusion Force Microscopy
PLC	Phospholipase C
PS	PhosphatidylSerin
OC	Osteoclasts
OT	Optical Tweezers
RANK-L	Receptor Activator of Nuclear factor $\kappa$ -B ligand
RBC	Red Blood Cell
ROCK	Rho kinase
ROS	Reactive Oxygen Species
TFM	Traction Force Microscopy
WASP	Wiskott-Aldrich Syndrom Protein

## LIST OF FIGURES

<b>Figure 1</b> : Simplified scheme of haematopoiesis.....	26
<b>Figure 2.</b> Macrophage polarization wheel .....	28
<b>Figure 3.</b> Origins and distribution of macrophages.....	29
<b>Figure 4.</b> Three types of filaments composing the cytoskeleton .....	32
<b>Figure 5.</b> Main phagocytic cells and their targets. ....	35
<b>Figure 6</b> The general process of phagocytosis .....	36
<b>Figure 7.</b> Schematic structure of Fcy receptors. ....	39
<b>Figure 8.</b> FcyR signalling for phagocytosis.....	40
<b>Figure 9.</b> CR receptors .....	41
<b>Figure 10.</b> Complement receptor signalling for phagocytosis. ....	42
<b>Figure 11.</b> Cooperation between phagocytic receptors. ....	44
<b>Figure 12</b> Schematic representation of trigger and zipper models .....	46
<b>Figure 13.</b> Phagocytic cup formation and closure.....	48
<b>Figure 14.</b> Dynamin localisation at the phagocytic cup .....	52
<b>Figure 15</b> Phagosome maturation.....	56
<b>Figure 16</b> Model of podosome architecture and interaction between its substructures. ....	64
<b>Figure 17</b> Podosome distribution among different cell types.....	65
<b>Figure 18</b> Functions of podosomes .....	66
<b>Figure 19.</b> Podosome-like structures during phagocytosis of beads or frustrated phagocytosis.....	72
<b>Figure 20.</b> MPA experimental setup. ....	77
<b>Figure 21</b> Optical and magnetic tweezers.....	77
<b>Figure 22</b> Experimental setup to evaluate stiffness of phagocytic cup using magnetic bead .....	80
<b>Figure 23.</b> Principle of AFM. ....	81
<b>Figure 24.</b> Traction Force Microscopy.....	85
<b>Figure 25.</b> MicroParticle Traction Force Microscopy .....	86

LIST OF TABLES

**Table 1.** Main human phagocytic receptors and their ligands..... 41  
**Table 2.** Available experimental techniques to decipher mechanical parameters during phagocytosis.  
..... 87

## TABLE OF CONTENT

RESUME.....	1
ABSTRACT.....	3
ACKNOWLEDGMENTS.....	7
PREFACE.....	11
LIST OF ABBREVIATIONS.....	15
LIST OF FIGURES.....	17
LIST OF TABLES.....	18
TABLE OF CONTENT.....	19
LITERATURE REVIEW.....	23
<b>CHAPTER I Immune and homeostatic role of macrophages.....</b>	<b>25</b>
I. Immune system and its cellular effectors.....	26
II. Macrophages.....	27
<b>CHAPTER II Role of the cytoskeleton in phagocytosis.....</b>	<b>31</b>
I. General definitions.....	32
II. First contact with the particle.....	36
III. Engagement of receptors.....	37
IV. Pseudopods extension.....	44
V. Phagosome closure.....	51
VI. Maturation of phagosome.....	55
<b>CHAPTER III Adhesion structures of macrophages: the podosomes.....</b>	<b>61</b>
I. Definition and description.....	62
II. Functions.....	65
III. Role in pathologies.....	69
IV. Role in phagocytosis.....	70
<b>CHAPTER IV Techniques to study mechanical properties and forces during phagocytosis.....</b>	<b>75</b>
I. Micropipette aspiration (MPA).....	76
II. Magnetic and optical tweezers.....	77
III. Atomic Force Microscopy (AFM).....	80
IV. Traction Force Microscopy (TFM).....	82
V. MP-TFM.....	85
<b>CHAPTER V Thesis objectives.....</b>	<b>89</b>

## TABLE OF CONTENT

<b>RESULTS</b> .....	<b>93</b>
<b>CHAPTER I Phagosome Associated Podosomes in Fc<math>\gamma</math> phagocytosis</b> .....	<b>95</b>
I. Objectives and summary of the article .....	96
II. Article: Phagocytosis is coupled to the formation of phagosome-associated podosomes and a transient disruption of podosomes in human macrophages .....	96
III. Perspectives.....	111
<b>CHAPTER II Development of a novel method to study the forces involved during phagocytosis and their molecular components</b> .....	<b>115</b>
I. Objectives and summary of the paper .....	116
II. Article: Compression force microscopy.....	117
III. Additional results.....	153
IV. Perspectives .....	157
<b>REFERENCES</b> .....	<b>162</b>
<b>Cover pages image credit</b> .....	<b>182</b>
<b>ANNEXES</b> .....	<b>183</b>

## Introduction

Phagocytosis is a cellular process consisting in the recognition, ingestion and degradation of large particles by dedicated cells, including the macrophages. By the clearance of microorganisms including bacteria, virus and fungi, or apoptotic cells and debris, phagocytosis is an essential component of the immune response and homeostasis.

Nevertheless, the act of engulfing large particles poses a significant challenge for phagocytic cells, also called phagocytes. This process necessitates the restructuration of the cell shape and organization around the target, subject to certain physical limitations. Numerous empirical and theoretical studies have emphasized the significant elements associated with the interconnected biophysical properties of receptors, the cell membrane, and the actin cytoskeleton. These factors are crucial in influencing the effectiveness of internalizing larger particles. However, unknowns remain regarding the mechanic of the process, in particular the forces exerted by cells to phagocyte. The methods used so far give only an incomplete picture of the nature and range of forces, their dynamic and their molecular determinants.

As an introduction, I will recall the basic concepts of cell biology that will be used throughout this study. More specifically, I will describe in the first chapter the immune system and its effectors cells, with a particular focus on macrophages. The second chapter is dedicated to the description of phagocytosis, one of the major functions of macrophages consisting in engulfing and degrading large particles, and the involvement of the actin-cytoskeleton in that process. The third chapter describes particular structures of macrophages, the podosomes, capable of local force generation recapitulates the techniques used up to date to study the cellular forces at stake during phagocytosis, and the fourth. Finally, the thesis objectives are listed in the fifth chapter, which concludes the literature review.

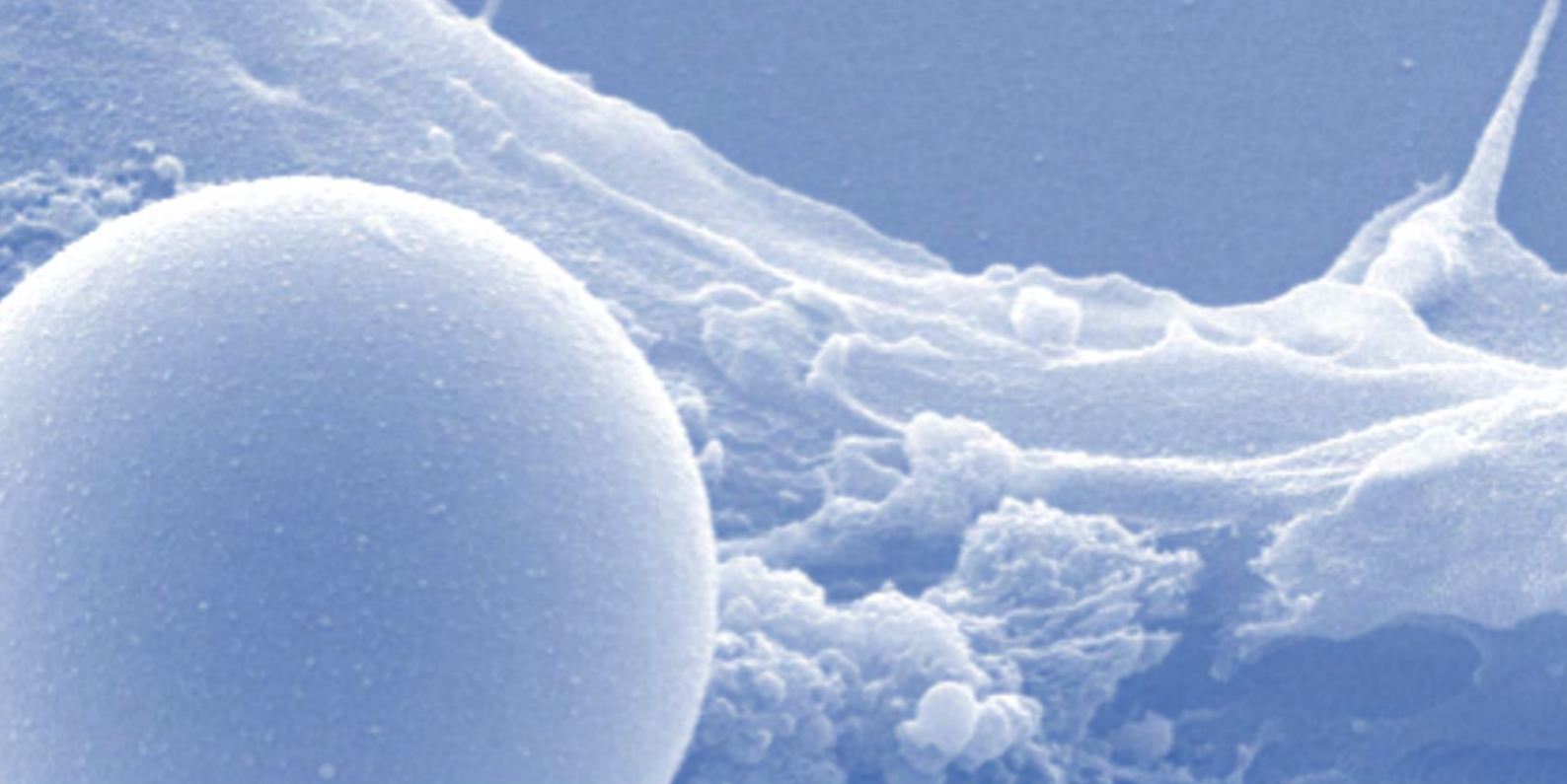
The “Results” part of this dissertation contains the experimental work performed along the thesis, presented in the form of two articles.

In the first one, phagocytosis assays were performed on monocyte-derived human macrophages (hMDM) with polystyrene beads or Zymosan, a component of the cell wall of the yeast *Saccharomyces cerevisiae*, typically used in phagocytosis experiments for its physiological relevance. Characterisation of actin-dots observed during phagocytosis reveals the presence of podosomes-like structures at the phagocytic site, which correlates with the disruption of ventral

## INTRODUCTION

podosomes and maturation of the vesicle containing the internalized target. The exact nature and role of these podosome-like structures are discussed.

In the second article, an innovative method of cellular force measurement during phagocytosis is proposed. I developed a system of deformable micropillars, whose dimension and stiffness can be tightly modulated. The functionalization of these pillars initiates their phagocytosis by macrophages which attempt to internalize them by exerting forces on their surface. The induced deformation is then converted into energy using a strategy of finite element mechanical simulations. The effect of stiffness and number of phagocytic targets per cell on the deformation energy is analysed, as well as the involvement of molecular actors previously described in force generation.



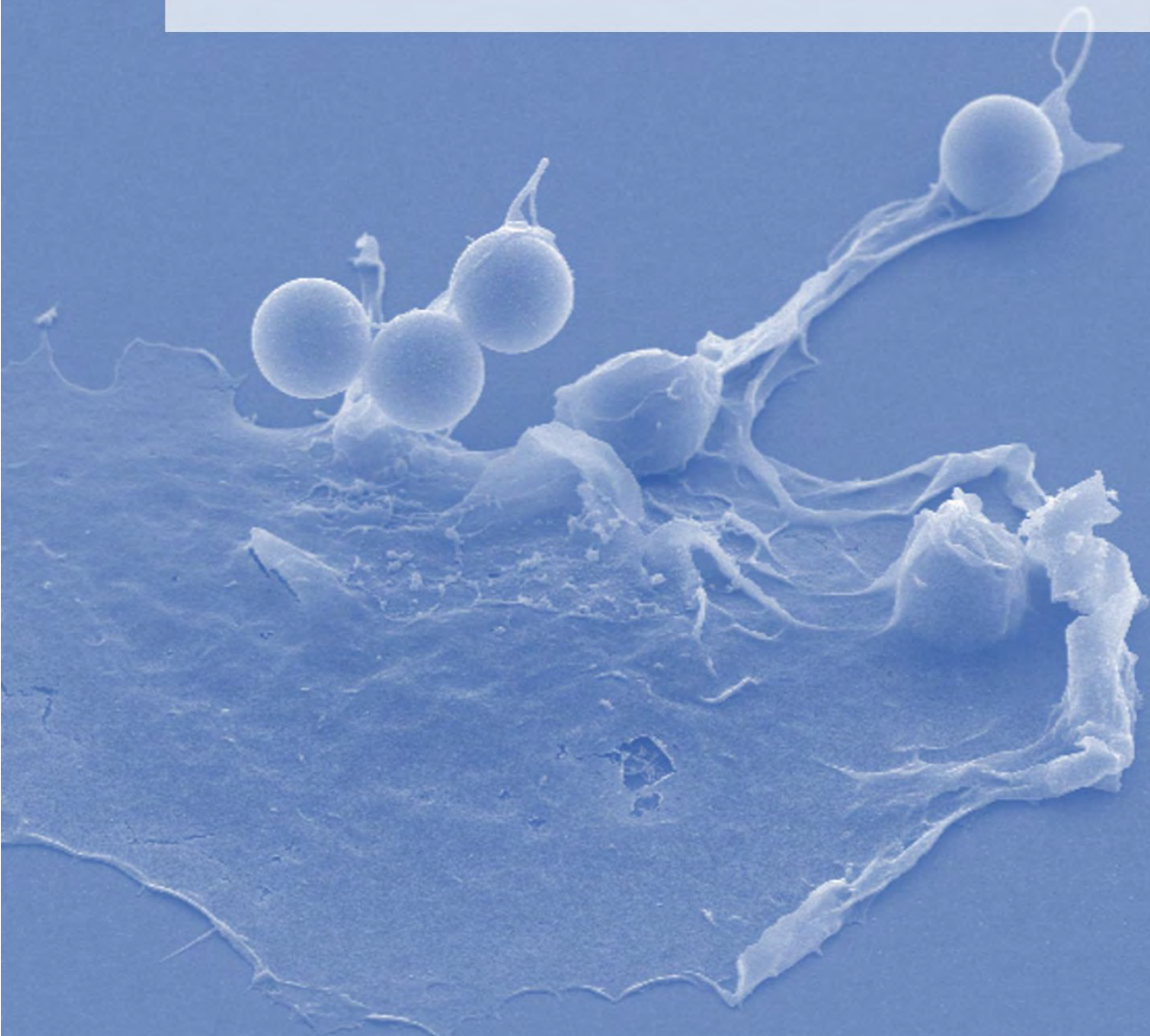
# **LITERATURE REVIEW**





# **· CHAPTER I ·**

## **Immune and homeostatic role of macrophages**



As an introduction, I will recall the basic concepts of cell biology that will be used throughout this study. More specifically, I will describe the immune system and its effector cells, with a particular focus on macrophages.

## I. Immune system and its cellular effectors

Upon infection by bacteria, virus, or fungus, innate immunity is triggered. It gives a rapid though possibly incomplete response when not all the pathogens can be eliminated. In that case, the adaptive immune system is activated after the recognition of specific antigens to neutralize the infection (Janeway and Medzhitov, 2002).

The combination of innate and adaptive immune responses provides the organism with a highly effective defence system. This system relies on cells called leukocytes (or white blood cells). Some of them originate from a common pluripotent precursor, the hematopoietic stem cells, in the bone marrow (Gordon and Taylor, 2005) (**Figure 1**), migrate and circulate through the bloodstream to the lymphatic system. Others, of distinct origin, reside in peripheral tissues to protect them from pathogens and are responsible for the clearance of debris and apoptotic cells.

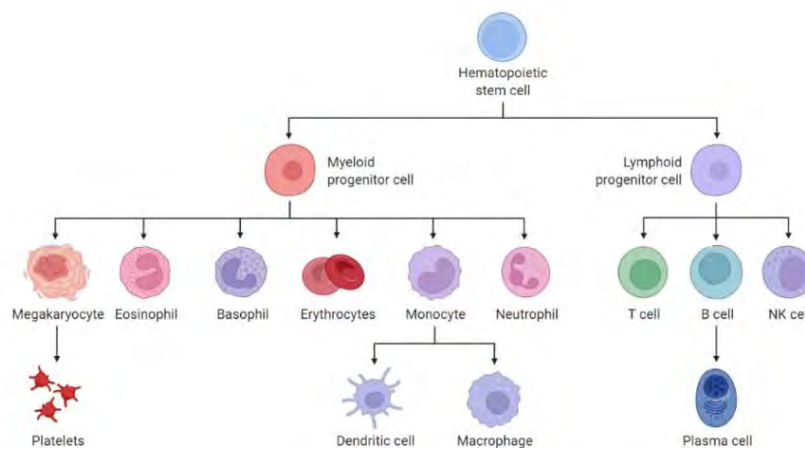


**Figure 1** : Simplified scheme of haematopoiesis  
From (Raza, Salman and Luberto, 2021).

Upon infection by a foreign agent, macrophages and neutrophils are the first innate immunity cells on site of infection to eliminate the particle via a process called phagocytosis. Phagocytosis refers to the ingestion and degradation of large particles ( $> 0.5\mu\text{m}$ ) (Uribe-Querol and Rosales, 2020) and is described more in depth in the Chapter II of this manuscript.

Macrophages and dendritic cells can also act as antigen-presenting cells (APCs). The digested peptide antigens from the pathogen are presented to the major histocompatibility complex class

II to activate helper T cells and thus adaptive immunity. Macrophages and dendritic cells present antigens within tissues and lymph nodes respectively (Guilliams *et al.*, 2014).

## II. Macrophages

### 1. Definition

Macrophages are present in all vertebrate tissues, from mid-gestation throughout life (Gordon and Martinez-Pomares, 2017). Their name comes from ancient Greek μακρός (*makrós*) - large and φαγεῖν (*phagein*) - to eat, which signifies they are large cells whose main role is to ingest particles. Indeed, they can eliminate pathogens through phagocytosis. Macrophages are among the most efficient cells to perform this biological process and are referred to as “professional phagocytes” along with monocytes, dendritic cells, neutrophils, and osteoclasts (Rabinovitch, 1995).

Beyond their immune function, macrophages are also vital key players in homeostasis. This role is independent of their involvement in immune responses (Mosser and Edwards, 2008). They also eliminate apoptotic cells, debris, tumour cells, and foreign materials through phagocytosis, and show trophic, regulatory, and repair functions (Adams and Hamilton, 1984; Gordon and Taylor, 2005; Pollard, 2009).

Therefore, their ability to phagocytose participates both in the defence against micro-organisms and clearance of dead and senescent cells.

### 2. Macrophage polarization

Although this parameter will not be considered in my experiments, I will now briefly describe the so-called "polarization" of macrophages. Macrophages are submitted to different stimuli that affect their phenotype. A first classification based on their functions was proposed by Mills *et al.* who propose to divide macrophages into two classes: M1 (classically activated, pro-inflammatory) or M2 (alternatively activated, pro-resolutive) (Mills *et al.*, 2000). In this classification, M1 phenotype corresponds to macrophages that produce cytokines, thus promoting and maintaining inflammation, while M2 phenotype mediates the control of the inflammation and promotes healing. However, this nomenclature has been questioned since many distinct polarization states have been described, being driven by different environmental stimuli. The plasticity of macrophage phenotype is now seen as a continuum, as shown in **Figure**

**2.**

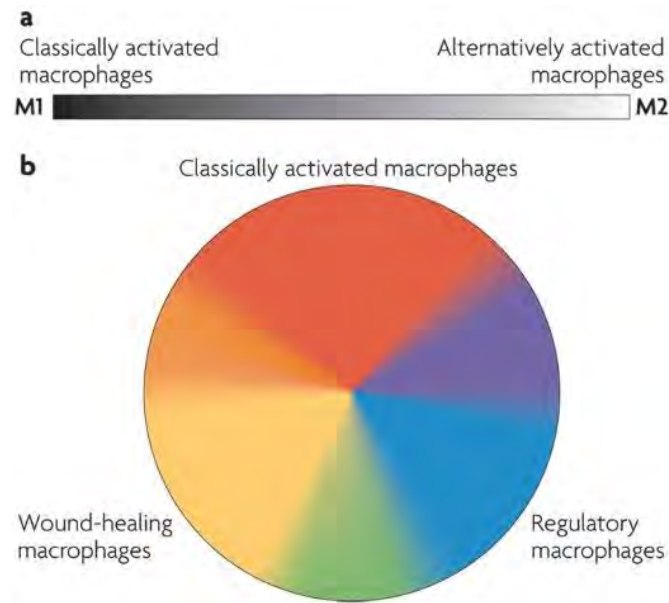


**Figure 2.** Macrophage polarization wheel  
Adapted from (Mosser and Edwards, 2008)

### 3. Origin of macrophages

After birth, macrophages can be derived from the differentiation of monocytes that leave the bloodstream and migrate to various tissues as mature macrophages (Aderem and Underhill, 1999; Taylor *et al.*, 2005). These monocytes are themselves derived from bone marrow myeloid progenitors. Macrophages can also come from fetal liver and yolk sac monocytes formed before birth, in that case they are specific to an organ (Gordon and Martinez-Pomares, 2017) and very long-lived, up to several months (Murphy *et al.*, 2008) (**Figure 3**).

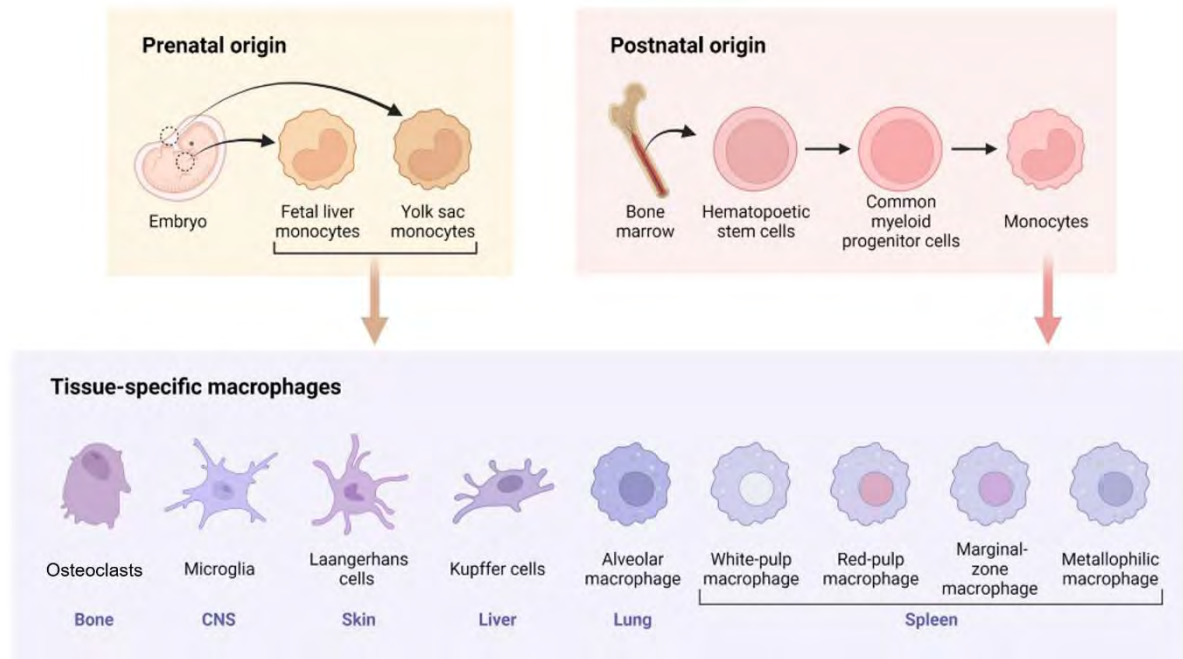


**Figure 3.** Origins and distribution of macrophages.  
From *microbenote.com*. Created with *Biorender*.

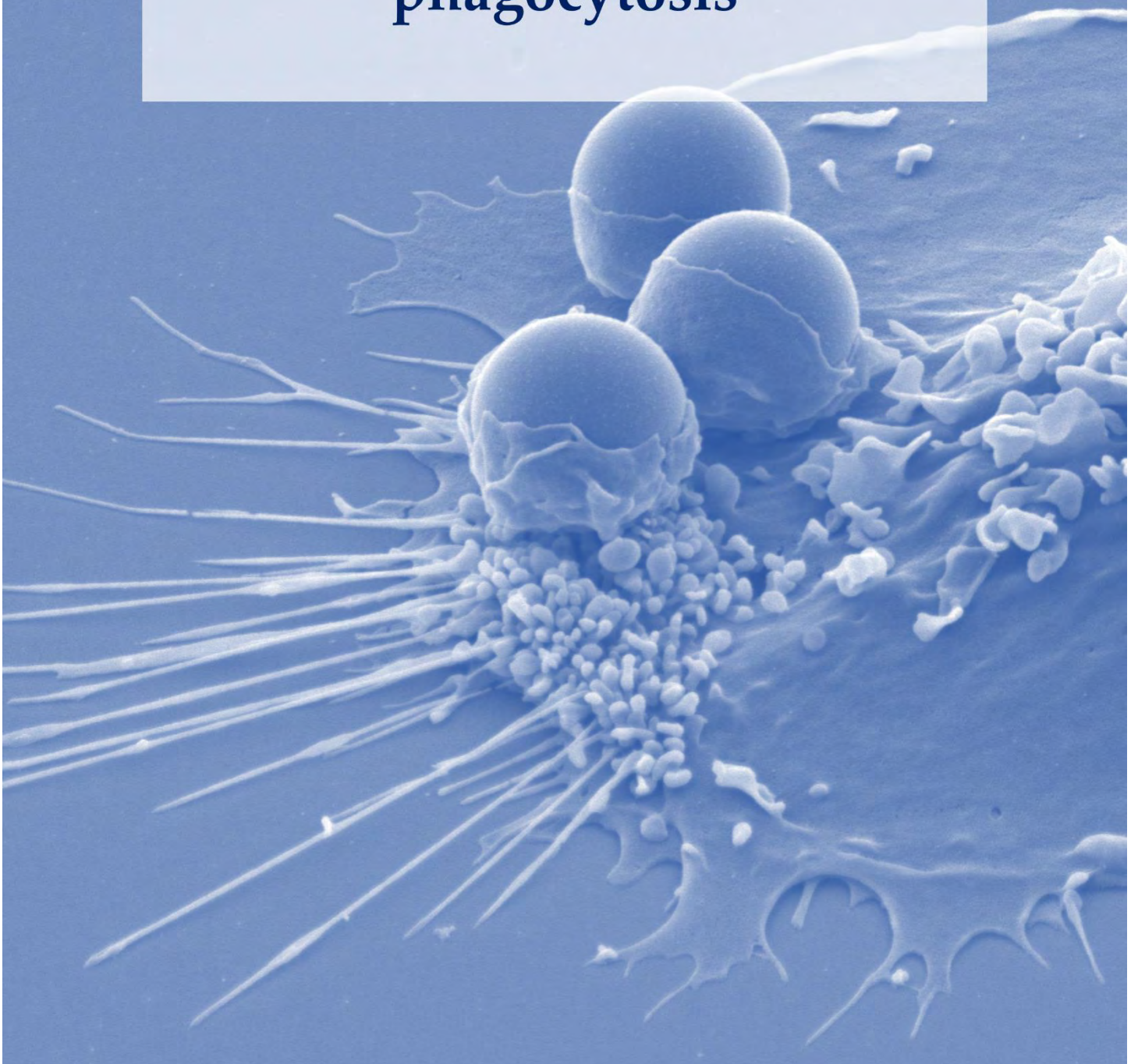
Depending on their tissue of residence, macrophages exhibit different phenotypes and specialized functions. For example, in bone tissue macrophages fuse to generate multinuclear cells called osteoclasts, that are responsible for the degradation of the bone. Similarly, alveolar macrophages are present in the lungs, Kupffer cells are found along certain blood vessels in the liver, and microglia reside in the brain and spinal cord (Pollard, 2009). These tissue resident macrophages play various role in physiological processes, such as clearance of cellular debris, metabolic function, tissue remodelling and defence.

*To conclude, macrophages are leukocytes of the innate immunity, capable of elimination of potential pathogens and activation of adaptative immunity. In addition to this immune role, they are also important for maintaining the body homeostasis by clearance of apoptotic cells, debris and tumour cells, all of the above being possible by their ability to phagocyte. This manuscript will concentrate on this critical function of phagocytosis, with a specific emphasis on the role of the cytoskeleton in its execution.*



# **· CHAPTER II ·**

## **Role of the cytoskeleton in phagocytosis**



## I. General definitions

### 1. Cytoskeleton

Cytoskeleton proteins form a tightly regulated network within the cell and are responsible for cell shape, cell division, motility and intracellular transport. Three distinct types of filaments enter its composition: microtubules, intermediate filament and microfilaments (**Figure 4**). If microtubules and intermediate filaments are mentioned here, this part focuses mainly on actin-cytoskeleton.

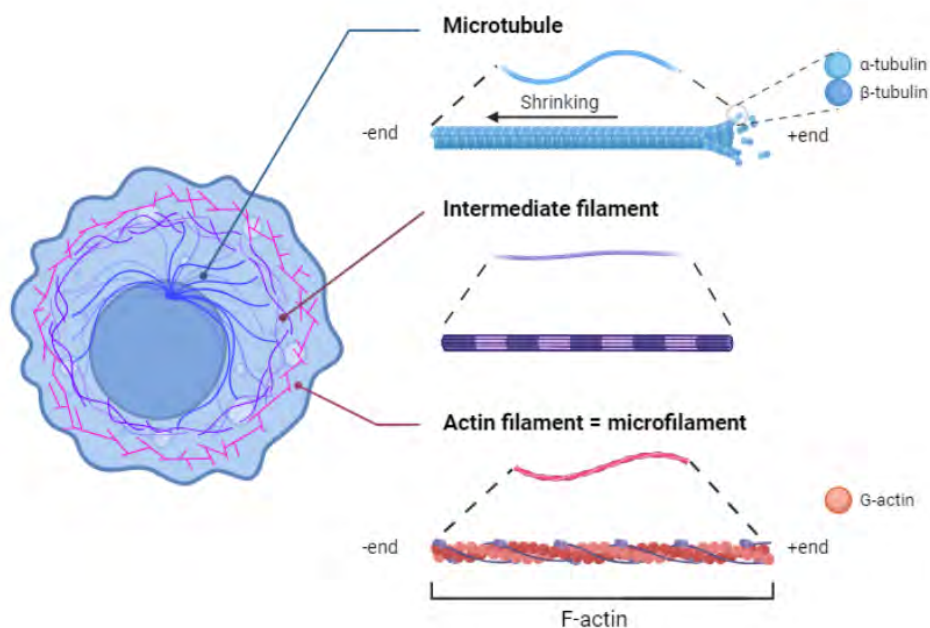


**Figure 4.** Three types of filaments composing the cytoskeleton  
Realized with Biorender

#### 1.1 Microtubules

Microtubules are long polymers of  $\alpha/\beta$  tubulin heterodimers forming hollow tubes. They mediate cell division in eukaryotic cells and are more specifically involved in some leucocyte function such as migration, phagocytosis and long range vesicle transport (Vicente-Manzanares and Sánchez-Madrid, 2004). Similarly to microfilaments, their dynamic is tightly regulated by interacting proteins and molecules (Nédélec, Surrey and Karsenti, 2003).

## 1.2 Intermediate filaments

Intermediate filaments are highly stable and they do not show polarized growth nor support motor-based transport. Most leukocyte intermediate filaments are composed of vimentin, and their functions remain elusive, although a role in the rigidity and structural integrity of lymphocytes during extravasation has been shown (Brown *et al.*, 2001).

## 1.3 Microfilaments, or actin filaments,

Microfilaments are homopolymers of actin, a protein of 42 kDa. Within the cell, half of the actin is assembled into filaments while the other half is free in the cytosol in the form of actin monomers. Actin in the filamentous form is sometimes referred to as F (Fibrillary) actin, while the monomeric form is referred to as G (Globular) actin. Microfilaments organize underneath the plasma membrane in a dense network called the cell cortex that produces tension controlling cell shape, polarization, motility and cell-cell interaction. Tension is produced through high rates of actin polymerization and depolarization (Pollard and Borisy, 2003), and contraction and relaxation, with the help of motor proteins such as myosins (Berg, Powell and Cheney, 2001). In leukocytes, the role of the actin cytoskeleton has been extensively studied and will be the main focus of this study.

Actin can be organized as branched or unbranched filaments, depending on the cell lineage, the region within a single cell or its activity (Mylvaganam, Freeman and Grinstein, 2021). Many proteins have been described to interact with actin and regulate its architecture and function.

Among these, the formin family of actin nucleation/elongation proteins polymerize the **unbranched filaments**. The literature reports 15 known formins in mammals (Chesarone, DuPage and Goode, 2010), and points out the involvement of diaphanous-related formins (DRFs), including mDia1 (mammalian diaphanous-related formin 1) in phagocyte cortical architecture. DRFs are regulated by the Rho-GTPase RhoA-C (Chugh and Paluch, 2018).

**Branched filaments** are nucleated from existing mother filaments by the Arp2/3 complex which is a heteromultimeric structure of seven stably associated proteins regulated by WASp (Mylvaganam, Freeman and Grinstein, 2021). Arp2/3 and formins crosstalk contribute to regulating the balance of F-actin cortical configuration.

## 2. Phagocytosis

Phagocytosis was first described by Elie Metchnikoff at the end of the 19<sup>th</sup> century, which led to the award of the Nobel prize for Physiology and Medicine in 1908. The word phagocytosis comes from ancient Greek *phagein* (“eat”) and *kutos* (“cell”) and illustrates the ability of a cell to internalize and destroy what was ingested. Phagocytosis is a cellular process consisting in the detection, internalization and elimination of particles larger than 0.5  $\mu\text{m}$  diameter. These particles can be agents such as bacteria, viruses and fungi or apoptotic cells. In this last case, the process is called efferocytosis, and consists in clearing every day billions of dying cells from the organism. Therefore, phagocytosis is essential for both pathogen elimination and tissue homeostasis (Uribe-Querol and Rosales, 2020).

Not all eukaryotic cells are able to perform phagocytosis. Phagocytosis is used for nutrition in unicellular organisms such as the amoeba *Dictyostelium discoideum*, a natural predator of bacteria which has been used as a model to understand cell defences (Dunn et al., 2018). In pluricellular organisms, this process is performed by a specialized type of cell called phagocytes. Among these cells, Rabinovitch distinguished professional phagocytes that are responsible for the clearance of microorganisms (Rabinovitch, 1995). They include monocytes, macrophages, neutrophils, dendritic cells, osteoclasts and eosinophils. Non-professional phagocytes including epithelial cells, endothelial cells and fibroblasts can perform phagocytosis of apoptotic cells, thus are important for maintaining homeostasis (Uribe-Querol and Rosales, 2020) (**Figure 5**).

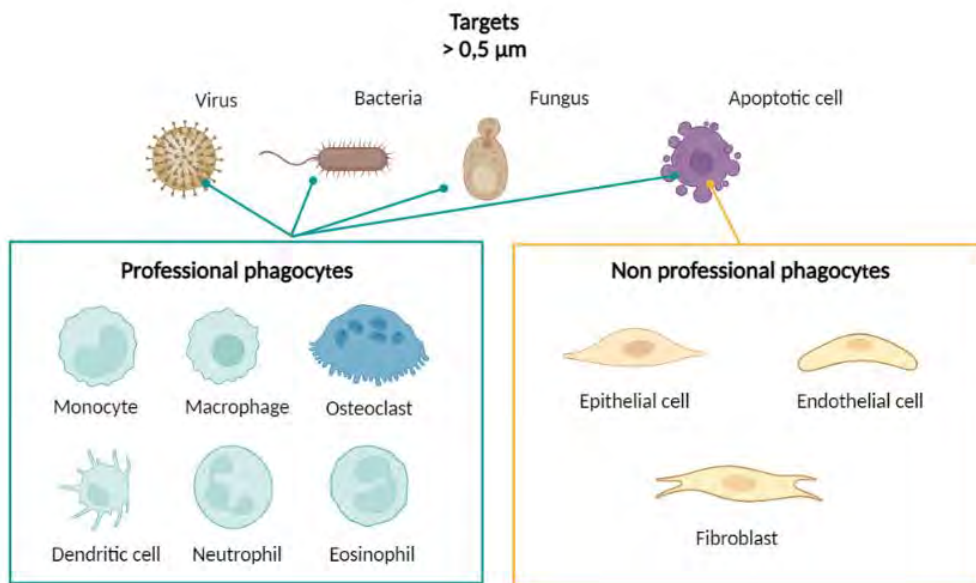


**Figure 5.** Main phagocytic cells and their targets.

Professional phagocytes (green frame) can efficiently phagocytose all sorts of microorganisms and apoptotic cells, while non-professional phagocytes (yellow frame) internalize apoptotic cells. Created from Biorender.

During phagocytosis, the target particle is recognized by dedicated receptors which are described in part II. Upon binding of the target to the phagocyte, downstream signalling pathways are initiated and lead to the remodelling of the actin cytoskeleton and plasma membrane to create protrusions called pseudopods (Freeman and Grinstein, 2014). These pseudopods cover the particle and distal ends of the membrane eventually close to create the phagosome which is a specific and transient compartment (Nüsse, 2011). The phagosome then matures through sequential fusion steps with late endosomes and lysosomes to form a phagolysosome (Desjardins, 1995) (**Figure 6**). Proteases are activated and reactive oxygen species (ROS) are generated via the NADPH Oxidase 2 (NOX2) enzyme (Dupré-Crochet, Erard and Nüße, 2013), making the content of the vesicle more acidic, leading to the degradation of the target particle and exposure of its cryptic sites (*i.e* sites that form a pocket in a ligand-bound structure), inaccessible before phagocytosis. The peptides of this target are then presented to other cells of the immune system via the CMH II (Underhill and Goodridge, 2012).

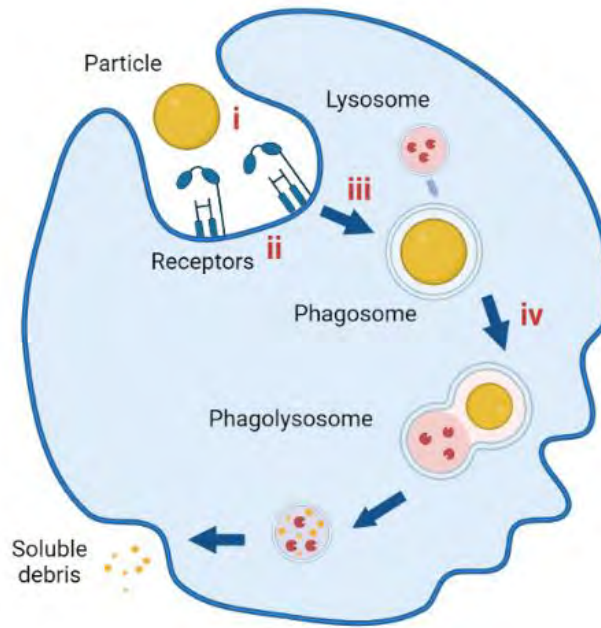


**Figure 6** The general process of phagocytosis

First, the particle to ingest is detected via specific receptors binding to surface ligands (i). Engagement of the receptors induces intracellular signalling to initiate phagocytosis (ii). Membrane protrusions surround the particle and fuse to engulf the particle into a specific compartment called the phagosome (iii). Phagosome undergoes several steps of maturation to degrade the ingested particle (iv). Created from Biorender.

This last part (presentation of antigen) is not developed here. However, I will describe more in-depth the first phases of phagocytosis, with a particular focus on the role of cytoskeleton and forces involved. First, we will describe the detection of the particle to be ingested, then, the clustering and engagement of the receptors, leading to intracellular signalling triggering the extension of the pseudopods and formation of the phagosome. Finally, the phagosome maturation will be briefly explained.

## II. First contact with the particle

Macrophages constantly survey their environment for potential targets to ensure efficient and timely responses. To this end, cells generate large membrane protrusions extending from the cell body (Stow and Condon, 2016). These protrusions, referred to as ruffles, promote surveillance functions by enabling the cell motility that is required to patrol and sample the surrounding microenvironment. They also serve as the first points of contact between the immune cell and target particles, thus initiating the process of phagocytosis. Ruffles are generally classified as *filopodia* which have a rod-like morphology, or as *lamellipodia*, which

are thin and flat. *Filopodia* have been reported to apply tensile forces to pull targets into contact with the cell body (Vonna *et al.*, 2003; Kress *et al.*, 2007), leading to a clustering of specific receptors at the plasma membrane.

### III. Engagement of receptors

Macrophages can efficiently identify and phagocytose different types of particles including apoptotic cells and microorganisms. This recognition is mediated by specific receptors at their plasma membrane which discriminate each type of particle to internalize. These receptors can bind directly to ligands present at the surface of their target, for instance in the case of pathogens which exhibit particular signature molecules grouped under the generic term of pathogen-associated molecular patterns (PAMPs). Other receptors recognize foreign particles indirectly by binding to opsonins that act as molecular bridges between the phagocyte and the particle to be internalized. Opsonins designate different sorts of host-derived proteins that coat particles to label them for more efficient phagocytosis (Uribe-Querol and Rosales, 2020). This process is called opsonisation, coined from the Latin *opsonare* ("to cater, to buy provisions") and from Greek *oponein* ("condiment, delicacy"). The opsonins include antibodies (including immunoglobulins IgG), fibronectin, complement components, milk fat globulin (lactadherin) and mannose-binding lectin (Flannagan, Jaumouillé and Grinstein, 2012). Their receptors are called opsonic receptors, and the most described in the literature are receptors for antibodies and complement which are both described next.

#### 1. Opsonic receptors and their signalling pathways

Among opsonic receptors, Fc receptors (FcR) and complement receptors (CR) are the best characterized to date. They respectively bind the fragment crystalline (Fc) portion of IgG, IgA or IgE antibodies, and iC3b, a complement component (van Lookeren Campagne, Wiesmann and Brown, 2007; Rosales and Uribe-Querol, 2013b).

When phagocytic receptors bind their ligand, they activate signalling pathways to initiate phagocytosis. This activation leads to the modification in the plasma membrane composition and actin cytoskeleton reorganization to form a phagocytic cup. If description and signalling

pathways of both FcR and CR families are detailed for the reader's understanding, it is to be noted that the rest of this work focuses on FcR mediated phagocytosis.

### 1.1 Fcγ receptors (FcγR)

- Description of the receptors

Fc receptors (FcR) are glycoproteins that bind specifically to the Fc part of immunoglobulin (also called Ig). Based on the type of antibody recognized, FcR are classified into FcαR, FcγR and FcεR, respectively binding to IgA, IgG and IgE (Nimmerjahn and Ravetch, 2010; Rosales and Uribe-Querol, 2013b). The most common class of antibody being IgG, we focus on its receptor Fcγ. After the engagement of FcγR with IgG molecules, the receptors cluster at the membrane of the cell and trigger cellular responses among which phagocytosis (Rosales and Uribe-Querol, 2013a; Uribe-Querol and Rosales, 2017).

On human cells, three types of FcγR are expressed: FcγRI (CD64), FcγRII (CD32), and FcγRIII (CD16) (Ravetch and Bolland, 2001). FcγRI displays a high affinity for IgG molecules and has three Ig-like domains. In contrast, FcγRII and FcγRIII display a low affinity for IgG molecules and have only two Ig-like domains. Each FcRγ contains tyrosine residues within an immunoreceptor tyrosine-based activation motif (ITAM) (Fodor, Jakus and Mócsai, 2006; Underhill and Goodridge, 2007). When activated, FcγRs cluster, without changing their conformation, and lead to the phosphorylation of tyrosine residues in the ITAM sequence. These tyrosine residues are phosphorylated upon activation and are essential for receptor signalling (Uribe-Querol and Rosales, 2020).

Both FcγRII and FcγRIII present two isoforms. FcγRII can be expressed in phagocytic cells mainly on its isoform FcγRIIa, and in B lymphocytes mainly on its isoform FcγRIIb (Ravetch and Bolland, 2001). This last isoform has the particularity to present an immunoreceptor tyrosine-based inhibition motif (ITIM) involved in negative signalling (Daéron and Lesourne, 2006). Indeed, upon phosphorylation, the tyrosin residues within ITIM downmodulate signals coming from ITAM receptors through the recruitment of phosphatases (Aman, Tosello-Tramont and Ravichandran, 2001; Daéron and Lesourne, 2006). Thus, FcγRIIb acts as a negative regulator of phagocytosis (Tridandapani et al., 2002; Nimmerjahn and Ravetch, 2010). FcγRIII can be expressed in its isoform FcγRIIIa in macrophages, natural killer (NK) cells,

basophils, mast cells and dendritic cells, or Fc $\gamma$ RIIIb exclusively on neutrophils (**Figure 7**). Specific ligands of these receptors are indicated in **Table 1**.

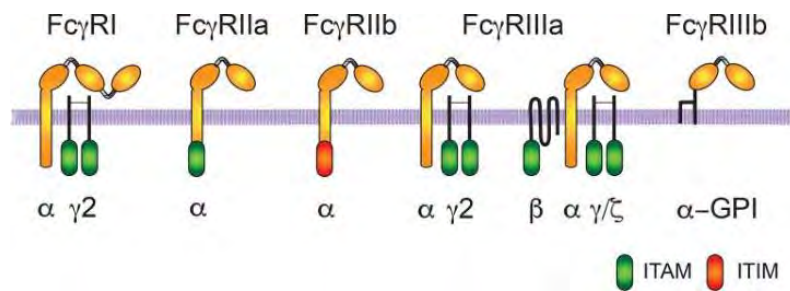


**Figure 7.** Schematic structure of Fc $\gamma$  receptors.

- Fc $\gamma$  Receptor signalling

Upon binding to antibodies, Fc $\gamma$  receptors get activated and cluster on the phagocyte membrane. Then, they co-localize with Src-family kinases (SFK, such as Lyn, Lck, and Hck), which phosphorylate tyrosines within the ITAM. Next, the phosphorylated ITAMs recruit Syk (spleen tyrosine kinase), which gets activated (Sánchez-Mejorada and Rosales, 1998; Rosales, 2007) and can in turn phosphorylate the adaptor molecule LAT (linker for activation of T cells), phosphatidylinositol 3-kinase (PI 3-K), and phospholipase C $\gamma$  (PLC $\gamma$ ) (Tridandapani *et al.*, 2002; Bezman and Koretzky, 2007).

The phosphorylation of PI 3-K leads to the transformation of phosphatidylinositol 4,5-bisphosphate (PIP<sub>2</sub>) to phosphatidylinositol-3,4,5-trisphosphate (PIP<sub>3</sub>) at the phagocytic cup (Cox *et al.*, 1999; Botelho *et al.*, 2000). This lipid regulates the activation of contractile proteins such as myosin and the GTPase Rac, both important for actin remodelling.

The Guanine nucleotide exchange factor (GEF) Vav activates GTPases of the Rho and Rac family (Hoppe and Swanson, 2004), which are involved in the regulation of the actin polymerization that drives pseudopod extension (Uribe-Querol and Rosales, 2020) (**Figure 8**).

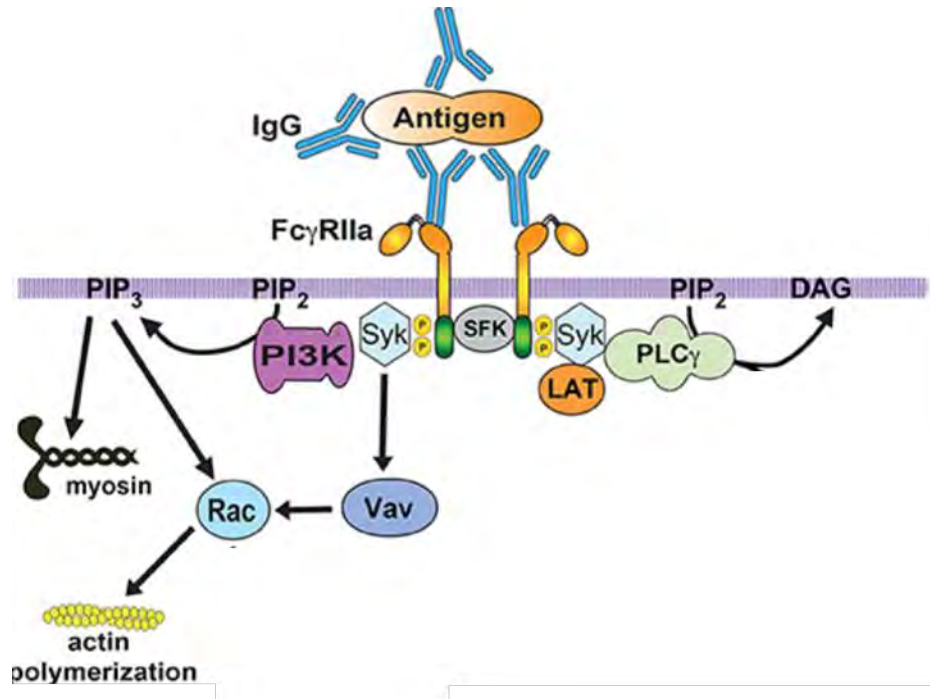


**Figure 8.** *FcγR* signalling for phagocytosis.

SFK: Src family kinases; Syk: Spleen tyrosine kinase; PLC: Phospholipase C gamma; IP<sub>3</sub>: inositoltrisphosphate; DAG: diacylglycerol; PI3K: phosphatidylinositol 3-kinase; PIP<sub>3</sub>: phosphatidylinositol-3,4,5-trisphosphate. Adapted from (Uribe-Querol and Rosales, 2020)

## 1.2 Complement Receptors

- Description

Complement receptors (CRs) bind the opsonins of the activated complement system (Brown, 2005; Dustin, 2016). This group of receptors counts three different types of molecules (**Figure 9**). First, CR1 and CR2 are formed by short consensus repeat (SCR) elements. Then, CR3 and CR4 belong to the  $\beta$ 2 integrin family (Dustin, 2016). More specifically, CR3 (also known as CD11b/CD18, Mac-1 or integrin  $\alpha$ M $\beta$ 2) binds the complement component iC3b, and represents the most efficient phagocytic receptor among complement receptors (Tohyama and Yamamura, 2006; Rosales, 2007; Dustin, 2016). Finally, CRiG belongs to the immunoglobulin Ig superfamily (Freeman and Grinstein, 2014). Specific ligands of these receptors are indicated in **Table 1**.

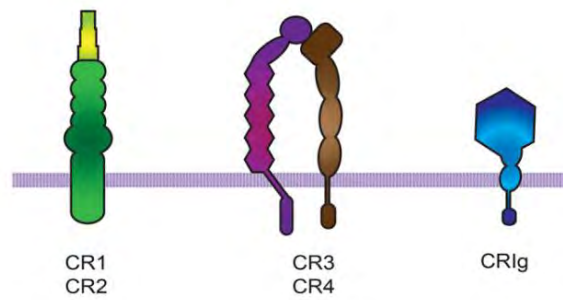


**Figure 9.** CR receptors

Receptors	Ligands	References
<b>FcR</b>		
FcγRI (CD64)	IgG <sub>1</sub> = IgG <sub>3</sub> > IgG <sub>4</sub>	(Anderson <i>et al.</i> , 1990)
FcγRIIa (CD32a)	IgG <sub>3</sub> ≥ IgG <sub>1</sub> = IgG <sub>2</sub>	
FcγRIIIa (CD16a)	IgG	
FcαRI (CD89)	IgA <sub>1</sub> , IgA <sub>2</sub>	(Bakema, van Egmond, 2011)
<b>CR</b>		
CR1 (CD35)	Mannan binding lectin; C1q; C4b; C3b	(Ghiran <i>et al.</i> , 2000)
CR3 (α <sub>M</sub> β <sub>2</sub> , CD11b/CD18, Mac-1)	iC3b	(Ross <i>et al.</i> , 1992)
CR4 (α <sub>V</sub> β <sub>2</sub> , CD11c/CD18, gp190/95)	iC3b	
α5β1 (CD49e/CD29)	Fibronectin; vitronectin	(Blystone <i>et al.</i> , 1994)

**Table 1.** Main human phagocytic receptors and their ligands

FcR: receptor fragment crystalline; CR: complement receptor

Adapted from (Uribe-Querol and Rosales, 2020) and (Fu and Harrison, 2021)

- Signalling

The most efficient receptor of this group is CR3 (Dustin, 2016). Studies have long proposed that the internalization process mediated by Fcγ-phagocytosis (called “zippering”), was different from CR, called “sinking”. The last is considered as a passive phenomenon where the target particle sank into the cell (Kaplan, 1977; Allen and Aderem, 1996). This concept has recently been challenged by several studies. Electron microscopy experiments revealed thin protrusions which surround iC3b-opsonized particles during phagocytosis (Hall *et al.*, 2006; Deschamps, Echard and Niedergang, 2013; Rotty *et al.*, 2017). Moreover, actin-based membrane protrusions were observed during phagocytosis of iC3b-opsonized particles through 3D live cell imaging (Jaumouillé, Cartagena-Rivera and Waterman, 2019). As a result, actin-based protrusions extending around a target particle seem to be a common feature of phagocytosis, regardless of the receptors involved (Jaumouillé and Waterman, 2020a).

This F-actin remodelling is under the control of the GTPase Rho (Caron and Hall, 1998; May *et al.*, 2000). Once activated, Rho can indeed promote actin polymerization. On one hand, Rho can activate Rho kinase (ROCK), resulting in phosphorylation and activation of myosin II which assists in actin assembly at CR phagosome, although the molecular mechanisms remain to be elucidated (Olazabal *et al.*, 2002). On the other hand, Rho can promote the polymerization of unbranched actin filaments through the accumulation of mDia1 (Colucci-Guyon *et al.*, 2005). At the phagocytic cup, this formin can also bind to the microtubule-associated protein CLIP-170 (Lewkowicz *et al.*, 2008), thus linking actin to the microtubule cytoskeleton (Newman, Mikus and Tucci, 1991; Allen and Aderem, 1996) (**Figure 10**).

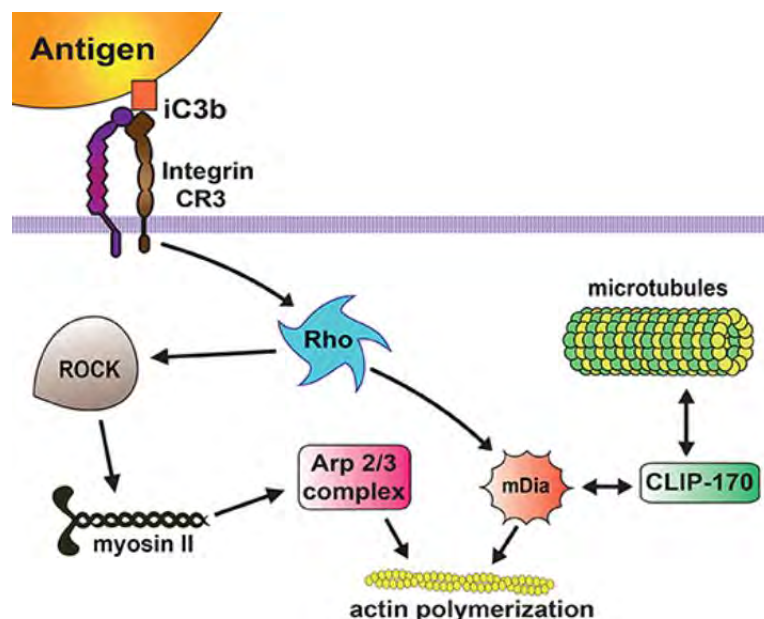


**Figure 10.** Complement receptor signalling for phagocytosis. ROCK: Rho kinase. From (Uribe-Querol and Rosales, 2020)

## 2. Phagocytic Receptors Cooperation

Initiation of phagocytosis requires the interaction of target-dense arrays of ligands with numerous phagocyte receptors. Upon engagement, receptors cluster and activate downstream signalling cascades. We focus here on the phagocytosis FcR-mediated.

Mobility of the receptors in the plasma membrane is essential to their clustering and activation (Jaumouillé and Grinstein, 2011). However, for most receptors, this diffusion is prevented by other transmembrane glycoproteins such as hyaluronan, CD45 and CD148 present on the cell surface (Springer, 1990). Many of these large glycoproteins can interfere with the lateral diffusion of receptors due to their link to the cytoskeleton (Ostrowski, Grinstein and Freeman,

2016) (**Figure 11A**). Moreover, on the macrophage surface, self-synthesized or acquired glycocalyx components cover phagocytic receptors, curtailing their ability to engage particles (Imbert *et al.*, 2021). Indeed, compared to the long glycoproteins composing this glycocalyx, phagocytic receptors are very short and therefore hidden among them (**Figure 11B**).

Accordingly, the interaction between Fc $\gamma$  receptors and possible targets is facilitated by the removal of these larger glycoproteins. This is achieved through cooperation between Fc $\gamma$  receptors and integrins such as CR3, a complement receptor. The Fc $\gamma$  receptors deliver inside-out signals to CR3 (Ortiz-Stern and Rosales, 2005) resulting in its activation and an increased affinity for its ligands (Brandsma *et al.*, 2015). Upon this activation through the small GTPase Rap1 (Botelho *et al.*, 2000), integrins extend their conformation (Lagarrigue, Kim and Ginsberg, 2016). This extended conformation, supported by the tight apposition of the membrane and the phagocytic target, creates a diffusion barrier excluding large glycoproteins from the phagocytic receptors area (Freeman *et al.*, 2016). Moreover, this extension allows integrins to bind ligands further on the particle while Fc $\gamma$  receptors aggregate in microclusters to bind ligands closer to the membrane surface (Ostrowski, Grinstein and Freeman, 2016) (**Figure 11C**). The engagement of both type of receptors (Fc and CR) mediates a strong adhesion between the phagocyte and the particle to be internalized as well as an increased downstream signalisation.

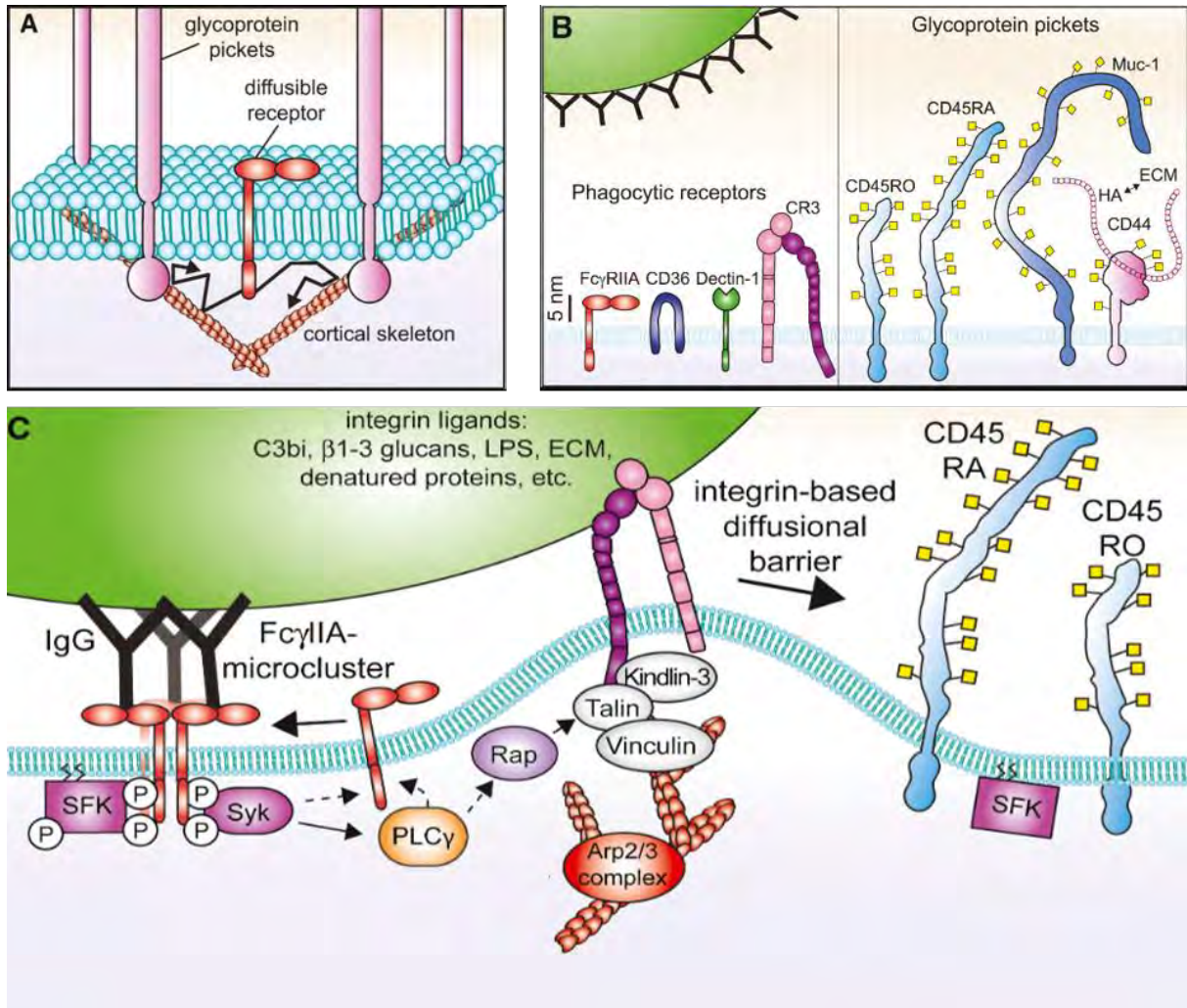


**Figure 11.** Cooperation between phagocytic receptors.  
Adapted from (Ostrowski, Grinstein and Freeman, 2016)

#### IV. Pseudopods extension

Upon engagement of the signalling pathways to initiate phagocytosis, the actin cytoskeleton is reorganized and the plasma membrane composition changes. These two phenomena result in a depression of the membrane area touching the particle called the phagocytic cup. This cup progresses around the particle in the form of membrane protrusions, the pseudopods, until the complete covering of this particle. Eventually, the membrane protrusions fuse and create a new vesicle, called the phagosome, containing the ingested particle.

## 1. Triggering or zippering?

Two distinct mechanisms have been discussed for the internalization of large particles: the trigger mechanism and the zipper one. Trigger mechanism has been proposed to be mediated by discreet signalling that mediates an all-or-none phagocytic response. In this mechanism, actin-based protrusions of plasma membrane form and surround nearby material in an adhesion-independent manner (**Figure 12**). The zipper mechanism consists in sequential engagement of cell surface receptors to the surface of the particle ligands, leading to formation of pseudopod which advance proceeds no further than receptor-ligand interactions permit. The engagement of receptors to the entire surface of the particle lead to a complete wrapping of the particle by the plasma membrane, and thus complete phagocytic uptake (**Figure 12**) (Swanson and Baer, 1995; Jaumouillé and Waterman, 2020a).

The **trigger mechanism** has been described for intracellular bacteria *Shigella* and *Salmonella* which can induce their own uptake by injecting effectors into a host cell. Those effectors hijack cellular signalling and actin polymerization machinery to trigger the formation of large ruffles leading to the internalization of the bacteria (Clerc and Sansonetti, 1987; Finlay, Ruschkowski and Dedhar, 1991). This was demonstrated in a study where a non-invasive strain of wild type *Salmonella* was added in epithelial cells, non-professional phagocytes, and triggered its internalization (Galán, Ginocchio and Costeas, 1992).

If the trigger mechanism does not require direct surface binding between the target and the phagocyte, on the contrary the **zipper model** implies a very close interaction between the two (Jaumouillé and Waterman, 2020a). Some studies have demonstrated particles internalization requires not only engagement of dedicated receptors, but also recruitment of receptors to sequentially engage the entire particle surface, like a zipper, to drive engulfment (Griffin *et al.*, 1975; Griffin, Griffin and Silverstein, 1976). Moreover, it seems that the protrusions are a product of active actin-remodelling programs (Kaplan, 1977; Allen and Aderem, 1996; Underhill and Goodridge, 2012).

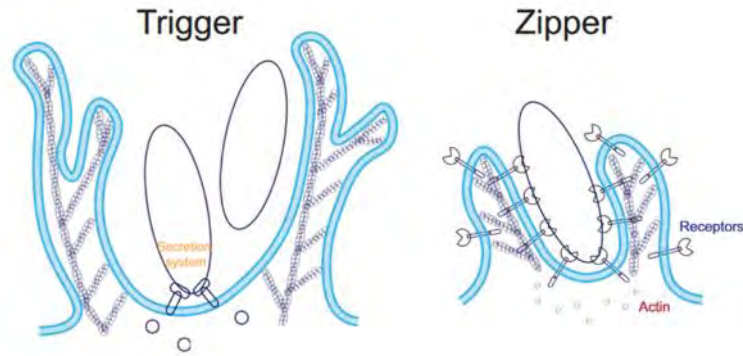


**Figure 12** Schematic representation of trigger and zipper models  
Adapted from (Jaumouillé and Waterman, 2020a).

Because the trigger mechanism is limited to very specific examples, and evidence supporting the zipper model, this report will focus on the phagocytic cup formation through a zipper mechanism.

## 2. Membrane

### 2.1 Changes in the membrane lipidic composition

The plasma membrane changes its lipid composition during phagosome formation. Fluorescence imaging techniques have shown that different lipids were formed and degraded in an orderly fashion (Levin, Grinstein and Schlam, 2015). For example, in Fc $\gamma$  mediated phagocytosis, there is an initial accumulation of phosphatidylinositol-4,5-bisphosphate [PI(4,5)P<sub>2</sub>] before rapid decline (Botelho *et al.*, 2000). This decrease likely eases actin disassembly at the base of the phagocytic cup that is necessary for the completion of phagocytosis (Scott *et al.*, 2005).

### 2.2 Deploying membrane surface reserve

To fully engulf its target, macrophage must completely envelop it with its membrane, and this can successfully occur even when the particle is larger than the initial diameter of the cell (Cannon and Swanson, 1992). However, the plasma membrane is poorly elastic and cannot expand more than 2 to 4% before rupture (Evans, Waugh and Melnik, 1976). In fact, some models predicted an absolute limit to phagocytosis that would be set by the availability of the membrane surface area (Herant, Heinrich and Dembo, 2005), supported by the observation that

macrophages reached a phagocytosis limit at a fixed surface area (Cannon and Swanson, 1992). So, how can macrophages engulf larger particles than themselves? Further studies suggest that they mobilize to their surface extra membrane from intracellular vesicles to furnish membrane component (Masters *et al.*, 2013). The exocytic delivery of endomembranes requires actin disassembly at the base of phagocytic cup, and is coordinated by molecular motors that transport vesicles along microtubules (Cannon and Swanson, 1992). Interestingly, disruption of microtubule formation by the use of colchicine and nocodazole affect pseudopods extension in macrophages, perhaps due to impaired focal exocytosis.

### 2.3 The Role of Membrane Tension

The regulation of membrane reservoir mobilization during phagocytosis remains poorly understood but is likely to involve membrane tension. In cells, membrane tension is defined as the membrane capacity to resist deformation and results from the combination of membrane in-plane tension, membrane bending stiffness and membrane attachment to the actin cortex (Hochmuth *et al.*, 1996). In experiments where macrophages were plated on a flat and infinite surfaces coated with IgG, they appeared to mobilize membrane reservoir sequentially, and an increase of plasma membrane tension through hypotonic shock resulted in exocytosis (Masters *et al.*, 2013). This suggests that the membrane reservoir exocytosis may be induced by an increase of membrane tension. The latest is affected by the membrane attachment to the actin cytoskeleton, which is drastically reorganized at the forming phagosome and thus could lead to a local increase of the membrane tension, along with the clearance of F-actin from the base of the cup. Signalling pathways mediating these events remain unclear, although it is known to involve the phosphoinositide 3 kinase (PI3K), which is required for internalization of particle larger than 3  $\mu\text{m}$  (Araki *et al.*, 2003; Masters *et al.*, 2013). Thus, phagocytosis of large or numerous particles appear to require mobilization of intracellular membrane reservoirs, possibly modulated by membrane tension, through a signalling pathway that is incompletely understood.

### 3. Actin cytoskeleton

The initiation of phagocytosis leads to re-arrangements of the cortical cytoskeleton to allow the pseudopod to extend and cover the particle to ingest. Proteins mediate polymerisation

of F-actin, when others debranch or sever the filaments in a coordinated manner to consistently supply pseudopods with monomeric actin. Briefly, the actin-cytoskeleton is disrupted (i), then F-actin polymerization forms pseudopods (ii), and finally, actin depolymerisation at the base of the phagocytic cup occurs while the membrane phagosome is sealed at the distal end (iii) (Freeman and Grinstein, 2014) (**Figure 13**).

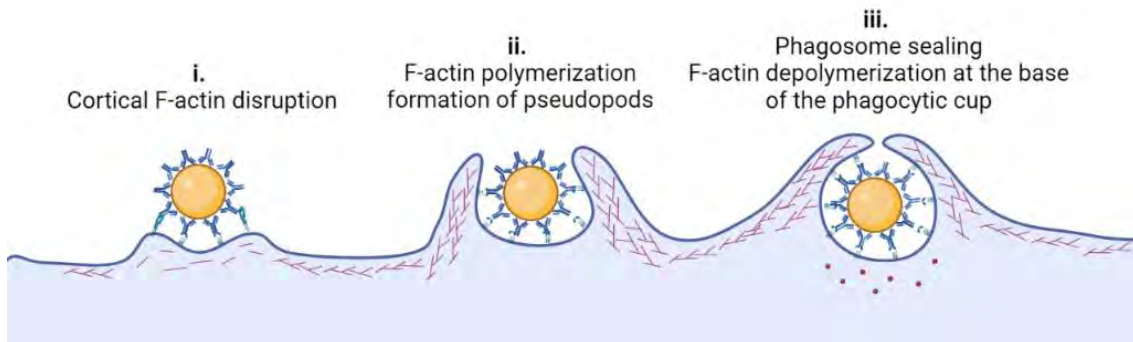


**Figure 13.** Phagocytic cup formation and closure.  
Adapted from (Freeman and Grinstein, 2014) and created on Biorender.

### 3.1 Arp2/3 and its regulators

Nucleation of branched-actin is promoted by the Arp2/3 complex, which activity is regulated by members of the Rho family of GTPases such as **Cdc42**, **Rac** and likely **RhoG**. Early during the process, Cdc42 is activated and recruits WASP and N-WASP, resulting in Arp2/3 activation. Soon thereafter, Rac1 and Rac2 are activated (Hoppe and Swanson, 2004). **Rac** is required for Fc $\gamma$  phagocytosis (Hall *et al.*, 2006), though its effectors are ill defined. **RhoG**, a Rac-like GTPase may also bolster Rac activity (Katoh and Negishi, 2003). Like Cdc42, Rac and RhoG generally promote Arp2/3 activity and branched-actin nucleation in the advancing pseudopod.

Intriguingly, **Arp2/3** has been shown to be not necessary for FcR-mediated phagocytosis, while it seems to be indispensable for integrin-mediated engulfment (Rotty *et al.*, 2017). Indeed, although the depletion of the Arp2/3 complex in bone marrow derived macrophages (BMDM Arpc2<sup>-/-</sup>) leads to protrusion and actin assembly defects, it did not affect competent phagocytosis *via* FcR. Wild type macrophages treated with CK-666, a potent inhibitor of Arp2/3 complex function, also showed preserved FcR phagocytic capability. However, CR3 phagocytosis was disrupted in Arp2<sup>-/-</sup> cells and WT cells treated with CK-666 (Rotty *et al.*,

2017). Authors suggest that FcR phagocytosis may have an Arp2/3 independent route to actin-polymerisation that can compensate for its loss (Rotty *et al.*, 2017).

Indeed, upon inhibition of Arp2/3 complex, compensatory F-actin assembly has been shown to occur via **formins** in fission yeast (Burke *et al.*, 2014). In mammalian cells, Arp2/3 complex-dependent and independent assembly pathways show a similar compensation, although the mechanism remain obscure (Hotulainen and Lappalainen, 2006; Steffen *et al.*, 2006; Suraneni *et al.*, 2012; Wu *et al.*, 2012). Recently, it was suggested that actin regulators, including **profilin** and Ena/VASP, could compensate for loss of Arp2/3 function (Rotty *et al.*, 2015; Suarez *et al.*, 2015). Profilin is a small actin-binding protein that directly binds monomers of G-actin and increases their rate of exchange of ADP for ATP around 1,000-fold (Goldschmidt-Clermont *et al.*, 1992). Profilin also favours F-actin polymerization by inhibiting unregulated, unproductive nucleation events (Suarez *et al.*, 2015). This protein can be recruited to the phagocytic cup *via* direct interactions with membrane PtdIns(4,5)P<sub>2</sub> (Goldschmidt-Clermont *et al.*, 1990) or by the Ena/ VASP family (Ferron *et al.*, 2007).

### 3.2 Ena/VASP family

Interestingly, the **Ena/VASP** family of actin-binding proteins is found to be present in the forming phagosome and appear necessary for completion of phagocytosis (Coppolino *et al.*, 2001). Ena/VASP family members not only recruit profilin but also protect growing barbed ends of actin from capping protein, thus promoting filament elongation (Bear *et al.*, 2002). Moreover, these proteins can interact directly with WASP. This tunes the degree of branching in the advancing pseudopod (Bear *et al.*, 2002) and stabilizes integrin-mediated adhesive structures (Carmona *et al.*, 2016). Ena/Vasp can be recruited by lamellipodin (Krause *et al.*, 2004), itself recruited to nascent phagosomes by PIP<sub>2</sub> (Montaño-Rendón *et al.*, 2022). Moreover, silencing of lamellipodin inhibits phagocytosis and produces aberrant pseudopodia with disorganized actin filaments (Montaño-Rendón *et al.*, 2022). Therefore, Ena/VASP and lamellipodin are attractive candidates to coordinate pseudopod extension and maintain pseudopod–target contacts.

#### 4. Mechanoresponsive feature of phagocytosis

During the pseudopods progression along the target particle, tight contact is established (Wright and Silverstein, 1984) and physical properties of this target can be sensed. It has been shown that some intrinsic parameters such as size, shape, and also importantly stiffness of the target greatly influence the outcome of phagocytosis: stiff particles are engulfed more efficiently than the soft ones (Beningo and Wang, 2002). Therefore, phagocytosis has been identified as a mechanosensitive process. Mechanosensing requires application of forces to the target, however no protein is known to couple Fc $\gamma$ Rs to the actin cytoskeleton, suggesting other actors are required. Some have been proposed, and appear here even if not strictly part of cytoskeleton.

##### 4.1 Integrins

Integrins are engaged in phagocytosis mediated by opsonic receptors, either as primary (in CR-phagocytosis), or secondary (in Fc-phagocytosis) receptors (Freeman and Grinstein, 2014). Their role in mechano-transduction is well established in the literature, thus integrin-mediated adhesions are of particular interest to mechanosensation in phagocytosis.

Upon binding to target particle ligands, integrins can recruit mechanoresponsive proteins such as talin which link their cytoplasmic tail to the actin cytoskeleton (Kanchanawong *et al.*, 2010). Mechanical stress on integrins stretches talin, resulting in the recruitment of other actin-binding proteins such as vinculin which reinforces the adhesion (del Rio *et al.*, 2009; Kanchanawong *et al.*, 2010). The involvement of talin in phagocytosis has been demonstrated by the use of a truncated form of talin preventing its association with actin and vinculin (Freeman *et al.*, 2016). Macrophages expressing this construct and plated on IgG-coated glass failed to assemble the actin belt usually formed at the site of phagocytosis, and CD45, a large glycoprotein, could pass through the contact zone, suggesting the diffusion barrier model is talin-dependant.

Thus, integrin engagement at the phagocytic site could mediate the response of the cytoskeleton to the extracellular phagocytic target.

## 4.2 Podosomes

Podosomes are another type of integrin-mediated adhesive structures and could also support the mechanoresponse of macrophages in phagocytosis. They have been found in the phagocytic cup during both Fc $\gamma$ R- and integrin-mediated phagocytosis (Ostrowski *et al.*, 2019) and can exert protrusive forces normal to the surface (Labernadie *et al.*, 2014; Vorselen *et al.*, 2021). This normal pushing could allow stiffness sensing at the phagocytic cup, therefore podosomes are good candidates to support the mechanoresponse of macrophages in phagocytosis. Their composition, function and potential roles in phagocytosis are discussed in Chapter III.

## V. Phagosome closure

The final and certainly least understood step for phagosome formation is its closure. At that particular moment, pseudopods completely surround the target and eventually merge, which lead to membrane fission and release of the phagosome from the plasma membrane. To mediate such event, two mechanisms has been proposed: membrane constriction by contractile proteins and membrane pushing by actin cytoskeleton (Jaumouillé and Waterman, 2020b).

### 1. Contractile proteins

#### 1.1 Dynamin

Dynamin is a membrane associated protein of the GTPase family involved in endocytosis and membrane traffic. Its isoform dynamin-1 is present exclusively in the brain and predominantly at the plasma membrane, while dynamin-2 is ubiquitous, and present both in endomembrane and plasma membrane. In macrophages, dynamin-2 has been described as recruited early and concomitantly with actin during phagosome formation (Gold *et al.*, 1999; Marie-Anaïs *et al.*, 2016). Inhibition of its activity resulted in the inhibition of the internalization of IgG-coated particles during the phase of pseudopod extension (Gold *et al.*, 1999).

Membrane extension such as pseudopodia is known to require the fusion of vesicles with the plasma membrane; thus, it has been speculated that dynamin role in phagocytosis is related to its capacity to recruit membrane to nascent phagosomes. This hypothesis is supported by a study where inhibition of dynamin-2, but not dynamin-1, lead to discernible defects in phagocytosis (Tse *et al.*, 2003). The localization of dynamin-2 in both endo- and plasma membrane would

allow such a phenomenon, while dynamin-1 is not expected to have any effect. Accordingly, another study reports inhibition of exocytosis of endomembranes related to phagocytosis upon dynamin-2 activity inhibition (Di *et al.*, 2003). If the above interpretation is correct, dynamin effects on the formation of phagosome are indirect. They would occur at remote location and may be size dependant. If the uptake of large particles requires insertion of internal membrane in a crucial manner, it might be dispensable for smaller targets (Huynh and Grinstein, 2008).

Another alternative role of dynamin has been proposed. Recent 3D-live imaging experiments revealed accumulation of dynamin-2 at the site of phagosome closure (**Figure 14**), and interestingly also on frustrated phagocytosis site, along with actin (Marie-Anaïs *et al.*, 2016). Sequential inhibition of dynamin-2 activity during phagocytosis resulted in stalled phagocytic cup at the pseudopod extension stage and also at phagosome closure stage. This inhibition was related to impaired F-actin polymerization in nascent phagocytic cups, suggesting a role of dynamin-2 in the assembly and remodelling of actin at the phagosomal cup (Marie-Anaïs *et al.*, 2016).

Moreover, dynamins have a well-documented role in the fission of vesicles at sites of endocytosis and have been reported to apply constrictive forces to drive membrane scission in a ring-shape conformation (Morlot and Roux, 2013). Therefore, Marie-Anaïs *et al.* suggest a critical role of dynamin-2 in scission of phagosome from plasma membrane. According to this study, in Fc $\gamma$  phagocytosis, dynamin-2 seems to play two distinct roles in the assembly of F-actin at the phagocytic cup and in phagosome scission from the plasma membrane. Of note, similar roles of dynamin-2 have been proposed in CR3-mediated phagocytosis (Mularski *et al.*, 2021).

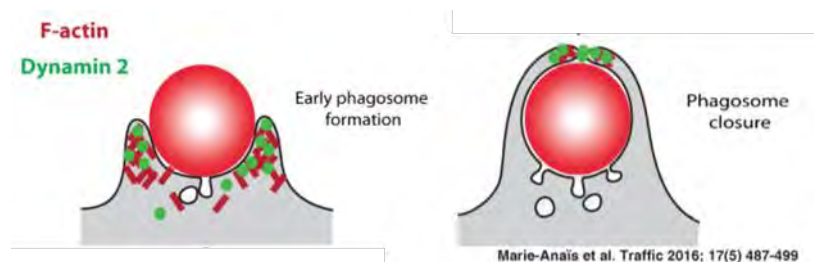


**Figure 14.** Dynamin localisation at the phagocytic cup  
From (Marie-Anaïs *et al.*, 2016)

## 1.2 Myosins

The molecular motors known as myosins, actin binding proteins, exert direct force on actin filaments. However, their mechanical function in phagocytosis is not completely comprehended, mainly because of the various myosin isoforms present in phagocytes and the intricate and rapid nature of phagocytosis. Myosins have the ability to control actin assembly, crosslink and rearrange actin filaments, facilitate actin-dependent membrane deformation, and regulate protein localization (Barger, Gauthier and Krendel, 2019).

In leukocytes, non-muscle myosin IIA is the predominantly expressed isoform. Myosin II has been localized at the phagosome, however its contribution in phagocytosis remains unclear (Swanson *et al.*, 1999). Studies suggest a role of myosin II in phagocytosis during both FcR and CR-mediated phagocytosis (Olazabal *et al.*, 2002; Tsai and Discher, 2008; Yamauchi, Kawauchi and Sawada, 2012; Vorselen *et al.*, 2021). when others claim no effect of myosin II inhibition on particle engulfment (Rotty *et al.*, 2017; Jaumouillé, Cartagena-Rivera and Waterman, 2019). During pseudopods extension, the phagocytic cup squeezes the particle to ingest (Araki, 2006) and this contractile activity is concomitant with the movement of F-actin ring from the bottom to the top of the phagocytic cup. The contraction is dependant of myosin light-chain kinase (MLCK), therefore myosin II activated by MLCK has been suggested to be required for the contractile activity of phagocytic cups (Araki *et al.*, 2003). However, in Fc $\gamma$ R phagocytosis, a myosin-II dependant contractility is observed only upon cell surface increase of more than 225% (Kovari *et al.*, 2016), thus myosin II does not seem required for pseudopods extension. It could be involved in phagocytosis through another effect: its role on cortical tension. In micropipette aspiration experiments, cortical tension of neutrophils was measured upon phagocytosis of IgG opsonized beads and subsequent modelling suggest the particles are not directly pulled by molecular motors, but that they are propelled inward through the increase of cortical tension (Herant, Heinrich and Dembo, 2006). Cortical tension can be increased by myosin II activity, and thus impair protrusions extension around the particle, but promote particle inward movement (van Zon *et al.*, 2009). Because phagocytes show distinct cortical tensions, the effect of myosin II inhibition may be variable (Bufi *et al.*, 2015).

In macrophages, others myosin isoforms concentrate at various stages of phagocytosis. Class IXb myosins are located at the base of phagocytic cups, while myosin Ic concentrates at the site

of phagocytic cup closure, and myosin V appears only after the phagosome closure (Diakonova, Bokoch and Swanson, 2002).

Similarly to myosin II, myosin IX appears in phagocytic cups (Swanson *et al.*, 1999; Diakonova, Bokoch and Swanson, 2002) and has also been proposed to be involved in its the contractile activity. Nevertheless, because class IX myosin contain a GTPase-activation protein (GAP) domain activating Rho GTPase (Chieriegatti *et al.*, 1998), it could act as a signalling molecule for actin remodelling. At the same time, myosin Ic concentrates at the tip of the phagocytic cup, and is suggested to mediate a purse-string-like contraction that closes phagosomes (Swanson *et al.*, 1999). Myosin X is also recruited to the phagocytic cup under PI-3-K control and appears to be important for pseudopod spreading in phagocytosis (Cox *et al.*, 2002). Finally, myosin V has been described on closed phagosomes. In other cells types, this class of myosin is involved in vesicular transport (Tabb *et al.*, 1998), thus is it possible that myosin V is related to phagosome movement rather than its closure (Araki, 2006).

In summary, myosins have been described as having potential different roles during phagosome formation: myosin II in the contractile activity of the phagocytic cup, myosin X in pseudopods extension, myosin Ic in phagocytic cup closing, myosin IX in actin remodelling via Rho activation and myosin V in movement of newly formed phagosomes.

## 2. Actin-driven protrusions

Lastly, cortical tension itself has been suggested to promote plasma membrane fusion. In a study on cell-cell fusion, Kim *et al.* describe fusion as being induced by invasive protrusions from an “attacking” cell on a “receiving” cell. The protrusive and resisting forces from the two fusion partners has been proposed to put the fusogenic area under high mechanical tension. This tension could help to overcome energy barriers for membrane apposition and drives cell membrane fusion (Kim *et al.*, 2015). In phagocytosis, it is tempting to assume a similar phenomenon, where the cortical tension of the progressing F-actin rich pseudopods could be sufficient to induce the fusion of their membrane.

## VI. Maturation of phagosome

### 1. Chemical degradation of the particle

After internalization, the newly formed phagosome undergoes several phenomena of fusion and fission with endosomes and lysosomes to become a new vesicle, the phagolysosome. This process is called phagosome maturation and aims at degrading the ingested particle (Fairn and Grinstein, 2012; Canton, 2014).

First, the new phagosome fuses with early endosomes (Levin, Grinstein and Canton, 2016) under the control of Rab5, a small GTPase present at the phagosome membrane (Kitano *et al.*, 2008; Gutierrez, 2013). Indeed, Rab5 recruits the molecule early endosome antigen 1 (EEA1) that acts as a bridge between early endosomes and endocytic vesicles (Callaghan *et al.*, 1999; Christoforidis *et al.*, 1999) and promotes the recruitment of Rab7 (Araki *et al.*, 2003; Vieira *et al.*, 2003) (**Figure 15A**).

Thereafter, Rab5 is lost to the profit of Rab7, which promotes the fusion of the phagosome with late endosomes (Vieira *et al.*, 2003). From that fusion, lysosomal-associated membrane proteins (LAMPs) and luminal proteases (cathepsins and hydrolases) are incorporated (Fairn and Grinstein, 2012; Canton, 2014). Simultaneously, V-ATPase molecules accumulate at the phagosome membrane. These molecules are responsible for the translocation of protons into the phagosome and thus acidification (pH 5,5 – 6) of the vesicle (Kinchen and Ravichandran, 2008; Marshansky and Futai, 2008) (**Figure 15B**).

Next, phagosomes and lysosomes fuse to form phagolysosomes (Levin, Grinstein and Canton, 2016). This particular vesicle is equipped with mechanisms of microorganism degradation and represents the fundamental microbiocidal and sterilization organelle (Uribe-Querol and Rosales, 2020). Indeed, the lumen contains many hydrolytic enzymes, such as cathepsins, proteases, lysozymes and lipases participating in the degradation of the internalized particle (Kinchen and Ravichandran, 2008). Moreover, the accumulation of V-ATPase molecules on the membrane promotes the decrease of the pH to 4.5 (Marshansky and Futai, 2008). NADPH-oxidase, also present at the membrane, produces reactive oxygen species (ROS), such as superoxide ( $O_2^-$ ), which produces hydrogen peroxide ( $H_2O_2$ ), a substance with strong microbiocidal activity (**Figure 15C**).

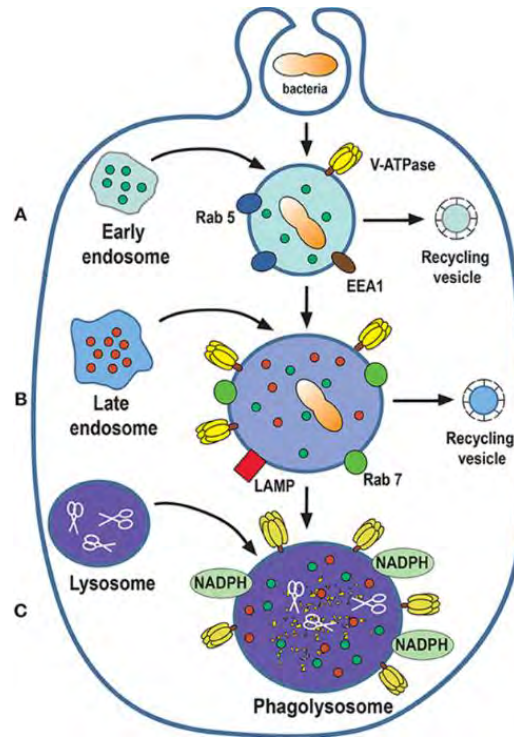


**Figure 15** Phagosome maturation.

*EEA1*, early endosome antigen 1; *LAMP*, lysosomal-associated membrane protein; *NADPH*, nicotinamide adenine dinucleotide phosphate oxidase. From (Uribe-Querol and Rosales, 2020)

## 2. Mechanical degradation: actin-flashes located at the phagosome

Transient recruitment of actin at the closed phagosome has been documented as “actin-flashes” by Yam and Theriot (Yam and Theriot, 2004). They observed rapid (<40 s) assembly and disassembly of F-actin at the phagosome membrane during phagocytosis by epithelial cells of *Listeria monocytogenes*, *Escherichia coli* and polystyrene beads coated with E-cadherin or transferrin. This phenomenon could occur repeatedly on phagosomes but its function was unexplained.

Later on, Liebl and Griffiths analysed phagosomes in primary mouse bone marrow-derived-macrophages (BMDMs), Raw macrophages and microglial cells phagocytosing various particles (zymosan, carbon particles, naked beads or IgG coated beads), and extend this observation of actin-flashes. The F-actin flashing occurred more frequently upon increased phagocytic load, with a slower cycle of assembly and disassembly (4 min) and appeared to be related to the maturation of the phagosome (Liebl and Griffiths, 2009). Indeed, the actin filaments are possibly forming a barrier excluding the endocytic organelles from accessing the phagosome membrane, thus inhibiting the fusion with lysosome (Liebl and Griffiths, 2009). Moreover, they show that dynamic interactions between membrane elastic tension and compression forces of

polymerizing actin can also lead to the constriction of macropinosomes. The latest is an intracellular fluid-containing compartment, more compressible than phagosome, which ease the analysis of the mechanical forces induced by the actin assembly on their membranes (Liebl and Griffiths, 2009).

This supposed mechanical role of F-actin flashes is supported by a study on macrophages CR-mediated phagocytosis where the flashes start a few minutes after internalization of C3b-opsonized beads or red blood cells (RBCs) (Poirier *et al.*, 2020). They confirm the dynamic of F-actin flashes at the phagosome (3min persistence and cycles of assembly and disassembly for one hour), which was increased upon phagocytosis of softer targets: twice as many flashes occurred over the first hour in RBCs compared with rigid latex beads of same size. Moreover, the appearance of the flashes correlated with the deformation and lysis of the RBCs internalized, and enhanced degradation of the phagosome content at later stages. Finally, the analysis of the molecular composition of the F-actin network revealed an enrichment in actomyosin, talin, and RhoA. The inhibition of the Arp3/3 complex and myosinIIA decreased the flashes and related deformations frequency. Therefore, the authors suggest a “mastication” role of these actomyosin mediated contractions that would ease the later degradation of softer particles (Poirier *et al.*, 2020).

Another role has been proposed by Bohdanowicz *et al.* who reported actin polymerization at the sealed phagosome 1 to 3 min after its closure. The F-actin surrounded transiently the phagosome before asymmetrical disassembly, leading to actin “comet tail” which were suggested to propel the phagosomes towards lysosomes (Bohdanowicz *et al.*, 2010). Also observed in later study on actin flashes (Poirier *et al.*, 2020), these comets are assumed to be distinct in nature as it appear only once and lead to translocation of the phagosome within the cytoplasm, whereas flashing phagosomes occurred on a repeated manner and were delayed in their maturation (Poirier *et al.*, 2020).

*To conclude on that chapter, phagocytosis is a cellular process consisting in the detection, engulfment and degradation of the target, realised by dedicated cells. Due to its crucial role in immunity and the maintenance of homeostasis, an excess or conversely a defect of this function can lead to pathologies. The actin cytoskeleton is actively involved in each step of phagocytosis. It is composed of actin filaments that can be organized as unbranched or branched filaments, mainly regulated by formin and Arp2/3 complex, respectively.*

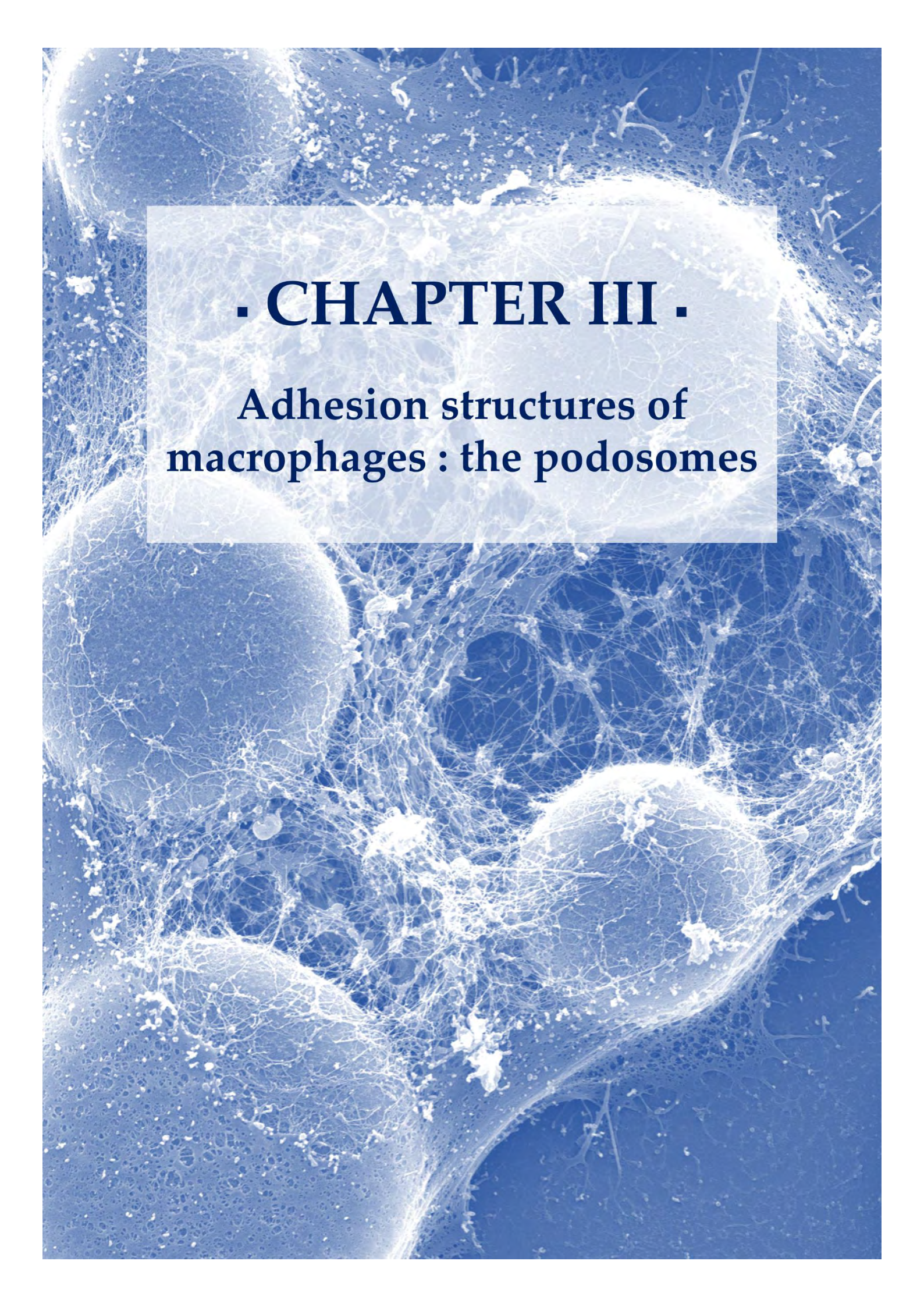
*Macrophages use membrane protrusions called ruffles, such as filopodia and lamellipodia, to interact with target particles and initiate phagocytosis. The engagement of receptors on the macrophage surface plays a crucial role in recognizing and binding to target particles. The most effective receptors are opsonic receptors, such as Fc receptors (FcR) and complement receptors (CR), which bind to specific ligands on the target particles. Upon ligand binding, these receptors activate signalling pathways that lead to membrane changes and actin cytoskeleton reorganization, forming a phagocytic cup. The signalling pathways differ for FcR and CR-mediated phagocytosis. I also discuss the types and functions of various Fc and complement receptors, their ligands, and their respective signalling mechanisms. Additionally, I highlight the cooperation of phagocytic receptors in initiating phagocytosis and the role of membrane mobility in receptor clustering.*

*The progression of the phagocytic cup involves the extension of actin-driven pseudopods and changes in membrane composition to capture the target particle. To engulf larger particles, macrophages mobilize extra membrane from intracellular vesicles. Membrane tension is indeed crucial and participates with actin cytoskeleton remodelling to pseudopod formation. The actin dynamics is regulated by the Arp2/3 complex and possibly Ena/VASP proteins. Phagocytosis is also influenced by mechanosensitive factors like integrins and likely podosomes.*

*Phagosome closure is a crucial step in phagocytosis, yet its mechanisms are not fully understood. Two proposed mechanisms involve contractile proteins such as dynamin-2 and myosin II, and actin-driven protrusions that would exert mechanical tension on the membrane, potentially facilitating fusion. The phagosome maturation involves chemical and potential mechanical degradation of the internalized particle. The chemical effect occurs through fusion of the phagosome with endosomes and lysosomes, acidification, and incorporation of degradative enzymes. The mechanical effect is proposed to be mediated by actin-flashes transiently occurring at the phagosome membrane and may regulate phagosome maturation.*

*We mentioned in this chapter the potential role of structures called podosomes on the mechanosensing feature of phagocytosis. These actin-rich structures have been described in macrophages as supporting many cellular functions. However, their role, and even presence during phagocytosis is far from consensual, and could be anything other than mechanosensing. Their definition, location, composition and cellular roles are detailed in the next section, with a particular focus on their description in phagocytosis contexts.*



The background of the slide is a high-magnification electron micrograph of a macrophage. It shows a complex, three-dimensional network of actin filaments. Several prominent, rounded structures called podosomes are visible, which are specialized for cell adhesion and migration. The overall appearance is that of a highly organized and dynamic cytoskeleton.

**· CHAPTER III ·**

**Adhesion structures of  
macrophages : the podosomes**

## I. Definition and description

### 1. What is a podosome?

Podosomes are dynamic adhesion structures, initially described in 2D cell culture in the context of migration on planar substrates. Their first observation in 1983 (Zallone *et al.*, 1983), describes peculiar punctate aggregations of actin in monocytes and osteoclasts. Their existence was then demonstrated in myeloid cells such as monocytes, macrophages, and immature (migrating) dendritic cells (Linder *et al.*, 2000; Burns *et al.*, 2004), as well as in smooth muscle cells, endothelial cells or fibroblasts (David-Pfeuty and Singer, 1980; Moreau *et al.*, 2003; Burgstaller and Gimona, 2004, 2005). In the case of cells of myeloid origin, the formation of podosomes is constitutive, whereas in the second case, their formation requires induction by soluble factors or oncogenes.

Podosomes are usually defined by their molecular composition (see I.2) and their ability to degrade the extracellular matrix (ECM) through a local proteolytic activity (Wiesner *et al.*, 2010). Typical dimensions of podosomes are 0.5 to 1  $\mu\text{m}$  in diameter and 0.5 to 0.8  $\mu\text{m}$  in height (Labernadie *et al.*, 2010).

In 3D, actin-rich protrusions of approximately 5  $\mu\text{m}$  diameter have been described in macrophages (Van Goethem *et al.*, 2010). These structures contain podosome components and recruit ECM-lytic enzymes, they were therefore called “3D podosomes” (Van Goethem *et al.*, 2010; Wiesner, Azzouzi and Linder, 2013). Physiologically, both 2D (i.e. vessel walls and tissue surface) and 3D conformations (network of ECM fibres) exist.

### 2. Architecture and components

The podosome proteome is composed of more than 300 proteins (Cervero *et al.*, 2012), among which cytoskeletal proteins arranged in a typical architecture.

Filamentous actin (F-actin) is assembled in a densely packed core of approximately 200 nm in diameter facing the membrane. Surrounding the core, integrins form a 200 nm wide ring in which are also found adaptor proteins linking them to actin filaments. This ring is located 350 nm away from the core (Proag *et al.*, 2015; Staszowska *et al.*, 2017). A third functional subdomain is located above the podosome core, namely the cap domain. Each of these domains is characterized by typical proteins and various regulatory pathways (**Figure 16**).

### 2.1. The core

The core is mainly constituted of F-actin and is under the control of N-WASp-mediated activation of the Arp2/3 complex (Linder *et al.*, 2000). Actin regulators such as cortactin (Tehrani *et al.*, 2006) and cofilin (Linder and Aepfelbacher, 2003) are also present. The adaptor protein TSK5, a SRC kinase substrate, acts as a central regulator of podosomes (Seals *et al.*, 2005; Crimaldi, Courtneidge and Gimona, 2009).

### 2.2 The ring

Around the core, a ring of integrins and their adaptor proteins such as talin and vinculin (Marchisio *et al.*, 1988; van den Dries *et al.*, 2013) links the actin cytoskeleton to the extracellular matrix. In addition, two types of unbranched actin filaments have been described: the lateral filaments which connect the ring to the top of the core, and the dorsal connecting cables, which link individual podosomes between them. In both situations, these actin cables were shown to be associated with myosin-IIA (van den Dries, Nahidiyar, *et al.*, 2019).

### 2.3. The cap

On top of the core, a structure called the cap extends laterally towards the ring. The proteins localised at the cap all bind actin or myosin, or are regulators of myosin activity, suggesting cap as a regulator of actomyosin contractility. Among these proteins, the formin INF2 (Panzer *et al.*, 2015), the lymphocyte-specific protein 1, LSP-1 (Cervero *et al.*, 2018), and  $\alpha$ -actinin (van den Dries, Nahidiyar, *et al.*, 2019) have been identified.

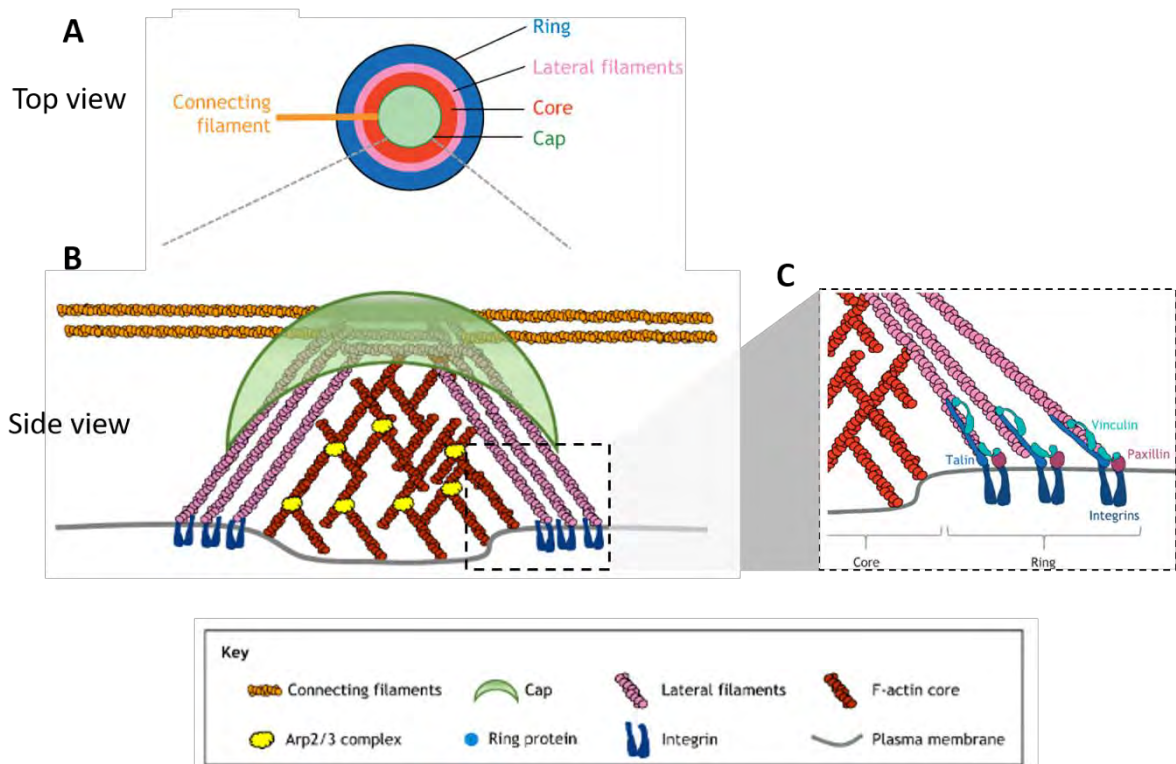


**Figure 16** Model of podosome architecture and interaction between its substructures. Adapted from (Dries *et al.*, 2019)

### 3. Distribution

Distribution of podosomes appears to be cell and adhesion dependent. In quiescent macrophages and dendritic cells they are mostly found as individual structures at the ventral face of the cell, but they group at the leading edge of migrating cells (Linder *et al.*, 1999; van den Dries, Bolomini-Vittori and Cambi, 2014). In human monocyte-derived macrophages, the individual podosomes are randomly distributed without an evident lattice pattern. Among this population, each podosome is spaced approximately 1.2  $\mu\text{m}$  apart from its nearest neighbouring podosome (Proag *et al.*, 2015). In osteoclasts, they can also arrange in a belt or sealing zone (Linder, Wiesner and Himmel, 2011). In endothelial cells and fibroblasts, podosomes form rosettes that are smaller in fibroblasts (Tarone *et al.*, 1985; Moreau *et al.*, 2003) (**Figure 17**).

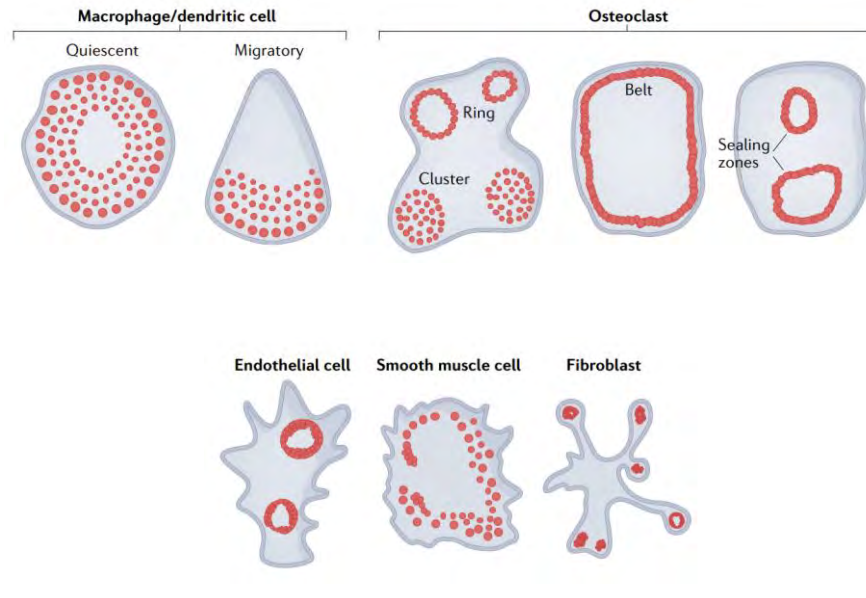


**Figure 17** Podosome distribution among different cell types. Podosomes are represented by red dots. Adapted from Linder, 2023

## II. Functions

Firstly defined by their proteic composition and their ability to degrade extracellular material, podosomes have progressively been recognized as multifunctional structures not only mediating matrix degradation, but also mechanosensing, directional migration, antigen uptake, topography sensing, and cell-cell fusion (**Figure 18**). The role of podosome-like structures in phagocytosis is not clearly identified yet and will be developed in the next part.

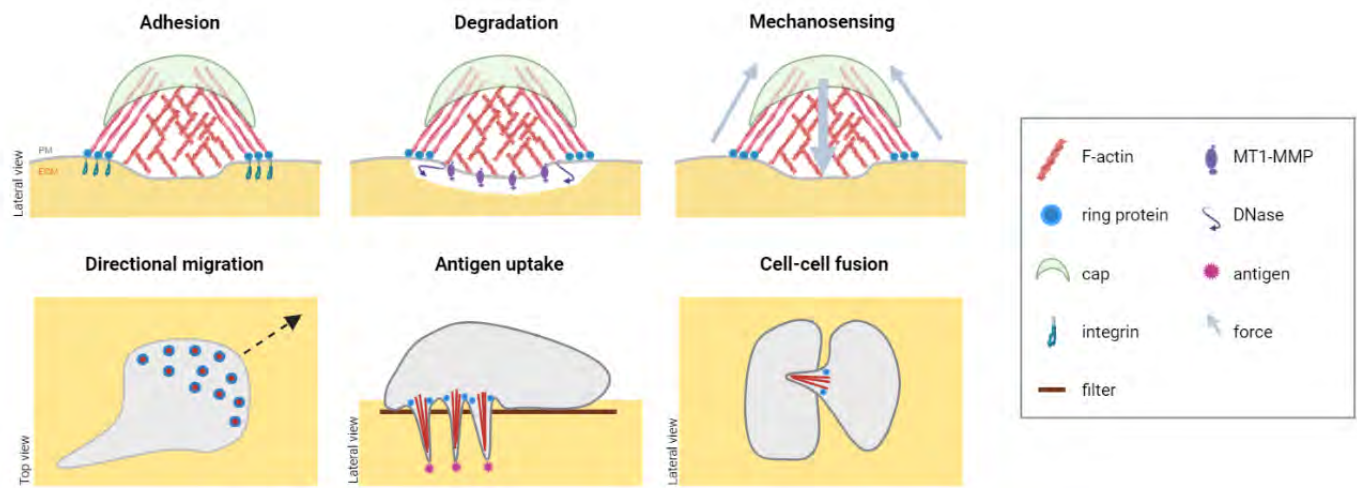


**Figure 18** Functions of podosomes

ECM: Extracellular Matrix; PM: Plasma Membrane. MMP: matrix metalloproteinase. Adapted from Linder *et al.* 2023

### 1. ECM adhesion

Through the adhesion of proteins of the ring, such as talin or paxillin binding to integrins, podosomes adhere to the substratum. Furthermore in osteoclasts, CD44, the cell surface adhesion receptor of hyaluronic acid, and collagens major components of extracellular matrix (ECM), has been proposed to localize underneath the core of belt superstructures (Chabadel *et al.*, 2007).

### 2. ECM degradation

One distinctive feature of podosomes is their ability to degrade components of the extracellular matrix in a localized manner. Due to the high turnover rate (persistence: 2 to 12 min) and large numbers of these structures (20 to 100) per cell, the degradation of ECM by these structures tends to be widespread and shallow (Linder, 2007). This degradation is achieved through the recruitment and release of various lytic enzymes, including matrix metalloproteinases (MMPs), cathepsins, and possibly ADAM proteins and serine proteinases. Specific MMP isoforms that are relevant to endosomes include MT1-MMP, MMP2, and MMP9, which have been observed in podosomes of macrophages (El Azzouzi, Wiesner and Linder, 2016), endothelial cells (Osiak, Zenner and Linder, 2005; Tatin *et al.*, 2006), phorbol ester-treated epithelial cells (Xiao and Liu, 2013) and smooth muscle cells (Thatcher and *et al.*, 2017). The activity of these enzymes covers a wide range of ECM substrates, including various

collagen isoforms, gelatin, fibronectin, vitronectin, and laminin, enabling podosomes to degrade virtually any ECM component they encounter. However, the release of lytic enzymes alone may not be sufficient to achieve ECM degradation, as most often, the activity of these enzymes requires an acidic pH. Additionally, matrix degradation requires not only protease activity but also the reduction of disulfide bonds between ECM fibres (Ros *et al.*, 2020), particularly collagen, which can be achieved by oxidoreductase, although its role is currently unclear in podosome-mediated ECM degradation (Linder and Aepfelbacher, 2003). Furthermore, DNase X, a glycosylphosphatidylinositol-anchored enzyme that degrades DNA, has been detected in podosomes in human, murine, and fish macrophages (Pal *et al.*, 2021). This suggests that podosomes may have additional roles in pathogen clearance and the general removal of extracellular DNA, in addition to their function in ECM degradation.

### 3. Mechanosensing

Macrophages encounter a wide range of substrates with different mechanical properties, including rigidity, density, crosslinking, and topography (Collin *et al.*, 2006). Therefore, the appropriate response of the cell to these environmental mechanical cues relies on the podosomes ability to probe these cues and transduce it into the cell.

Subsequently, traction force microscopy (TFM) has revealed that podosomes in v-src-transformed fibroblasts generate local force in response to substratum rigidity, which correlates with the lifetime and stability of these podosomes (Collin *et al.*, 2006, 2008). Moreover, an oscillatory behaviour of podosomes has been shown by protrusion force microscopy (PFM) on macrophages (Labernadie *et al.*, 2014; Proag *et al.*, 2015, 2016), later supported by elastic resonator interference stress microscopy on osteoclasts (Kronenberg *et al.*, 2017). In PFM, deformation induced by macrophages adhering to a compliant Formvar sheet are measured by atomic force microscopy (AFM) and the height of resulting protrusions serve to estimate the related exerted force, within the nN range per podosome. It was shown that a decrease in the substrate stiffness correlated with a decrease in forces applied by individual podosome and a lower density of podosomes at the cell level (Labernadie *et al.*, 2010) This hallmark of mechanosensing activity points podosomes as mechanosensitive cell structure capable of protrusive force exertion.

Finally, podosomes appear to sense substrate topography as their organization differs in osteoclasts when seeded in substrates of different roughness (Geblinger, Geiger and Addadi,

2009). Similarly, in dendritic cells, podosomes align along micropatterned substrates (van den Dries *et al.*, 2012).

#### 4. Directional migration

Although podosomes can be present over the whole ventral face of cells, they are mostly recruited in cellular migratory-related protrusions (Linder and Aepfelbacher, 2003). Since they adhere to the substrate, podosomes have been proposed to promote stabilization of cellular protrusions, leading to cell polarity which supports directional cell migration (Dovas *et al.*, 2009). In primary macrophages, a subpopulation of precursor podosomes has been described at the cell periphery and site of protrusions, which are larger, more dynamic, and display higher turnover rates than the successor podosomes. In this second subpopulation, podosomes are indeed smaller, more stable, and located in the inner part of the cell (Evans *et al.*, 2003; Kopp *et al.*, 2006). Such dynamics likely allows more rapid adaptation of the actin cytoskeleton at protrusion sites. This is supported by the observation that in dendritic cells, only immature but not mature ones form podosomes (Burns *et al.*, 2004). Moreover, in a 3D context, the podosomes ability to degrade the ECM is necessary to perform mesenchymal migration (Van Goethem *et al.*, 2010, 2011).

#### 5. Antigen uptake

Podosomes-like structures have been described in dendritic cells plated on porous filters. These actin rich protrusions show sites of endocytosis (Gawden-Bone *et al.*, 2010) and antigen uptake (Geijtenbeek *et al.*, 2000; Burgdorf, Lukacs-Kornek and Kurts, 2006; Baranov *et al.*, 2014), as well as an adhesive ring structure.

#### 6. Cell-cell fusion

Multinucleated giant cells (MGCs), including osteoclasts, sometimes referred to as “bone RANK-L macrophages”, undergo several steps of fusion before being considered as mature and functional. First, individuals fuse into multinucleated cells that will eventually fuse to form multinucleated giant cells. It has been reported that podosome-like structures support both phases. Oikawa and colleagues showed that actin-rich protrusions drive contact and fusion with neighbouring cells in RANK-L-treated RAW264.7 macrophages (Oikawa *et al.*, 2012).

During the following phase, the fusion of multinucleated cells, the periphery of the fusing cells exhibits actin-rich zipper-like structures, which share many components with podosomes.

Indeed, Arp2/3 complex, TKS5, vinculin, zyxin, talin, and integrin  $\alpha_M\beta_2$  have been observed on these structures that originate from successive addition of peripheral podosomes (Balabiyev *et al.*, 2020). It is thought that zipper-like structures enable the formation of cell-cell junctions by allowing close contact between fusing cells (Balabiyev *et al.*, 2020).

### 7. Other functions

Finally, in non-myeloid cell types, clearly identified podosomes or podosome-like structures are involved in other processes such as angiogenesis and vasculature remodelling in endothelial cells (Paterson and Courtneidge, 2018), myoblast fusion (Sens *et al.*, 2010) maturation of the postsynaptic membrane in myotube, and embryonic and postnatal development (Paterson and Courtneidge, 2018).

## III. Role in pathologies

The formation of podosomes in specific cells allows the degradation of ECM and invasion of their microenvironment, leading to physiological processes like cell migration, bone remodelling, or embryonic development. Therefore, a defective function of the podosomes can cause pathological states.

### 1. Wiskott-Aldrich syndrome (WAS)

WAS is due to a recessive mutation within the WAS gene and leads to an immunodeficiency characterized by recurrent infections, thrombocytopenia (i.e. a low number of platelets), and eczema (Thrasher and Burns, 2010). The activation of the Arp2/3 complex on podosomes to nucleate the branched F-actin network of the podosome core, requires the WAS protein (WASp) family (Linder *et al.*, 1999). Patients affected by WAS present macrophages devoid of podosomes with defects in chemotaxis (Dovas *et al.*, 2009). Experimentally, WASp deficiency in murine osteoclasts results in the non-formation of podosomes and impaired bone resorption (Calle *et al.*, 2004).

Other mutations of WASp can be pathogenic: Ile294Thr and Ser270Pro lead to an increased function of WASp, thus favouring Arp2/3 mediated actin polymerization. At the cellular level, irregular morphology, impaired motility, and abnormal organization of podosomes have been reported in macrophages (Ancliff *et al.*, 2006). Symptoms include myelodysplasia (blood cancer affecting the bone marrow) and severe congenital neutropenia.

The Arp2/3 complex consists of seven subunits (Arp2, Arp3 and ARPC1–5) among which ARPC1 and ARPC5 are encoded by two different isoforms that confer them distinct properties in actin assembly and disassembly (Abella *et al.*, 2016). Mutations of Arp2/3 subunits can be pathogenic: mutations in the ARPC1 isoform B lead to major defects in the actin cytoskeleton and podosome formation of megakaryocytes, causing micro thrombocytopenia (decrease in number and size of platelets), eosinophilia (high levels of eosinophils) and inflammatory disease (Kahr *et al.*, 2017).

## **2. Pyogenic sterile arthritis, pyoderma gangrenosum, and acne syndrome (PAPA)**

This rare autosomal dominant autoinflammatory disorder is characterised by severe arthritis, skin ulcerations, and acne. PAPA is due to mutations in the PSTPIP1 gene coding for an F-BAR and adaptor protein linking the actin cytoskeleton to the plasma membrane. In some patients, specific mutations affect the interaction of PSTPIP1 with PTP-PEST (a protein-tyrosine phosphatase) or WASp, resulting in severe defects in podosome formation and functionality and impaired macrophage chemotaxis and migration (Cortesio *et al.*, 2010; Starnes *et al.*, 2014). Unlike patients with WAS, who display immunodeficiency, PAPA patients rather show chronic tissue inflammation and destruction. Authors speculate that the impairment of macrophage migratory function leads to their retention within tissues and contributes to the development of chronic inflammation through neutrophil recruitment, a hallmark of PAPA syndrome (Cortesio *et al.*, 2010).

## **3. Frank-TerHaar Syndrome (FTHS)**

FTHS is an autosomal recessive genetic disorder whose symptoms include skeletal dysplasia (which most common form is achondroplasia, also called dwarfism), eye and cardiac abnormalities occurring during development (Iqbal *et al.*, 2010). The mutations of the Tsk4 gene induce reduced levels of Tsk4 protein, which is essential for the functional formation of podosomes. As functional podosomes are needed for development and tissue remodelling, these defects could lead to the symptoms described (Paterson and Courtneidge, 2018).

## **IV. Role in phagocytosis**

Despite the well-documented role of podosomes in many myeloid cell functions, their presence and exact contribution to phagocytosis, one of the main roles of macrophages, remain unclear and have only been studied recently. The next part will review the available literature

on the matter, including the work published in the frame of this thesis, which will be described in more detail in the “Results” section of this dissertation.

Over the last years, evidence has accumulated for the formation of actin-rich punctiform structures at the phagocytic cup containing typical components of podosomes such as  $\beta 2$  integrin, paxillin, talin, vinculin, myosin motors such as myosin IIA, myo1e, and myo1f, as well as Arp2/3 complex-generated actin networks, either during frustrated phagocytosis (Labrousse, 2011; Jaumouillé, Cartagena-Rivera and Waterman, 2019; Ostrowski *et al.*, 2019) (**Figure 19C**) or phagocytosis of beads (Barger *et al.*, 2019; Tertrais *et al.*, 2021; Vorselen *et al.*, 2021). (**Figure 19A,B**). These structures have been called podosome-like structures (Allen and Aderem, 1996; Labrousse, 2011; Ostrowski *et al.*, 2019), phagocytic teeth (Vorselen *et al.*, 2021), and phagosome-associated podosomes (Tertrais *et al.*, 2021).

A recent study using Raw264.7 macrophages plated on IgG disks deciphers the ultrastructure of these phagocytic podosomes using interferometric photoactivated localization microscopy (iPALM). It reveals an hourglass-shaped core of F-actin associated with paxillin, talin, and myosin IIa, and connected to other podosomes through F-actin cables. (Herron *et al.*, 2022) (**Figure 19D**).

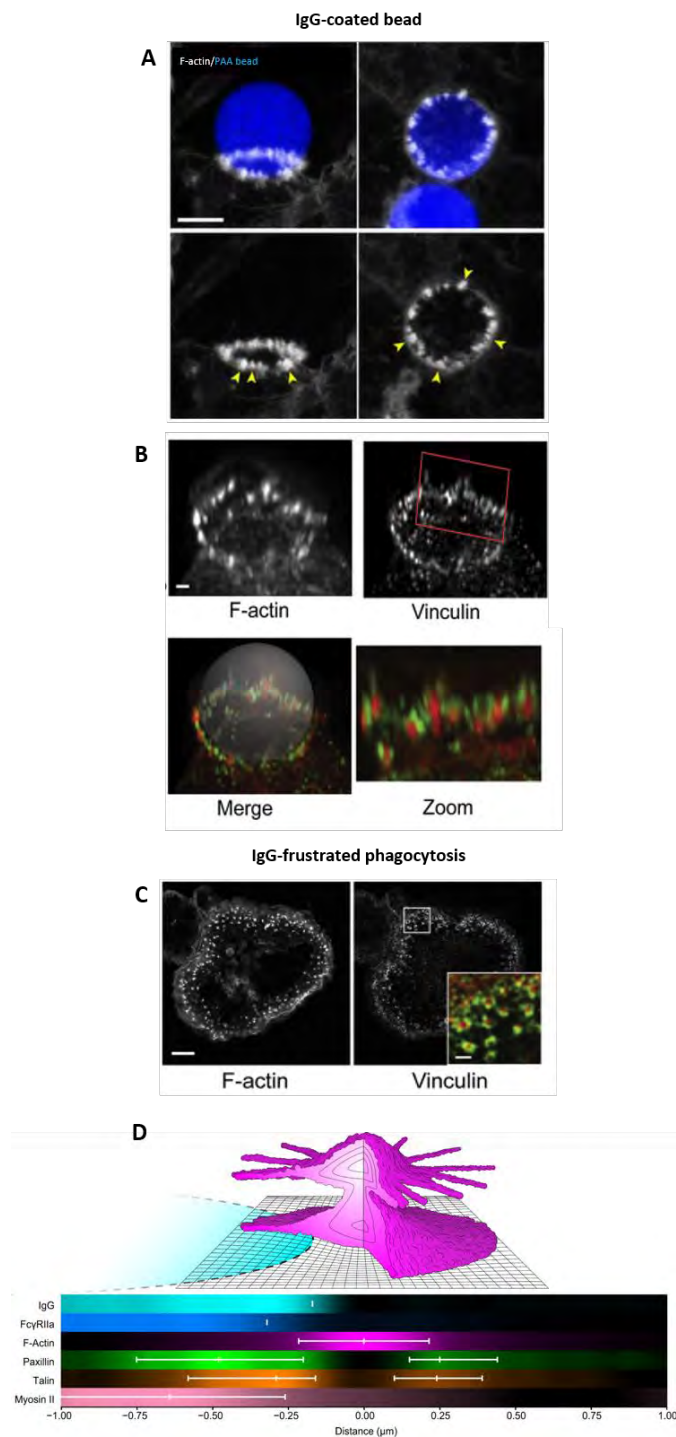


**Figure 19.** Podosome-like structures during phagocytosis of beads or frustrated phagocytosis  
From (Vorselen *et al.*, 2021), (Ostrowski *et al.*, 2019) & (Herron *et al.*, 2022)

Although phagocytic podosomes share similar proteic composition to “classical” podosomes, they show some notable differences in their dynamic. Ostrowski *et al.* described a higher turnover of phagocytic podosomes on the site of frustrated phagocytosis and a shorter life span (Ostrowski *et al.* 2019). Their sensitivity to inhibition of F-actin nucleation is not consensual: on closed phagosomes, they were either found partially resistant (Tertrais *et al.*, 2021), or

significantly reduced in number upon inhibition of Arp2/3 complex (Vorselen *et al.*, 2021). This discrepancy might be explained by the different cell types (primary human macrophages or Raw264.7).

The role of these podosome-like structures in the phagocytic cup is currently unclear. Several hypotheses have been proposed and remain to be demonstrated.

Because of an observation of the reciprocal relationship between phagocytic podosomes and conventional podosomes, where the formation of the first correlates with the reduction in the number of the second (West *et al.*, 2004; Tertrais *et al.*, 2021), it has been proposed that the podosomes of the resting ventral face relocate at the phagocytic cup.

Moreover, it has been speculated that dissolving enzymes released at the tip of podosomes in the context of ECM degradation could be incorporated into nascent phagosomes to digest the internalized particle during phagocytosis (Tertrais *et al.*, 2021). Podosome-like structures were also reported to mediate tight sealing with the phagocytic target, and thought to act like a scaffold for encapsulation as well as a diffusion barrier for signalling molecules at the phagocyte membrane (Ostrowski *et al.*, 2019).

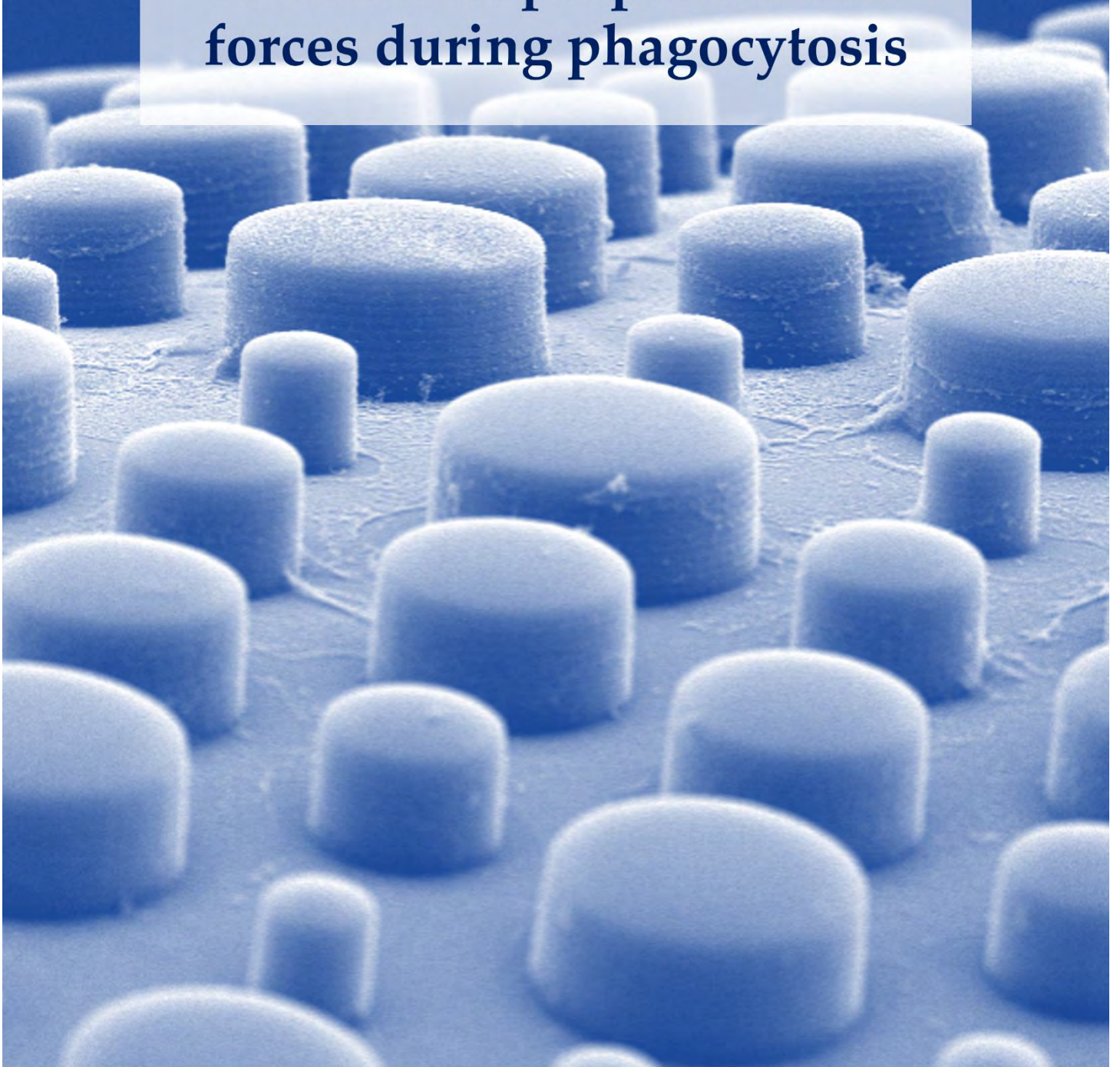
In a recent innovative study, soft polyacrylamide beads covered with IgG have been used as a phagocytic target for macrophages. The deformation of the beads during internalisation correlate with the presence of phagocytic podosomes and shed light on the local forces involved, which would be mediated by myosin II dependant contractility (Vorselen *et al.*, 2021). This assumption is supported by another study where macrophages internalize the yeast *Candida hyphae*. Indeed, podosome-like structures have been described and correlated with the folding of the filamentous form of the yeast inside the phagosome (Bain *et al.*, 2021), suggesting force application at this site. In this context, the role of these podosome-like structures would be to generate protrusive forces to ease the internalisation process or as a mechanical pre-digestion of the target (Vorselen *et al.*, 2021).

*In conclusion, podosomes are dynamic structures formed constitutively in myeloid cells and composed of an actin core, an adhesion ring of integrins and adaptor proteins, and a cap domain composed of actomyosin regulators. Podosomes can be present individually or form specific structures, their location depends on the cell type and adhesion state. Their functions in the myeloid lineage include adhesion, degradation of the ECM, mechanosensing, directional migration, antigen uptake, cell-cell fusion and recent studies report a potential mechanical role in phagocytosis. This last point is particularly interesting since the studies carried out until now do not seem to agree on the exact nature of the observed “podosome-like” structures nor on their role. A part of the thesis work was to characterise these structures in human macrophages and elucidate how their presence affected the fate of the internalized particle. Results are presented in the first chapter of the “Results” section.*

*The ability of podosomes to generate protrusive forces against their substrate has been demonstrated through an ingenious microscopy technique. It is important to note that measuring forces at the cellular scale poses significant challenges and necessitates innovative approaches. The primary techniques employed thus far to study these forces, along with the mechanical parameters of phagocytizing cells, are detailed in the following section.*

# **. CHAPTER IV .**

**Techniques to study  
mechanical properties and  
forces during phagocytosis**



During phagocytosis, several mechanical events can be defined: the physical act of finding a target, adhere to it, and then pulling it toward the cell body for engulfment (Kalashnikov and Moraes, 2022). Different systems have been developed to transduce forces into measurable physical quantities such as a mechanical deformation. This part describes the principal techniques that have been referenced in the literature to evaluate the mechanical properties of phagocytosing cells and the forces at stake during the early stage of the process, *i.e.* during the formation of the phagocytic cup. The principal results of studies using these techniques are also detailed.

## I. Micropipette aspiration (MPA)

This technique consists in entrapping a part of a cell into a micropipette and bringing a phagocytic target at its free ends. (**Figure 20**). The pipette pressure to maintain the cell into the pipette can be related to the cellular tension through Laplace's law. It is important to note that the measured tension results both from the acto-myosin cortical tension (Chugh and Paluch, 2018) and the membrane tension, and their relative contribution is difficult to differentiate (Diz-Muñoz, Fletcher and Weiner, 2013; Sens and Plastino, 2015).

In a specific version of this technique, where the cell body is almost completely drawn into the pipette, Evans, Leung and Zhelev showed that target engulfment and contraction of the phagocyte occur sequentially until the phagosome closes. They evaluated that cell contracts with an equivalent force of 10nN, that would be equivalent to a stress of 1kPa, if distributed uniformly over the cell cross section (Evans, Leung and Zhelev, 1993). Herant *et al.* demonstrated that throughout the whole process of phagocytosis, membrane tension remains low (Herant, Heinrich and Dembo, 2005). Through comparison of MPA experimental results and finite element simulations, the same group determined an optimal model for mechanistic of phagocytosis (Herant, Heinrich and Dembo, 2006). This model involves two key mechanical interactions. First, a repulsion between the cytoskeleton and the plasma membrane drives membrane protrusions. Then, when the membrane has just adhered to the target, it is drawn to the cytoskeleton, and the cell flattens into a thin lamella.

An additional setup has been developed to extend this methodology. A micro-indenter placed on the phagocyte side allows for measurements of cellular viscosity and Young's modulus. Both are found to be increasing during phagocytosis, 2-3 folds for T and B cells, 11 folds for neutrophils -like PLB. (Zak *et al.*, 2019) (**Figure 20**).

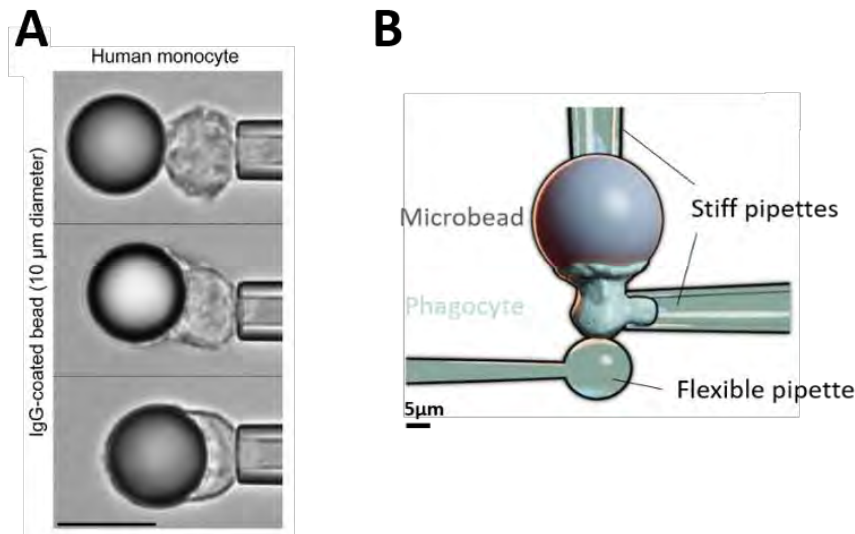


**Figure 20.** MPA experimental setup.  
Adapted from (Heinrich, 2015) and (Zak et al., 2019).

## II. Magnetic and optical tweezers

Optical and magnetic tweezers are two methods using force spectroscopy that are powerful approaches to study single molecules, micromolar assemblies, or cells (Sarkar and Rybenkov, 2016). Optical tweezers (OT) were first introduced to manipulate microscopic particles which are trapped into a focused light beam (Ashkin *et al.*, 1986). Further developments led to the magnetic tweezers technique, which manipulate para or super-paramagnetic beads in a gradient of magnetic field (Strick *et al.*, 1996) (**Figure 21**).

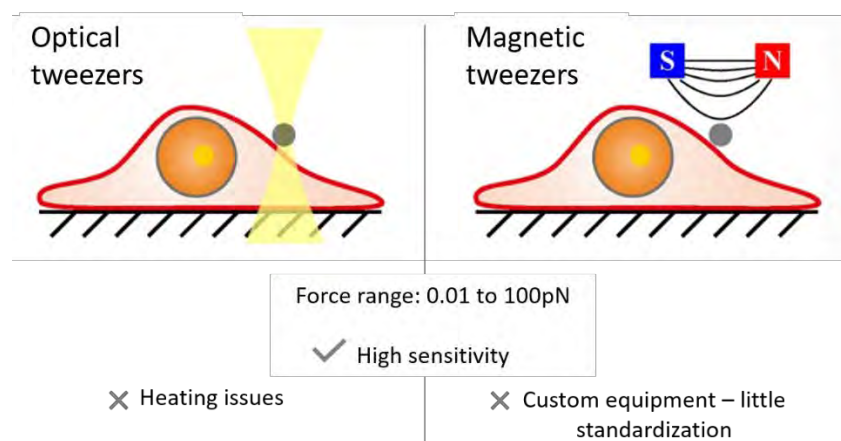


**Figure 21** Optical and magnetic tweezers  
Adapted from (Basoli et al., 2018; Ito and Kaneko, 2020)

## 1. Optical tweezers

Arthur Ashkin, the inventor of OT, was lauded with the 2018 Nobel Prize in Physics for the development of this technique. He also pioneered its applications to cell biology, employing infrared laser light to avoid cell damage, thus allowing *in vivo* observation. To investigate membrane surface tension, OT pull on microspheres attached to the cell membrane. This extracts long cylindrical nanotubes named tethers, which force square is proportional to the membrane tension (Sheetz, 2001). This result suggests that no cytoskeleton content is present within tethers. Experimental curves of force-displacement revealed that this assumption is actually incorrect (Nussenzveig, 2018) and it appears that adhesive interaction between plasma membrane and cytoskeleton contributes to the measured tether forces (Diz-Muñoz, Fletcher and Weiner, 2013; Sens and Plastino, 2015).

In phagocytosis, this technique has been used to study the dynamic and mechanical properties of macrophages filopodia upon binding to IgG-coated beads (Kress *et al.*, 2007). Authors describe filopodia as cellular tentacles: a few seconds after particle binding particle, filopodia retract and pull the bound particle toward the cell. This retraction is F-actin stepwise dependant, with a mean step size of 36 nm, and occurs in three phases: an initial slow phase followed by rapid retraction (average velocity 85 nm/s) and finally slow uptake (10 nm/s). This stepwise process suggests molecular motor activity during filopodial pulling. The pulling velocity depended strongly on the counteracting force and ranged between 600 nm/s at forces <1pN and 40 nm/s at forces above 15 pN. (Kress *et al.*, 2007)

Other researchers used macrophages seeded on IgG-opsonized glass surface to study the pseudopods extension phase (Masters *et al.*, 2013), while measuring membrane tension with OT. Upon contact, the cells spread out as if trying to engulf the surface, without succeeding to and never leading to closure of the phagosome. This process has been called frustrated phagocytosis. In this state, cells first rapidly extend pseudopods (in about 2 min) with actin polymerization pushing the plasma membrane forward and increase of membrane tension up to 58pN counteracting forces. Then, when the membrane area from pre-existing reservoirs is depleted, a transition phase occurs where cells wait for exocytosis to relieve this tension in order to continue. Once past the transition, large actin bundles appear in the central part of the cell, whereas the cell extends outward only slowly, with small and local cycles of protrusion–retraction, restoring pre-existing dorsal membrane folds. (Masters *et al.*, 2013). Increasing

membrane tension with hypotonic buffers increases phagocytosis efficiency and can even overcome pseudopod extension inhibitors (Masters *et al.*, 2013)

## 2. Magnetic tweezers and derived technologies using magnetic beads

In the context of integrin-mediated phagocytosis, magnetic tweezers were used to study response of macrophages to local forces (Vonna *et al.*, 2003). In this study, superparamagnetic beads were coated with invasins, a  $\beta$ 1-integrin-binding protein, and attached to J774 murine macrophages. Under forces exceeding  $\sim 0.5$  nN an initial elastic deflection occurs, and after 30 seconds, trumpet-shaped protrusions “pseudopodia-like” formed actively. The speed of advancement of the protrusion was about  $0.065 \mu\text{m/s}$ , appears force-independent and attributed to the actin cortex growth in the direction of the force. After prolonged application of the external force (about 100 s), the cells retract their protrusions against the largest external forces available (5 nN) to internalize the bead. This value is in the order of magnitude of the cell contraction estimated by Evans *et al.* (Evans, Leung and Zhelev, 1993). Later study by Vonna *et al.* shows that very thin filopodia can generate retraction forces over  $>0.5$  nN over large distances ( $>10 \mu\text{m}$ ) (Vonna *et al.*, 2007).

Spherical probes used in magnetic tweezers can also be used to study the predatory behaviour of macrophages, by guiding translational and rotational movement of micromagnets preys (Schuerle *et al.*, 2017). When confronted with passive targets, mimicking free floating preys, macrophages identify these targets, co-align them with their long axis and first push the probes with forces in the pN range. Then, they slowly pull the beads inward along a C-shape trajectory (Schuerle *et al.*, 2017). Interestingly, for resistive prey, the realignment is disrupted and macrophages are not always able to perform phagocytosis. Macrophages appear to keep producing larger pushing forces, likely to ensure sufficient physical contact by engaging more stable receptor–ligand bonding (Schuerle *et al.*, 2017).

Alternatively, magnetic tweezers can be used to measure mechanical properties of phagocytosing cell. Using functionalized oscillating magnetic particles as phagocytic targets on macrophages, Irscher *et al.* measured stiffness of the phagocytic cup over time by measuring its resistance or stiffness to motion of the beads (Irscher *et al.*, 2013) (**Figure 22**). Evolution of the stiffness revealed an increase (double values in about 30 to 50 s) up to a pronounced peak immediately preceding the internalization, followed by a slow decrease. This observation demonstrated the existence of a mechanical bottleneck that must be overcome for phagocytosis to occur, already suggested by van Zon *et al.* (van Zon *et al.*, 2009). If membrane extrusion comes to its limit

and reach its maximum capacity when the phagocytic cup extends to the equator of a particle, the phagocytic cup cannot proceed past it and phagocytosis stalls. Comparison of the model and experimental data suggested the membrane progresses around the particle with a speed of 20 nm/s (Irmscher *et al.*, 2013).

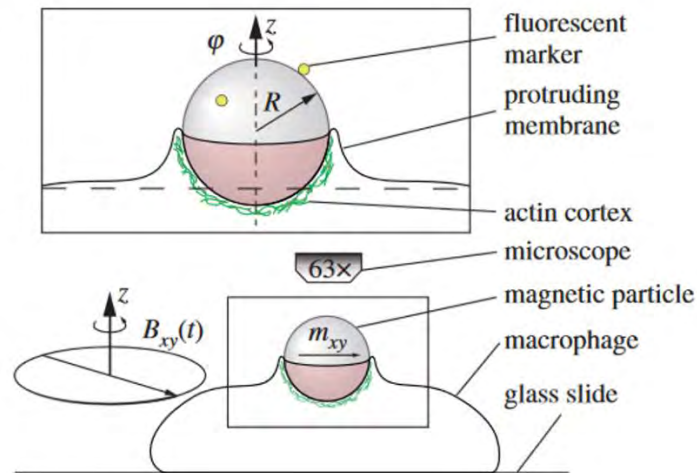


**Figure 22** Experimental setup to evaluate stiffness of phagocytic cup using magnetic bead  
From (Irmscher *et al.*, 2013)

### III. Atomic Force Microscopy (AFM)

Atomic force microscopy (AFM) is a high-resolution non-optical imaging technique first demonstrated in 1986 (Binnig, Quate and Gerber, 1986). Since these first demonstrations it has been developed into a powerful measurement tool for surface analysis. Notably, AFM allows accurate and non-destructive measurements of the topographical, and mechanical (among others parameters) properties of a sample surface. The basic principle of AFM system involves scanning an AFM probe over a sample surface, the probe being composed of a flexible cantilever with a prominent tip near its free end. As the AFM tip moves over features of different height, the interaction of the tip with the surface induces deflection of the AFM cantilever. This deflection is tracked by a laser beam reflected from the back side of the AFM cantilever and directed into a position-sensitive photodetector. A feedback loop controls the vertical extension of the scanner in order to maintain a near-constant AFM cantilever deflection or a constant interaction force. (**Figure 23A**)

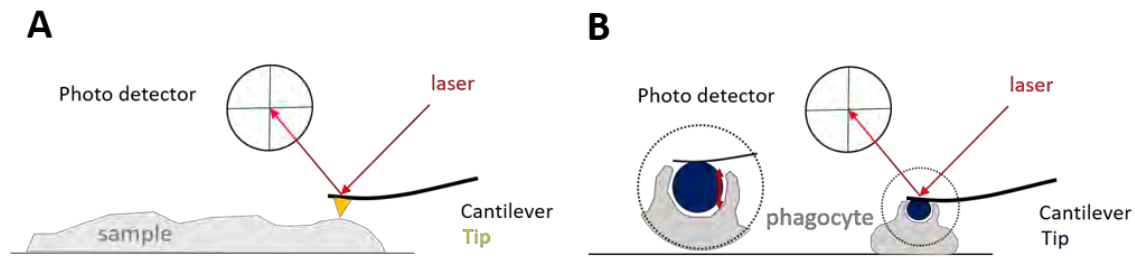


**Figure 23.** Principle of AFM.

This characteristic can be used to measure forces exerted during phagocytosis, by confronting macrophages with AFM probes as targets (**Figure 23B**). Indeed, thanks to the deflection of the cantilever, forces generated by the cell to engulf the probe can be measured. AFM can accurately measure net forces in a range from 10 pN to 10 nN, depending on the selected the spring constant of the cantilever. It thus appears as a relevant technique for measuring forces in phagocytosis (Vorselen, Labitigan and Theriot, 2020). Recently this technique has been combined with light sheet microscopy to perform simultaneous AFM fast fluorescent imaging (Nelsen et al., 2019). The study revealed that macrophages engaging in a process of phagocytosis first push the probe with 50pN forces, and then pull on it with forces reaching up to 1nN (Nelsen et al., 2019).

Moreover, the probe can indent the cell to determine its mechanical properties. In that case AFM serves to estimate membrane rigidity during phagocytosis (Flannagan et al., 2010). Nevertheless, the measure corresponds more to the response of the cytoskeleton and cytosol than that of the membrane (Krieg et al., 2018).

If these studies provided numerous insights in cellular mechanical properties, cellular tension changes and pulling forces exerted by cells during phagocytosis, these techniques still fail to analyse the distribution of forces directly exerted by the cell on its environment. Other methods, including traction force microscopy (TFM) and microparticle force microscopy (MP-TFM), allow such measurements and are described next.

## IV. Traction Force Microscopy (TFM)

### 1. Classical TFM coupled with frustrated phagocytosis

#### 1.1 Experimental approach

The first experimental set up called “Traction force microscopy” in reference to “the traction an automobile’s wheel exerts on the highway surface” was invented by Harris et al. The authors seeded fibroblasts on a thin silicon rubber and showed that cells generate elastic wrinkles when crawling (Harris, Wild and Stopak, 1980). Nevertheless, the forces could not be accurately quantified, because of the nonlinear and complex nature of wrinkling phenomenon (Mustapha, Sengupta and Puech, 2022).

The most commonly used TFM approach was officially introduced in 1999 by Dembo and Wang. To quantify forces exerted by adherent cells on their substrate, they propose to use linearly elastic hydrogels containing fluorescent beads reporting its deformation (Dembo and Wang, 1999) (**Figure 24.A**).

#### 1.2 Substrate properties

The most popular substrate is polyacrylamide, sometimes referred as PAG for polyacrylamide gels, PAA or PAM. In this manuscript, the term PAA is used for polyacrylamide. PAA is chemically stable and non-adherent hydrogel, meaning no protein or cell surface receptor can directly bind to it, and that only covalently grafted molecules can act as ligand for the cells (Mustapha, Sengupta and Puech, 2022), allowing a precise control of the substrate surface ligands. PAA exhibits a wide range of stiffness that can be adapted by simply modulating the ratio of acrylamide - the polymer - and N,N'-methylenebisacrylamide - the crosslinker. The range of Young’s modulus, from 1 to 100 kPa, reproduces typical stiffnesses of biological tissues. One important feature of TFM is the thickness of the substrate, as cells may sense the stiffness of a rigid support located underneath the hydrogel layer (e.g. glass or silicon), even without being in direct contact with it. If the substrate is too thin, the cells respond to the rigidity of the underlying glass; if it is too thick, advanced microscopy might be impeded.

#### 1.3 TFM in frustrated phagocytosis context

When used in the context of phagocytosis, this approach consists in functionalizing a large flat 2D surface of hydrogel (typically polyacrylamide) with phagocytosis ligands to induce frustrated phagocytosis. In their internalization attempt, cells apply forces on the surface

that induce displacement of the fluorescent nanobeads in the gel. These displacements can be related to forces via the classical laws of physics, notably Hooke's law for the deformation of a linear elastic spring:  $F = k \cdot \Delta x$  (with  $F$ : force,  $k$ : spring constant,  $\Delta x$  extension of the spring). To access  $F$ ,  $k$  can be obtained through calibration experiments and  $\Delta x$  has to be measured (Mustapha, Sengupta and Puech, 2022). To measure the latest, two sequential images of the substrate must be acquired: one of the beads displaced, in the stressed state when cellular forces are applied, and one of the non-perturbed beads, in the relaxed state (without cellular forces). The relaxed state image can be obtained either before cell engagement or after. In that case, cells must be detached from the substrate through the use of EDTA, trypsin or accutase (Mustapha, Sengupta and Puech, 2022). Displacements can be tracked either by single particle tracking (SPT) or particle image velocimetry (PIV) and then converted to forces, although this last step can be challenging and source of bias (Mustapha, Sengupta and Puech, 2022). Another limitation to this technique is the frustrated phagocytosis state does not recapitulate entirely the process of phagocytic cup formation, although it keeps the cell in a phagocytic behaviour for much longer than a classical phagocytosis assay with free particles, easing the observation of the process. This technique presents the advantage to confine phagocytosis to a single plane and thus allows high-resolution microscopy. Cell behaviour can be then imaged with high spatial and temporal precision.

Consistent with frustrated phagocytosis experiments performed on glass (Masters *et al.*, 2013), macrophages seeded on PAA attempt to phagocytose PAA substrate in a sequential way: they first spread and then F-actin bundles into fibres at the periphery of the cells (Kovari *et al.*, 2016). This last phase is shown to be a period of contraction where cells exert significant strain on the substrate, whereas only little strain is described during the spreading phase. Therefore, authors suggest that active constriction is applied by phagocytes only during late stages of phagocytosis. This contraction phase only appears when the cell surface area has increased by 225%, and decreasing membrane tension with hypertonic buffers increases spreading and delay contraction phase, which is also consistent with the cortical tension hypothesis of Masters *et al.* (Masters *et al.*, 2013; Kovari *et al.*, 2016). Interestingly, opsonin density at the substrate surface appears to affect the likelihood of spreading, but not its speed (Kovari *et al.*, 2016).

Macrophages plated on opsonized polyacrylamide sheets of increasing stiffness showed a preference for the stiffer ones (0.2% bis): approximately sixfold more cells engage in frustrated phagocytosis compared to those plated on the softer sheets (0.05% bis) at similar ligand

concentration (Beningo and Wang, 2002). In contrast with this observation, Rougerie and Cox describe the proportion of cells entering frustrated phagocytosis is not affected by the substrate stiffness, despite similar experimental setup (macrophages seeded on polyacrylamide sheet of same stiffness range and coated with IgG) (Rougerie and Cox, 2020). However, magnitude of mechanical stress generated downstream of Fc $\gamma$ R engagement is found to be linearly proportional to the substrate stiffness: approximately 4.5 Pa and 19.5 Pa stress for 1.25 kPa and 15.6 kPa PAA respectively. Because no force is recorded during the spreading phase, authors propose that macrophages adapt their mechanical response only during contraction phase by modulating the magnitude of mechanical stress exerted (Rougerie and Cox, 2020).

Other molecular actors of phagocytosis have been identified through TFM: myosin1e/f. In Fc $\gamma$  mediated phagocytosis, these actin dependent molecular motors are localized between F-actin and membrane at the Fc receptors adhesion sites and appears necessary for efficient phagocytosis (Barger *et al.*, 2018). This is due to the linking role of these myosins between actin and membrane, but not to a contractile activity. Indeed, depletion of these myosins did not affect traction forces applied on TFM substrate.

## 2. Micropillar array TFM

A few years after TFM introduction, an alternative method was developed by Tan *et al.* to simplify the force calculations required for continuous hydrogels (Tan *et al.*, 2003). Although this system has not been used in the context of phagocytosis to our knowledge, it is mentioned here to ease the understanding of the method developed during my thesis.

The setup involves a regular arrangement of cylindrical pillars created through soft lithography, which allows for the separation of cellular forces into individual strain gauges. As the cells attach to the protein-coated tops of the pillars, they apply forces and pillars bend away from their initial position. By utilizing the principles of classical beam bending theory, it becomes possible to estimate this deformation and calculate the local traction forces exerted by the cells on each individual structure (Tan *et al.*, 2003; Hur *et al.*, 2020). (**Figure 24.B**)

The use of these discrete adhesive surfaces offers significant benefits such as the availability of a load-free position, that is a position without cellular constraints, and a direct relationship between the deflection of a given pillar and the force applied to that specific pillar. However, this approach also imposes certain limitations on the size, shape, and location of cellular adhesions, which can restrict how and where cells are able to transmit forces. (Schoen *et al.*,

2010; Schwarz and Soiné, 2015). Moreover, if the cells adhesion extends beyond the top of the pillar down onto the substrate, it becomes impossible to accurately resolve exerted forces.

Despite the elegant calculations that can be performed using this system, it is still uncertain how these calculations correlate with the forces that are actually transmitted in the natural cellular environment.

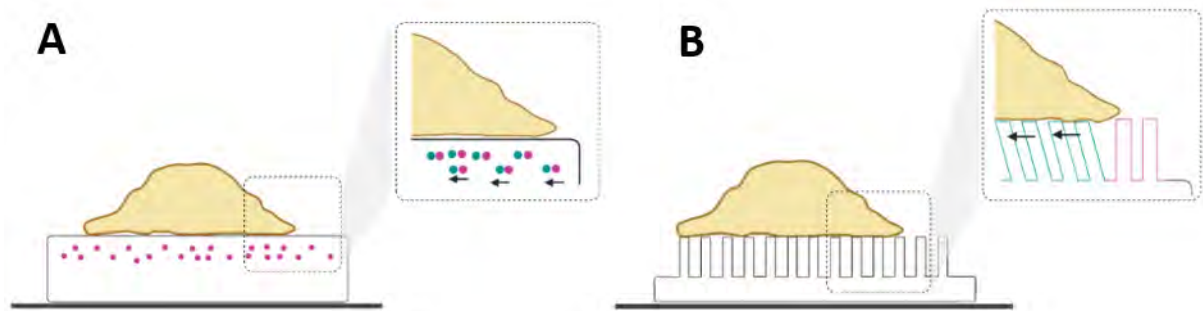


**Figure 24.** Traction Force Microscopy  
Adapted from (Mustapha, Sengupta and Puech, 2022)

TFM is a commonly used method for evaluation of force distribution. However, the use of large 2D flat surface as phagocytic target does not recapitulate the 3D architecture of the microenvironment of cells. Moreover, it does not reproduce the shape of natural biological target and does not allow for the formation of the full phagocytic cup, which may affect cytoskeletal dynamic and force generation. In addition, TFM only measures tangential forces without accounting for forces normal to the surface of the target. (Kovari et al., 2016; Barger et al., 2018; Jaumouillé, Cartagena-Rivera and Waterman, 2019). New experimental methods are critical to explore net forces and their distribution exerted during phagocytosis

## V. MP-TFM

Recently, TFM methods based on flat traction have been extended into microspheres that are used as phagocytic target and force sensors (Mohagheghian *et al.*, 2018; Träber *et al.*, 2019). This technique has been further developed by Vorselen *et al.* to synthesize on a batch-scale deformable and tuneable polyacrylamide beads. Using confocal microscopy, the surface of the particles can be resolved with a <50 nm height accuracy and then reconstituted in 3D (**Figure 25A,B**). From this 3D shape mapping the deformations, a computational method is applied to evaluate the relative forces exerted in each point of the particle surface (**Figure 25C**). The use of this non-invasive technique reveals that at the beginning of phagocytosis,

macrophages generate protrusive force onto the particle at the initial point of contact, that are compensated by pulling forces from the surrounding adhesion complexes around it. These forces spatiotemporally evolve into a contractile punctate ring moving along the particle, progressively squeezing it until closure of the phagocytic cup. Moreover, shear forces are applied at the equator of the particle, resulting in torsion of the bead (Vorselen *et al.*, 2020). The punctate feature of this contractile belt and Arp2/3 dependant constriction suggest the presence of podosome-like structures at the phagocytic cup, although another explanation is proposed. Vorselen *et al.* suggest that actin protrusions containing myosin 1e and 1f acts like “teeth”, connected together in a ring. Finally, this technique supports the myosin-II contractile role in phagocytic cup closure, as it contributes to late-stage force generation. Myosin-II are thus described as a “jaw”. Together, these structures would mechanically initiate the process of particle degradation. (Vorselen *et al.*, 2021)

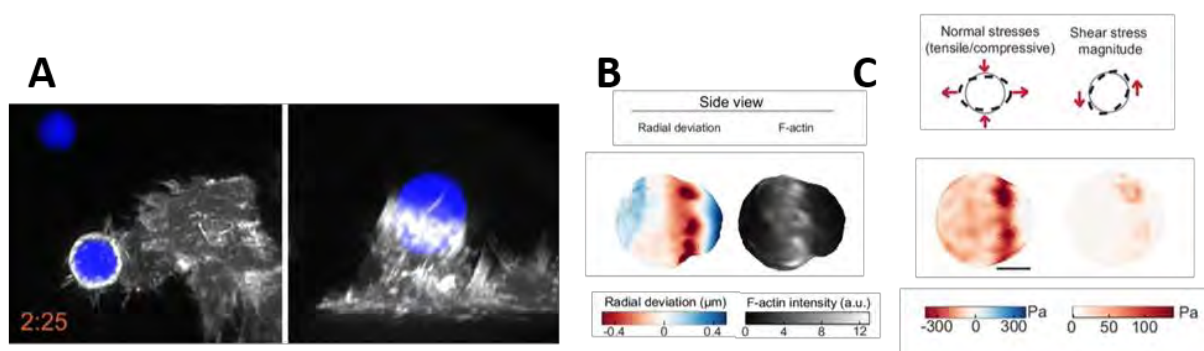


**Figure 25.** MicroParticle Traction Force Microscopy

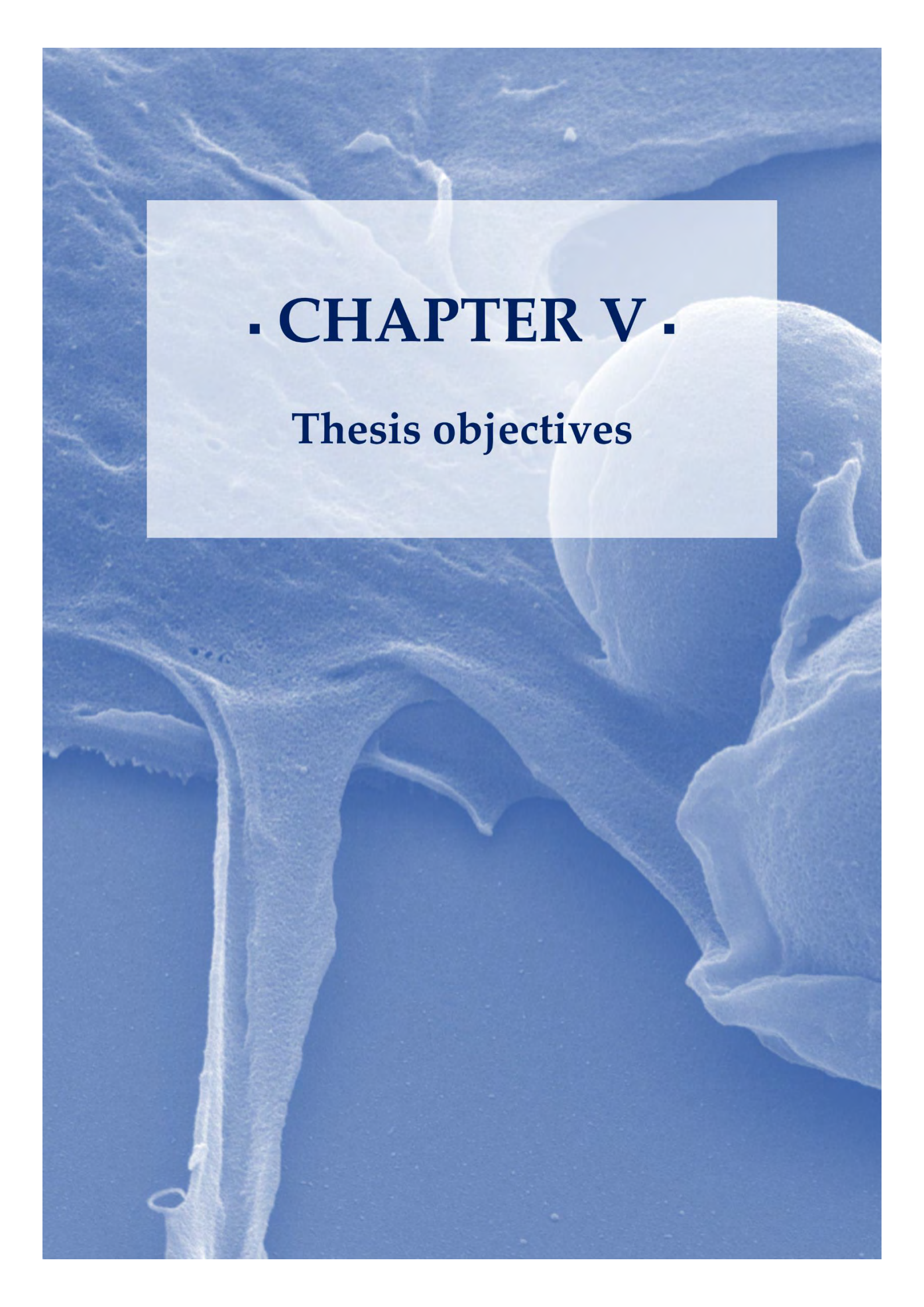
To conclude, techniques used to decipher cellular mechanical properties or distribution and values of forces are summarized in **Table 2**.

<b>Technique</b>	<b>Measured quantity</b>	<b>Cell state</b>	<b>Advantage</b>	<b>Limitation</b>
<b>MPA</b>	<ul style="list-style-type: none"> <li>Cellular tension = membrane tension + cortical tension</li> </ul>	S	<ul style="list-style-type: none"> <li>Physiologically relevant target</li> </ul>	<ul style="list-style-type: none"> <li>Invasive</li> <li>Single cell analysis</li> </ul>
<b>Tether pulling</b>	<ul style="list-style-type: none"> <li>Membrane tension + membrane-cytoskeleton adhesion</li> </ul>	A	<ul style="list-style-type: none"> <li>External control over target dynamics</li> </ul>	<ul style="list-style-type: none"> <li>Invasive</li> <li>Single cell analysis</li> <li>Technical expertise is necessary</li> <li>Limited physiological relevance</li> <li>Poor control over target physical properties</li> </ul>
<b>AFM</b>	<ul style="list-style-type: none"> <li>Exerted net force (normal)</li> <li>Cellular mechanical properties</li> </ul>	A	<ul style="list-style-type: none"> <li>External control over target dynamics</li> </ul>	<ul style="list-style-type: none"> <li>Single cell analysis</li> <li>Technical expertise is necessary</li> <li>Limited physiological relevance</li> <li>Poor control over target physical properties</li> </ul>
<b>TFM</b>	<ul style="list-style-type: none"> <li>Distribution of exerted force (shear)</li> </ul>	S	<ul style="list-style-type: none"> <li>Some control over target physical properties</li> </ul>	<ul style="list-style-type: none"> <li>Measures only tangential forces</li> <li>Severely limited physiological relevance (no phagocytic cup)</li> </ul>
<b>MP-TFM</b>	<ul style="list-style-type: none"> <li>Exerted net forces (shear and normal)</li> <li>Distribution of exerted force (shear and normal)</li> </ul>	A	<ul style="list-style-type: none"> <li>3D forces</li> <li>Non-invasive</li> <li>Relative control of target physical properties</li> </ul>	<ul style="list-style-type: none"> <li>Technical expertise is necessary</li> <li>Statistical analysis of forces requires fixation of samples</li> <li>Inert target</li> </ul>

**Table 2.** Available experimental techniques to decipher mechanical parameters during phagocytosis. S: suspended; A: adherent. Adapted from (Vorselen, Labitigan and Theriot, 2020) and (Kalashnikov and Moraes, 2022)

While these methods have greatly contributed to a better understanding of the mechanics of phagocytosis, the extraction of forces is sometimes limited by experimental constraints. Ideally, to study the dynamics of these forces, a system should allow the observation of live phagocytosis in a non-invasive way, while controlling the physical parameters of the target, and keeping a temporal control of the phenomenon on a large number of phagocytic events. To answer these requirements, we thus propose an experimental and analysis approach that is described in the results part of this dissertation

LITERATURE REVIEW · CHAPTER IV ·  
Techniques to study mechanical properties and forces during phagocytosis



**· CHAPTER V ·**

**Thesis objectives**

Phagocytosis is a well-conserved phenomenon in evolution and is crucial to maintain homeostasis and defence against pathogens. Therefore, a better understanding of its mechanics is not only interesting for fundamental research in cell biology, but also for potential therapeutic applications in the future.

Although it had been first described more than a century ago, many unknowns remain about the process of phagosome formation and maturation, and its relationship with the actin cytoskeleton. As professional phagocytes, macrophages are a model of choice to study this process. Its specific mechanosensitive structure, the podosome, is involved in many cell functions, but its role in phagocytosis remains unclear. Therefore, the two first objectives of this work were:

- i. To study the presence of podosome-like structures at the closed phagosome membrane;
- ii. To propose a role for these structures.

Moreover, podosomes have been demonstrated to exert protrusive forces on their substrate and may apply these forces on the phagosome. Interestingly, over the last years, studies have started to focus on the mechanical aspect of phagocytosis, and the development of techniques allows to better decipher forces and intracellular pathways at stake. These techniques have revealed the existence of contraction and traction forces. However, these techniques do not allow the study of all the forces a phagocytic target is submitted to simultaneously, at least not without fixing the samples. Fixation may modify the actual local actin organisation, dynamics and forces applied to the phagosomal membrane. Therefore, we decided to develop new tools to measure the net forces a cell can exert, in live conditions upon phagocytosis. In particular, studies must be conducted to determine how cells apply forces during the early stage of phagocytosis, which might be critical for phagocytic cup closure and phagosome formation.

The last objective of my thesis was therefore

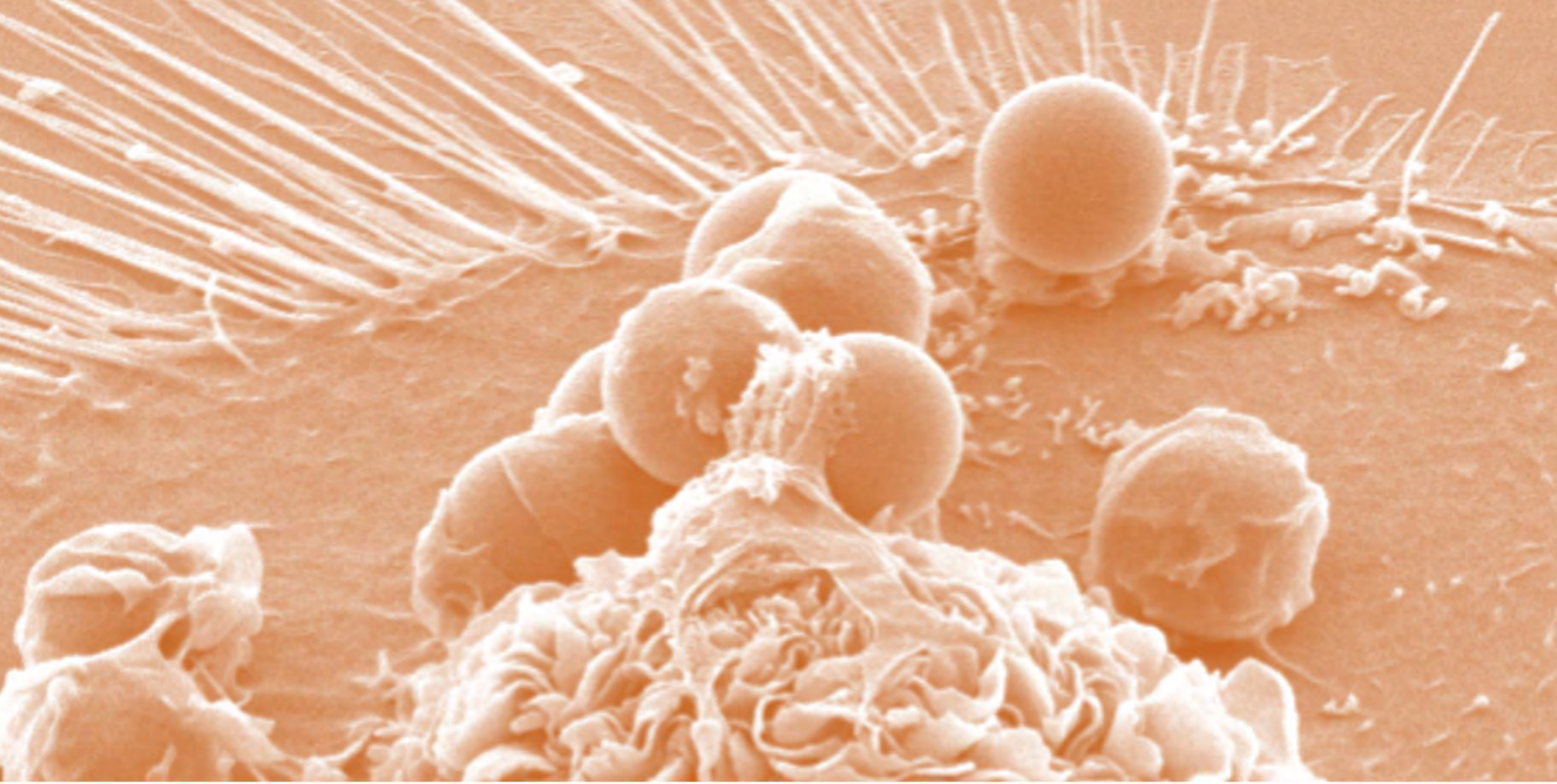
- iii. To develop a tool allowing the measurement of forces on a large number of living cells during the early stage of phagocytosis.

The next part of this dissertation, consisting in two chapters, describes the results of my investigations related to these objectives. The first chapter concerns the study of podosome-like structures at the level of the phagocytic cup and the closed phagosome, their characterization as well as their proposed role. It is written in the form of an article, published

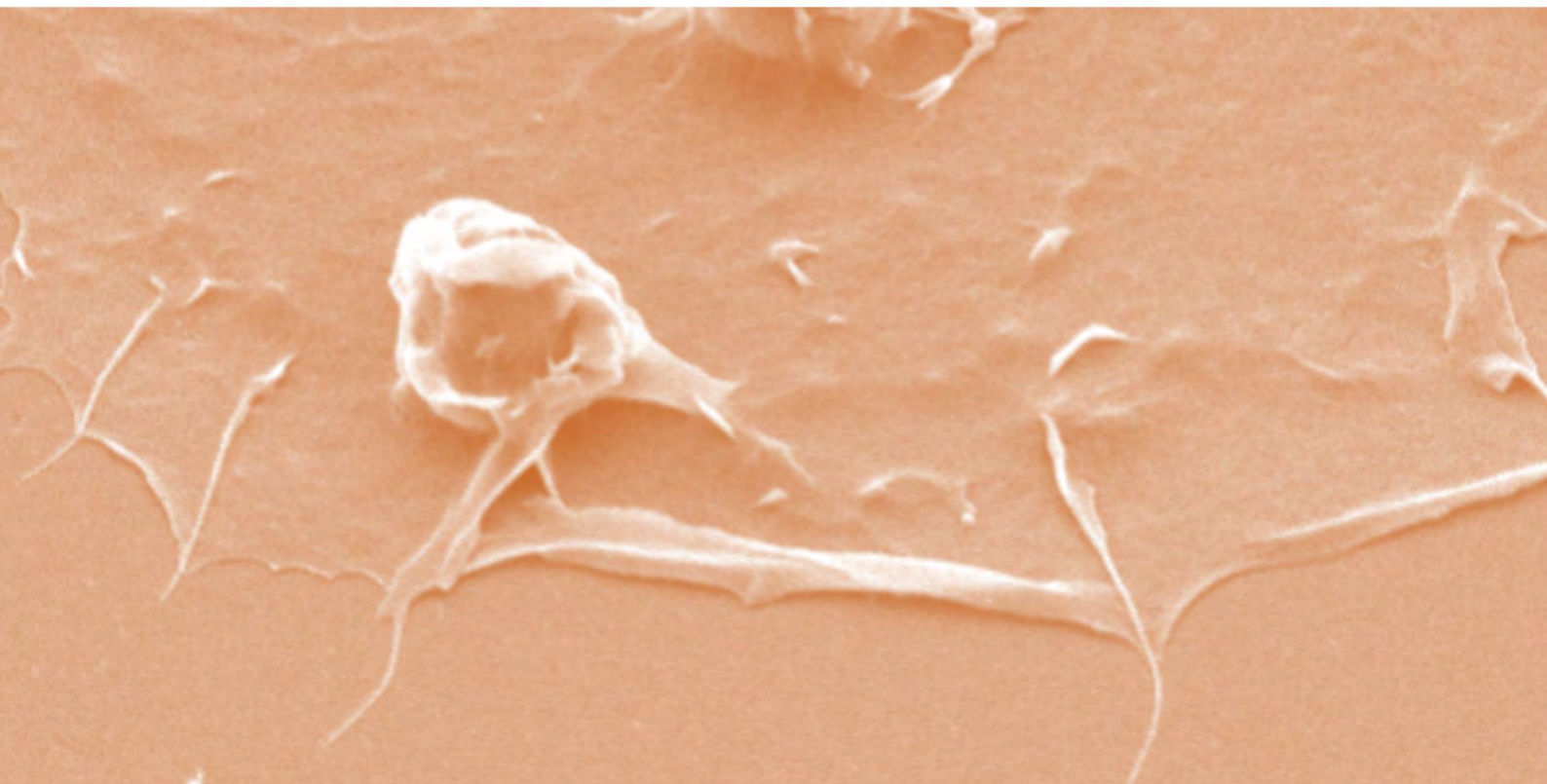
by European Journal of Cell Biology (EJCB) in 2021. This article is first briefly introduced and then perspectives are launched on this work.

The second chapter explains the method developed to analyse in a simple and precise way the forces applied during phagocytosis. It describes the microfabrication process of hydrogel pillars used as phagocytic targets, the method for analysing their deformation, as well as the model used to evaluate the forces applied by macrophages to phagocyte them. I also present the results of the modulation of these pillars stiffness, and the effect of several cytoskeleton inhibitors on the forces values. Finally, I discuss dynamics of these forces and how the number of phagocytic targets per cell can affect them. Also written in the form of an article, this work has not yet been submitted for publication.

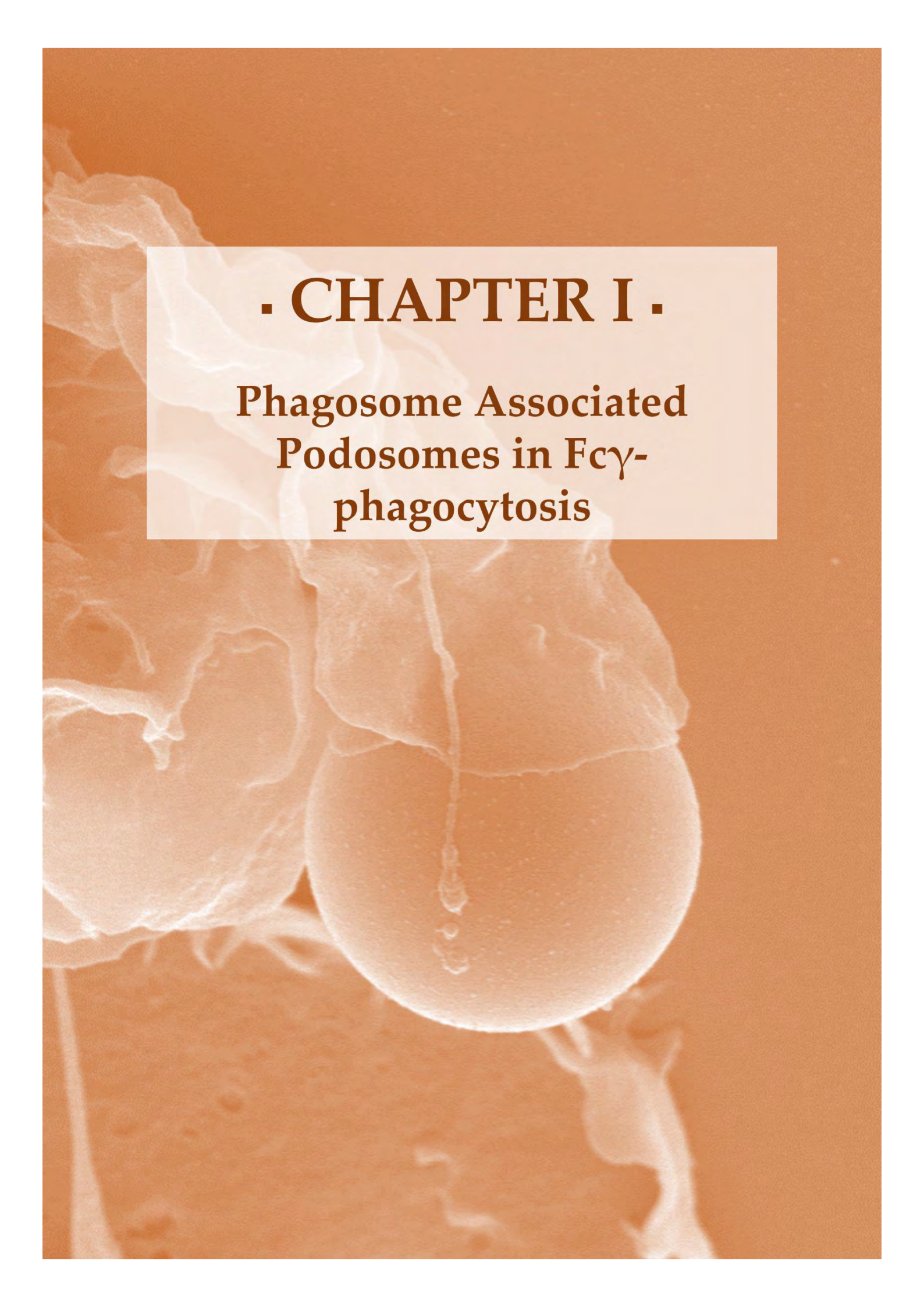




# RESULTS





The background of the slide is a scanning electron micrograph (SEM) showing a cell with a large, spherical phagosome and several smaller, rounded podosomes. The cell surface is highly textured and irregular. The phagosome is a large, smooth sphere, and the podosomes are smaller, rounded structures. The overall color is a warm, orange-brown hue.

**· CHAPTER I ·**

**Phagosome Associated  
Podosomes in Fc $\gamma$ -  
phagocytosis**

## I. Objectives and summary of the article

Phagocytic cups and podosomes share several common components, and numerous studies have reported the presence of podosome-like structures in early phagosomes, as discussed in Chapter III (Allen and Aderem, 1996; Labrousse, 2011; Ostrowski *et al.*, 2019). Interestingly, we also noted the disappearance of podosomes in macrophages during phagocytosis. This observation led us to explore a possible correlation between these two phenomena, focusing specifically on phagocytosis mediated by Fc $\gamma$  receptors. For this investigation, we utilized polystyrene beads as phagocytic targets, either coated with IgG to initiate Fc $\gamma$  receptor-mediated phagocytosis or uncoated as a control. Additionally, we employed Zymosan, a polysaccharide component of the yeast *Saccharomyces cerevisiae* cell wall, which is commonly used in phagocytic assays due to its physiological relevance compared to polystyrene beads. Zymosan was used either directly or after opsonization with serum to induce Fc $\gamma$  receptor-mediated phagocytosis.

I took up this project at the beginning of my thesis, following a post-doctoral student with whom I co-authored the paper presented below, which appeared in a special issue of the European Journal of Cell Biology entitled "Mechano-chemical signals in the invasion". Our results confirm the presence of podosome-like structures, on the surface of both forming and closed phagosomes during phagocytosis of IgG-coated polystyrene beads, but not naked beads. The presence of these so-called Phagosome associated podosomes (PAPs) correlates with phagosome maturation and leads us to hypothesize about the role of PAPs.

## II. Article: Phagocytosis is coupled to the formation of phagosome-associated podosomes and a transient disruption of podosomes in human macrophages



# Phagocytosis is coupled to the formation of phagosome-associated podosomes and a transient disruption of podosomes in human macrophages

Margot Tertrais<sup>a,1</sup>, Claire Bigot<sup>a,1</sup>, Emmanuel Martin<sup>b</sup>, Renaud Poincloux<sup>a</sup>,  
Arnaud Labrousse<sup>a</sup>, Isabelle Maridonneau-Parini<sup>a,\*</sup>

<sup>a</sup> Institut de Pharmacologie et Biologie Structurale, IPBS, Université de Toulouse, CNRS, UPS, Toulouse, France

<sup>b</sup> MCD, Centre de Biologie Intégrative (CBI), Université de Toulouse, CNRS, UPS, Toulouse, France

## ARTICLE INFO

**Keywords:**  
Podosome  
Phagocytosis  
Macrophage  
Phagolysosome

## ABSTRACT

Phagocytosis consists in ingestion and digestion of large particles, a process strictly dependent on actin re-organization. Using synchronized phagocytosis of IgG-coated latex beads (IgG-LB), zymosan or serum opsonized-zymosan, we report the formation of actin structures on both phagocytic cups and closed phagosomes in human macrophages. Their lifespan, size, protein composition and organization are similar to podosomes. Thus, we called these actin structures phagosome-associated podosomes (PAPs). Concomitantly to the formation of PAPs, a transient disruption of podosomes occurred at the ventral face of macrophages. Similarly to podosomes, which are targeted by vesicles containing proteases, the presence of PAPs correlated with the maturation of phagosomes into phagolysosomes. The ingestion of LB without IgG did not trigger PAPs formation, did not lead to podosome disruption and maturation to phagolysosomes, suggesting that these events are linked together. Although similar to podosomes, we found that PAPs differed by being resistant to the Arp2/3 inhibitor CK666. Thus, we describe a podosome subtype which forms on phagosomes where it probably serves several tasks of this multifunctional structure.

## 1. Introduction

Macrophages are immune cells that are involved in both innate and adaptive immune responses (Jakubzick et al., 2017). They migrate to reach infectious sites and ingest microorganisms, debris and foreign bodies, a process called phagocytosis (Jaumouille and Grinstein, 2016; Uribe-Querol and Rosales, 2020). Both migration and phagocytosis rely on a strong and coordinated re-organization of the actin cytoskeleton. Phagocytosis is the specialized capacity of a subpopulation of immune cells called phagocytes to ingest particles larger than 0.5  $\mu\text{m}$ . Despite the discovery of phagocytosis at the end of the 19th century, many aspects of this process remain unclear. During phagocytosis, actin polymerization is responsible for engulfment of particles and phagosome maturation (Freeman and Grinstein, 2014; Gray and Botelho, 2017). However, the dynamics of actin polymerization at phagosomes is regulated differently when Fc $\gamma$ R for IgG or CR3 receptors are engaged (Allen and Aderem, 1996; Caron and Hall, 1998; Jaumouille and Waterman, 2020; Rotty

et al., 2017).

During the first steps of phagocytosis, actin filaments organize as a dense meshwork underlying the plasma membrane in a structure called the phagocytic cup. Following the formation of this cup, actin re-organizes progressively all around the particle until closure of the phagosome membrane. Then, the phagosome traffics along microtubules and sequentially fuses with endosomes and lysosomes to form phagolysosomes (Uribe-Querol and Rosales, 2020). Along this maturation process, the phagosome progressively loses its F-actin coat. The abundance of actin around the phagosome determines its capacity to fuse with lysosomes. The presence of a dense actin meshwork inhibits the fusion of phagosomes with lysosomes (Jahraus et al., 2001; Liebl and Griffiths, 2009), whereas a less abundant organization of actin filaments at the phagosome membrane can serve as tracks for lysosomes to move forward phagosomes (Anes et al., 2003; Jahraus et al., 2001; Kjekten et al., 2004). Moreover, flashes of actin have been described on a small proportion of mature phagosomes in RAW 264.7 macrophages that

**Abbreviations:** PAP, phagosome-associated podosome; LB, latex beads; IgG-LB, IgG-coated latex beads; Z, zymosan; OZ, serum-opsonized zymosan.

\* Corresponding author at: Institut de Pharmacologie et Biologie Structurale, CNRS UMR5089, 205 route de Narbonne, 31400 Toulouse, France.

E-mail address: [maridono@ipbs.fr](mailto:maridono@ipbs.fr) (I. Maridonneau-Parini).

<sup>1</sup> Co-first authors.

<https://doi.org/10.1016/j.ejcb.2021.151161>

Received 16 October 2020; Received in revised form 8 March 2021; Accepted 29 March 2021

Available online 31 March 2021

0171-9335/© 2021 The Author(s).

Published by Elsevier GmbH. This is an open access article under the CC BY-NC-ND license

(<http://creativecommons.org/licenses/by-nc-nd/4.0/>).

ingest IgG-coated particles, as well as in non-phagocytic cells infected by *Listeria monocytogenes* (Liebl and Griffiths, 2009; Yam and Theriot, 2004). More recently, flashes have been shown to form on the phagosome surface when phagocytosis is mediated by complement receptors but not by Fc receptors and they are more abundant when particle stiffness decreases (Poirier et al., 2020). Dynamic analysis of these flashes indicated that actin filaments follow several assembly/disassembly cycles, a phenomenon that lasts the first hour of the phagocytic process and that is Arp2/3-dependent. Despite some contradictory results, the proposed function of actin flashes is to contract phagosomes and improve the degradation of the phagosome content (Liebl and Griffiths, 2009; Poirier et al., 2020).

In addition to these actin structures present on closed phagosomes, podosome-like structures have also been observed at phagocytic cups (Allen and Aderem, 1996; Labrousse et al., 2011; Ostrowski et al., 2019). Podosomes, constitutively form in macrophages, dendritic cells and osteoclasts, and participate in cell adhesion, proteolysis of the extracellular matrix and mechanosensing of the cellular environment. They comprise a dense core of F-actin, surrounded at its basis by a ring of adhesion complexes linked to the actin cytoskeleton (van den Dries et al., 2019). In dense and non-penetrable environments, podosomes are involved in opening paths that allow the migration of macrophages (Maridonneau-Parini, 2014). The podosome-like structures described at phagocytic cups are similar to podosomes in term of composition and architecture but can be distinguished by their lifespan and distinct regulators of their formation (Allen and Aderem, 1996; Labrousse et al., 2011; Ostrowski et al., 2019). The podosome-like structures found on early phagosomes were proposed to mediate particle internalization (Allen and Aderem, 1996) and to perform a mechanical sealing of the phagosome membrane with the ingested particle (Ostrowski et al., 2019). This mechanical function is reminiscent of the force that is required to zip the phagosome membrane around particles and to detect the rigidity of the extracellular environment by podosomes (Jaumouille and Grinstein, 2016; Labernadie et al., 2014; Mylvaganam et al., 2018). Podosomes are targeted by late endosomes/lysosomes that deliver proteases, including MT1-MMP, in their close vicinity (Cougoule et al., 2005, 2010; Jeannot and Besson, 2020; Marchesin et al., 2015; Monteiro et al., 2013; Wiesner et al., 2010). Phagosomes also fuse with endosomes and lysosomes, a process known as phagosome maturation, the resulting phagolysosome offers a specialized acidic and hydrolytic milieu dedicated to degradation of the engulfed particle. It is therefore tempting to hypothesize that podosome-like structures are not only involved in the early stages of phagocytosis but also play a role all along phagosome maturation. However, it is still unknown whether podosome-like structures are present after phagosome closure.

We therefore examined whether podosome-like structures i) are present on closed phagosomes, ii) form around any particles regardless of the phagocytic pathway, iii) correlate with phagolysosome formation, and iv) impact the formation of podosomes at the ventral membrane of macrophages.

## 2. Materials and methods

### 2.1. Products and antibodies

Zymosan A (Z4250) was provided by Sigma-Aldrich. Latex microbeads (Fluoresbrite Yellow Green Microspheres, 17155-2) was from Polyscience. CK-666 (ab141231) was purchased from Abcam. Phalloidin-546 and -647, secondary antibodies donkey anti-mouse (Alexa Fluor 647) and goat anti-mouse (Alexa Fluor 647) were purchased from Fischer Scientific and all used at a 1:200 dilution. Mouse monoclonal antibodies anti-Cortactin (1:100, p80/85, clone 4F11), and rabbit anti-ovalbumin (1:10, ab1225) were from Millipore. Anti-vinculin (1:100, V9131, clone HVIN-1) antibodies and goat anti-rabbit TRITC were purchased from Sigma. Paxillin antibodies (1:100, P13520) was from BD Transduction Laboratories and anti-LAMP1

(1:100, clone H4A3) from Santa Cruz. Rab 5 antibodies (1:100, clone 2E8B11) were from ThermoFischer. CD18 antibodies (1:100, clone MHM23) from Dako. Human MCSF (130–096-489) was purchased from Miltenyi (France). Fluorescein isothiocyanate (F1906) was provided by Molecular Probes.

### 2.2. Cells

Human monocytes were isolated from the blood of healthy donors (buffy coats obtained from Etablissement Français du Sang) and differentiated into human monocyte-derived macrophages (hMDMs) as previously described (Van Goethem et al., 2010). After cell sorting with CD14-magnetic beads, monocytes were differentiated in RPMI culture medium with 10% FCS (Fisher Scientific, France) containing 20 ng/mL of human M-CSF for 7–8 days before their use. The culture medium was usually renewed on the third or fourth day. In experiments with CK666, macrophages were pre-incubated for 15 min with either the drug solubilized in DMSO or vehicle.

### 2.3. Phagocytosis assays

Zymosan A (Z, 10 mg) was placed overnight at 4 °C in rotation with FITC (0.5 mg/mL) in 1 mL of bicarbonate reaction buffer (0.25 M pH 9) then washed with PBS (Fisher Scientific). For opsonisation, FITC-labelled zymosan was incubated at 37 °C under agitation with human serum (H4522, Sigma-Aldrich) at 37 °C for 30 min then washed with PBS.

Latex beads (LB, Fluoresbrite yellow green, Polyscience, diameter : 3 µm) were coated with ovalbumin (1 mg/mL in PBS) for 1 h at room temperature and washed with PBS containing BSA (10 mg/mL, 115004696, Fisher Scientific). To obtain IgG-opsonized latex beads, ovalbumin-coated beads were then incubated with anti-ovalbumin antibodies for a hour (1:10, room temperature) and washed 3 times.

Particles were added to macrophages at several multiplicity of infection (MOI) to obtain equivalent rates of phagocytosis. Z and LB were used at MOI 30:1; IgG-LB and OZ at MOI 10:1 with macrophages plated on coverslips. Phagocytosis was synchronized with a centrifugation at 170 g for 5 min. Unbound beads were washed off with culture medium and cells were then incubated at 37 °C for the indicated time points. In some experiments, to chelate divalent cations, EDTA (5 mM) was added to the medium concomitantly to IgG-LB and the phagocytosis assay was carried-out for 5 min.

### 2.4. Immunofluorescence

After cell fixation for 30 min at RT with 3.7 % paraformaldehyde in PBS containing 15 mM sucrose, unreacted aldehyde functions were quenched with 50 mM NH<sub>4</sub>Cl in PBS for 5 min at RT as previously described (Labernadie et al., 2010). Cells were then washed and permeabilized with 0.1 % Triton X100 in PBS for 10 min at RT before being saturated with 5% BSA in PBS for 30 min at RT. Cells were then stained with primary antibodies in the presence of 5% BSA (PBS/BSA) for 30 min at RT, washed three times in PBS and incubated in the dark with a mixture of secondary antibodies and fluorescent phalloidin (546 or 647, to detect F-actin) for 30 min at RT. Samples were then mounted with the fluorescent mounting medium from DAKO.

To determine whether green latex beads were internalized or not, cells challenged with IgG-coated LB were fixed and subjected to TRITC-conjugated goat anti-rabbit secondary antibodies (1:150 dilution) without cell permeabilization. When cells were challenged with LB, they were fixed and not permeabilized, subjected to anti-ovalbumin antibodies and revealed by TRITC secondary antibodies. Thus, yellow beads (green + red) are those remained outside while green beads were inside phagosomes. This approach also attested that phagosomes are sealed when they contain green beads.

2.5. Microscopy and image analysis

Immunofluorescent samples were observed using a PL Fluotar 40x/NA 1.0–0.5 oil immersion objective on a Leitz DM-RB microscope, equipped with a CoolSnap HQ CCD camera (Roper Scientific) and the Metaview software (Roper Scientific).

When indicated, super-resolution images were obtained using a LSM880 confocal microscope equipped with a Fast Airyscan module (Carl Zeiss) and is with and a Plan-Apochromat 40x/NA 1.3 oil DIC UV-IR M27 objective. Z-stack were acquired using the Super Resolution mode (Airyscan), set with a pixel size of 0.053 μm/pixel and a z-step of 0.249 μm. Airyscan Z-stacks were processed in ZEN software using the automatic strength (6 by default) and the 3D method.

Podosomes in F-actin stained cells were quantified with Fiji software. Briefly, podosome cores were detected using the “Find Maxima” function of the software. To calculate the number of cells with podosomes, cells with less than 10 podosomes were considered as podosome-free. Podosome density was calculated for each cell by dividing the podosome number by the cell surface (measured by manual cell delimitation).

Intensity profiles of vinculin, paxillin, talin, cortactin, CD18 and F-actin were measured on the phagosome surface in the area of PAPs by using the « Plot profile » function of Image J. The maximal fluorescence intensity of each profile was normalized to 100. Mean values were calculated on PlotTwist application (Goedhart, 2020). The height of PAPs was determined by the full width at half maximum of the intensity peak of F-actin from Airyscan acquisition.

2.6. Live cell imaging

Human macrophages were transduced with Lifeact-mCherry expressing lentiviruses as previously described (Van Goethem et al., 2011) after 4 days of differentiation. Two days later, cells were harvested and seeded in Lab-tek™ glass based chambers and kept in a humidified atmosphere at 37 °C and 5% CO<sub>2</sub> for at least 18 h. Live cell imaging was performed using an Olympus IX81 microscope equipped with a 100X oil immersion objective, a Yokogawa CSU22 confocal unit and an Andor iXon 888-BVEM–CCD back illuminated camera. Stacks of 11 sections spaced by 0.7 μm were acquired every 30 s using Andor IQ 1.9 Software.

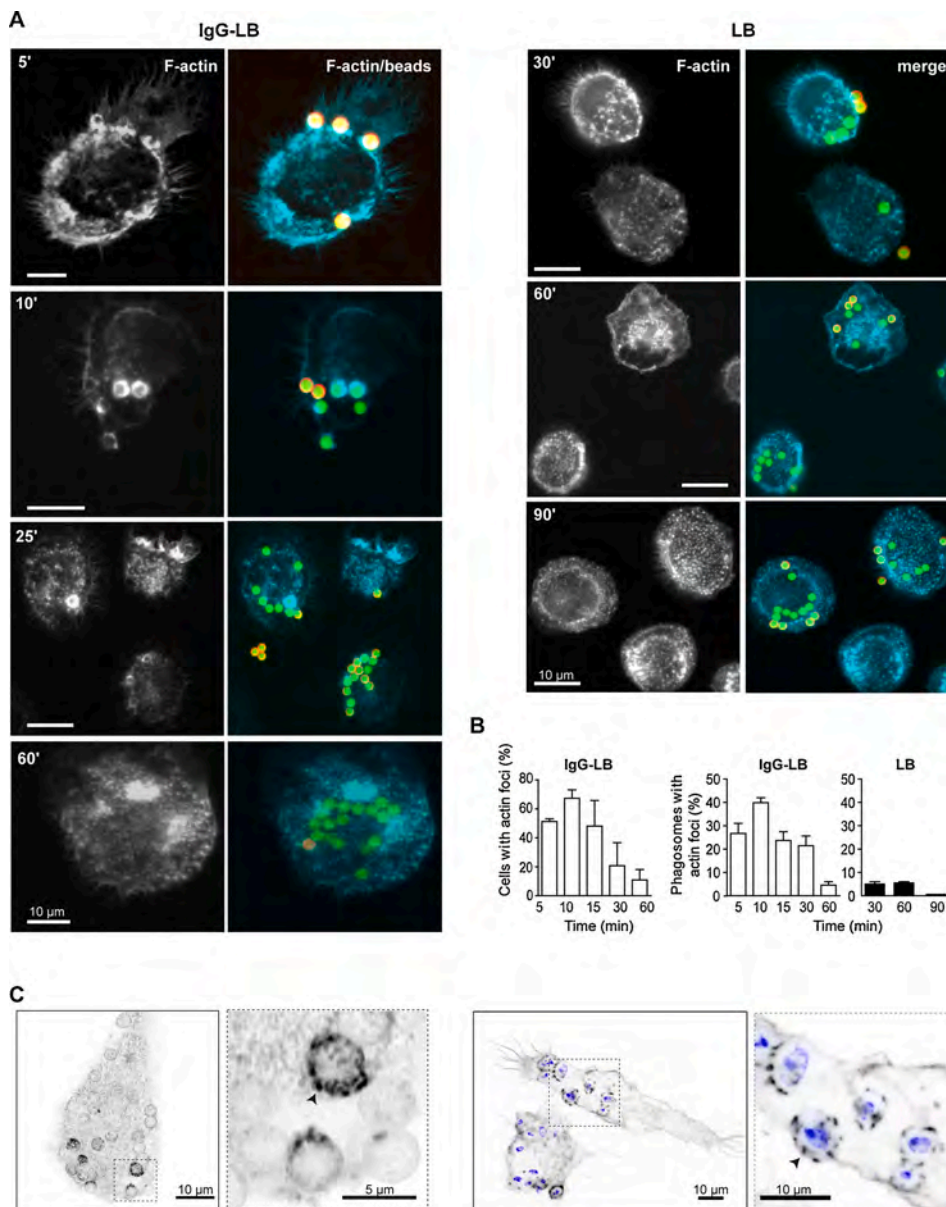


**Fig. 1.** F-actin structures are present at the membrane of nascent and closed phagosomes. Images of fluorescence microscopy (A). Human macrophages cultured on glass coverslips were exposed to fluorescent latex beads (green) coated with IgG (IgG-LB : MOI 10:1) or not (LB : MOI 30:1). The beads were centrifuged to synchronize phagocytosis and the experiments were carried out for the indicated times. F-actin (cyan) structures form on phagocytic cups (5 min) and closed phagosomes containing IgG-LB, they did not form on phagosomes containing LB. Beads inside sealed phagosomes are green, beads outside were stained in red (they appear yellow in merge images). Scale bars: 10 μm. (B) Quantification of the percentage of cells with actin structures on phagosomes (left) and the percentage of phagosomes containing IgG-LB (middle) or LB (right) with actin structures. Results from at least 25 cells per time point from 2 to 5 donors are expressed as mean +/- SD. (C) Macrophages containing IgG-LB were fixed at 10 min, those containing LB, fixed at 15 min, and stained for F-actin and analyzed by Airyscan super-resolution microscopy. In the cropped images, arrowheads point to F-actin foci on phagosomes. (For interpretation of the references to colour in this figure legend, the reader is referred to the web version of this article).

2.7. Statistics

Statistical analyses were performed using Prism 5 (GraphPad). Statistical comparison of the data was performed using one-way Anova followed by Dunnett's comparison test or by Kruskal-Wallis test, followed by Dunn's multiple comparisons test for not normally distributed data. For EDTA, statistical comparison was performed using paired *t*-test followed by Wilcoxon test. In the figures, statistical significance is indicated as follows: \* *p* < 0.05; \*\* *p* < 0.01 and \*\*\* *p* < 0.001.

3. Results

3.1. F-actin structures form on phagocytic cups and closed phagosomes

To determine whether F-actin structures are present on closed

phagosomes, experiments of synchronized phagocytosis were performed with fluorescent 3 μm-large latex beads that were coated with IgG (IgG-LB) or not (LB). Phagocytosis of IgG-LB and LB was carried out with 10 and 30 particles/cell, respectively, in order to obtain similar phagocytic rates (Suppl. Fig. 1A). Next, as shown in Fig. 1, beads inside sealed phagosomes (green) were distinguished from beads that were not internalized (yellow, see Materials and Methods). At 5 min of phagocytosis of IgG-LB, we noticed that F-actin structures were present on phagocytic cups (see phagocytic cups containing beads with a yellow/red apex attesting that phagosomes are unclosed) and, at later time points, they were also observed on closed phagosomes (Fig. 1A). The percentage of cells with F-actin foci at phagosomes was maximal at 10 min and then decreased until 60 min (Fig. 1B). The percentage of phagosomes with actin structures was 25 % at 5 min; it peaked at 10 min at about 40 % and went back to almost zero at 60 min. Contrasting with

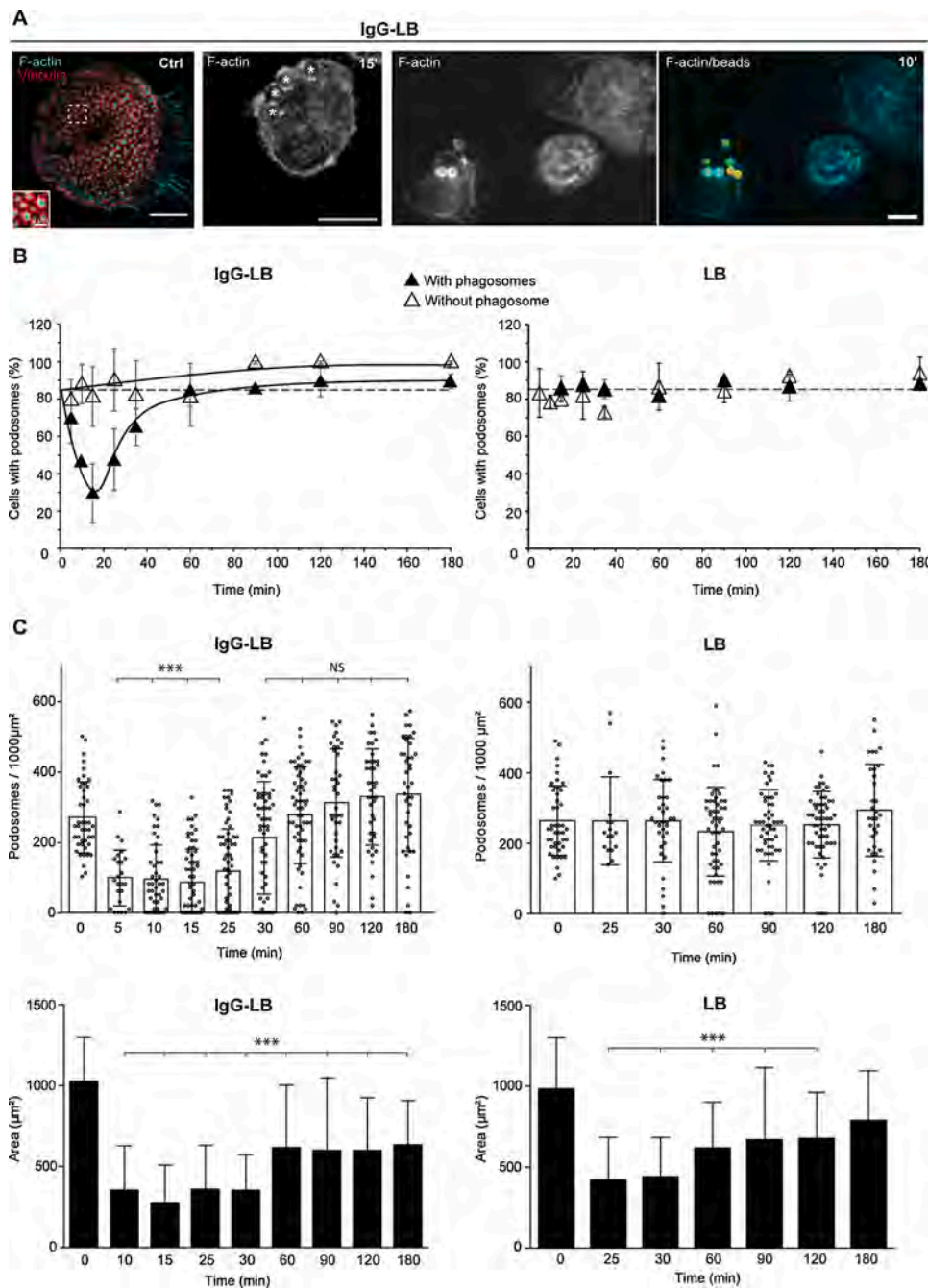


**Fig. 2. Phagocytosis of IgG-IgG-LB leads to transient disruption of podosomes.** Human macrophages cultured on glass coverslips were exposed to IgG-LB (MOI 10:1) or LB (MOI 30:1). The beads were centrifuged to synchronize phagocytosis and the experiments were carried out for the indicated times (5 to 180 min). Images of fluorescence microscopy (A): the left image shows podosomes in a control cell not exposed to beads, the neighbor image shows podosome disruption at 15 min in a cell with phagosomes (materialized by stars); the two images on the right show that podosomes remain in cells that do not ingest beads while they disappear in the neighbor cells with phagosomes. Beads inside cells are green, beads outside are yellow, F-actin is cyan. Scale bars: 10 μm. (B) The percentage of cells with podosomes were quantified in cells containing phagosomes and in neighbor cells without phagosomes. The dash line is the percentage of macrophages with podosomes in control cells that were not exposed to beads. Results are expressed as mean ± SD of at least 50 cells/time point from 3 donors; and analyzed with Kruskal-Wallis test, followed by Dunn's multiple comparisons test. (C) The podosome density was quantified by measuring the cell area (lower panels) and counting the number of podosomes. Results are expressed as mean ± SD of at least 20 cells/time point from 3 donors, and analyzed using a Kruskal-Wallis test, followed by Dunn's multiple comparisons test. (For interpretation of the references to colour in this figure legend, the reader is referred to the web version of this article).

these results, phagosomes containing LB only occasionally presented F-actin at their surface (Fig. 1B). Next, the actin structures were examined by super-resolution microscopy on closed phagosomes. They looked similar in size and distribution when either IgG-LB or serum-opsonized zymosan (OZ) were used (Fig. 1C, Video 1). Thus, in human macrophages, F-actin structures formed at the surface of phagocytic cups and closed phagosomes containing IgG-LB, OZ but not LB.

### 3.2. Podosomes are transiently disrupted concomitantly to the formation of actin structures on phagosomes

While we were imaging actin structures on phagosomes at different time points, we noticed that podosomes at the ventral face of macrophages disappeared (Fig. 1A). We therefore quantified it.

As observed in Fig. 1A, at early time points of the phagocytosis process (5 and 10 min), podosomes disappeared and they re-appeared later on (30 and 60 min). In Fig. 2A, the superresolution images on the left show podosomes in a macrophage devoid of phagosomes to compare with a macrophage containing phagosomes in which podosomes were disrupted (neighbor image). Interestingly, only cells that ingested particles lost transiently their podosomes, neighbor cells

without phagosomes kept their podosomes (Fig. 2A, right panels). Podosome quantification was performed. It showed that phagocytosis of IgG-LB induced a loss of podosomes in 70 % of the cells with phagosomes at 15 min and then the number of cells with podosomes raised back to normal at 60 min (Fig. 2). In contrast, phagocytosis of LB was not associated with podosome loss over the 3 h time-course of the experiments (Fig. 2). When phagocytosis was performed with zymosan (Z) and OZ used at 30 and 10 particles/cells respectively to keep comparable phagocytosis rates than latex beads (Suppl. Fig. 2A), transient podosome disappearance was observed with both types of particles (Suppl. Fig. 2B). Similarly to IgG-LB, only cells with phagosomes had transient podosome disruption (Suppl. Fig. 2B).

Next, the podosome number was quantified by cell surface unit in cells with phagosomes containing IgG-LB. After 5 min, the podosome number rapidly dropped down from 264 to 96 podosomes / 1000  $\mu\text{m}^2$  and went back to control at 60 min (270 podosomes /1000  $\mu\text{m}^2$ ) (Fig. 2C). We also quantified podosomes per cell surface unit in cells that ingested LB and no change was noticed (Fig. 2C). During phagocytosis of IgG-LB, the cell area of macrophages was reduced concomitantly to podosome disruption. When podosomes re-appeared, macrophage spreading increased without reaching the control value (Fig. 2).

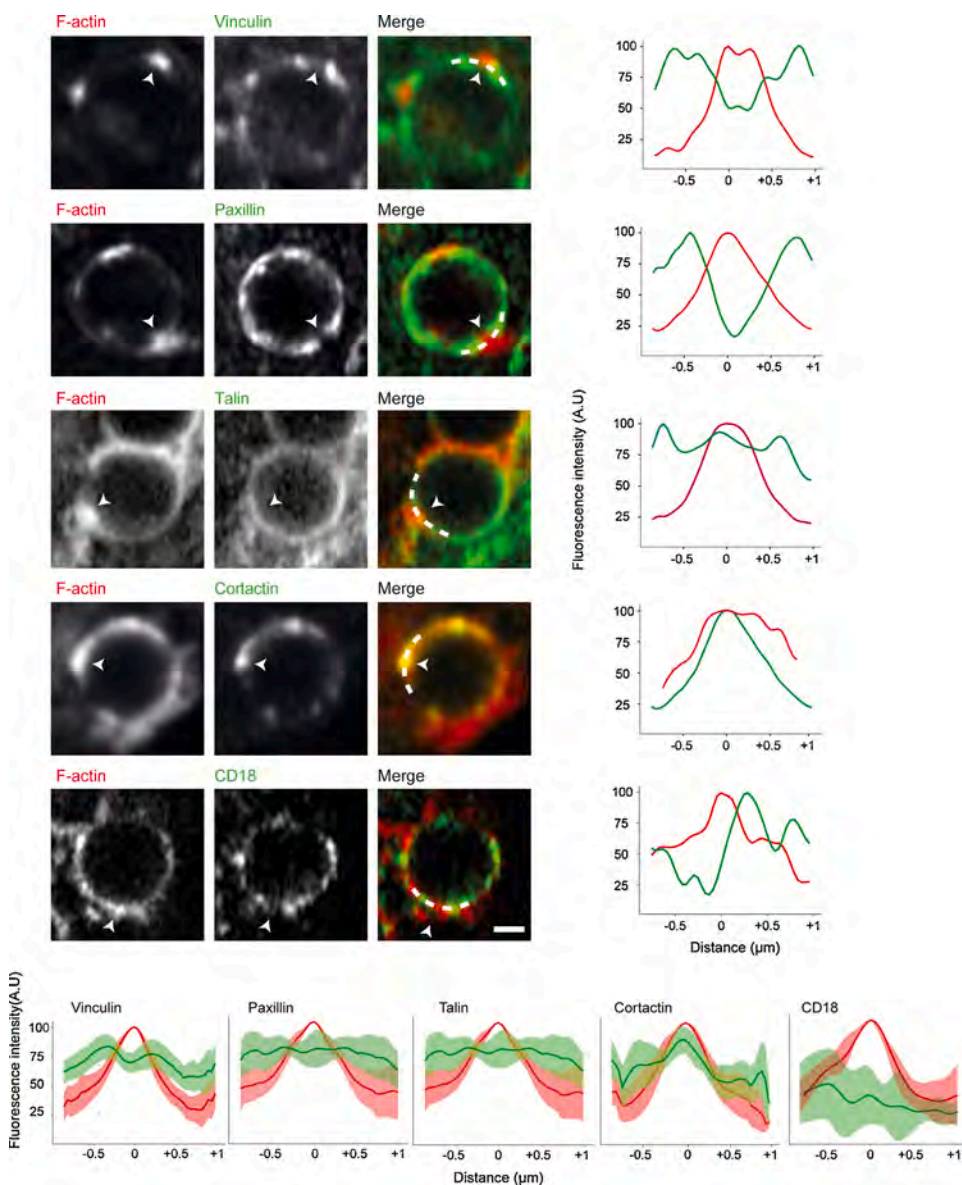


**Fig. 3. F-actin structures present on closed phagosomes have podosome characteristics.** Macrophages were exposed to IgG-LB for 10 min and F-actin (red), vinculin, paxillin, talin and cortactin were stained (green) or for 5 min and F-actin and CD18 were stained. Super-resolution images show phagosomes (scale bar : 1  $\mu\text{m}$ ) used for the line scans (right) with zero on the horizontal axis corresponding to the center of PAPs. Line scan mean values were calculated from at least 10 PAPs from 3 donors, using PlotTwist application (lower panels). (For interpretation of the references to colour in this figure legend, the reader is referred to the web version of this article).

However, this transient decrease of the cell spreading also occurred in cells ingesting LB that do not lose their podosomes suggesting that the two events are not correlated.

These experiments revealed that upon phagocytosis of most but not all phagocytic particles, those that trigger formation of actin structures at phagosomes also trigger transient podosome disruption. This occurred exclusively in cells with phagosomes suggesting that a coupling exists between phagocytosis, formation of actin structures at phagosomes and podosome disruption.

3.3. F-actin structures present on closed phagosomes have podosome characteristics

The actin structures present on closed phagosomes were

characterized to determine whether they share common features with podosome-like structures that were already described in phagocytic cups. Using confocal and super-resolution fluorescence microscopy, the height of F-actin foci on phagosomes was estimated to be 511 +/-107 nm (mean +/-SD of 16 actin foci from 7 cells, from 2 donors). We observed that podosome components belonging to the adhesion complex (integrins, vinculin, paxillin, talin) that are present in the ring of podosomes, also localized in close proximity of actin foci on phagosomes (Fig. 3). Analysis of fluorescence intensity profiles revealed that, similarly to podosomes, cortactin co-localized with F-actin and vinculin, paxillin and talin accumulated around the peak of F-actin (Fig. 3, Video 2). The  $\alpha$ M $\beta$ 2 integrin (CD18/CD11b) is involved in both adhesion complexes and Fc $\gamma$ R-mediated phagocytosis (Graham et al., 1989; Jongstra-Bilen et al., 2003). We observed that 91.7 +/- 18.5 %, n = 2 of

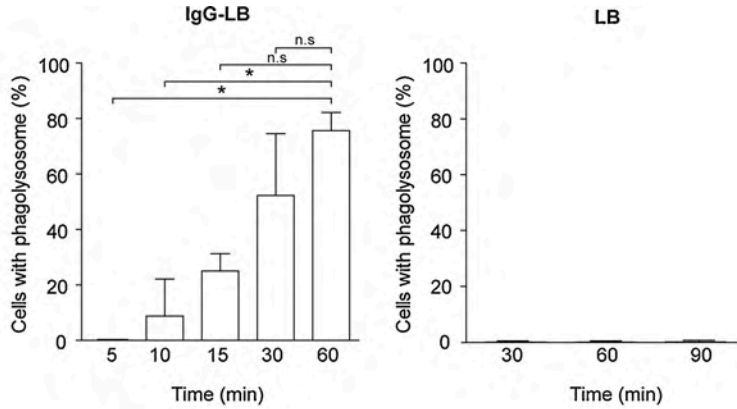
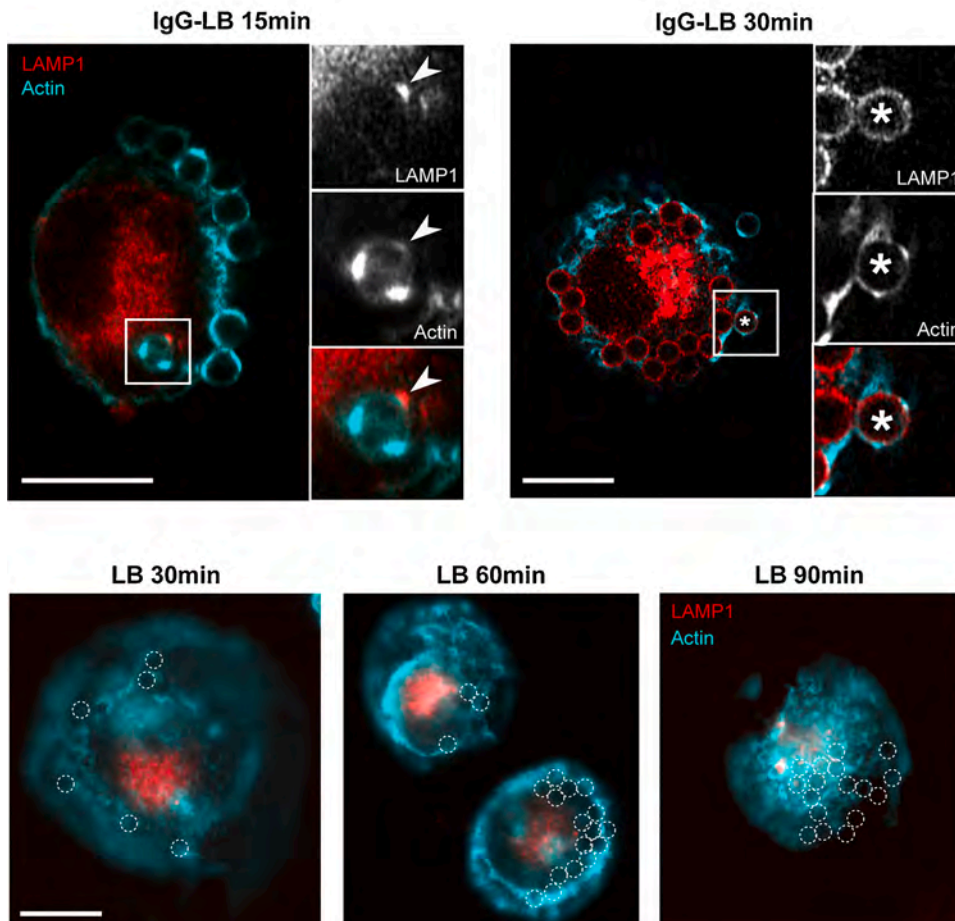


Fig. 4. Differential phagolysosome formation upon ingestion of IgG-LB or LB by human macrophages. Upper panels: Phagolysosomes (Lamp-1 positive) were quantified at different time points in cells challenged with IgG-LB or LB. The results are expressed as mean +/- SD, n = 3 and analyzed using Kruskal-Wallis test, followed by Dunn's multiple comparisons test. Middle panels: representative superresolution microscopy images of macrophages exposed to IgG-LB stained for LAMP-1 (red) and F-actin (cyan) at 15 and 35 min. The arrowheads show a LAMP-1 positive vesicle in proximity of a phagosome with PAPs. The stars show a phagosome with both LAMP-1 and PAPs at its membrane. Lower panels : Fluorescence microscopy images of F-actin and LAMP-1 are not recruited to phagosomes containing LB (represented by dash circles) at different time points. (For interpretation of the references to colour in this figure legend, the reader is referred to the web version of this article).



actin-positive phagosomes were also CD18 positive. Analysis of the fluorescence intensity profiles revealed that CD18 was present in close proximity of F-actin foci (Fig. 3).

Next, the life-time of these phagosome-associated F-actin structures was determined by confocal microscopy in macrophages transduced with LifeAct-mCherry. F-actin was monitored for an hour in single cells (Video 3) that perform phagocytosis of IgG-LB in a non-synchronized way. We found that the mean life-span of F-actin foci on phagosomes was  $5.0 \pm 3.3$  min (Suppl. Fig. 3). In the meantime, podosomes progressively disappeared from the ventral face of macrophages (Video 3).

Thus, podosomes and F-actin foci at phagosomes share common characteristics: similar size since podosomes are structured as an actin core of 5–600 nm high surrounded by a ring of adhesion proteins of 0.8–1  $\mu\text{m}$  (Labernadie et al., 2010; Wiesner et al., 2010); similar life span; similar protein components (integrin, talin, vinculin, paxillin, cortactin) with similar localizations to podosomes. We therefore propose to call these F-actin structures phagosome-associated podosomes (PAPs).

### 3.4. The presence of PAPs correlates with phagolysosome formation

Podosomes are docking sites for intracellular vesicles that subsequently fuse with the membrane and deliver metalloproteases and cathepsins involved in extracellular matrix degradation (Cougoule et al., 2005; Jevnikar et al., 2012; Van Goethem et al., 2010; Wiesner et al., 2010). Hence we wondered whether PAPs would display similar functionality, since phagosomes fuse with endosomes and lysosomes to form phagolysosomes along the maturation process.

The formation of phagolysosomes was examined by monitoring the transfer of lysosome-associated membrane protein 1 (LAMP-1) to the membrane of phagosomes. During phagocytosis of IgG-LB by human macrophages, LAMP-1 positive phagosomes were detected from 10 min on (Fig. 4). As shown in Fig. 4 (15 min, arrowhead), a LAMP-1-positive vesicle was in close proximity to an IgG-LB phagosome with PAPs. In Fig. 4 (30 min, star) a phagosome with both PAPs and LAMP-1 is shown. When this phenomenon was quantified, only  $15 \pm 6\%$  ( $n = 3$  donors) of phagosomes were F-actin and LAMP-1 double positive suggesting that PAPs rapidly disappeared after LAMP-1 transfer. Supporting this, PAPs decreased with time (Fig. 1B left graph) while phagolysosomes increased (Fig. 4, left graph).

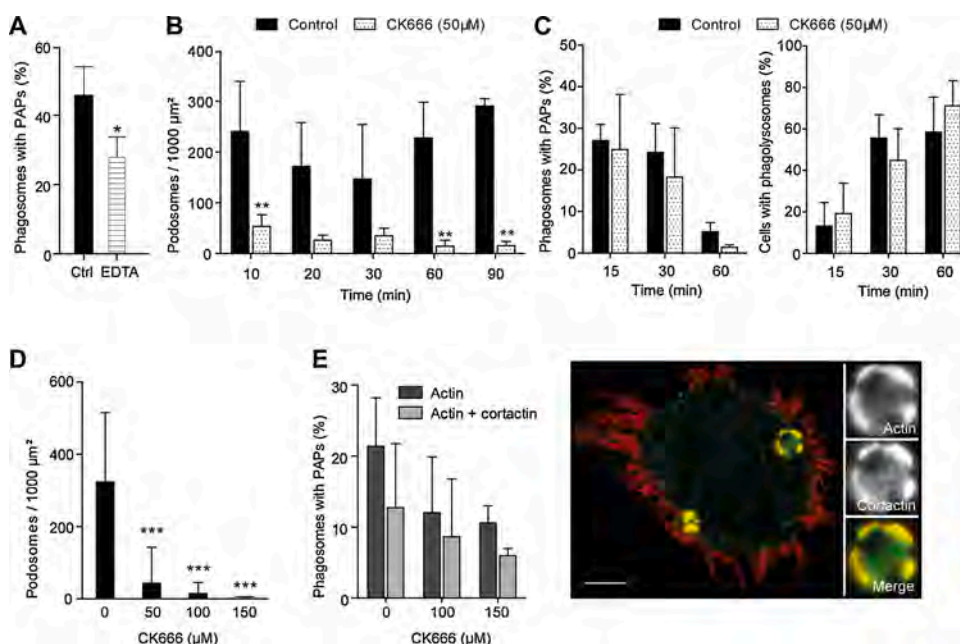


**Fig. 5.** Arp2/3 inhibition disrupts podosomes but PAPs and phagolysosomes are only slightly affected. (A) EDTA (5 mM) inhibited the formation of PAPs on IgG-LB containing phagosomes. Data from at least 180 cells from 6 donors are expressed as mean  $\pm$  SD and analyzed using paired *t*-test followed by Wilcoxon test. (B–C) The podosome density was markedly decreased by 50  $\mu\text{M}$  CK666; PAPs persisted on IgG-phagosomes and phagolysosome formation was not affected by CK666. Data from at least 50 cells from 3 donors are expressed as mean  $\pm$  SD and analyzed using two-way ANOVA followed by Bonferroni's multiple comparison test. (D) High concentrations of CK666 abolished the formation of podosomes. (E) The localization of cortactin was not modified by 150  $\mu\text{M}$  CK666 in macrophages ingesting IgG-LB for 30 min, a merge Airyscan microscopy image shows that cortactin (green) co-localized with F-actin (red) in PAPs. Scale bar 5  $\mu\text{m}$ . For D and E: data from at least 70 cells from 3 donors are expressed as mean  $\pm$  SD and were analyzed using Kruskal-Wallis test. (For interpretation of the references to colour in this figure legend, the reader is referred to the web version of this article).

In contrast to IgG-LB, phagosomes containing LB did not become LAMP-1 positive at any time point examined until 90 min (Fig. 4).

These results suggest that phagocytic particles that do not trigger the formation of PAPs do not end up in phagolysosomes.

### 3.5. Formation of PAPs involves integrins and is resistant to Arp2/3 inhibition

CD11b/CD18 is involved in phagocytosis of IgG, it accumulates at phagocytic cups and podosome-like structures (Graham et al., 1989; Jongstra-Bilen et al., 2003; Freeman et al., 2016; Ostrowski et al., 2019). When integrins were inhibited with EDTA which chelates divalent cations (Zhang and Chen, 2012), we observed that the percentage of phagosomes with PAPs was decreased, suggesting that integrin activation was involved, at least for a part, in PAPs formation (Fig. 5A).

The formation of podosomes is Arp2/3-dependent (Faust et al., 2019; Jeannot and Besson, 2020; van den Dries et al., 2019; Yamaguchi et al., 2005), and the formation of actin flashes at the phagosomal membrane as well (Poirier et al., 2020). Thus we questioned the involvement of Arp2/3 in the formation of PAPs. Recently, the role of Arp2/3 in the process of phagocytosis has been re-evaluated (Rotty et al., 2017). Indeed, macrophages from Arp2c $^{-/-}$  mice or macrophages treated with the Arp2/3 inhibitor CK666 are still capable of ingesting IgG-coated particles. So, we compared the effect of CK666 (Baggett et al., 2012) on podosomes, PAPs and phagolysosome formation in macrophages ingesting IgG-LB. We first determined the lowest concentration of CK666 sufficient to abolish the formation of podosomes without major effect on phagocytosis of IgG-LB. Using 50  $\mu\text{M}$  CK666, podosomes were almost fully disrupted while phagocytosis of IgG-LB, formation of PAPs and LAMP-1 translocation to the phagosomal membrane were not significantly modified (Fig. 5B–C). In other studies, CK666 has been used at 150  $\mu\text{M}$  to inhibit the formation of F-actin flashes on phagosomes (Poirier et al., 2020) or phagocytosis of C3bi-coated particles by macrophages (Rotty et al., 2017). Thus, we examined whether higher concentrations of CK666 would affect PAPs. Using CK666 at 100 and 150  $\mu\text{M}$  we observed that podosomes were completely disrupted (Fig. 5D), phagocytosis of IgG-LB was slightly inhibited (21 % with 150  $\mu\text{M}$  CK666 at 30 min), and the percentage of phagosomes with PAPs was decreased but not significantly (Fig. 5E). In the presence of 150  $\mu\text{M}$  CK666, cortactin which is known as a regulator of Arp2/3 (Kirkbride et al., 2011)

still co-localized with the actin core of PAPs, like it does in untreated cells (Fig. 5E). Thus, even at high CK666 concentration, PAPs are still present and organized like in controls. These results indicate that PAPs, like podosomes, involve integrin activation but they can be distinguished from podosomes by being partially resistant to Arp2/3 inhibition by CK666.

#### 4. Discussion

Actin polymerization at nascent phagosomes has been studied with interest in order to understand how pseudopodia progress around the particle, how the membrane adheres to the particle and senses its stiffness (Jaumouille and Waterman, 2020; Liebl and Griffiths, 2009; Ostrowski et al., 2019). There are podosomes-like structures on phagocytic cups (Allen and Aderem, 1996; Labrousse et al., 2011; Ostrowski et al., 2019) and, actin flashes on closed phagosomes (Liebl and Griffiths, 2009; Poirier et al., 2020). These two structures can be distinguished by several aspects including their size, life span, duration and the phagocytic receptors involved (Liebl and Griffiths, 2009; Ostrowski et al., 2019; Poirier et al., 2020).

Here, we describe actin structures that form on both phagocytic cups and closed phagosomes containing various particle types. They have structural characteristics of podosomes, and, similarly to podosomes that are targeted by vesicles, they are involved in phagosome maturation into phagolysosomes. We called these actin structures phagosome-associated podosomes (PAPs). Concomitant to PAP formation, podosomes transiently disappeared in macrophages containing phagosomes, not in cell neighbors devoid of phagosomes suggesting that PAPs form at the expense of podosomes.

We noticed that PAPs did not form when LB were ingested, whereas they appeared on IgG-LB phagosomes. Depending on the concerned particle, phagocytosis involves the complex interplay of receptors for serum opsonins, microbes or senescent cell motifs that initiate a diversity of signaling pathways. In the case of LB, CD36 and P2×7 scavenger receptors have been proposed to participate in their internalization, but the signals they elicit during that process have not been identified (Wiley and Gu, 2012; Yun et al., 2014). The receptors of OZ, zymosan and IgG-LB have been better characterized. OZ is recognized by several receptors which bind to IgG (FcγRs) and by the integrin αMβ2, also called Complement Receptor 3 (CR3), which binds to the complement fragment C3bi. Receptors for zymosan include the mannose receptor, dectin1 and the lectin domain of the CR3 (Astarie-Dequeker et al., 1999; Ganbold and Baigude, 2018; Le Cabec et al., 2002; Ross et al., 1985). The receptors involved in ingestion of IgG-LB are FcγRs and, interestingly, during phagocytosis of IgG, β2 integrins and integrin-associated proteins have been described to accumulate on phagosomes (Allen and Aderem, 1996; Freeman et al., 2016; Greenberg et al., 1990; Jaumouille and Grinstein, 2016; Labrousse et al., 2011). More specifically, in the context of IgG-mediated frustrated phagocytosis, activated β2 integrins accumulate in the environment of podosome-like structures (Ostrowski et al., 2019) and, during phagocytosis of IgG-LB, β2 integrins were observed on phagosomes in close proximity with PAPs (this report). It is well established that integrins and FcγRs trigger actin polymerization but it is not known whether the receptors involved in phagocytosis of LB induce actin polymerization which was only occasionally observed on LB phagosomes.

Another difference between the particles we used, is the process of phagosome maturation. Once phagosomes are closed, approximately 5 min after the beginning of particle engulfment, they migrate towards the cell center and mature by sequential fusion with vesicles of the endosome-lysosome compartments to form phagolysosomes. In a few examples however, ingested cargos are not routed to phagolysosomes (Armstrong and Hart, 1971). In the case of phagosomes containing LB, most of them (>95 %, n = 4) remained negative for both the early endosome protein Rab5 and the late endosome/lysosome protein LAMP-1 (this report), and were previously shown to by-pass the production of

O<sub>2</sub>, a major bactericidal response of human macrophages (Astarie-Dequeker et al., 1999). This is different from phagosomes containing LB previously shown to become Rab 5 and LAMP-1 positive in the J774 cell line (Houde et al., 2003). However, several differences between human primary macrophages and this particular mouse macrophage-like cell line isolated from a murine sarcoma have been reported (Andreu et al., 2017; Chamberlain et al., 2015; Hall et al., 2006), so we assume that phagosome maturation proceeds differently in these two cell types. Contrasting with LB, phagosomes containing IgG-LB, Z and OZ formed PAPs and became LAMP-1 positive (this report). These observations allowed to propose that the presence of PAPs is related to late endosome/lysosome fusion. Dense actin meshworks that make a physical barrier around early phagosomes impair their fusion with vesicles (Burgoyne and Cheek, 1987; Liebl and Griffiths, 2009), and progressively disappear during phagosome maturation. However, F-actin is still assembling at discrete sites of the phagosome membrane, a process required for fusion of late endosomes/lysosomes with phagosomes (Anes et al., 2003; Hasegawa et al., 2016; Kalamidas et al., 2006; Kjekken et al., 2004; Liebl and Griffiths, 2009; Marion et al., 2011; Wang et al., 2008). Thus, in the light of these observations, we propose that PAPs on closed phagosomes could be the F-actin structures that serve as docking sites for vesicles. In fact, in the vicinity of PAPs, LAMP1-positive vesicles were observed. However, phagosomes were more frequently PAPs positive or LAMP-1 positive rather than double-positive suggesting that co-existence of both staining should be a short-lasting event. Similarly, in RAW264.7 macrophages, phagosomes containing IgG-LB have been shown to lose actin at their surface while acquiring LAMP-2 (Liebl and Griffiths, 2009). Thus, PAPs could serve as furtive docking and fusion sites for vesicles and subsequently disappear.

Like podosomes that are involved in cell adhesion, generation of protrusive forces, mechano- and topography-sensing, proteolysis of the extracellular matrix and cell migration, we propose that PAPs could be also multifunctional structures. Actually podosome-like structures on phagocytic cups have been described to seal the membrane to the phagocytic prey suggesting that the protrusion force generated by podosomes to sense the environment (Bouissou et al., 2017; Labernadie et al., 2014; van den Dries et al., 2019) is also operating in podosome-like structures to seal the membrane onto the ingested particle and, possibly, sense its stiffness (Ostrowski et al., 2019). Whether mechanosensing property is also functional in PAPs remains to be demonstrated, but the presence of proteins belonging to the adhesion complex spatially organized like in podosomes and podosome-like structures on frustrated phagosomes is in favor of this hypothesis. The Arp2/3 complex is a major regulator of actin filament assembly involved in podosome formation. Here, we show that PAPs are poorly disturbed by the presence of 150 μM CK666, a concentration that abolished the formation of podosomes in the same cells (this report), the formation of actin flashes (Poirier et al., 2020) and phagocytosis of C3bi coated beads (Rotty et al., 2017). Similarly to PAPs formation, phagocytosis of IgG particles, triggers an Arp2/3-independent route to actin polymerization which compensates for Arp2/3 inhibition (Rotty et al., 2017). Formins are actin nucleators which function independently of Arp2/3. They generate unbranched actin filaments. The formin family comprises 15 proteins, several of them have been implicated in the formation of podosomes and invadopodia, and degradation of the extracellular matrix (Lizarraga et al., 2009; Mersich et al., 2010; Miller et al., 2017; Panzer et al., 2016; Ren et al., 2018; Tsuboi et al., 2009). Thus we propose that formins could complement Arp2/3 in the formation of PAPs, explaining their pretty good resistance to Arp2/3 inhibition. Actually, in addition to its role in Arp2/3 activation, cortactin which co-localized with F-actin in PAPs has been described to recruit formins in invadopodia (Li et al., 2010; Ren et al., 2018; Suman et al., 2018). To explore whether formins could be involved in actin polymerization in PAPs, 25 μM SMIFH2, a formin pan-inhibitor (Isogai et al., 2015) was used but it did not affect PAP formation (data not shown), pointing to the need of more specific approaches.

So, podosome-like structures and PAPS share many structural and functional characteristics with podosomes but differ by a few aspects. In the case of podosome-like structures, inhibition of two PI(3,4,5)P3 effectors Akt and ARNO required for podosomes formation have no obvious effect (Ostrowski et al., 2019). In the case of PAPS, inhibition of Arp2/3 has almost undetectable effect whereas, in the same cells, podosomes are completely dismantled. It is possible that the structural differences have consequences on the functions served by podosome-like structures and PAPS at the phagosomal membrane compared to podosomes at the interface between the plasma membrane and the substratum. In addition to podosomes at phagosomes, other “unusual localizations” of podosomes have been reported including at cell interfaces during cell-cell fusion and at the immunological synapse (Faust et al., 2019; Oikawa et al., 2012; Wernimont et al., 2008). Whether podosomes in these localizations also present some signaling, structural and functional differences from “classical” podosomes has not been explored and this opens a new research field.

In this study, we also show that podosomes were temporarily dismantled concomitantly to the formation of PAPS. Strikingly, it occurred during ingestion of IgG-opsonized particles, zymosan and serum-opsonized zymosan, but not that of LB. PAPS were present at 5 min, the earliest time point of our experiments and disappeared about 60 min later. Podosomes disappeared and reappeared with almost the same kinetics. Transient disruption of podosomes was only observed in cells that had ingested particles, podosomes remained unaffected in neighboring cells that lacked phagosomes. It indicates that the process of phagocytosis by itself is involved in a way that is not triggered by LB. One hypothesis is that the signaling of phagocytic receptors involved in ingestion of IgG-LB, Z and OZ triggers podosome disruption. A molecule which spreads from a cell to another such as PGE2, known to disrupt podosomes in dendritic cells (Cougoule et al., 2018; van Helden et al., 2008), can be excluded because macrophages without phagosomes keep their podosomes. Podosomes and PAPS share adhesion complexes containing talin, paxillin and vinculin that link integrins to actin. Several actors regulating this process such as FAK/Pyk2 and Src kinases could be potential limiting factors. As a consequence, their recruitment on forming phagosomes to initiate the ingestion process and form PAPS would deplete them at the ventral face of macrophages, which could induce podosome disruption. Interestingly, podosome disruption would be potentially a way to redirect lysosomes to PAPS and no longer to podosomes, and thus prioritize the destruction of phagocytic particles at the expense of podosome-mediated matrix degradation.

To conclude, we propose that PAPS and podosome-like structures described in phagocytic cups are similar structures, themselves related to podosomes. Formation of PAPS leads to phagosome maturation and to podosome disruption in a synchronized manner. The rationality to disrupt podosomes when PAPS are present is not understood yet, it could help at redirecting vesicles containing proteases to phagosomes to digest microorganisms, which is undoubtedly a life priority.

## Fundings

This work was supported by the Human Frontier Science Program (RGP0035/2016), Fondation pour la Recherche MedicaleDEQ2016 0334894RGP0035/2016, Inserm Plan Cancer, Fondation Toulouse Cancer Santé. CB is a recipient of a CNRS 80 Prime fellowship.

## Declaration of Competing Interest

The authors have no competing interests to declare.

## Acknowledgements

The authors thank TRI imaging facility, Veronique Le Cabec for critical reading of the manuscript, Christel Verollet and Remi Mascarau for helpful discussions.

## Appendix A. Supplementary data

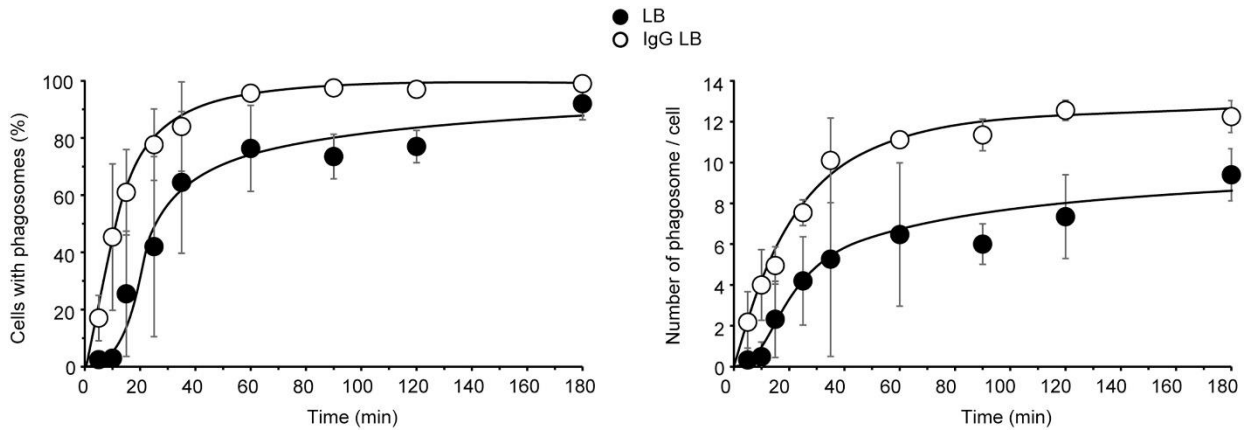
Supplementary material related to this article can be found, in the online version, at doi:<https://doi.org/10.1016/j.ejcb.2021.151161>.

## References

- Allen, L.A., Aderem, A., 1996. Molecular definition of distinct cytoskeletal structures involved in complement- and Fc receptor-mediated phagocytosis in macrophages. *J. Exp. Med.* 184, 627–637.
- Andreu, N., Phelan, J., de Sessions, P.F., Cliff, J.M., Clark, T.G., Hibberd, M.L., 2017. Primary macrophages and J774 cells respond differently to infection with *Mycobacterium tuberculosis*. *Sci. Rep.* 7, 42225.
- Anes, E., Kuhnle, M.P., Bos, E., Moniz-Pereira, J., Habermann, A., Griffiths, G., 2003. Selected lipids activate phagosome actin assembly and maturation resulting in killing of pathogenic mycobacteria. *Nat. Cell Biol.* 5, 793–802.
- Armstrong, J.A., Hart, P.D., 1971. Response of cultured macrophages to *Mycobacterium tuberculosis*, with observations on fusion of lysosomes with phagosomes. *J. Exp. Med.* 134, 713–740.
- Astarié-Dequeker, C., N'Diaye, E.N., Le Cabec, V., Rittig, M.G., Prandi, J., Maridonneau-Parini, I., 1999. The mannose receptor mediates uptake of pathogenic and nonpathogenic mycobacteria and bypasses bactericidal responses in human macrophages. *Infect. Immun.* 67, 469–477.
- Baggett, A.W., Cournia, Z., Han, M.S., Patargias, G., Glass, A.C., Liu, S.Y., Nolen, B.J., 2012. Structural characterization and computer-aided optimization of a small-molecule inhibitor of the Arp2/3 complex, a key regulator of the actin cytoskeleton. *ChemMedChem* 7, 1286–1294.
- Bouissou, A., Proag, A., Bourg, N., Pingris, K., Cabriel, C., Balor, S., Mangeat, T., Thibault, C., Vieu, C., Dupuis, G., Fort, E., Leveque-Fort, S., Maridonneau-Parini, I., Poincloux, R., 2017. Podosome force generation machinery: a local balance between protrusion at the core and traction at the ring. *ACS Nano* 11, 4028–4040.
- Burgoyne, R.D., Cheek, T.R., 1987. Reorganisation of peripheral actin filaments as a prelude to exocytosis. *Biosci. Rep.* 7, 281–288.
- Caron, E., Hall, A., 1998. Identification of two distinct mechanisms of phagocytosis controlled by different Rho GTPases. *Science* 282, 1717–1721.
- Chamberlain, L.M., Holt-Casper, D., Gonzalez-Juarrero, M., Grainger, D.W., 2015. Extended culture of macrophages from different sources and maturation results in a common M2 phenotype. *J. Biomed. Mater. Res. A* 103, 2864–2874.
- Cougoule, C., Carreno, S., Castandet, J., Labrousse, A., Astarié-Dequeker, C., Poincloux, R., Le Cabec, V., Maridonneau-Parini, I., 2005. Activation of the lysosome-associated p61Hck isoform triggers the biogenesis of podosomes. *Traffic* 6, 682–694.
- Cougoule, C., Le Cabec, V., Poincloux, R., Al Saati, T., Mege, J.L., Tabouret, G., Lowell, C.A., Lavolette-Malirat, N., Maridonneau-Parini, I., 2010. Three-dimensional migration of macrophages requires Hck for podosome organization and extracellular matrix proteolysis. *Blood* 115 (7), 1444–1452.
- Cougoule, C., Lastrucci, C., Guiet, R., Mascarau, R., Meunier, E., Lugo-Villarino, G., Neyrolles, O., Poincloux, R., Maridonneau-Parini, I., 2018. Podosomes, but not the maturation status, determine the protease-dependent 3D migration in human dendritic cells. *Front. Immunol.* 9, 846.
- Faust, J.J., Balabiyev, A., Heddleston, J.M., Podolnikova, N.P., Baluch, D.P., Chew, T.L., Ugarova, T.P., 2019. An actin-based protrusion originating from a podosome-enriched region initiates macrophage fusion. *Mol. Biol. Cell* 30, 2254–2267.
- Freeman, S.A., Grinstein, S., 2014. Phagocytosis: receptors, signal integration, and the cytoskeleton. *Immunol. Rev.* 262, 193–215.
- Freeman, S.A., Goyette, J., Furuya, W., Woods, E.C., Bertozzi, C.R., Bergmeier, W., Hinz, B., van der Merwe, P.A., Das, R., Grinstein, S., 2016. Integrins form an expanding diffusional barrier that coordinates phagocytosis. *Cell* 164, 128–140.
- Ganbold, T., Baigude, H., 2018. Design of mannose-functionalized curdlan nanoparticles for macrophage-targeted siRNA delivery. *ACS Appl. Mater. Interfaces* 10, 14463–14474.
- Goedhart, J., 2020. PlotTwist: a web app for plotting and annotating continuous data. *PLoS Biol.* 18, e3000581.
- Graham, L.L., Gresham, H.D., Brown, E.J., 1989. An immobile subset of plasma membrane CD11b/CD18 (Mac-1) is involved in phagocytosis of targets recognized by multiple receptors. *J. Immunol.* 142, 2352–2358.
- Gray, M., Botelho, R.J., 2017. Phagocytosis: hungry, hungry cells. *Methods Mol. Biol.* 1519, 1–16.
- Greenberg, S., Burridge, K., Silverstein, S.C., 1990. Colocalization of F-actin and talin during Fc receptor-mediated phagocytosis in mouse macrophages. *J. Exp. Med.* 172, 1853–1856.
- Hall, A.B., Gakidis, M.A., Glogauer, M., Wilsbacher, J.L., Gao, S., Swat, W., Brugge, J., 2006. Requirements for Vav guanine nucleotide exchange factors and Rho GTPases in FcγR- and complement-mediated phagocytosis. *Immunity* 24, 305–316.
- Hasegawa, J., Iwamoto, R., Otomo, T., Nezu, A., Hamasaki, M., Yoshimori, T., 2016. Autophagosome-lysosome fusion in neurons requires INPP5E, a protein associated with Joubert syndrome. *EMBO J.* 35, 1853–1867.
- Houde, M., Bertholet, S., Gagnon, E., Brunet, S., Goyette, G., Laplante, A., Princiotta, M. F., Thibault, P., Sacks, D., Desjardins, M., 2003. Phagosomes are competent organelles for antigen cross-presentation. *Nature* 425, 402–406.
- Isogai, T., van der Kammen, R., Innocenti, M., 2015. SMIFH2 has effects on Formins and p53 that perturb the cell cytoskeleton. *Sci. Rep.* 5, 9802.

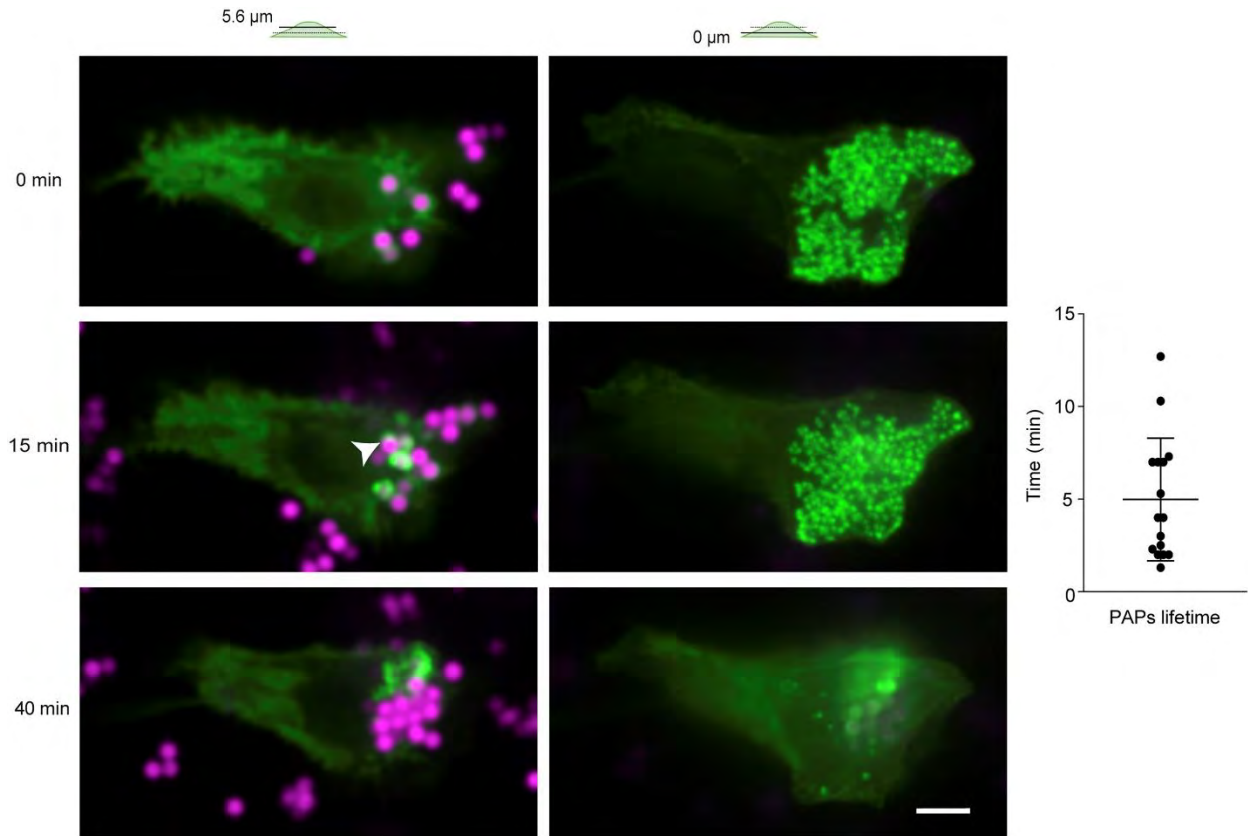
- Jahraus, A., Egeberg, M., Hinner, B., Habermann, A., Sackman, E., Pralle, A., Faulstich, H., Rybin, V., Defacque, H., Griffiths, G., 2001. ATP-dependent membrane assembly of F-actin facilitates membrane fusion. *Mol. Biol. Cell* 12, 155–170.
- Jakubczik, C.V., Randolph, G.J., Henson, P.M., 2017. Monocyte differentiation and antigen-presenting functions. *Nat. Rev. Immunol.* 17, 349–362.
- Jaumouille, V., Grinstein, S., 2016. Molecular mechanisms of phagosome formation. *Microbiol. Spectr.* 4.
- Jaumouille, V., Waterman, C.M., 2020. Physical constraints and forces involved in phagocytosis. *Front. Immunol.* 11, 1097.
- Jeannot, P., Besson, A., 2020. Cortactin function in invadopodia. *Small GTPases* 11, 256–270.
- Jevnikar, Z., Mirkovic, B., Fonovic, U.P., Zidar, N., Svajger, U., Kos, J., 2012. Three-dimensional invasion of macrophages is mediated by cysteine cathepsins in protrusive podosomes. *Eur. J. Immunol.* 42, 3429–3441.
- Jongstra-Bilen, J., Harrison, R., Grinstein, S., 2003. Fcγ-receptors induce Mac-1 (CD11b/CD18) mobilization and accumulation in the phagocytic cup for optimal phagocytosis. *J. Biol. Chem.* 278, 45720–45729.
- Kalamidas, S.A., Kuehnel, M.P., Peyron, P., Rybin, V., Rauch, S., Kotoulas, O.B., Houslay, M., Hemmings, B.A., Gutierrez, M.G., Anes, E., Griffiths, G., 2006. cAMP synthesis and degradation by phagosomes regulate actin assembly and fusion events: consequences for mycobacteria. *J. Cell. Sci.* 119, 3686–3694.
- Kirkbride, K.C., Sung, B.H., Sinha, S., Weaver, A.M., 2011. Cortactin: a multifunctional regulator of cellular invasiveness. *Cell Adh. Migr.* 5, 187–198.
- Kjeken, R., Egeberg, M., Habermann, A., Kuehnel, M., Peyron, P., Floetenmeyer, M., Walther, P., Jahraus, A., Defacque, H., Kuznetsov, S.A., Griffiths, G., 2004. Fusion between phagosomes, early and late endosomes: a role for actin in fusion between late, but not early endocytic organelles. *Mol. Biol. Cell* 15, 345–358.
- Labernadie, A., Thibault, C., Vieu, C., Maridonneau-Parini, I., Charriere, G.M., 2010. Dynamics of podosome stiffness revealed by atomic force microscopy. *Proc. Natl. Acad. Sci. U. S. A.* 107, 21016–21021.
- Labernadie, A., Bouissou, A., Delobelle, P., Balor, S., Voituriez, R., Proag, A., Fourquaux, I., Thibault, C., Vieu, C., Poincloux, R., Charriere, G.M., Maridonneau-Parini, I., 2014. Protrusion force microscopy reveals oscillatory force generation and mechanosensing activity of human macrophage podosomes. *Nat. Commun.* 5, 5343.
- Labrousse, A., Record, J., Labernadie, A., Beduer, A., Vieu, C., Ben Safta, T., Maridonneau-Parini, I., 2011. Frustrated phagocytosis on micro-patterned immune complexes to characterize lysosome movements in live macrophages. *Front. Immunol.* 2, 51. <https://doi.org/10.3389/fimmu.2011.00051>.
- Le Cabec, V., Carreno, S., Moisan, A., Bordier, C., Maridonneau-Parini, I., 2002. Complement receptor 3 (CD11b/CD18) mediates type I and type II phagocytosis during nonopsonic and opsonic phagocytosis, respectively. *J. Immunol.* 169, 2003–2009.
- Li, A., Dawson, J.C., Forero-Vargas, M., Spence, H.J., Yu, X., Konig, I., Anderson, K., Machesky, L.M., 2010. The actin-bundling protein fascin stabilizes actin in invadopodia and potentiates protrusive invasion. *Curr. Biol.* 20, 339–345.
- Liebl, D., Griffiths, G., 2009. Transient assembly of F-actin by phagosomes delays phagosome fusion with lysosomes in cargo-overloaded macrophages. *J. Cell. Sci.* 122, 2935–2945.
- Lizarraga, F., Poincloux, R., Romao, M., Montagnac, G., Le Dez, G., Bonne, I., Rigail, G., Raposo, G., Chavrier, P., 2009. Diaphanous-related formins are required for invadopodia formation and invasion of breast tumor cells. *Cancer Res.* 69, 2792–2800.
- Marchesin, V., Castro-Castro, A., Lodillinsky, C., Castagnino, A., Cyrta, J., Bonsang-Kitzis, H., Fuhrmann, L., Irondelle, M., Infante, E., Montagnac, G., Rey, F., Vincent-Salomon, A., Chavrier, P., 2015. ARF6-JIP3/4 regulate endosomal tubules for MT1-MMP exocytosis in cancer invasion. *J. Cell Biol.* 211, 339–358.
- Maridonneau-Parini, I., 2014. Control of macrophage 3D migration: a therapeutic challenge to limit tissue infiltration. *Immunol. Rev.* 262, 216–231.
- Marion, S., Hoffmann, E., Holzer, D., Le Clairche, C., Martin, M., Sachse, M., Ganeva, I., Mangeat, P., Griffiths, G., 2011. Ezrin promotes actin assembly at the phagosome membrane and regulates phago-lysosomal fusion. *Traffic* 12, 421–437.
- Mersich, A.T., Miller, M.R., Chkourko, H., Blystone, S.D., 2010. The formin FRL1 (FMNLI) is an essential component of macrophage podosomes. *Cytoskeleton Hoboken (Hoboken)* 67, 573–585.
- Miller, M.R., Miller, E.W., Blystone, S.D., 2017. Non-canonical activity of the podosomal formin FMNLI gamma supports immune cell migration. *J. Cell. Sci.* 130, 1730–1739.
- Monteiro, P., Rosse, C., Castro-Castro, A., Irondelle, M., Lagoutte, E., Paul-Gilloteaux, P., Desnos, C., Formstecher, E., Darchen, F., Perrais, D., Gautreau, A., Hertzog, M., Chavrier, P., 2013. Endosomal WASH and exocyst complexes control exocytosis of MT1-MMP at invadopodia. *J. Cell Biol.* 203, 1063–1079.
- Mylvaganam, S.M., Grinstein, S., Freeman, S.A., 2018. Picket-fences in the plasma membrane: functions in immune cells and phagocytosis. *Semin. Immunopathol.* 40, 605–615.
- Oikawa, T., Oyama, M., Kozuka-Hata, H., Uehara, S., Udagawa, N., Saya, H., Matsuo, K., 2012. Tks5-dependent formation of circumferential podosomes/invadopodia mediates cell-cell fusion. *J. Cell Biol.* 197, 553–568.
- Ostrowski, P.P., Freeman, S.A., Fair, G., Grinstein, S., 2019. Dynamic podosome-like structures in nascent phagosomes are coordinated by phosphoinositides. *Dev. Cell* 50 (397–410), e393.
- Panzer, L., Trube, L., Klose, M., Joosten, B., Slotman, J., Cambi, A., Linder, S., 2016. The formins FHOD1 and INF2 regulate inter- and intra-structural contractility of podosomes. *J. Cell. Sci.* 129, 298–313.
- Poirier, M.B., Fiorino, C., Rajasekar, T.K., Harrison, R.E., 2020. F-actin flashes on phagosomes mechanically deform contents for efficient digestion in macrophages. *J. Cell. Sci.* 133.
- Ren, X.L., Qiao, Y.D., Li, J.Y., Li, X.M., Zhang, D., Zhang, X.J., Zhu, X.H., Zhou, W.J., Shi, J., Wang, W., Liao, W.T., Ding, Y.Q., Liang, L., 2018. Cortactin recruits FMNL2 to promote actin polymerization and endosome motility in invadopodia formation. *Cancer Lett.* 419, 245–256.
- Ross, G.D., Cain, J.A., Lachmann, P.J., 1985. Membrane complement receptor type three (CR3) has lectin-like properties analogous to bovine conglutinin as functions as a receptor for zymosan and rabbit erythrocytes as well as a receptor for iC3b. *J. Immunol.* 134, 3307–3315.
- Rotty, J.D., Brighton, H.E., Craig, S.L., Asokan, S.B., Cheng, N., Ting, J.P., Bear, J.E., 2017. Arp2/3 complex is required for macrophage integrin functions but is dispensable for FcR phagocytosis and in vivo motility. *Dev. Cell* 42 (498–513), e496.
- Suman, P., Mishra, S., Chander, H., 2018. High expression of FBP17 in invasive breast cancer cells promotes invadopodia formation. *Med. Oncol.* 35, 71.
- Tsuboi, S., Takada, H., Hara, T., Mochizuki, N., Funiyu, T., Saitoh, H., Terayama, Y., Yamaya, K., Ohyama, C., Nonoyama, S., Ochs, H.D., 2009. FBP17 mediates a common molecular step in the formation of podosomes and phagocytic cups in macrophages. *J. Biol. Chem.* 284, 8548–8556.
- Uribe-Querol, E., Rosales, C., 2020. Phagocytosis: our current understanding of a universal biological process. *Front. Immunol.* 11, 1066.
- van den Dries, K., Linder, S., Maridonneau-Parini, I., Poincloux, R., 2019. Probing the mechanical landscape - new insights into podosome architecture and mechanics. *J. Cell. Sci.* 132.
- Van Goethem, E., Poincloux, R., Gauffre, F., Maridonneau-Parini, I., Le Cabec, V., 2010. Matrix architecture dictates three-dimensional migration modes of human macrophages: differential involvement of proteases and podosome-like structures. *J. Immunol.* 184, 1049–1061.
- Van Goethem, E., Guet, R., Balor, S., Charriere, G.M., Poincloux, R., Labrousse, A., Maridonneau-Parini, I., Le Cabec, V., 2011. Macrophage podosomes go 3D. *Eur. J. Cell Biol.* 90, 224–236.
- van Helden, S.F., Oud, M.M., Joosten, B., Peterse, N., Figdor, C.G., van Leeuwen, F.N., 2008. PGE2-mediated podosome loss in dendritic cells is dependent on actomyosin contraction downstream of the RhoA-Rho-kinase axis. *J. Cell. Sci.* 121, 1096–1106.
- Wang, Q.Q., Li, H., Oliver, T., Glogauer, M., Guo, J., He, Y.W., 2008. Integrin beta 1 regulates phagosome maturation in macrophages through Rac expression. *J. Immunol.* 180, 2419–2428.
- Wernimont, S.A., Cortesio, C.L., Simonson, W.T., Huttenlocher, A., 2008. Adhesions ring: a structural comparison between podosomes and the immune synapse. *Eur. J. Cell Biol.* 87, 507–515.
- Wiesner, C., Faix, J., Himmel, M., Bentzien, F., Linder, S., 2010. KIF5B and KIF3A/KIF3B kinesins drive MT1-MMP surface exposure, CD44 shedding, and extracellular matrix degradation in primary macrophages. *Blood* 116, 1559–1569.
- Wiley, J.S., Gu, B.J., 2012. A new role for the P2X7 receptor: a scavenger receptor for bacteria and apoptotic cells in the absence of serum and extracellular ATP. *Purinergic Signal.* 8, 579–586.
- Yam, P.T., Theriot, J.A., 2004. Repeated cycles of rapid actin assembly and disassembly on epithelial cell phagosomes. *Mol. Biol. Cell* 15, 5647–5658.
- Yamaguchi, H., Lorenz, M., Kempik, S., Sarmiento, C., Coniglio, S., Symons, M., Segall, J.E., Eddy, R., Miki, H., Takenawa, T., Condeelis, J., 2005. Molecular mechanisms of invadopodium formation: the role of the N-WASP-Arp2/3 complex pathway and cofilin. *J. Cell Biol.* 168, 441–452.
- Yun, M.R., Seo, J.M., Park, H.Y., 2014. Visfatin contributes to the differentiation of monocytes into macrophages through the differential regulation of inflammatory cytokines in THP-1 cells. *Cell. Signal.* 26, 705–715.
- Zhang, K., Chen, J., 2012. The regulation of integrin function by divalent cations. *Cell Adh. Migr.* 6, 20–29.

## Supplementary material

**Suppl. Fig. 1. Phagocytosis of LB and IgG-LB**

Human macrophages were exposed to IgG-LB (MOI 10:1) or LB (MOI 30:1) and phagocytosis was synchronized as described in the legend of Fig. 1. The percentage of cells with phagosomes and the number of phagosomes per cell was quantified. Results from at least 45 cells/time point from 3 (IgG-LB) or 2 to 3 donors (LB) are expressed as mean  $\pm$  SD.





### Suppl. Fig. 3. PAPA are dynamic actin structures

F-actin (artificially coloured in green) was monitored by confocal microscopy in macrophages expressing Life-Act cherry exposed to IgG-LB (artificially coloured in pink) for 2 hours. Z stacks at the indicated time points show phagosomes and podosomes (dorsal and ventral sections of macrophages, respectively). A PAP is pointed by an arrowhead. The lifetime of PAPs expressed as mean  $\pm$  SD of 16 PAPs is shown in the dot plot.

### Video 1. Phagosomes with actin structures.

Macrophages challenged with OZ (blue) were fixed, stained and imaged with a super-resolution confocal microscope equipped with a Fast Airyscan module. Actin structures (grey) on phagosomes are shown, scale bar 10  $\mu$ m.

Link to the online version: <https://ars.els-cdn.com/content/image/1-s2.0-S0171933521000121-mmc7.mp4>

### Video 2. Phagosome-associated podosomes (PAPA) on phagosomes containing IgG-LB

Macrophages were challenged with IgG-LB, fixed, stained and imaged with a super-resolution confocal microscope equipped with a Fast Airyscan module. A PAP is pointed by an arrowhead, latex bead (blue), vinculin (green) F-actin (red), scale bar: 10  $\mu$ m

Link to the online version: <https://ars.els-cdn.com/content/image/1-s2.0-S0171933521000121-mmc5.mp4>

**Video 3.** Monitoring of PAPs and podosomes in macrophages ingesting IgG-LB.

Macrophages expressing Life-Act cherry were incubated with IgG-LB and monitored by confocal microscopy. An arrowhead points to a PAP forming on a phagosome. Beads (magenta), F-actin (green).

Link to the online version: <https://ars.els-cdn.com/content/image/1-s2.0-S0171933521000121-mmc6.mp4>

### III. Perspectives

In this work, we demonstrated the presence of actin *foci* at the phagosome surface which associated with characteristic podosome proteins around the F-actin peak, and showed similar life-time and size as podosomes. We therefore named these structures PAPs, for phagosomes associated podosomes. This finding is in accordance with previous literature also describing podosomes-like structures at the phagocytic cup (Allen and Aderem, 1996; Labrousse, 2011; Ostrowski *et al.*, 2019). These PAPs formed only during phagocytosis of opsonized particles (polystyrene beads or zymosan) and concomitantly correlated with the disappearance of podosomes at the ventral face of macrophages, suggesting a re-localisation of podosomes during phagocytosis. Moreover, the presence of PAPs has been shown to correlate with the phagosome maturation, thus, PAPs are proposed to act as furtive docking and fusion site for late endosomes/lysosomes with the phagosome.

#### 1. Proteic composition and structure of podosome

Ever since publication of this work, other groups have described the structure of podosome-like structures at the phagocytic site (Vorselen *et al.*, 2021; Herron *et al.*, 2022).

Using super-resolution microscopy and frustrated phagocytosis assay with macrophages, Herron *et al.* reported so called “phagocytic podosomes” at Fc-phagocytosis sites (Herron *et al.*, 2022). This 3D nano-architecture study revealed an hourglass shape of podosomes, instead of the commonly described cone-shape (Dries *et al.*, 2019). The podosome height is found to be  $330 \pm 20$  nm, when our study report a  $511 \pm 107$ nm height and previous literature 400 to 700nm (Linder, 2007; Labernadie *et al.*, 2010; van den Dries, Nahidiazar, *et al.*, 2019). Discrepancies observed might be due to the different cell lines (Raw264.7 in this study, primary human macrophages in ours); the frustrated phagocytosis state or the better resolution of their imaging technique. However, similarly to our results, Herron *et al.* showed that cortactin co-localizes with actin; and talin and paxillin accumulate around the peak of F-actin (Herron *et al.*, 2022).

Vorselen *et al.* used polyacrylamide deformable beads to quantify actin dynamics and subcellular forces during macrophage Fc $\gamma$  - phagocytosis (Vorselen *et al.*, 2021). At the phagocytic cup, they showed actin protrusions called “teeth” resembling 2D podosomes by their size (1 $\mu$ m diameter) and protrusive nature. If cortactin also co-localises with F-actin, paxillin and vinculin appear in a punctate-like pattern behind the teeth, which is different from the

distribution around the F-actin described in our study, closer to the ring model of 2D podosomes (Dries *et al.*, 2019). This could be due to the difficulty to visualize the supramolecular architecture of these structures in a 3D context, where phagocytosis occurs on targets with different curvature angle and size (3  $\mu\text{m}$  in our study, 10  $\mu\text{m}$  in Vorselen).

In short, further studies on the composition of podosome-like structures at the phagosome do not allow to formally conclude on their exact nature.

## 2. Role of the Arp2/3 complex

The mild effect of Arp2/3 inhibitor CK666 is intriguing. Rotty *et al.* show that the Arp2/3 complex is not necessary to induce Fc $\gamma$ -mediated phagocytosis, although uptake of large (> 6 $\mu\text{m}$ ) targets is delayed upon inhibition of the above mentioned complex (Rotty *et al.*, 2017). Additionally, Vorselen *et al.* reported that phagocytic teeth are strongly affected by 150  $\mu\text{M}$  of CK666, with a decrease of 80% of the number of teeth (Vorselen *et al.*, 2021), while same dose of CK666 in our study poorly disrupts PAPs. This discrepancy could be explained by the difference in phagocytic targets used: small and stiff in our study (3  $\mu\text{m}$  in diameter, MPa range), large and soft in Vorselen's (9  $\mu\text{m}$  in diameter, 1,4 kPa).

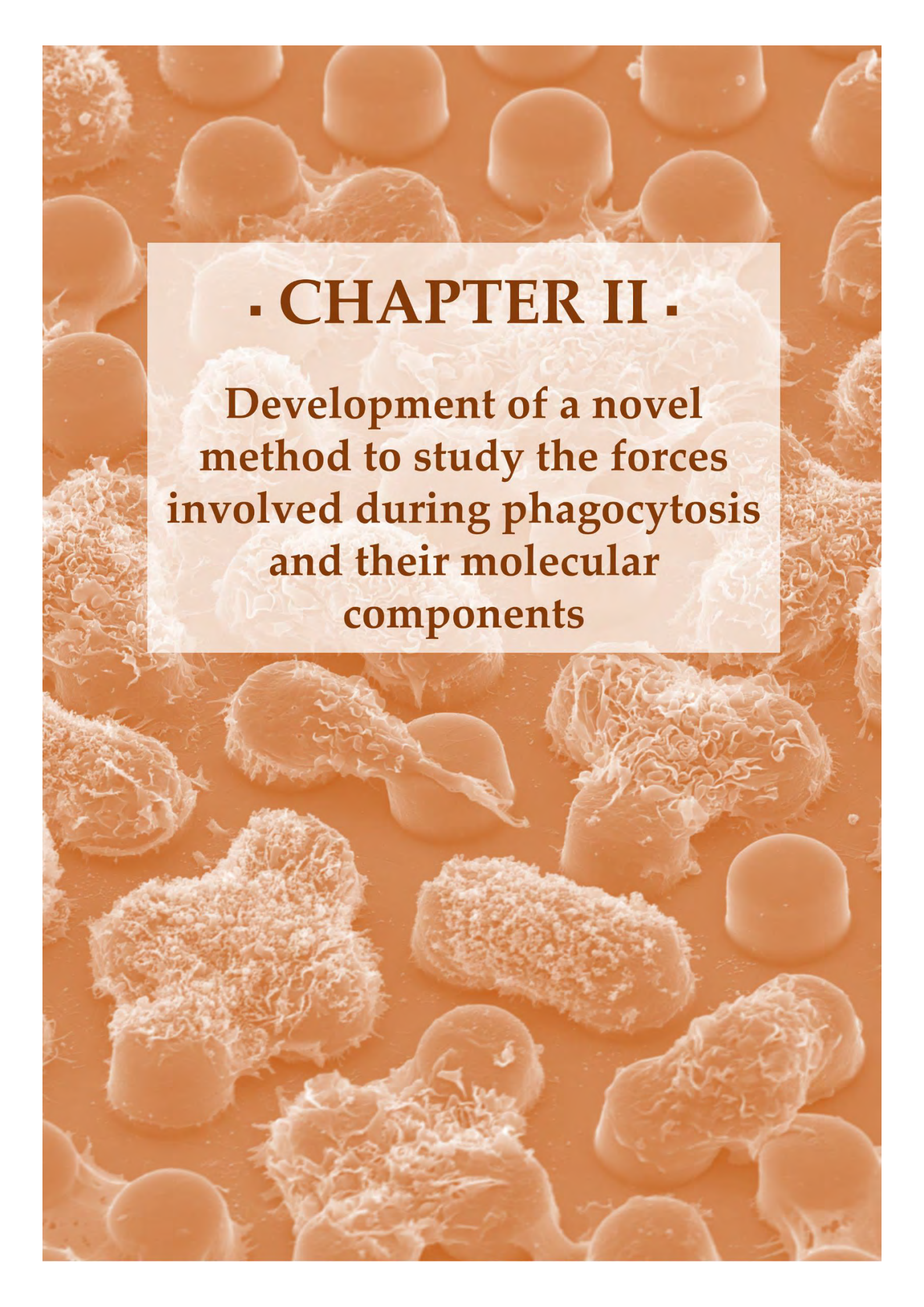
Another explanation could be the sensitivity to the inhibitor used. If 50  $\mu\text{M}$  of CK666 were sufficient to disrupt podosomes at the ventral face of macrophages, 150  $\mu\text{M}$  didn't seem to affect much the PAPs formation. The Arp2/3 complex consists of seven subunits, with some (ARPC1 and ARPC5) encoded by different isoforms, which confer them distinct properties in actin assembly and disassembly (Abella *et al.*, 2016). It is possible that PAPs and podosomes don't require the same isoforms of Arp2/3 complex subunits for their F-actin nucleation. The efficacy of commercially available inhibitors such as CK666, used in this study, or others (i.e CK869) on different isoforms of Arp2/3 complex have not been investigated to our knowledge, but might explain the discrepancies observed in this work.

## 3. A competition between phagocytosis and migration?

The concomitant disappearance of podosomes from the ventral face and the apparition of PAPs suggest a re-localisation of these structures during phagocytosis. Furthermore, if podosome number decrease during phagocytosis of IgG-LB, their migratory function supported by podosomes is certainly defective. Both migration and phagocytosis require actin-cytoskeletal remodelling to produce F-actin-rich membrane structures, mediated by the Arp2/3 complex

(Rougerie, Miskolci and Cox, 2013). It is thus tempting to assume a competitive relationship between these two processes. It would be interesting to test on migrating cells whether the presence of phagocytic targets on their way slows down their migration, by prioritizing phagocytosis over migration. Paterson and Lämmermann investigated the influence of cell shape and motility of macrophages on efferocytosis, a specific type of phagocytosis targeting apoptotic cells and mediated through phosphatidylserine (PS). Macrophages were challenged with PS coated beads or apoptotic bodies when in 3D matrix (Matrigel or Collagen) to evaluate clearance of the latest (Paterson and Lämmermann, 2022). If this experimental configuration would allow to answer our question, no look has been given to the speed of migration upon phagocytosis.



A scanning electron micrograph (SEM) showing a dense population of cells. The cells exhibit various morphologies, including smooth, rounded spheres and more complex, irregular shapes with prominent surface ruffles and filaments. The overall color is a monochromatic orange-brown. A semi-transparent white rectangular box is centered over the image, containing the chapter title and subtitle.

## **· CHAPTER II ·**

**Development of a novel  
method to study the forces  
involved during phagocytosis  
and their molecular  
components**

## **I. Objectives and summary of the paper**

Our observation of PAPs confirms the previous papers relating to the presence of podosome-like structures in forming phagosomes. As mentioned previously, Vorselen et al. later describe the presence of “phagocytic teeth” at the forming phagosome, which is related to the compressive forces of macrophages on the phagocytic target (Vorselen et al., 2021). Total compressive forces measured on 1.4 kPa polyacrylamide beads range from 1 to 10 pN at the phagocytic rim around the beads and are reported to be regulated based on target stiffness. However, the fact that measurements were performed on fixed cells could result in an underestimation of these forces, since fixation relaxes the internal tension within the cell (Vorselen *et al.*, 2021). Lead by this observation, we thus chose to develop a method to evaluate forces during phagocytosis on living cells. The next part will describe this development, the forces evaluated and the involvement of molecular components of the phagocytic cup to generate these forces. It is written as an article that will be completed before submission.

## II. Article: Compression force microscopy

### Compression Force Microscopy: a simple method to evaluate phagocytic forces

Claire Bigot<sup>1,2</sup>, Javier Rey Barroso<sup>1</sup>, Marjolaine Malgeri<sup>2</sup>, Adrian Laborde<sup>2</sup>, Isabelle Maridonneau-Parini<sup>1</sup>, Christel Vérolet<sup>1</sup>, Laurent Malaquin<sup>2,#</sup>, Renaud Poincloux<sup>1,#</sup>

<sup>1</sup> Institut de Pharmacologie et de Biologie Structurale, Université de Toulouse, CNRS, UPS, France

<sup>2</sup> LAAS-CNRS, Université de Toulouse, CNRS, INSA, Toulouse, France

# co-corresponding authors

Correspondence: [laurent.malaquin@laas.fr](mailto:laurent.malaquin@laas.fr) and [renaud.poincloux@ipbs.fr](mailto:renaud.poincloux@ipbs.fr)

#### Abstract

Macrophages are innate immune cells that are present in all tissues to maintain immune surveillance and homeostasis, in particular through the ingestion of bacteria or apoptotic cells. This process, called phagocytosis, involves a dynamic reorganization of the actin cytoskeleton and the generation of traction and compression forces. Despite the importance of this mechanism, the molecular mechanisms involved in force generation during phagocytosis are still poorly documented and understood. This is mainly due to the lack of a simple method for the evaluation of these forces on a large number of living cells. We, therefore, propose a new method, called Compression Force Microscopy, that consists in analyzing the forces applied by macrophages phagocytosing polyacrylamide micropillars of controlled size and stiffness. We developed an automated procedure to measure with high accuracy the displacement and radius reduction of the pillars upon phagocytosis by living human monocyte-derived macrophages. Finite element-based mechanical simulations were then used to estimate the amplitude and direction of compression and traction forces generated, revealed that the deformation energy per pillar does not vary with its stiffness, and confirmed the involvement of actomyosin machinery for phagocytic force generation. Finally, our model of 2.5D frustrated phagocytosis enabled the analysis of the dynamics of the forces generated over several hours and on a large number of cells in parallel. It revealed that traction and compression forces are not coupled nor simultaneous and that the magnitude of the forces decreases with the number of phagocytosis events, which suggests that macrophages are more efficient at phagocytosing one particle at a time.

## Introduction

Phagocytosis is a cellular mechanism that consists in the detection, internalization and elimination of particles larger than 0.5  $\mu\text{m}$  diameter, such as bacteria, viruses and fungi or apoptotic cells. In pluricellular organisms, this process is mainly performed by a set of specialized cells called phagocytes, which includes monocytes, macrophages, neutrophils, dendritic cells, osteoclasts and eosinophils (Rabinovitch, 1995). Given the crucial role of phagocytosis in immune response and homeostasis, a better understanding of its regulation is not only interesting for fundamental research but has also important potential therapeutical applications (Uribe-Querol and Rosales, 2020).

Although it had been first described more than a century ago (Metchnikoff, 1905), there are still unknowns about this process. In particular, the mechanisms used by phagocytes to apply forces onto their targets during phagocytosis are very poorly known. This is mainly due to a lack of a simple and large-scale strategy to evaluate mechanical forces and their dynamics.

Several methods have been proposed to address the mechanics of phagocytosis. Micropipette aspiration revealed the evolution of phagocyte membrane tension during phagocytosis (Evans, Leung and Zhelev, 1993; Herant, Heinrich and Dembo, 2005; Zak *et al.*, 2019). Atomic force microscopy and magnetic and optical tweezers showed the dynamics and amplitude of traction forces used by cells to attract particles for phagocytosis (Vonna *et al.*, 2003, 2007; Kress *et al.*, 2007; Schuerle *et al.*, 2017; Nelsen *et al.*, 2019). Traction force microscopy (TFM) allowed the evaluation of the forces generated by cells during 2D frustrated phagocytosis and revealed centripetal forces (Kovari *et al.*, 2016). These inward directed forces could be reminiscent either of the traction forces used by phagocytes to attract particles or of contraction forces generated on the particles during phagocytosis.

Recently, Vorselen *et al.* proposed an intriguing approach where polyacrylamide substrates typically used for TFM were turned into microspheres and used as force sensors (Mohagheghian *et al.*, 2018; Träber *et al.*, 2019). The author synthesized such deformable and tuneable polyacrylamide beads on a batch scale and coated them with IgG to trigger FcR-phagocytosis. The shape of the particles could be resolved with high,  $<50$  nm, precision using regular confocal microscopy. From the 3D mapping of the deformations imposed by macrophages phagocytosing the particle, a computational method then allowed the evaluation of the forces responsible for the deformations. The use of that elegant technique revealed that at the beginning of phagocytosis, macrophages generate both pushing forces into the particle at the initial point of contact and pulling forces around it. These forces spatiotemporally evolve into a contractile punctate ring moving along the particle, progressively squeezing it until the closure of the phagocytic cup. Moreover, shear forces are applied at the equator of the particle,

resulting in longitudinal deformation of the bead (Vorselen *et al.*, 2020). Vorselen *et al.* suggest that actin protrusions containing myosin 1e and 1f act like “teeth”, connected together in a ring. Moreover, this technique supports the myosin-II contractile role in phagocytic cup closure, since it contributes to late-stage force generation, actomyosin networks being described as the “jaw” (Vorselen *et al.*, 2021). However, using this approach at a larger scale to study biological mechanisms would involve either very long hours of microscopy or fixing the samples, which induces relaxation of the samples and significantly affects the measurement of the forces involved (Vorselen *et al.*, 2021).

In this context, we propose a simple and complementary method to evaluate both compression and traction forces during phagocytosis. It consists of the microfabrication of hexagonal lattices of polyacrylamide IgG-coated micropillars, the dynamic measurement of their deformations during phagocytosis and the analysis of mechanical forces responsible for the deformation using mechanical simulations. This method confirmed the involvement of actomyosin for phagocytosis contractions and revealed how macrophages apply higher forces when trying to phagocyte one vs several pillars at the same time, which suggests that macrophages are most effective when they concentrate their forces on phagocytosing particles one by one.

## Results

### Fabrication of polyacrylamide micropillars for the observation of the phagocytosis-associated forces

Observing the forces at work during phagocytosis is challenging because this process lasts only a few minutes (Horsthemke et al., 2017; Vorselen et al., 2021) and its occurrence under the microscope is difficult to be managed. To control where the phagocytosis events will take place, and to be able to observe and measure, for several hours, the mechanical action of macrophages on the particles to be ingested, we propose a new approach. It consists in analysing the forces applied by macrophages phagocytosing polyacrylamide micropillars of controlled size and stiffness (**Fig.1A**). Microfabrication allows large-scale fabrication and precise control of the location and geometry of the pillars to be phagocytosed. In this configuration, macrophages will not be able to fully engulf the pillars, and the phagocytosis process will be frustrated. Despite this limitation, this particular setup allows the observation of a large number of phagocytosis events in parallel during the hour range, with no need to fix the samples which risks releasing cellular tension (Vorselen et al., 2021). The second advantage of this approach is that both compression and traction forces can be evaluated in a very simple way, in real-time, by measuring the radius and position of the pillar, respectively (**Fig.1A**).

For this purpose, silicon moulds were fabricated by photolithography. Silicon wafers covered with 1  $\mu\text{m}$ -thick resin (ECI1.1) were UV exposed through masks with hexagonal patterns of holes. The areas of the wafers not covered by the resin were plasma etched to a depth of 5  $\mu\text{m}$ . After the removal of resin with acetone and plasma cleaning, the moulds were characterized by scanning electron microscopy (SEM) (**Fig.S1A-B**). Two moulds were used in this study: a first mould with various hole diameters (from 3 to 9  $\mu\text{m}$ ) with a centre-to-centre spacing of 12  $\mu\text{m}$  (upper panel) and a second mould with a single hole diameter of 9  $\mu\text{m}$  and centre-to-centre spacing of 15  $\mu\text{m}$  (lower panel) (**Fig.S1B**).

We chose to use polyacrylamide (PAA), because of its chemical stability and non-adherent properties that allow to precisely monitor the ligands on its surface by covalently linking them through adapted functionalization. Furthermore, PAA exhibits a large and easily obtainable range of stiffness by simply modulating the ratio of acrylamide - the polymer - and N, N'-methylene bisacrylamide - the crosslinker (Mustapha, Sengupta and Puech, 2022). The range of stiffness, from 3 to 40 kPa considered in this study, replicates well the one of potential phagocytic targets a macrophage is susceptible to encounter. To keep the same amount of

polymer in each condition, the quantity of crosslinker only was adapted to tune the stiffness of the gel. Polyacrylamide micropillars lie on a base of the same material of 10  $\mu\text{m}$  so that the cells would not respond to the rigidity of the underlying glass (Tusan *et al.*, 2018).

Pre-gel solution of polyacrylamide (PAA) incorporating rhodaminB methacrylate was cast onto the silicon mould, which surface was previously activated by a 15 min UV-Ozone treatment (Shibata, Heo and Takeuchi, 2011). Before their complete reticulation, hydrogels were covered with an amino silanized glass coverslip. Once full polymerization was completed, top coverslips were gently removed from the silicon mould and micro structured polyacrylamide gels were functionalised, first with ovalbumin, then with IgG to trigger Fc phagocytosis (**Fig.S1C**). Confocal microscopy revealed the successful fabrication and labelling of the pillars, both in their volume and on their surface (**Fig.S1D**).

We then sought to assess the behaviour of macrophages on the pillars. We first observed by SEM human macrophages derived from primary monocytes on IgG-coated micropillars obtained in PDMS (Poly(Dimethyl Siloxane)) using the same moulds. It revealed that macrophages adhered and appeared to engulf up to 7 pillars at the same time (**Fig.1B**). Observations by confocal microscopy further showed that, in comparison to control pillars not in contact with macrophages, engulfed pillars could appear smaller and deflected (**Fig.1C**), which suggested that macrophages applied compression and traction forces during the phagocytosis of the pillars.

We, therefore, sought to develop a procedure to automatically evaluate the compression and traction forces from the images of the pillars.

### **Automated analysis coupled with finite element simulations allows the evaluation of phagocytic forces**

To convert the images of the pillars into force values, we first developed and evaluated the precision of two different algorithms that measure pillar dimensions and positions. Given the ideal geometry of the pillars and their orientation for observation by light microscopy, we opted for the simplest possible procedure, using only one illumination correction to segment as many pillars as possible in a single step, and thus locate their geometrical centre and radius, evaluated by considering the segmented surface as a circle (**Fig.S2A**).

To assess the deformation of a pillar, it is necessary to know the original position and diameter of the pillar, before any contact with a cell. Thanks to microfabrication, two options are available. One can either determine the original position and shape of the pillar by considering

the control, i.e. non-phagocytosed, pillars surroundings the pillar of interest (method #1, **Fig.S2B**). Or one can use the geometry of the pillar of interest if it was imaged before the cells arrived (method #2, **Fig.S2B**). We aimed at comparing the precision of both approaches.

The precision of the radius measurement was evaluated as the standard deviation of the radius of control, uncompressed, pillars, and the precision of the deflection measurement was assessed as the deviation from the mean of the uncompressed, control pillar positions. Despite their simplicity, both methods were revealed to be extremely precise in radius and position measurement. Methods #1 and #2 yielded precision for the measurement of the pillar radius of 23 nm, regardless of the number of control pillars considered, and 8 nm, respectively (**Fig.S2C**). These values correspond to the accuracy of undistorted pillar measurements, not to the resolution of the images. Such precision, well below optical resolution, is possible due to the very high reproducibility of the microfabrication process. These experimental measurements prove that similar to the high accuracy of measuring the position of a molecule in single-molecule localisation microscopy, the measurement of an object can be done with very high fidelity. Precisions of 125 to 93 nm were achieved for the measurements of the pillar deflection, for methods #1 and #2, respectively (**Fig.S2D**). As both are effective, we have chosen to use them according to the type of acquisition. Method #2 for live acquisitions allowing access to the initial, cell-free positions of the pillars and method #1 for single time point acquisitions.

Analysis of pillars of different radius showed that the measurement of large (6.3  $\mu\text{m}$  radius) pillars are relatively more accurate than that of thinner pillars (**Fig.S2E**). Of note, the measurement of these pillars revealed that the pillar radius is larger than that of the mould, suggesting a swelling behaviour of the polyacrylamide (Subramani *et al.*, 2020). For instance, moulds of 1.5  $\mu\text{m}$  radius give 2.3  $\mu\text{m}$  radius pillars, and moulds of 4.5  $\mu\text{m}$  radius give 6.3  $\mu\text{m}$  radius pillars for 10 kPa PAA. Compressive deformations being more easily detectable on large pillars, relative to their size, we chose to use them for the rest of the work.

In order to evaluate the distribution and values of forces responsible for the pillar deformations, we performed mechanical simulations using the finite element-based method (COMSOL<sup>®</sup> Multiphysics software). In the case of pillar compression, the approach consists in reproducing the pillar geometry from experimental observation and resolving equation of deformation considering an elastic model (see Methods). We selected phagocytic events where one cell is engaged on a single pillar. For each simulated pillar, the range of deformation in xy plan (purple/orange), pressure (green/yellow), normal and shear stress were plotted. Representative pillars deformed on their top, middle or bottom are represented (**Fig.2A-C**). The calculated strain energy for each pillar was found to fit using a square function with the

total volume compression of the pillar (**Fig.2D**). These simulations reveal that it is sufficient to measure the total compression of the pillars to be able to evaluate the strain energy of the pillar and thus understand the forces applied to it.

It is to be noted that the 40 kPa condition has been simulated over a small number of pillars (6), thus providing less accuracy in the correlation as compared with other conditions ( $R^2=0.95$ , 0.94 and 0.08 for 3, 10 and 40 kPa, respectively). For the remainder of this study, we have chosen to use 10 kPa as the stiffness because the deformations at this stiffness are below 10%, and are therefore compatible with a linear elastic regime while being high enough to be well above the measurement accuracy.

For the estimation of traction strain energies, we could not use the beam theory classically used for pillar based TFM (Mustapha, Sengupta and Puech, 2022) as both the aspect ratio of our pillars and the presence of a 10  $\mu\text{m}$  layer of PAA under the pillar are incompatible with these equations. We therefore simulated increasing shear forces on a pillar top surface and established a calibration curve between the resulting deflection and the pillar strain energy (**Fig.S3**).

### **Influence of the substrate stiffness and actomyosin on compression forces**

We started addressing the molecular mechanisms responsible for pillar compression. Confocal imaging on fixed samples stained for F-actin and SEM acquisitions on unroofed macrophages showed enrichment in punctate F-actin around the pillars. (**Fig.3A-B**).

We then analysed the deformations of the pillars by living macrophages, and quantified pillar compression, expressed either as their maximal radius compression (i.e. the most reduced radius along the pillar height) or their total volume compression. Cytochalasin D, a potent inhibitor of actin polymerisation, and nitro-blebbistatin, an inhibitor of non-muscular myosin II, significantly reduced the pillar compression and strain energy. More surprisingly, a 50  $\mu\text{M}$  dose of CK666, an inhibitor of the Arp2/3 complex, did not affect the pillar compression, in contradiction with previous work where CK666 significantly inhibits contraction (Vorselen *et al.*, 2021), although at a higher dose of 150  $\mu\text{M}$  which will be tested on our system. Also surprisingly, the inhibition of dynamin-II with dynasore did not affect pillar compression (**Fig.3C**), while dynamin-2 has been proposed as important for Fc-phagocytosis (Marie-Anaïs *et al.*, 2016)

Next, we evaluated how pillar stiffness influences phagocytic forces. Pillars of different stiffness (Young's modulus of 3, 10 and 40 kPa) showed a different rate of compression in terms of

radius and volume reduction. However, the related strain energy shows no significant differences for 3, 10 and 40 kPa pillars (94 +/- 97; 95 +/- 106; and 65 +/- 48 fJ respectively) (**Fig.3D**). This may suggest that Fc phagocytosis is not a mechanosensitive process, what would contradict recent work (Beningo and Wang, 2002; Rougerie, Miskolci and Cox, 2013; Vorselen *et al.*, 2021). Another hypothesis could explain this apparent contradiction: in the context of frustrated phagocytosis of an opsonized target, macrophages could be triggered to apply a maximum of forces in an attempt to detach and complete pillars phagocytosis. Following this hypothesis, we reasoned that macrophages should reach their maximum effort when attempting to phagocytose one pillar, and that the simultaneous engulfment of multiple pillars would not lead to an increase in total effort but to its distribution among the different targets. For this purpose, we addressed the dynamics of phagocytosis-associated forces.

### **Compression and traction amplitudes depend on the number of pillars phagocytosed**

To reveal the dynamics of compression and traction forces in macrophage phagocytosis we followed by time-lapse confocal microscopy pillar deformations upon contact with macrophages over two hours (**Fig.4A** and **VideoS1**). Macrophages spread upon contact with the pillars, quickly covering one or several pillars. Pillars being phagocytosed could be both compressed and deflected or only compressed or only deflected (**Fig.4A**), suggesting that compression and traction mechanisms are probably uncoupled. Analyses showed that pillar compression was triggered just after cell arrival, and then increased progressively until it arrived at a plateau. Compression energy curves were fitted using a “plateau followed by one phase association” equation:  $E = E_{\text{plateau}} * (1 - e^{-(t-t_0)/\text{Tau}})$ , where E is the compression energy, t the time and Tau the time constant. Measurement of the Tau, which corresponds to the time required for compression up to 63% of the plateau value, yielded an average value of 11min and 20s (**Fig.4B-C**). This stable phase lasted at least 30 min for most of the pillars analysed, decreasing slightly afterwards for some pillars. This plateau supports the assumption of maximum effort per pillar.

The traction forces were found to be much lower than the compressive forces and showed a smooth progression along the length of the video for some of the pillars, whereas the compression reached a plateau much faster (**Fig.4B-C**). This completely different dynamic suggests that different molecular mechanisms and cellular structures may be at play for the compression and traction of the particles.

To evaluate the behaviour of macrophages facing several pillars at the same time, we compared the forces and strain energy corresponding to macrophages trying to engulf one,

two or three pillars. Analyses on compression energy at 30, 60, 90 and 120-time points showed a two or three-fold decrease of the energy at the plateau phase (60 and 90 min time points), per pillar, when the cell phagocytosed two or three pillars, respectively (**Fig.4D**, left). Thus, macrophages facing multiple targets lose progressively their ability to compress each of them. We further investigated the impact of the number of phagocytic targets on the total compressive energy by evaluating the energy values for each targeted pillar. At the plateau, results indicated no significant increase in the total compression energy exerted by a cell when phagocytosing multiple pillars but no difference between 2 and 3 targets (**Fig.4D**, right). This confirms that would mean that cells exert most of their compression forces from the first target, and they cannot escalate in response to several ones.

In sharp contrast, the analysis on traction forces confirmed that they are much lower than compression forces, and showed that cells engulfing one pillar hardly displaced it, while cells phagocytosing multiple pillars pulled them efficiently, especially in the case of two facing pillars (**Fig.4E**, left). This trend was maintained when the total traction energy was calculated (**Fig.4E**, right).

Altogether, time-lapse analyses reveal that traction and compression forces are not necessarily coupled and that the magnitude of the compression forces on pillars, which does not depend on the pillar stiffness, quickly reaches a plateau whose value decreases with the number of phagocytosis events. This suggests that macrophages are more efficient at phagocytosing one particle at a time.

## Discussion

In the present study, we developed PAA micropillars to evaluate normal and shear forces applied by macrophages during frustrated phagocytosis. Using confocal imaging and a simple method of analysis, we were able to estimate both the deflection and compression of the pillars for several hours. Finite element-based simulations permitted to associate strain energy values to these measured deformations at the pillar level, which ease the comparison of each culture condition further tested. We confirmed that contraction forces are actomyosin-dependent (Vorselen *et al.*, 2021). The strain energy in this configuration of frustrated phagocytosis appears however independent of material stiffness, which is in contrast with literature establishing Fc-phagocytosis as a mechanosensitive process (Beningo and Wang, 2002; Rougerie, Miskolci and Cox, 2013; Vorselen *et al.*, 2021). Finally, investigating the dynamics of the process suggests that if trying to engulf several targets at the same time, macrophages apply lower maximal force and lower energy values than when facing a single particle.

Polyacrylamide has long been used as a substrate for force measurements, in the form of a flat substrate (Mustapha, Sengupta and Puech, 2022), or more recently in the shape of beads (Mohagheghian et al., 2018; Träber et al., 2019). Elegantly adapted to the study of phagocytosis by Vorselen et al. (Vorselen et al., 2021), polyacrylamide beads allow the evaluation of the distribution and amplitude of normal and shear stresses. In our approach, the pillar configuration permits precise control of localisation of the phagocytic event, and enables the simultaneous measurement of compression and deflexion forces of phagocytic events involving multiple targets as well as evaluation of forces on longer times. Together, these parameters allowed observations of this dynamic process in living cells. This particular setup is also the first, to our knowledge, to allow the estimation of normal forces in a frustrated phagocytosis configuration.

The actomyosin dependence of the contractile forces demonstrated *via* direct inhibitions of actin polymerisation and myosin-II, is in accordance with previous studies and validates the hypothesis of myosin-II contractile role in the phagocytic cup closure in FcR phagocytosis (Swanson et al., 1999; Araki, 2006; Tsai and Discher, 2008; Kovari et al., 2016; Vorselen et al., 2021). However, the inhibition of Arp2/3 using a 50  $\mu$ M dose of CK666 did not show any effect on the compression rate. This is in contrast with previous work (Vorselen et al., 2021), although in that case the dose was three times higher, and higher concentrations should be tested to conclude. The role of the Arp2/3 complex has already been debated. Long considered as the major actor of actin polymerisation in phagocytosis (Caron and Hall, 1998; May et al., 2000), its role has been proposed to be modulated by the target size, since it was described as non-required for FcR phagocytosis of small, 2  $\mu$ m, targets (Rotty et al., 2017). Because the dimension of the target pillars used in this study does not fit this range, either the CK666 dose employed was too low, as mentioned previously, either compensatory mechanism for actin polymerisation occurred. Upon inhibition of the Arp2/3 complex, formins have already been shown to mediate a compensatory F-actin assembly (Hotulainen and Lappalainen, 2006; Steffen et al., 2006; Suraneni et al., 2012; Wu et al., 2012), although in FcR phagocytosis, their inhibition via the poorly specific formin inhibitor SMIFH2 did not affect the constriction magnitude of polyacrylamide beads (Vorselen et al., 2021). Another candidate could also be Ena/VASP family proteins that were found in the forming phagosome (Coppolino et al., 2001) and promoting F-actin filament elongation *via* recruitment of profilin, protection of growing barbed ends of actin from capping proteins, and direct interaction with WASP (Bear et al., 2002).

Also surprisingly, dynasore, an inhibitor of dynamin-2, had no significant effect on compression forces. Dynamin has been proposed to play different roles in Fc phagocytosis. First, dynamin was related to its capacity to recruit membrane to nascent phagosomes during pseudopod

extension, particularly for the internalization of large targets (Tse et al., 2003) (Huynh and Grinstein, 2008). According to this hypothesis, the extension of pseudopods in an attempt of internalising large pillars would require dynamin-II to deliver intracellular vesicles membrane to the phagocytic site. Because we have not analysed the rate of extension of the advancing pseudopods, it is difficult to conclude on that hypothesis. One could speculate that upon dynamin-2 inhibition, the constriction would occur upper in the pillar: limited by the amount of membrane available, the cell could start to apply forces, as it has been described previously (Masters et al., 2013; Kovari et al., 2016). Second, dynamin-2 was proposed to mediate F-actin recruitment at the phagocytic cup, since its inhibition in FcR phagocytosis impairs the initial step of phagosome formation and actin recruitment (Marie-Anaïs et al., 2016). The absence of phenotype on force generation in our system is in contradiction with this hypothesis or suggests the existence of a compensation mechanism. Last, dynamin-2 was also proposed to close the phagosome *via* its contractile activity (Marie-Anaïs et al., 2016). Given the frustrated phagocytosis state and the relatively low rate of compression, it seems unlikely that the pseudopods get close enough to each other for the ring-shaped configuration of dynamin-2 to form (Morlot and Roux, 2013). With our experimental configuration of frustrated phagocytosis, we cannot address this hypothesis and a dedicated system allowing the measurement of forces during the complete steps of phagocytosis could be necessary.

Microfabrication allowed accurate control of the position of the pillars, and thus of the phagocytic events. We could advantageously benefit from this feature to design arrays of pillars so that a single cell would encounter several phagocytic targets at the same time, and strain energies of each target could be obtained individually or added up to estimate the total energy deployed by the cell to induce the observed deformations. The total strain energy per cell remained stable upon phagocytosis of one, two or three pillars at the same time. This suggests that phagocytic forces reach a maximum value that cannot be overcome by the uptake of additional targets. This would imply that forces exerted to pull or mechanically remodel the target macrophages are applied by macrophages preferentially on one target. Interestingly, phagocytosis efficiency, i.e. the average number of internalized particles per phagocytic cell within a definite time (Leishman, 1902), has been shown to decrease with the number, or the size, of particles (Roberts and Quastel, 1963; Simon and Schmid-Schönbein, 1988; Pacheco, White and Sulchek, 2013), supporting studies interpreting membrane availability as a limiting factor for phagocytosis (Cannon and Swanson, 1992; Herant, Heinrich and Dembo, 2005). According to this hypothesis, more membrane surface is involved upon ingestion of multiple particles at once. Whether the limiting factor is the amount of force and/or the availability of plasma membrane is an intriguing question.

This method should pave the way for the investigation of the molecular mechanisms and dynamics of the force generation during phagocytosis, but also for other applications such as the immunological synapse or trogocytosis, a process used by cells to physically extract and ingest bites of cellular material from another cell (Bettadapur, Miller and Ralston, 2020).

## **Methods**

### **Differentiation and culture of human primary monocyte-derived macrophages**

Human peripheral blood mononuclear cells were isolated from the blood of healthy donors by centrifugation through Ficoll-Paque Plus (Dutscher), resuspended in cold phosphate-buffered saline (PBS) supplemented with 2 mM EDTA, 0.5% heat-inactivated Fetal Calf Serum (FCS) at pH 7.4 and monocytes were magnetically sorted with magnetic microbeads coupled with antibodies directed against CD14 (Miltenyi Biotec # 130-050-201). Monocytes were then seeded on glass coverslips at  $1.5 \times 10^6$  cells/well in six-well plates in RPMI 1640 (Invitrogen) without FCS. After 2 h at 37°C in a humidified 5% CO<sub>2</sub> atmosphere, the medium was replaced by RPMI containing 10% FCS and 20 ng/mL of Macrophage Colony-Stimulating Factor (M-CSF) (Miltenyi 130096489). For experiments, cells were harvested on day 7 using trypsin-EDTA (Fisher Scientific).

In experiments analyzing the effect of cytoskeleton inhibitors, macrophages were pre-incubated for 15 min with either the drug solubilized in DMSO or a vehicle.

### **Silicon Mould Fabrication**

Microfabricated polyacrylamide pillars can be reproduced from a single silicon mould comprising the desired micropattern made from photolithography. An initial silicon wafer is spin-coated with ECI1.1 resist and exposed to UV through a mask (Methods\_Figure S1) allowing the specification of an arbitrary two-dimensional pattern (disk of 3 to 9 µm diameter). The wafer is then etched with plasma O<sub>2</sub> to a height determined by the user, typically ranging from 5 to 6 µm. Once fabricated, the silicon moulds were treated with UV-Ozone for 15 min (Jelight) for PAA moulding or using FluoroDecyltrichloroSilane (FDTS) using the SPD system for PDMS moulding. PDMS (Sylgard 184, Dow Corning) was prepared in a 10:1 (Base: Curing agent) ratio, degassed under vacuum and poured into the silicon mould. Crosslinking of PDMS was performed for 2 h at 60°C.

### **Fabrication of polyacrylamide pillar arrays**

PAA hydrogel preparation was adapted from (Tse, J. R. & Engler, 2010). Briefly, silicon moulds were treated with UV-Ozone cleaner for 15 min and covered with solutions containing a ratio of acrylamide, bis-acrylamide (Sigma) and distilled water to tune the elastic modulus as desired

(see Table S1); 2.5 mg/mL rhodamine B methacrylate for staining, and 0.15% TEMED and 1% ammonium persulfate in distilled water to allow reticulation. Before their complete reticulation, hydrogels were covered with an amino silanized glass coverslip. Once full polymerization was completed, top coverslips were gently removed from the silicon mould and micropatterned polyacrylamide was washed with 50 mM HEPES buffer at pH 8.4. Ovalbumin (Sigma) was covalently linked at the surface of the PAA gels using the photoactivable heterobifunctional reagent sulfosuccinimidyl-6-(4'-azido-2'-nitrophenyl amino) hexanoate (sulfo-SANPAH, VWR). After photoactivation with ultraviolet light, a 1 mg. mL<sup>-1</sup> ovalbumin solution (in 50 mM HEPES buffer) was incubated onto the PAA hydrogels for 30min at RT. To obtain IgG-opsonized pillars, ovalbumin-coated pillars were then incubated with anti-ovalbumin antibodies for 30 min (1:20, room temperature) and washed 3 times.

Before use, PAA hydrogels were washed three times with HEPES buffer (50 mM, pH 8.4), and incubated for 30 min at 37 °C in a cell culture medium before plating cells.

Supplementary Table 1: Composition of PAA gels

	Acrylamid (30%)	Bisacrylamid (1%)	TEMED	APS	H <sub>2</sub> O	RhodaminB-MA
3 kPa	166.7 µL (10%)	15 µL (0.03%)	0.75 µL	5 µL	312.6 µL	5 µL
10 kPa	166.7 µL (10%)	50 µL (0.1%)	0.75 µL	5 µL	278 µL	5 µL
40 kPa	166.7 µL (10%)	150 µL (0.3%)	0.75 µL	5 µL	178.4 µL	5 µL

### Frustrated phagocytosis assays

Glass coverslips with polyacrylamide pillars were placed at 37°C and controlled CO<sub>2</sub> on an AttoFluor® chamber (Invitrogen A7816) with pillars facing up and immersed with 500 µL of RPMI (Invitrogen) for 10 minutes to equilibrate. Macrophages were added in 500 µL RPMI supplemented with FCS 10% (Invitrogen) and allowed to contact and phagocyte pillars for 15 min before the beginning of acquisitions, then imaged for a maximum of 45 min. During observations, samples were maintained at 37 °C in humidified 5% CO<sub>2</sub> atmosphere.

Confocal images were taken using a Spinning Disc Confocal system mounted on a Nikon Eclipse Ti-E microscope equipped with a Hamamatsu C9100-50 EMCCD camera, a 63× (1.4 NA) PlanApo objective, and controlled by Micromanager software. Images were acquired every 0.3 µm and covered the full pillar length.

For phagocytosis dynamics experiments, videos were taken using a CSU-X1 Spinning Disc Confocal scanner mounted on a Nikon microscope equipped with a FLASH4 camera, a 60× (1.4 NA) PlanApo objective, and controlled by Metamorph software. Images were acquired every 2.1 µm stack with a time-lapse of 40 s for a total of 2 h.

### Immunofluorescence

After cell fixation for 15 min at RT with 3.7 % paraformaldehyde in PBS containing 15 mM sucrose, unreacted aldehyde functions were quenched with 50 mM NH<sub>4</sub>Cl in PBS for 5 min at RT as previously described (Labernadie *et al.*, 2010). Cells were then washed and permeabilized with 0.1 % Triton X100 in PBS for 10 min at RT before being saturated with 3% BSA in PBS for 30 min at RT. Cells were then stained with fluorescent phalloidin 546 (Invitrogen) for 30 min at RT to detect F-actin. Samples were imaged using a PL Fluotar 40x/ NA 1.0–0.5 oil immersion objective on a Leitz DM-RB microscope, equipped with a CoolSnap HQ CCD camera (Roper Scientific) and the Metaview software (Roper Scientific).

### Scanning electron microscopy

Macrophages plated on IgG-coated PDMS pillars for 30 min were fixed for 10 min in a 0.2 M sodium cacodylate buffer (pH 7.4) containing 2.5% glutaraldehyde (Electron Microscopy Sciences 16220), then washed with distilled water. The samples were then prepared for observation following the protocol: they were dehydrated through a graded series (25–100%) of ethanol, transferred in acetone and subjected to critical point drying with CO<sub>2</sub> in a Leica EM CPD300, then sputter-coated with 3 nm platinum with a Leica EM MED020 evaporator, and were examined and photographed with an FEI Quanta FEG250.

### Image analysis

Acquired image stacks were treated with Image J to extract pillar shapes and positions (**Fig.S2A**). Local illumination heterogeneity was corrected by duplicating the original stack, applying a Gaussian blur of 10  $\mu$ m then dividing each original image by the blurred one. An automatic threshold (default method) was then applied to the corrected stack to generate a binary mask. Then, for fixed imaging, the contrast phase channel was used to select the Regions of Interest (a central pillar covered by a cell, encircled by untouched pillars) and “Analyze particles” was launched in the ROI, using the binary mask, extracting pillars shape and position. Then, for each image on the stack, the deflection was calculated as the Euclidean distance between the central pillar barycentre position and its theoretical position, calculated as the mean position of the barycentre of the surrounding control pillars (method #1, **Fig.S2B**). Compression of the central pillar was calculated as the difference between the measured radius of the central pillar and the mean of the surrounding pillar's radius. Volume displacement was further integrated from the full z-stack.

For time lapse experiments, auto-thresholder pillars were segmented using the *Analyze particles* function of ImageJ. The phase contrast channel was used to identify the cell responsible for the deformations, and 12 cell-free pillars were measured for each video to be

used as controls. Lateral drift over time was first registered using the ImageJ stackreg plugin, then by subtracting the average position of the cell-free pillars. For each image on the stack at 8  $\mu\text{m}$  height, the deflection was calculated as the Euclidean distance between the pillar geometrical centre and its original position, calculated as the mean position of the first 5 time points (method #2, **Fig.S2B**). The deflection at the top of the pillars was evaluated by applying a multiplying factor of 1.2 to the position obtained at 8  $\mu\text{m}$ . Pillar compression was calculated as the difference between the measured radius pillar at each time point and the mean of the measured radius on the first 5 time points. Volume displacement was integrated from the full z-stack.

### **Finite element mechanical simulations**

The approach for numerical simulation of compression consisted in reproducing a pillar geometry from experimental data and applying an equation of deformation to reproduce the mean variation of the pillar radius along the z-axis.

We considered that the pillars are cylinder-shaped, and compressed homogeneously *i.e.* that macrophages are exerting a uniform strain around the pillar for each z value. This approach permits to perform simulations in a 2D axisymmetric conformation. Polyacrylamide was defined as an elastic material possessing a density of  $1 \text{ kg}\cdot\text{m}^{-3}$ , a biaxial Young's modulus  $E_m$  (3, 10 or 40 kPa) and a Poisson' ratio of 0.48. A 10  $\mu\text{m}$  thick and 10  $\mu\text{m}$  radius base was built under the pillar to recapitulate the polyacrylamide layer between the glass coverslip and pillar from the experimental system.

The initial geometry of each pillar was defined in Comsol<sup>®</sup> through experimental data of height and radius. The original curve of radius given height was applied an order 3 polynomial fit. Values of radius from this smoothed curve were then entered for each z in Comsol<sup>®</sup> with a 0.3  $\mu\text{m}$  step.

To model the compression induced by macrophages action on the pillar, the curve of radius reduction issued from the experiment was applied on the surface of the reconstructed pillar. An order 6 polynomial fit was applied to the original curve. The equation of this smoothed curve was imported in Comsol<sup>®</sup> as an applied deformation on the surface of the pillar. A tetrahedral mesh was used and set as "ultrafine". Simulations were performed using a linear elastic deformation model.

Traction simulations were performed in a 3D configuration using the geometry of the pillar observed experimentally. The geometries were generated by exporting a 3D model of the

pillars from the 2D axisymmetric models previously described for compression analysis. A tetrahedral mesh was used and set as “ultrafine”. Increasing values of shear forces were applied on the top surface of the pillar resulting in pillar deflection and base deformation. All simulations were performed using a linear elastic deformation model

**Supplementary table 2: product list**

Product	Supplier	Reference	Concentration
Acrylamid	Sigma	A-9099	10% (see suppl. Table 1)
Bisacrylamid	Sigma	146072	0.03 to 0.3% (see suppl. Table 1)
APTMS (3-aminopropyl trimethoxysilane)	Sigma	281778	pure
Rhodamin B methacrylate	Sigma		2.5 mg/mL
XLINKER Sulfo-SANPAH	VWR	GENOBC 38	1 mg/mL
HEPES	Sigma	H3375	50 mM
TEMED	Sigma	T9281	(see suppl. Table 1)
Glutaraldehyde 25%	EMS	16210	2.5%
APS (ammonium peroxydisulfate)			(see suppl. Table 1)
Ovalbumin	Sigma	A5503	1 mg/mL
Anti-ovalbumin IgG (rabbit polyclonal)	Millipore	AB1225	0.5 mg/mL

**Statistics**

Statistical analyses were performed using Prism 5 (GraphPad). Statistical comparison of the data was performed using one-way ANOVA followed by Dunnett’s comparison test or by Kruskal-Wallis test, followed by Dunn’s multiple comparisons test for not normally distributed data. In the figures, statistical significance is indicated as follows: \*  $p < 0.05$ ; \*\*  $p < 0.01$  and \*\*\*  $p < 0.001$ .



Figures

Bigot et al. Figure 1

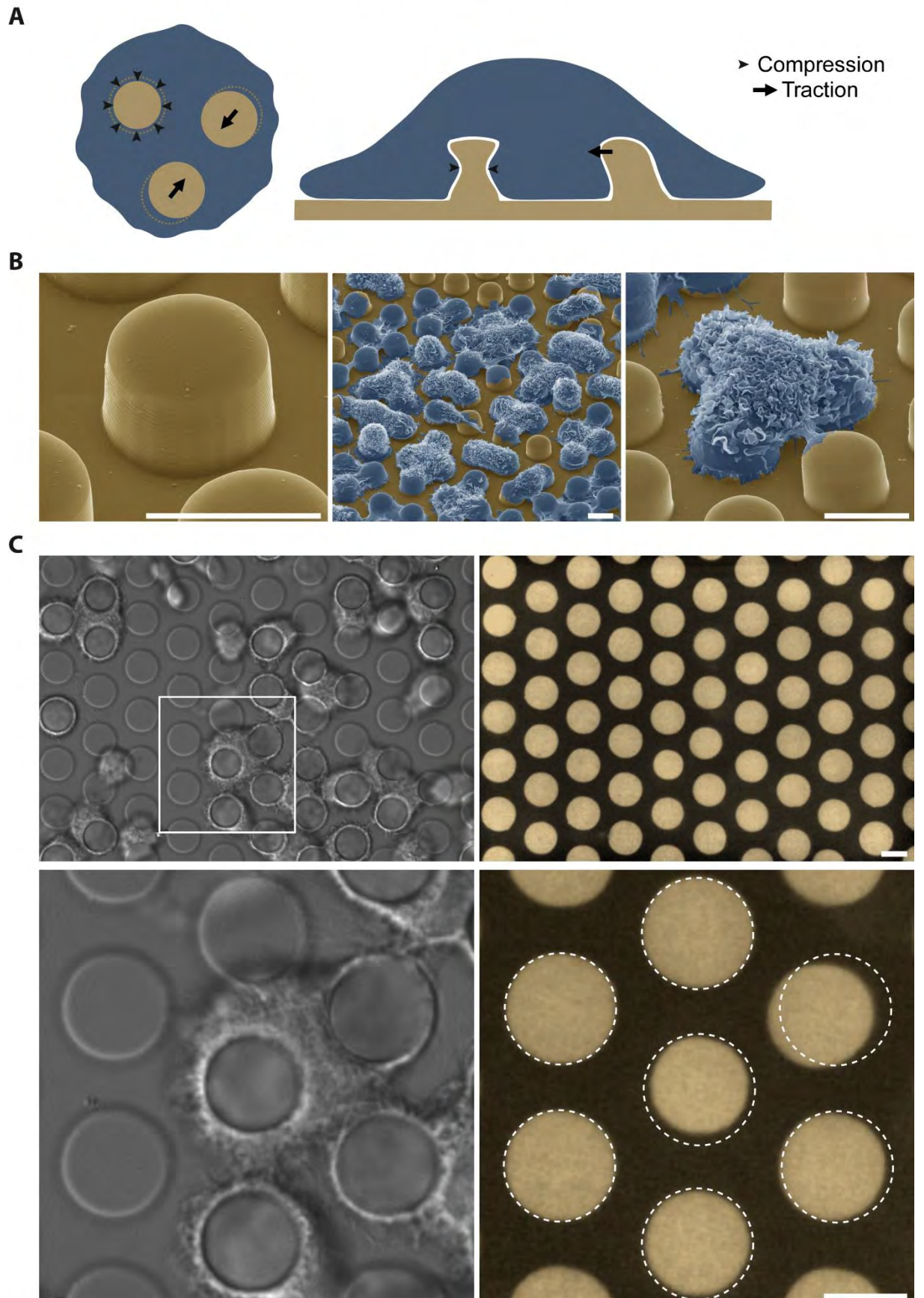


**Figure 1. Principle of the method**

**A.** Schematic representation of the principle of the method. Top view (left) of a macrophage (blue) seeded on polyacrylamide pillars (gold) and exerting compression and traction forces in an attempt to engulf them. Side view (right) of same phenomenon where squeezing and deflection of pillars can be appreciated. Created on Biorender.

**B.** SEM images of a PDMS pillar (in gold) of controlled dimensions, coated with IgG (left panel). Human monocytes-derived macrophages (hMDMs, in blue) can extend and initiate phagocytosis on one to up to 7 pillars (middle panel). Zoom on a macrophage engulfing 3 pillars (right panel). Scale bar 10µm.

**C.** Dynamic of hMDMs (bright field) seeded on polyacrylamide pillars (gold). Application of cell forces deforms the pillars in two distinct ways. Reduction of their radius can be related to the compression forces, and displacement of their barycentre can be related to the traction forces. Initial radius and position are indicated by white dashed circles. Scale bar 10µm.

Bigot et al. Figure 2

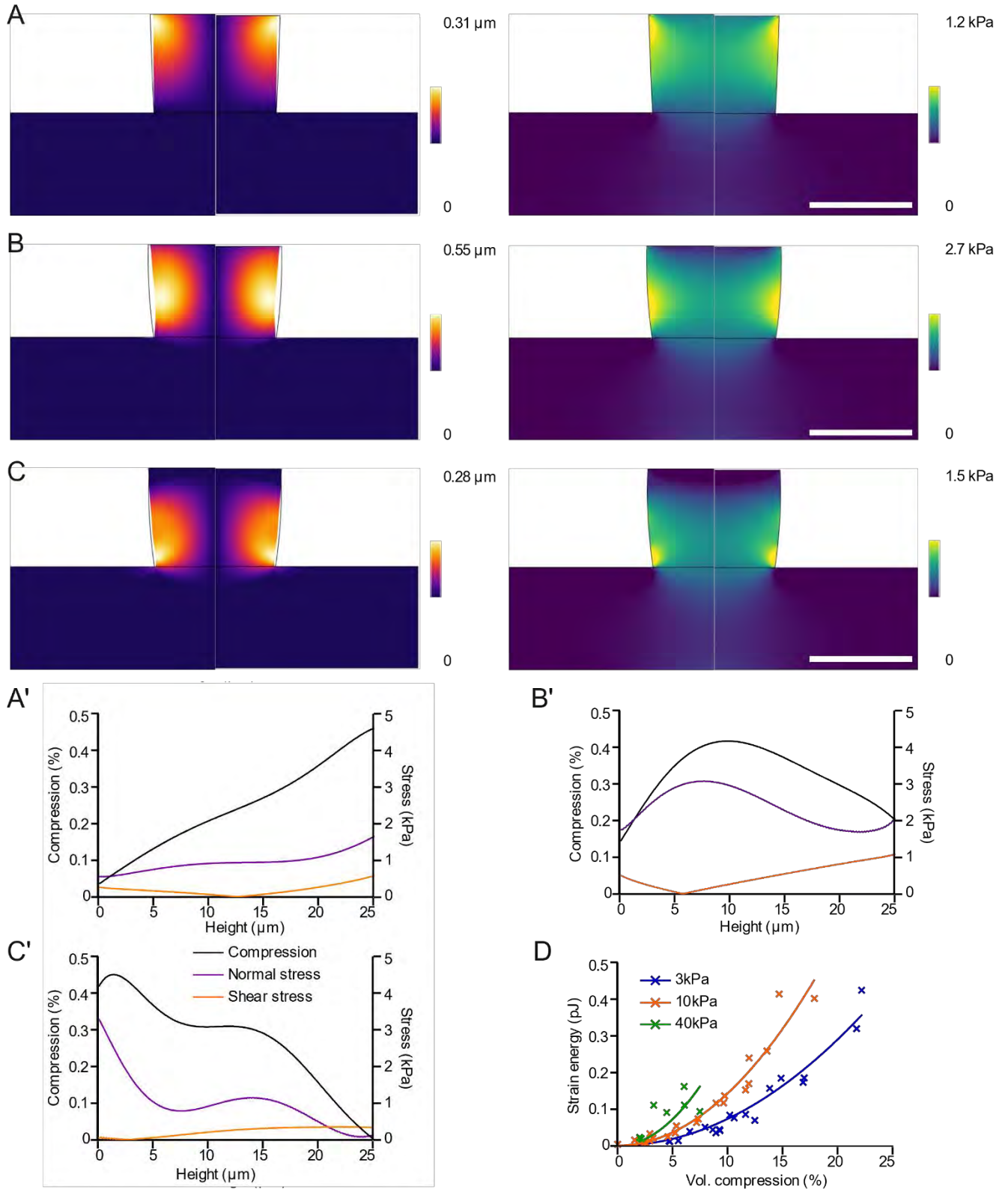


**Figure 2. Modelisation of compression energy via finite elements simulation**

**A.** 2D axisymmetric reconstruction of a 10 kPa pillar. Initial geometry is represented by a black line and deformed geometry by the full colorized theme, with a colour code on the amplitude of deformation in the longitudinal axis xy (purple to yellow, left) and pressure (blue to yellow, right). Maximum deformation is observed at the top of the pillar.

**A'** Compression rate of the pillar on A along its height (black, left axis) and corresponding normal (purple) and shear (orange) stresses (right axis).

**B. and B'** Similar representation of a 10 kPa pillar deformed on its middle.

**C and C'** Similar representation of a 10 kPa pillar deformed on its bottom.

**D.** Calibration curve relating strain energy to rate of volume compression from at least 21 pillars of each Young's modulus, from at least 2 independent experiments (see **Table S3**).

**Supplementary table 3: statistics corresponding the Fig.2**

	<b>Configuration</b>	<b>N. pillars simulated</b>	<b>Fit</b>
3kPa	2D axisymmetric	22 (experimental data from 2 different experiments)	Non linear fit $x^2$ on Prism5
10kPa		22 (experimental data from 2 different experiments)	Non linear fit $x^2$ Prism5
40kPa		21 (experimental data from 3 different experiments)	Non linear fit $x^2$ Prism5

Bigot et al. Figure 3

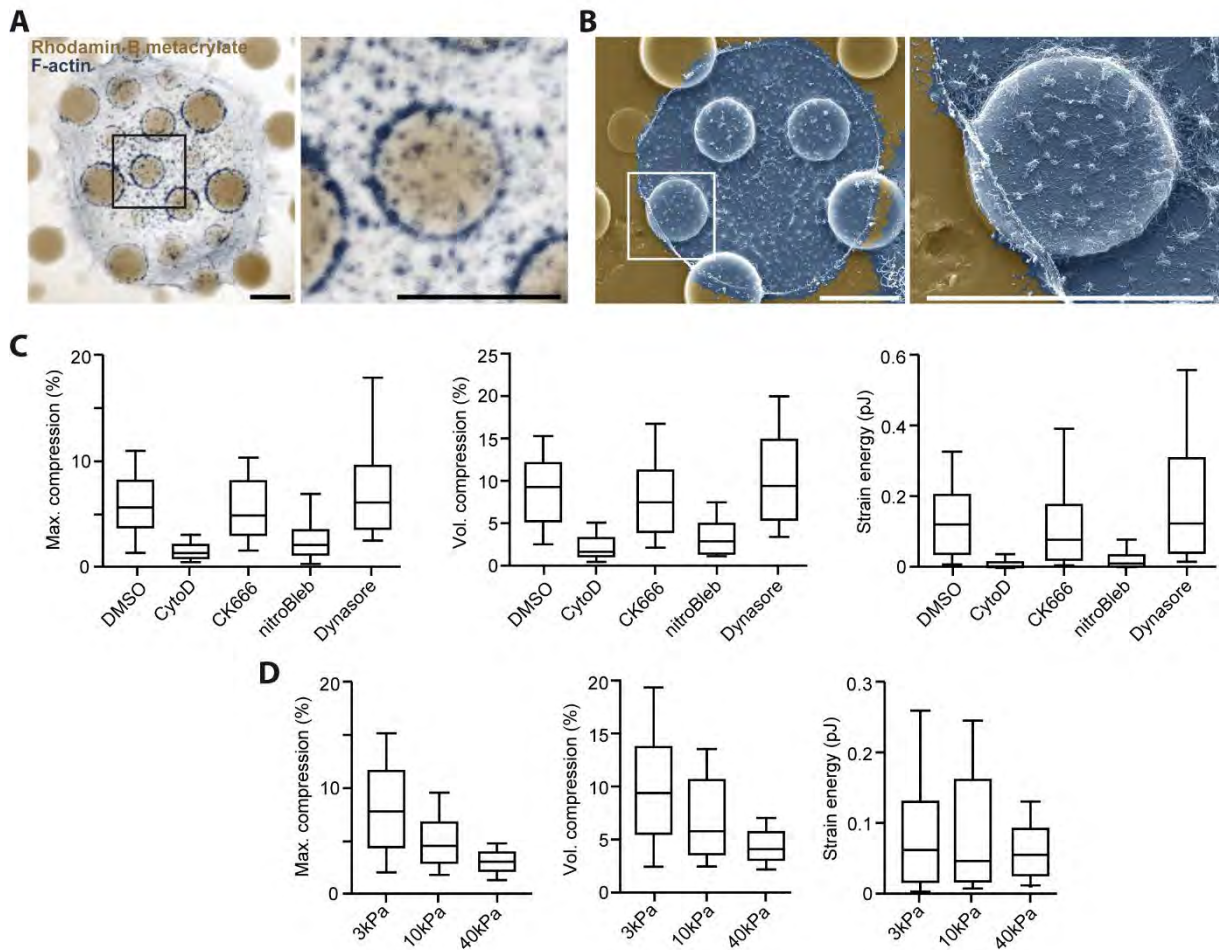


**Figure 3. Compression force dependence on acto-myosin cytoskeleton and mechanosensing**

**A.** Representative confocal image of a human macrophage (stained for F-actin in blue) engulfing polyacrylamide pillars (gold) of various diameters, one hour after seeding. A dot-shaped enrichment in F-actin is observed around the pillars.

**B.** SEM image of an unroofed human macrophage (colorized in blue) on PDMS pillars (colorized in gold) of various diameters, one hour after seeding. Punctate structures identified as podosomes are present at the top of the pillars.

**C.** Quantifications of compression rate expressed in maximum radius reduction (left), overall volume reduction (middle) or related strain energy (right) of 10 kPa polyacrylamide pillars phagocytosed by human macrophages in the presence of cytoskeleton-related inhibitors. One-time acquisitions of macrophages phagocytosing one pillar were performed and the compression rate was analysed by comparison with control neighbour pillars (method #1). Effects were analysed for the actin-polymerisation inhibitor cytochalasinD (2  $\mu$ M), Arp2/3 complex inhibitor

CK666 (50  $\mu$ M), myosin-II inhibitor nitroblebbistatin (20  $\mu$ M) and dynamin-2 inhibitor dynasore (50  $\mu$ M) and DMSO was used as control condition.

**D.** Same representation and analysis method for macrophages phagocytosing one pillar of either 3, 10 or 40 kPa.

Statistical comparison of the data was performed using one-way Anova followed by Dunnett's comparison test or by Kruskal-Wallis test, followed by Dunn's multiple comparisons test for not normally distributed data. In the figures, statistical significance is indicated as follows: \*  $p < 0.05$ ; \*\*  $p < 0.01$  and \*\*\*  $p < 0.001$ . The number of pillars quantified for each experiment is indicated in **Table S4**.

**Supplementary table 4: statistics corresponding the Fig.3**

	N. pillars quantified	N. experiments
<b>Drugs</b>		
DMSO (1/1000)	71	5
CK666 (50 $\mu$ M)	46	3
NitroBlebbistatin (20 $\mu$ M)	59	3
Dynasore (50 $\mu$ M)	55	3
CytochalasinD (2 $\mu$ M)	29	2
<b>Mechanosensing</b>		
3 kPa	38	3
10 kPa	44	3
40 kPa	45	3

Bigot et al. Figure 4

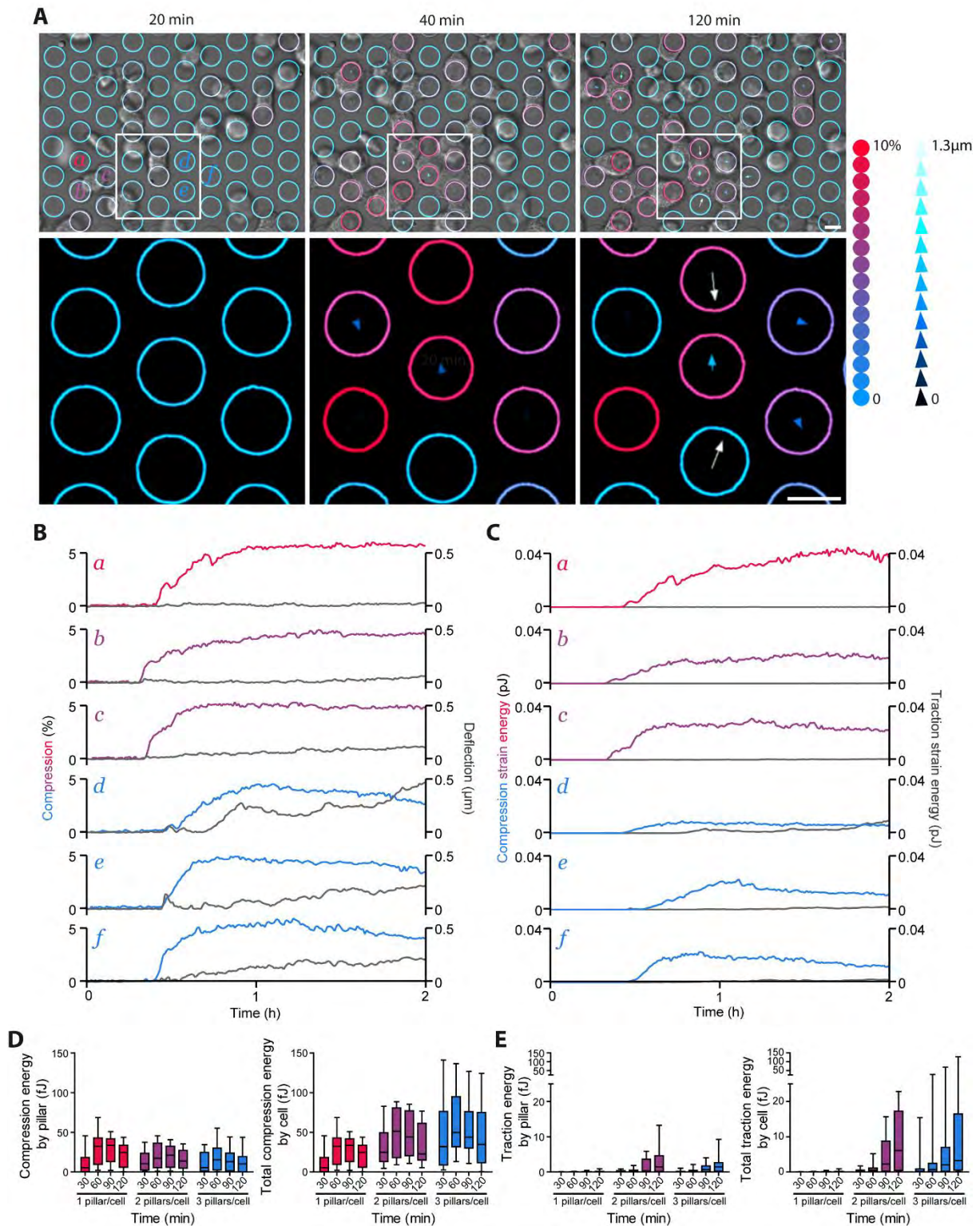


**Figure 4. Force dynamics of macrophage phagocytosis on IgG coated 10kpa pillars**

**A.** Different time points from a representative video (see **VideoS1**) of 10 kPa pillars coated with IgG and stained with rhodaminB, recording cells arrival and phagocytosis dynamics. Bottom panels show a zoom on a region of interest. A Z stack covering the full pillars height

was taken each 40 s for a total of 120 min. Pillars radius compression and deflection respect to original size and position (method #2) were calculated using the rhodamin channel, and colour coded for visualisation. The lengths of deflection arrows were multiplied by 3 to increase visibility.

**B.** Evolution of compression rate (expressed as pillar radius reduction) and deflection at 8  $\mu\text{m}$  of height of representative pillars (*a* to *f*) on the video. Compression curves (left Y axis) are color-coded to identify the cell inducing the deformations deflection curves (right Y axis) are represented in black.

**C.** Compression and traction strain energies calculated for each selected pillar, same colour code.

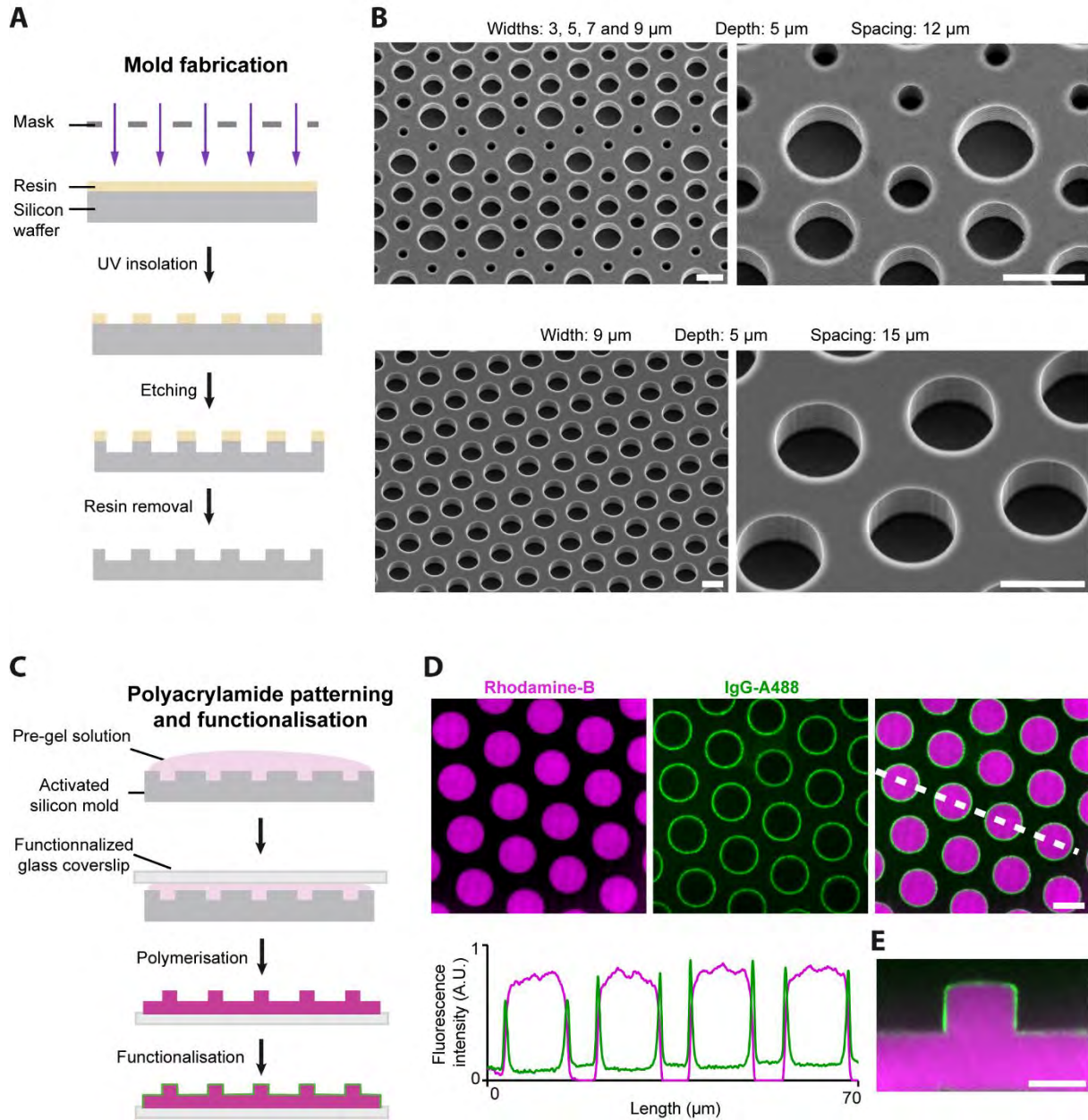
**D.** Compression strain energy values of pillars phagocyted alone, or in 2- or 3-packs were compared at 30, 60, 90 and 120 min time points (left). Then, for each cell, values from its simultaneously phagocyted pillars were added and total compression energy per cell represented.

**E.** Traction strain energy per pillar and per cell were calculated and plotted similarly to compression strain energy.

**Supplementary table 4: statistics corresponding the Fig.4**

	Nb pillars quantified	Nb cells quantified	Nb videos
<b>Drugs</b>			
Alone	23	23	4
2-pack	36	18	4
3-pack	27	9	4

Bigot et al. Figure S1



**Supplementary Figure 1. Fabrication and characterisation of micropillars**

**A.** Process of photolithography to create the silicon mould. A thin (1.1 µm) layer of resin is spin-coated on a silicon wafer and insulated by UV through a mask with desired patterns. Plasma etching hollows zones of the wafer not protected by the resin to the desired depth (5µm) and the residual resin is removed.

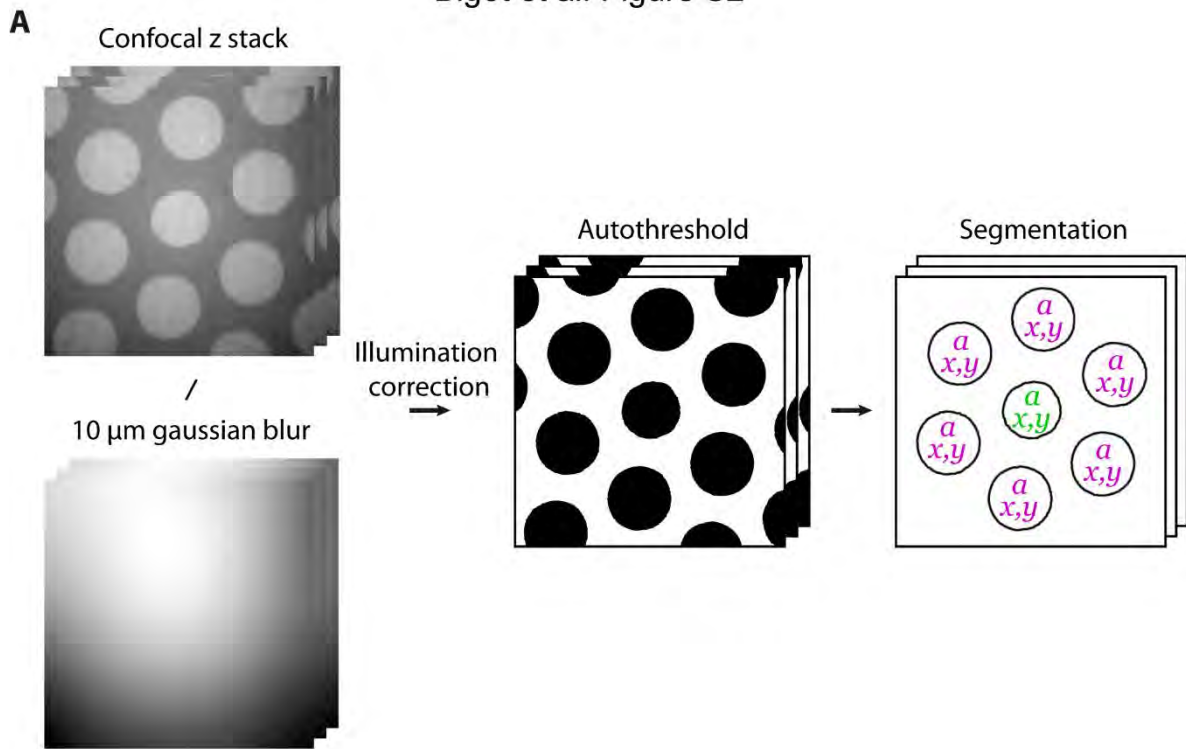
**B.** SEM images of silicon moulds with a regular hexagonal pattern of wells of diameters ranging from 3 to 9 µm, depth of 5 µm, with a spacing of 12 µm (upper panel), and mould with wells of 9 µm diameter, 5 µm depth and 15 µm spacing (lower panel). Scale: 10µm

**C.** Polyacrylamide moulding process: a pre-gel solution of polyacrylamide containing rhodamin B methacrylate for staining is casted into the pre-activated silicon mould. A functionalised glass coverslip is added on top and after 15 min of polymerisation, gently removed. The obtained micropatterned polyacrylamide is functionalised with ovalbumin and IgG to trigger FcR phagocytosis.

**D.** Top view of confocal images of polyacrylamide pillars stained with rhodamin B methacrylate (magenta) and functionalized with Alexa488-IgG (green). The distribution of the relative fluorescence intensity of both markers along the white dashed line is represented in the bottom panel. Scale 10 $\mu$ m

**E.** Side view of the same pillar. Scale 10 $\mu$ m

Bigot et al. Figure S2



**B**

method #1 (1 time acquisition)

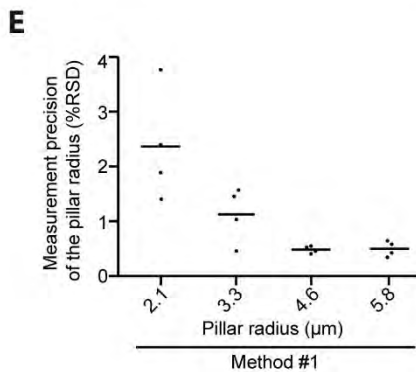
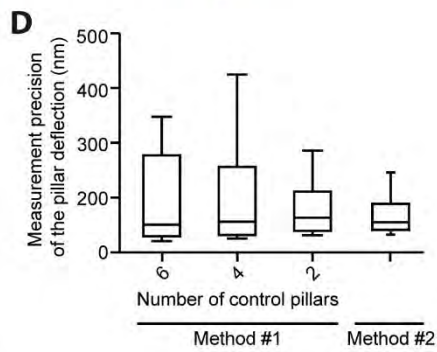
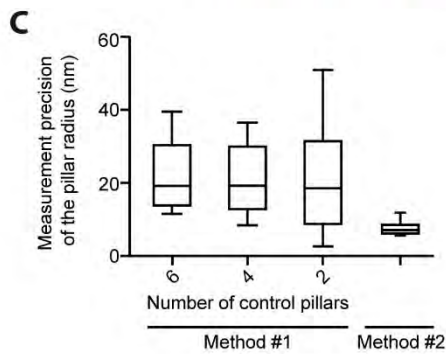
$$d = \sqrt{(x_i - \bar{x}_c)^2 + (y_i - \bar{y}_c)^2}$$

$$c = \frac{\bar{r}_i - \bar{r}_c}{\bar{r}_c}$$

method #2 (2 h acquisition)

$$d = \sqrt{(x_i - \bar{x}_{t0})^2 + (y_i - \bar{y}_{t0})^2}$$

$$c = \frac{\bar{r}_i - \bar{r}_{t0}}{\bar{r}_{t0}}$$



### Supplementary Figure 2. Method of analysis

**A.** Automated image treatment on ImageJ. For each image on a z-stack acquisition over the height of a pillar, the original image is divided by its replicate on which has been applied a 10  $\mu\text{m}$  Gaussian blur to remove the background noise. Through a single illumination correction and using the auto threshold function of ImageJ, all of the pillars from same image are segmented and their dimension and barycenter xy position is extracted.

**B.** Pillar deflection ( $d$ ) and compression ( $c$ ) were calculated for each frame using two different methods. Method #1 compared the pillar of interest size and position to the mean of the surrounding control pillars while method #2 calculated pillar deformation respect to its own size and position before the cell arrival.

**C.** Standard deviation on the radius measurement of pillar of interest for the two analysis methods, depending on the number of surrounding control pillars used for comparison in method #1.

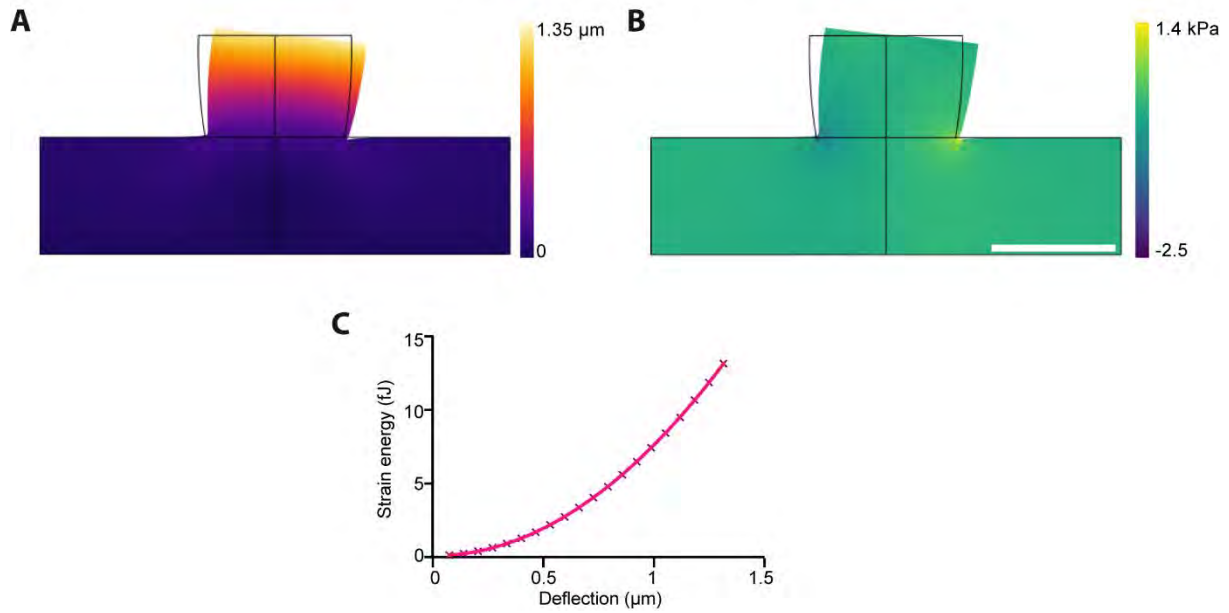
**D.** Standard deviation on the xy barycentre displacement (deflection) for the two analysis methods, depending on the number of surrounding control pillars used for comparison in method #1.

**E.** For method #1, relative standard deviation on the radius measurement respect to the mean value, depending on the pillar radius category.

**Supplementary table 5: statistics corresponding the Fig.S2**

Figure S2	N. pillars quantified	N. images or videos	N. experiments
<b>Figure S2.C</b>			
Method #1	90	82	3
Method #2	46	4	1
<b>Figure S2.D</b>			
Method #1	18	17	3
Method #2	20	2	2
<b>Figure S2.E</b>			
Radius = 2.1 $\mu\text{m}$	46	4	2
Radius = 3.6 $\mu\text{m}$	48	4	2
Radius = 4.9 $\mu\text{m}$	48	4	2
Radius = 6.3 $\mu\text{m}$	47	4	2

Bigot et al. Figure S3



**Supplementary Figure 3 Finite element simulation of traction energy**

**A.** 3D reconstruction of a 10 kPa pillar. Initial geometry is represented by the black line and deformed geometry by the full-colored theme. Colour codes for the amplitude of the deformation in the longitudinal axis x.

**B.** Corresponding pressure map.

**C.** Calibration curve relating strain energy to deflection is a result of simulations where shear forces were applied on top of the pillar.

**Supplementary table 6: statistics corresponding the Fig.S3**

DEFLECTION			
10kPa	3D	3 (experimental data form 1 experiment)	Non-linear fit x <sup>2</sup> Prism5

**Supplementary Video 1:**

Representative video of 10 kPa pillars coated with IgG and stained with rhodamin (left), recording cell arrival and force dynamics. Pillars radius compression and deflection respect to original size and position were calculated and colour coded for visualisation. The lengths of deflection arrows were multiplied by 3 to increase visibility

## References

- Araki, N. (2006) 'Role of microtubules and myosins in Fc gamma receptor-mediated phagocytosis', *Frontiers in Bioscience*, 11(1), p. 1479. Available at: <https://doi.org/10.2741/1897>.
- Bear, J.E. *et al.* (2002) 'Antagonism between Ena/VASP Proteins and Actin Filament Capping Regulates Fibroblast Motility', *Cell*, 109(4), pp. 509–521. Available at: [https://doi.org/10.1016/S0092-8674\(02\)00731-6](https://doi.org/10.1016/S0092-8674(02)00731-6).
- Beningo, K.A. and Wang, Y. (2002) 'Fc-receptor-mediated phagocytosis is regulated by mechanical properties of the target', *Journal of Cell Science*, 115(4), pp. 849–856. Available at: <https://doi.org/10.1242/jcs.115.4.849>.
- Bettadapur, A., Miller, H.W. and Ralston, K.S. (2020) 'Biting Off What Can Be Chewed: Trophocytosis in Health, Infection, and Disease', *Infection and Immunity*. Edited by K.M. Ottemann, 88(7), pp. e00930–19. Available at: <https://doi.org/10.1128/IAI.00930-19>.
- Cannon, G.J. and Swanson, J.A. (1992) 'The macrophage capacity for phagocytosis', *Journal of Cell Science*, 101(4), pp. 907–913. Available at: <https://doi.org/10.1242/jcs.101.4.907>.
- Caron, E. and Hall, A. (1998) 'Identification of Two Distinct Mechanisms of Phagocytosis Controlled by Different Rho GTPases', *Science*, 282(5394), pp. 1717–1721. Available at: <https://doi.org/10.1126/science.282.5394.1717>.
- Coppolino, M.G. *et al.* (2001) 'Evidence for a molecular complex consisting of Fyb/SLAP, SLP-76, Nck, VASP and WASP that links the actin cytoskeleton to Fcγ receptor signalling during phagocytosis', *Journal of Cell Science*, 114(23), pp. 4307–4318. Available at: <https://doi.org/10.1242/jcs.114.23.4307>.
- Evans, E., Leung, A. and Zhelev, D. (1993) 'Synchrony of cell spreading and contraction force as phagocytes engulf large pathogens', *Journal of Cell Biology*, 122(6), pp. 1295–1300. Available at: <https://doi.org/10.1083/jcb.122.6.1295>.
- Herant, M., Heinrich, V. and Dembo, M. (2005) 'Mechanics of neutrophil phagocytosis: behavior of the cortical tension', *Journal of Cell Science*, 118(9), pp. 1789–1797. Available at: <https://doi.org/10.1242/jcs.02275>.
- Horsthemke, M. *et al.* (2017) 'Multiple roles of filopodial dynamics in particle capture and phagocytosis and phenotypes of Cdc42 and Myo10 deletion', *Journal of Biological Chemistry*, 292(17), pp. 7258–7273. Available at: <https://doi.org/10.1074/jbc.M116.766923>.
- Hotulainen, P. and Lappalainen, P. (2006) 'Stress fibers are generated by two distinct actin assembly mechanisms in motile cells', *Journal of Cell Biology*, 173(3), pp. 383–394. Available at: <https://doi.org/10.1083/jcb.200511093>.
- Kovari, D.T. *et al.* (2016) 'Frustrated Phagocytic Spreading of J774A-1 Macrophages Ends in Myosin II-Dependent Contraction.' Available at: <https://doi.org/10.1016/j.bpj.2016.11.009>.
- Kress, H. *et al.* (2007) 'Filopodia act as phagocytic tentacles and pull with discrete steps and a load-dependent velocity', *Proceedings of the National Academy of Sciences*, 104(28), pp. 11633–11638. Available at: <https://doi.org/10.1073/pnas.0702449104>.

Labernadie, A. *et al.* (2010) 'Dynamics of podosome stiffness revealed by atomic force microscopy', *Proceedings of the National Academy of Sciences*, 107(49), pp. 21016–21021. Available at: <https://doi.org/10.1073/pnas.1007835107>.

Leishman, W.B. (1902) 'NOTE ON A METHOD OF QUANTITATIVELY ESTIMATING THE PHAGOCYTOTIC POWER OF THE LEUCOCYTES OF THE BLOOD', *BMJ*, 1(2141), pp. 73–75. Available at: <https://doi.org/10.1136/bmj.1.2141.73-a>.

Marie-Anaïs, F. *et al.* (2016) 'Dynamin-Actin Cross Talk Contributes to Phagosome Formation and Closure: Role of Dynamin in Phagosome Formation and Closure', *Traffic*, 17(5), pp. 487–499. Available at: <https://doi.org/10.1111/tra.12386>.

Masters, T.A. *et al.* (2013) 'Plasma membrane tension orchestrates membrane trafficking, cytoskeletal remodeling, and biochemical signaling during phagocytosis', *Proceedings of the National Academy of Sciences*, 110(29), pp. 11875–11880. Available at: <https://doi.org/10.1073/pnas.1301766110>.

May, R.C. *et al.* (2000) 'Involvement of the Arp2/3 complex in phagocytosis mediated by FcγR or CR3', *Nature Cell Biology*, 2(4), pp. 246–248. Available at: <https://doi.org/10.1038/35008673>.

Metchnikoff, E. (1905) 'Immunity in infective diseases', *Cambridge University Press*.

Morlot, S. and Roux, A. (2013) 'Mechanics of Dynamin-Mediated Membrane Fission', *Annual Review of Biophysics*, 42(1), pp. 629–649. Available at: <https://doi.org/10.1146/annurev-biophys-050511-102247>.

Mustapha, F., Sengupta, K. and Puech, P.-H. (2022) 'May the force be with your (immune) cells: an introduction to traction force microscopy in Immunology', *Frontiers in Immunology*, 13, p. 898558. Available at: <https://doi.org/10.3389/fimmu.2022.898558>.

Nelsen, E. *et al.* (2019) 'Combined Atomic Force Microscope and Volumetric Light Sheet System for Mechanobiology'. Available at: <https://doi.org/10.1101/812396>.

Olazabal, I.M. *et al.* (2002) 'Rho-Kinase and Myosin-II Control Phagocytic Cup Formation during CR, but Not FcγR, Phagocytosis', *Current Biology*, 12(16), pp. 1413–1418. Available at: [https://doi.org/10.1016/S0960-9822\(02\)01069-2](https://doi.org/10.1016/S0960-9822(02)01069-2).

Pacheco, P., White, D. and Sulchek, T. (2013) 'Effects of Microparticle Size and Fc Density on Macrophage Phagocytosis', *PLoS ONE*. Edited by Y. Wang, 8(4), p. e60989. Available at: <https://doi.org/10.1371/journal.pone.0060989>.

Rabinovitch, M. (1995) 'Professional and non-professional phagocytes: an introduction', *Trends in Cell Biology*, 5(3), pp. 85–87. Available at: [https://doi.org/10.1016/S0962-8924\(00\)88955-2](https://doi.org/10.1016/S0962-8924(00)88955-2).

Roberts, J. and Quastel, J. (1963) 'PARTICLE UPTAKE BY POLYMORPHONUCLEAR LEUCOCYTES AND EHRLICH ASCITES-CARCINOMA CELLS', *Biochemical Journal*, 89(1), pp. 150–156. Available at: <https://doi.org/10.1042/bj0890150>.

Rotty, J.D. *et al.* (2017) 'Arp2/3 Complex Is Required for Macrophage Integrin Functions but Is Dispensable for FcR Phagocytosis and In Vivo Motility', *Developmental Cell*, 42(5), pp. 498–513.e6. Available at: <https://doi.org/10.1016/j.devcel.2017.08.003>.

Rougerie, P., Miskolci, V. and Cox, D. (2013) 'Generation of membrane structures during phagocytosis and chemotaxis of macrophages: role and regulation of the actin cytoskeleton', *Immunological Reviews*, 256(1), pp. 222–239. Available at: <https://doi.org/10.1111/imr.12118>.

Schuerle, S. *et al.* (2017) 'Robotically controlled microprey to resolve initial attack modes preceding phagocytosis', *Science Robotics*, 2(2), p. eaah6094. Available at: <https://doi.org/10.1126/scirobotics.aah6094>.

Shibata, H., Heo, Y.J. and Takeuchi, S. (2011) 'Simple molding fabrication for poly acrylamide hydrogel', in *2011 IEEE 24th International Conference on Micro Electro Mechanical Systems. 2011 IEEE 24th International Conference on Micro Electro Mechanical Systems (MEMS)*, Cancun, Mexico: IEEE, pp. 885–888. Available at: <https://doi.org/10.1109/MEMSYS.2011.5734567>.

Simon, S.I. and Schmid-Schönbein, G.W. (1988) 'Biophysical aspects of microsphere engulfment by human neutrophils', *Biophysical Journal*, 53(2), pp. 163–173. Available at: [https://doi.org/10.1016/S0006-3495\(88\)83078-9](https://doi.org/10.1016/S0006-3495(88)83078-9).

Steffen, A. *et al.* (2006) 'Filopodia Formation in the Absence of Functional WAVE- and Arp2/3-Complexes', *Molecular Biology of the Cell*. Edited by M. Ginsberg, 17(6), pp. 2581–2591. Available at: <https://doi.org/10.1091/mbc.e05-11-1088>.

Subramani, R. *et al.* (2020) 'The Influence of Swelling on Elastic Properties of Polyacrylamide Hydrogels', *Frontiers in Materials*, 7, p. 212. Available at: <https://doi.org/10.3389/fmats.2020.00212>.

Suraneni, P. *et al.* (2012) 'The Arp2/3 complex is required for lamellipodia extension and directional fibroblast cell migration', *Journal of Cell Biology*, 197(2), pp. 239–251. Available at: <https://doi.org/10.1083/jcb.201112113>.

Swanson, J.A. *et al.* (1999) 'A contractile activity that closes phagosomes in macrophages', *Journal of Cell Science*, 112(3), pp. 307–316. Available at: <https://doi.org/10.1242/jcs.112.3.307>.

Tsai, R.K. and Discher, D.E. (2008) 'Inhibition of "self" engulfment through deactivation of myosin-II at the phagocytic synapse between human cells', *Journal of Cell Biology*, 180(5), pp. 989–1003. Available at: <https://doi.org/10.1083/jcb.200708043>.

Tse, S.M.L. *et al.* (2003) 'Differential Role of Actin, Clathrin, and Dynamin in Fcγ Receptor-mediated Endocytosis and Phagocytosis', *Journal of Biological Chemistry*, 278(5), pp. 3331–3338. Available at: <https://doi.org/10.1074/jbc.M207966200>.

Tusan, C.G. *et al.* (2018) 'Collective Cell Behavior in Mechanosensing of Substrate Thickness', *Biophysical Journal*, 114(11), pp. 2743–2755. Available at: <https://doi.org/10.1016/j.bpj.2018.03.037>.

Uribe-Querol, E. and Rosales, C. (2020) 'Phagocytosis: Our Current Understanding of a Universal Biological Process'. Available at: <https://doi.org/10.3389/fimmu.2020.01066>.

Vonna, L. *et al.* (2003) 'Local force induced conical protrusions of phagocytic cells', *Journal of Cell Science*, 116(5), pp. 785–790. Available at: <https://doi.org/10.1242/jcs.00230>.

Vonna, L. *et al.* (2007) 'Micromechanics of filopodia mediated capture of pathogens by macrophages', *European Biophysics Journal*, 36(2), pp. 145–151. Available at: <https://doi.org/10.1007/s00249-006-0118-y>.

Vorselen, D. *et al.* (2020) 'Microparticle traction force microscopy reveals subcellular force exertion patterns in immune cell–target interactions', *Nature Communications*, 11(1), p. 20. Available at: <https://doi.org/10.1038/s41467-019-13804-z>.

Vorselen, D. *et al.* (2021) *Phagocytic “teeth” and myosin-II “jaw” power target constriction during phagocytosis*. preprint. *Cell Biology*. Available at: <https://doi.org/10.1101/2021.03.14.435346>.

Wu, C. *et al.* (2012) 'Arp2/3 Is Critical for Lamellipodia and Response to Extracellular Matrix Cues but Is Dispensable for Chemotaxis', *Cell*, 148(5), pp. 973–987. Available at: <https://doi.org/10.1016/j.cell.2011.12.034>.

Yamauchi, S., Kawauchi, K. and Sawada, Y. (2012) 'Myosin II-dependent exclusion of CD45 from the site of Fcγ receptor activation during phagocytosis', *FEBS Letters*, 586(19), pp. 3229–3235. Available at: <https://doi.org/10.1016/j.febslet.2012.06.041>.

Zak, A. *et al.* (2019) *Single-cell immuno-mechanics: rapid viscoelastic changes are a hall-mark of early leukocyte activation*. preprint. *Biophysics*. Available at: <https://doi.org/10.1101/851634>.

### **Declaration of Competing Interest**

The authors have no competing interests to declare.

### **Contributions**

LM, RP designed and supervised the project. CB, JRB performed experiments and analysed the data. CB, MM, LM performed mechanical simulations. AL, CB developed the pillar micro fabrication process. LM, CV, IMP, RP, CB obtained funding. CB, JRB, LM, RP wrote the manuscript.

### **Acknowledgements**

This work was partially supported by TRI facilities and by the LAAS-CNRS micro and nanotechnologies platform, a member of the French Renatech network. The authors thank Maureen Verdier and Ugo Arles Bottega for their help with image analysis and Daan Vorselen for helpful discussions. This work was supported by a CNRS 80 Prime fellowship, la Fondation pour la Recherche Médicale (FRM), the Agence Nationale de Recherche sur le Sida et les hépatites virales (ANRS, ECTZ 205320/305352), the Agence Nationale de la Recherche and the ITMO Cancer of Aviesan on funds managed by Inserm (ITMO PCSI Grant number 266430).

### III. Additional results

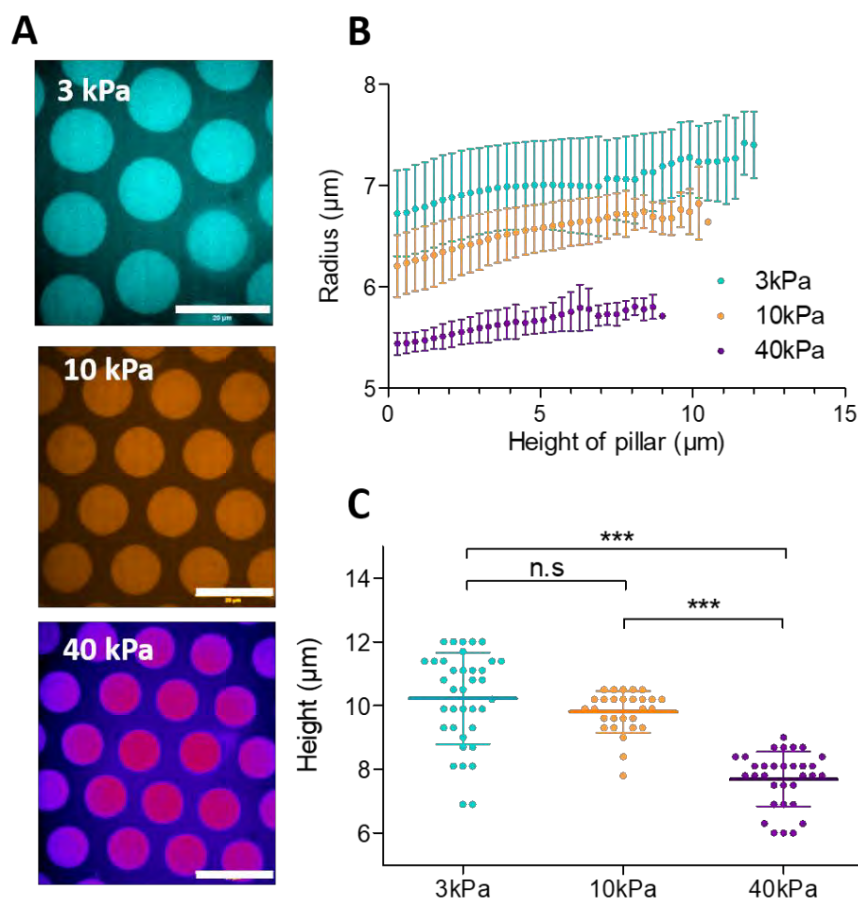
During this study, further experiments have been carried out to ensure effective control of the microfabrication process (Additional Figure 1 – 2), and to begin to investigate molecular mechanisms in force generation (Additional Figure 3). The results are presented and discussed here to enrich the discussion during the defence and open up perspectives for new experiments to come.

#### 1. Pillar dimensions depend on the PAA Young's modulus

Polyacrylamide gels of different Young's modulus were moulded using the same mould with wells of 5  $\mu\text{m}$  depth and 4.5  $\mu\text{m}$  radius. Surprisingly, it resulted in different pillar dimensions: the mean dimensions for 3 kPa pillars are 10.23 (+/- 1.43)  $\mu\text{m}$  height and 7.01 (+/- 0.44)  $\mu\text{m}$  radius at mid-height, while 40 kPa pillars show a mean height of 7.70 (+/-0.86)  $\mu\text{m}$  and radius at mid-height of 5.64 (+/-0.15). It thus appears that a change in the relative concentration of acrylamide and bis-acrylamide in the initial solution not only results in a change in the elastic modulus of the polymerized hydrogel but also affects the dimensions of the microfabricated pillars.

The swelling characteristic of the polyacrylamide could explain this behaviour (Subramani *et al.*, 2020). The pore sizes of the PAA hydrogels, in the order of 20-200 nm, have been reported to decrease with increasing monomer and cross-linker concentration (Stellwagen, 1998). Therefore, the smallest elastic moduli pillars are more prone to swell which extends their dimensions.

A second effect has been observed: regardless of the elastic modulus considered, the pillar shape was not perfectly cylindrical but rather resembles a truncated cone, which either might be due to the etching technique employed to create the mould, or to the fact that the pillar is constrained on its base through attachment to the underlying substrate. Indeed, the PAA swelling is maximized on its top-free ends, resulting in an increase of the pillar radius. To consider these particular effects, we optimised the strategy of the finite element-based simulations, and numerous pillars of each Young's modulus were imaged on confocal acquisition and reproduced in Comsol® to obtain a “calibration curve” (**Figure 3**).

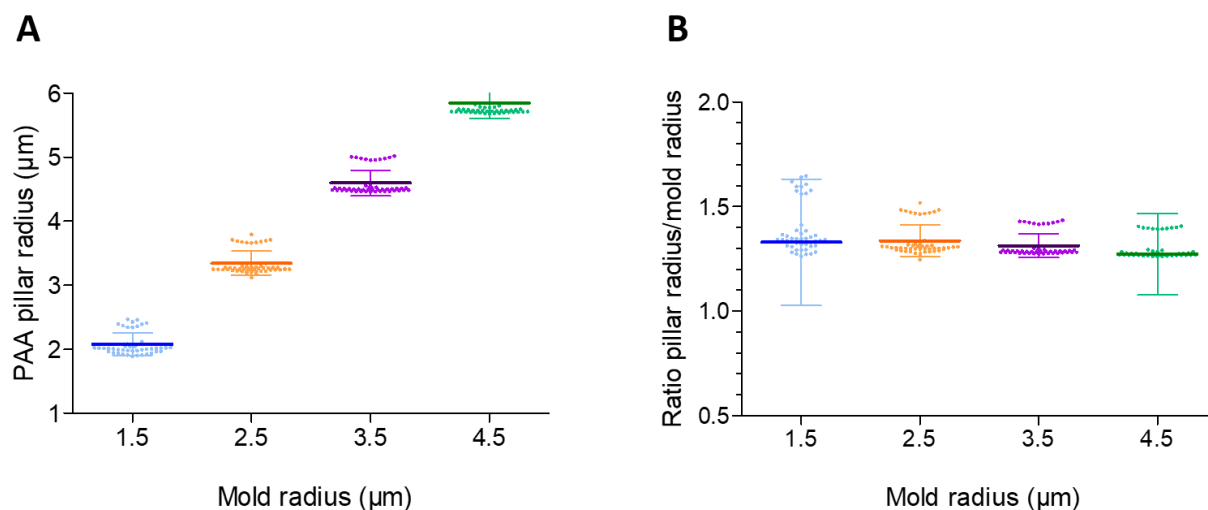


**Additional Figure 1. Representative dimension of pillar for Young's moduli of 3, 10 and 40 kPa**

**A.** Representative confocal image of pillars of 3 (cyan), 10 (orange) or 40 kPa (purple). **B.** Radius of the pillar along the height. The elastic modulus is inversely proportional to the radius: the smaller the elastic modulus, the larger the pillar. In each configuration, the radius increases with height, indicating a non-perfect cylindrical shape but rather a truncated cone shape. **C.** The pillar height is inversely dependant to the elastic modulus. Data of 150 to 250 pillars per condition. Mean is represented with SD. Statistical analyses were performed using Prism 5 (GraphPad). Statistical comparison of the data was performed using the Kruskal-Wallis test, followed by Dunn's multiple comparisons tests. In the figure, statistical significance is indicated as follows: \*  $p < 0.05$ ; \*\*  $p < 0.01$  and \*\*\*  $p < 0.001$ . Scale bar: 20  $\mu\text{m}$

## 2. The radius of the pillars is larger than the mould wells

Polymerization of 10 kPa polyacrylamide in a multi radius size mould (Figure S1.B), resulted in pillars larger than the wells they were moulded into (A). Regardless of the initial mould radius, the pillars show a 1.3-fold increase (B). Discrepancies observed may be due to the swelling behaviour of polyacrylamide previously described, and should be considered for further mould creation.



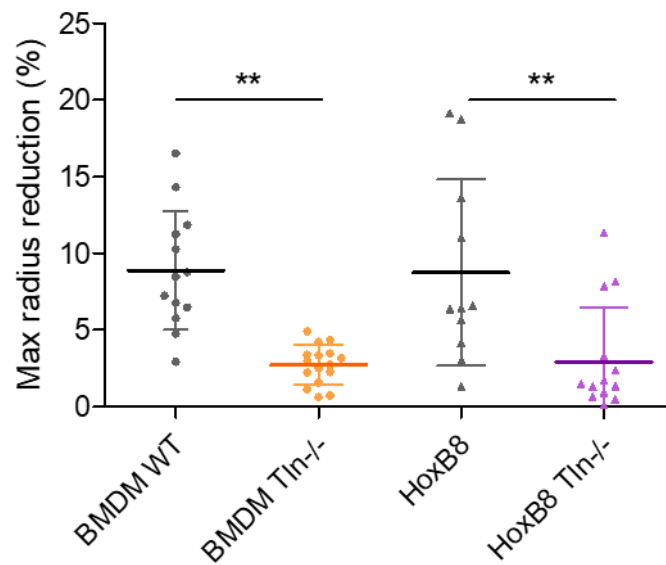
**Additional figure 2.** Ratio of pillar radius on mould radius.

**A.** Radius of PAA pillars measured on confocal images are larger than the mould wells used for their fabrication. **B.** Ratio of each pillar radius value on corresponding mould radius value. Radius of polyacrylamide pillars were measured in confocal imaging through ImageJ software. Mould wells radius was measured by SEM. For each condition, 50 PAA pillars of 10 kPa were measured and came from 4 different images of two different experiments.

## 3. Involvement of Talin in compression forces

Talin role in mechanotransduction has been established *via* its linking role between the actin cytoskeleton and integrins (Kanchanawong *et al.*, 2010). In phagocytosis, it has been proposed to mediate mechanosensing of the target during internalisation of opsonized particles, since integrins are engaged either as direct receptors in CR-mediated phagocytosis, either as secondary receptors in Fc-phagocytosis (Jaumouillé and Waterman, 2020a). Therefore, in collaboration with the group “Integrins in immune cells” of Frederic Lagarrigues at IPBS, I proposed to test its involvement in the generation of compressive forces at the phagocytic cup.

Using the same methodology as described previously, a first experiment has been performed on HoxB8 macrophages modified through CRISPR-Cas9 technology to knock-out the Talin gene. A second experiment uses Bone Marrow-Derived Macrophages (BMDM) from a mouse depleted in Talin. In both cases, macrophages were seeded on 10 kPa pillars and a decrease in the rate of compression upon Talin inhibition is observed. These preliminary data, from a few pillars and a single experiment, need to be confirmed.



**Additional Figure 3.** Talin seems to be involved in compressive force generation

Data come from a single experience for BMDM, and a single experience for HoxB8 macrophages, where 11 to 16 pillars were quantified for each condition. Statistical comparison of the data was performed using the Kruskal-Wallis test, followed by Dunn's multiple comparisons tests. In the figure, statistical significance is indicated as follows: \*  $p < 0.05$ ; \*\*  $p < 0.01$  and \*\*\*  $p < 0.001$ .

## IV. Perspectives

### 1. Refinement of the model through further simulations

#### Compression

Strain energy estimations rely on mechanical simulations performed in Comsol<sup>®</sup> software. For the estimation of the compressive strain energy, an empirical approach has been chosen by simulating geometry and deformations observed from experiments, resolving an inverse problem to calculate stresses and energy. To obtain the most accurate results, a precise measurement of the geometry is thus needed.

However, the limited resolution and signal to noise ratio impairs our analysis of how pillars are deformed at their top. A way to overcome this limitation would be to image the pillar system at 90°, using for example an additional mirror in the optical system (Hajjoul *et al.*, 2009). Performing accurate measurement of the top part of the pillar would permit to propose a more accurate model of deformation, improving the accuracy in the spatial distribution of deformation and thus the energy values obtained for each pillar.

Of note, results of strain energy presented for the 40 kPa pillars need to be confirmed: although the calibration curve seems consistent with results from others stiffnesses (**Figure 2**), it comes from a few (6) simulations. Thus, the strain energy calculated from it should be taken with care and must be validated by further simulations.

#### Traction

For the estimation of traction strain energies, we could not use the beam theory classically used for pillar based TFM (Mustapha, Sengupta and Puech, 2022) as both the aspect ratio of our pillars and the presence of a 10 µm layer of PAA under the pillar are incompatible with these equations. Comsol<sup>®</sup> simulations indeed confirmed discrepancies with analytical model proposed for high aspect ratio structures (not shown). A semi-empirical approach was then proposed: we simulated increasing shear forces on the top surface of the pillar and took opportunity of the elastic behaviour of the system to establish a calibration curve between the resulting deflection and the pillar strain energy. Expressing the results in terms of total energy per pillar could advantageously replace force calculations to compare deformation induced during phagocytosis by a large number of cells. The predicted values using this approach were

in the order of femto joules, which is consistent with the literature on 2D frustrated phagocytosis (Barger *et al.*, 2018).

In order to propose a general equation taking into account the mechanical properties and dimensions of the pillars, simulations will be further performed by varying systematically the height, radius, Young's modulus of the pillars, and evaluate how they affect the spring constant of the pillars.

## 2. What about the podosome like-structures for phagosome force generation?

In the first part of the results of this dissertation, I focused on the presence and role of podosomes-like structures, called "PAPs", and previously described in both frustrated phagocytosis (Labrousse, 2011; Jaumouillé, Cartagena-Rivera and Waterman, 2019; Ostrowski *et al.*, 2019) and phagocytosis of free particles (Allen and Aderem, 1996; Barger *et al.*, 2018; Vorselen *et al.*, 2021). They have been proposed to exert protrusive force on the phagocytic target (Vorselen *et al.*, 2021), as they do on flat substrate (Labernadie *et al.*, 2014). However, neither result from Vorselen *et al.*, neither ours allow to formally identify podosomes at the phagocytic cup.

Indeed, Vorselen *et al.* rather describe actin "teeth" that do not exhibit same typical ring-like organization of adhesion proteins surrounding the F-actin core of 2D podosomes. The dynamic appears also different since actin teeth form more frequently upon phagocytosis of soft target, which is in contrast with previous works reporting higher turnover of 2D when macrophages were plated on stiff substrates (Labernadie *et al.*, 2014; van den Dries, Linder, *et al.*, 2019; van den Dries, Nahidiazar, *et al.*, 2019).

As we have not specially investigated the composition nor dynamic of the actin dots observed in confocal imaging (Figure 3), further characterisation will be needed to conclude on that part. We will perform immunofluorescence of the typical podosome ring proteins: paxillin and vinculin, and then investigate the dynamics of F-actin during phagocytosis of the pillars by using LifeAct transformed human macrophages.

Moreover, the force profile observed through deformation of beads (Vorselen *et al.*) or pillars (this report) appear on a larger scale than expected by the protrusive activity of teeth or

podosome alone: the relatively homogeneous deformation suggest that the pillar compression is more due to a contractile ring rather than individual podosomes.

### 3. Candidate molecular actors on force generation

The method developed here allowed the evaluation of the effect of molecular actors on the contractile activity present in phagocytosis. The surprising result on Arp2/3 inhibition will first need to be confirm by repeating the experiment with higher doses of CK666 (150  $\mu$ M). Then, others potential candidate could be tested.

#### Piezo-1

As mentioned in the introduction of this dissertation, the membrane tension appears to play a critical role in the completion of phagocytosis, while being itself subject to modulation by the forces involved. Interestingly, the plasma membrane incorporates ion channels, that are pores allowing an electrical and chemical gradient across the membrane through active or passive transport of ions. The opening and closing of the channel can be triggered by *stimuli* such as voltage, temperature or chemical ligands, but also, for specific channels such as Piezo-1, by mechanical forces.

Recently, this non-specific cation channel, has been described as a mechanosensor of stiffness in macrophages, and modulator of polarization responses (Atcha *et al.*, 2021). Piezo-1 is activated by traction forces generated at integrin-rich focal adhesion zones by the actomyosin machinery (Nourse and Pathak, 2017). In phagocytosis, it has been shown to exhibit a critical role in cytoskeleton remodelling *via* Rac-1, ROS production, and bactericidal activity in response to various infectious cues (Geng *et al.*, 2021). Whether its role on cytoskeleton remodelling affect the phagocytic cup contractily remain to be investigated and could be assessed through our system with the use of its agonist Yoda-1 and its inhibitor GsMTx4.

#### Talin

The effect of Talin on force generation could be of great interest given its already described role in mechanotransduction in adhesive and migratory context. Our preliminary results on mouse macrophages devoid of Talin seem to support its role during Fc $\gamma$ R phagocytosis, although further experiments are required to confirm this hypothesis.

#### 4. Force application at the phagocytic cup: to fold or to break ?

##### Forces to fold target when full engulfment is compromised

To evade phagocytosis, some pathogens exhibit mechanisms of escape from recognition, engulfment and killing. For instance, *Candida albicans*, a commensal yeast usually found in skin and mucosa, can cause infection and escape phagocytosis by adapting its morphology in an elongated tubular hyphae, more difficult to internalize (Erwig and Gow, 2016).

While challenging macrophages with *Candida albicans*, Bain et al. observed a folding of this hyphae form within the phagocytic cup, promoted by actomyosin polymerisation. They speculate this folding eases internalisation of long hyphae and attenuates its growth, thus promoting successful phagocytosis (Bain *et al.*, 2021). It is still to be elucidated if this folding is an active mechanism of the phagocyte applying additional forces or a physical response from the pathogen to its uptake. This study focuses on the phagocytosis on *Candida* already in its hyphae form, which is known to be initiated by physicochemical parameters of the environment such as pH, temperature, and growth factors (Desai, 2018). Nevertheless, a recent work by Lucie Albert, from the group “Micronanofluidics for Life Science and environment” in LAAS, revealed that the yeast-to-hypha phenotype transition could also be modulated by mechanical forces (Albert, 2022). Through a collaboration with this group, we would like to realise phagocytosis assay with macrophages and ovaloid-shaped *Candida albicans* to test if the physical constrains and forces exerted at the phagocytic cup on the yeast could induce its transition to a hyphae form, and thus, promote escape of the pathogen from phagocytosis.

##### Forces to break target when full engulfment is not possible

On large beads of soft polyacrylamide coated with PS (10  $\mu\text{m}$  diameter – 0.3 kPa Young’s modulus) mimicking apoptotic cells, macrophages has been shown to break covalent links within the particle and thus separate the target in two parts (Vorselen *et al.*, 2022). This suggests a macrophages capacity to break particles to ingest them, although the very soft nature of the target used in this study does not recapitulate the wide range of rigidity a phagocyte can encounter. Specially, bacteria are way stiffer (within the MPa range) and their glycocalyx might make it more difficult for the macrophages to access its surface and apply forces to break it. Based on this observation, one can wonder if macrophages are capable of breaking stiff targets such as bacteria or if there is a maximum force that the macrophage is able to exert in order to break a phagocytic target. A proposed experiment would be to study the phagocytosis of *cocci*

bacteria chains, such as *Streptococcus*, and the possibility for macrophages to break up such assemblies.

## REFERENCES

- Abella, J.V.G. *et al.* (2016) 'Isoform diversity in the Arp2/3 complex determines actin filament dynamics', *Nature Cell Biology*, 18(1), pp. 76–86. Available at: <https://doi.org/10.1038/ncb3286>.
- Adams, D.O. and Hamilton, T.A. (1984) 'The Cell Biology of Macrophage Activation', *Annual Review of Immunology*, 2(1), pp. 283–318. Available at: <https://doi.org/10.1146/annurev.iy.02.040184.001435>.
- Aderem, A. and Underhill, D.M. (1999) 'MECHANISMS OF PHAGOCYTOSIS IN MACROPHAGES', *Annual Review of Immunology*, 17(1), pp. 593–623. Available at: <https://doi.org/10.1146/annurev.immunol.17.1.593>.
- Albert, L. (2022) *Candida albicans sur puce : approche biomécanique de la plasticité morphogénétique de c. albicans*. Université Paris sciences et lettres.
- Allen, L.A. and Aderem, A. (1996) 'Molecular definition of distinct cytoskeletal structures involved in complement- and Fc receptor-mediated phagocytosis in macrophages.', *Journal of Experimental Medicine*, 184(2), pp. 627–637. Available at: <https://doi.org/10.1084/jem.184.2.627>.
- Aman, M.J., Tosello-Trampont, A.-C. and Ravichandran, K. (2001) 'FcγRIIB1/SHIP-mediated Inhibitory Signaling in B Cells Involves Lipid Rafts', *Journal of Biological Chemistry*, 276(49), pp. 46371–46378. Available at: <https://doi.org/10.1074/jbc.M104069200>.
- Ancliff, P.J. *et al.* (2006) 'Two novel activating mutations in the Wiskott-Aldrich syndrome protein result in congenital neutropenia', *Blood*, 108(7), pp. 2182–2189. Available at: <https://doi.org/10.1182/blood-2006-01-010249>.
- Anderson, C.L. *et al.* (1990) 'Phagocytosis mediated by three distinct Fc gamma receptor classes on human leukocytes.', *Journal of Experimental Medicine*, 171(4), pp. 1333–1345. Available at: <https://doi.org/10.1084/jem.171.4.1333>.
- Araki, N. *et al.* (2003) 'Phosphoinositide-3-kinase-independent contractile activities associated with Fcγ-receptor-mediated phagocytosis and macropinocytosis in macrophages', *Journal of Cell Science*, 116(2), pp. 247–257. Available at: <https://doi.org/10.1242/jcs.00235>.
- Araki, N. (2006) 'Role of microtubules and myosins in Fc gamma receptor-mediated phagocytosis', *Frontiers in Bioscience*, 11(1), p. 1479. Available at: <https://doi.org/10.2741/1897>.
- Ashkin, A. *et al.* (1986) 'Observation of a single-beam gradient force optical trap for dielectric particles', *Optics Letters*, 11(5), p. 288. Available at: <https://doi.org/10.1364/OL.11.000288>.
- Atcha, H. *et al.* (2021) 'Mechanically activated ion channel Piezo1 modulates macrophage polarization and stiffness sensing', *Nature Communications*, 12(1), p. 3256. Available at: <https://doi.org/10.1038/s41467-021-23482-5>.
- Bain, J.M. *et al.* (2021) 'Immune cells fold and damage fungal hyphae', *Proceedings of the National Academy of Sciences*, 118(15), p. e2020484118. Available at: <https://doi.org/10.1073/pnas.2020484118>.

## REFERENCES

- Bakema, J.E. and van Egmond, M. (2011) 'The human immunoglobulin A Fc receptor Fc $\alpha$ RI: a multifaceted regulator of mucosal immunity', *Mucosal Immunology*, 4(6), pp. 612–624. Available at: <https://doi.org/10.1038/mi.2011.36>.
- Balabiyev, A. *et al.* (2020) 'Transition of podosomes into zipper-like structures in macrophage-derived multinucleated giant cells', *Molecular Biology of the Cell*. Edited by A. Dunn, 31(18), pp. 2002–2020. Available at: <https://doi.org/10.1091/mbc.E19-12-0707>.
- Baranov, M. *et al.* (2014) 'Podosomes of dendritic cells facilitate antigen sampling', *Journal of Cell Science*, p. jcs.141226. Available at: <https://doi.org/10.1242/jcs.141226>.
- Barger, S.R. *et al.* (2018) 'Membrane-cytoskeleton mechanical feedback mediated by myosin-I controls phagocytic efficiency'. Available at: <https://doi.org/10.1101/433631>.
- Barger, S.R. *et al.* (2019) 'Membrane-cytoskeletal crosstalk mediated by myosin-I regulates adhesion turnover during phagocytosis'. Available at: <https://doi.org/10.1038/s41467-019-09104-1>.
- Barger, S.R., Gauthier, N. and Krendel, M. (2019) 'Squeezing in a Meal: Myosin Functions in Phagocytosis.' Available at: <https://doi.org/10.1016/j.tcb.2019.11.002>.
- Basoli, F. *et al.* (2018) 'Biomechanical Characterization at the Cell Scale: Present and Prospects', *Frontiers in Physiology*, 9, p. 1449. Available at: <https://doi.org/10.3389/fphys.2018.01449>.
- Bear, J.E. *et al.* (2002) 'Antagonism between Ena/VASP Proteins and Actin Filament Capping Regulates Fibroblast Motility', *Cell*, 109(4), pp. 509–521. Available at: [https://doi.org/10.1016/S0092-8674\(02\)00731-6](https://doi.org/10.1016/S0092-8674(02)00731-6).
- Beningo, K.A. and Wang, Y. (2002) 'Fc-receptor-mediated phagocytosis is regulated by mechanical properties of the target', *Journal of Cell Science*, 115(4), pp. 849–856. Available at: <https://doi.org/10.1242/jcs.115.4.849>.
- Berg, J.S., Powell, B.C. and Cheney, R.E. (2001) 'A Millennial Myosin Census', *Molecular Biology of the Cell*. Edited by T.D. Pollard, 12(4), pp. 780–794. Available at: <https://doi.org/10.1091/mbc.12.4.780>.
- Bettadapur, A., Miller, H.W. and Ralston, K.S. (2020) 'Biting Off What Can Be Chewed: Trophocytosis in Health, Infection, and Disease', *Infection and Immunity*. Edited by K.M. Ottemann, 88(7), pp. e00930-19. Available at: <https://doi.org/10.1128/IAI.00930-19>.
- Bezman, N. and Koretzky, G.A. (2007) 'Compartmentalization of ITAM and integrin signaling by adapter molecules', *Immunological Reviews*, 218(1), pp. 9–28. Available at: <https://doi.org/10.1111/j.1600-065X.2007.00541.x>.
- Binnig, G., Quate, C.F. and Gerber, Ch. (1986) 'Atomic Force Microscope', *Physical Review Letters*, 56(9), pp. 930–933. Available at: <https://doi.org/10.1103/PhysRevLett.56.930>.
- Blystone, S.D. *et al.* (1994) 'Integrin alpha v beta 3 differentially regulates adhesive and phagocytic functions of the fibronectin receptor alpha 5 beta 1.', *Journal of Cell Biology*, 127(4), pp. 1129–1137. Available at: <https://doi.org/10.1083/jcb.127.4.1129>.
- Bohdanowicz, M. *et al.* (2010) 'Class I and class III phosphoinositide 3-kinases are required for actin polymerization that propels phagosomes', *Journal of Cell Biology*, 191(5), pp. 999–1012. Available at: <https://doi.org/10.1083/jcb.201004005>.

## REFERENCES

- Botelho, R.J. *et al.* (2000) 'Localized Biphasic Changes in Phosphatidylinositol-4,5-Bisphosphate at Sites of Phagocytosis', *Journal of Cell Biology*, 151(7), pp. 1353–1368. Available at: <https://doi.org/10.1083/jcb.151.7.1353>.
- Brandsma, A.M. *et al.* (2015) 'Fc receptor inside-out signaling and possible impact on antibody therapy', *Immunological Reviews*, 268(1), pp. 74–87. Available at: <https://doi.org/10.1111/imr.12332>.
- Brown, E. (2005) 'Complement Receptors, Adhesion, and Phagocytosis', in *Molecular Mechanisms of Phagocytosis*. Boston, MA: Springer US (Medical Intelligence Unit), pp. 49–57. Available at: [https://doi.org/10.1007/978-0-387-28669-3\\_4](https://doi.org/10.1007/978-0-387-28669-3_4).
- Brown, M.J. *et al.* (2001) 'Rigidity of Circulating Lymphocytes Is Primarily Conferred by Vimentin Intermediate Filaments', *The Journal of Immunology*, 166(11), pp. 6640–6646. Available at: <https://doi.org/10.4049/jimmunol.166.11.6640>.
- Bufi, N. *et al.* (2015) 'Human Primary Immune Cells Exhibit Distinct Mechanical Properties that Are Modified by Inflammation', *Biophysical Journal*, 108(9), pp. 2181–2190. Available at: <https://doi.org/10.1016/j.bpj.2015.03.047>.
- Burgdorf, S., Lukacs-Kornek, V. and Kurts, C. (2006) 'The Mannose Receptor Mediates Uptake of Soluble but Not of Cell-Associated Antigen for Cross-Presentation', *The Journal of Immunology*, 176(11), pp. 6770–6776. Available at: <https://doi.org/10.4049/jimmunol.176.11.6770>.
- Burgstaller, G. and Gimona, M. (2004) 'Actin cytoskeleton remodelling via local inhibition of contractility at discrete microdomains', *Journal of Cell Science*, 117(2), pp. 223–231. Available at: <https://doi.org/10.1242/jcs.00839>.
- Burgstaller, G. and Gimona, M. (2005) 'Podosome-mediated matrix resorption and cell motility in vascular smooth muscle cells', *American Journal of Physiology-Heart and Circulatory Physiology*, 288(6), pp. H3001–H3005. Available at: <https://doi.org/10.1152/ajpheart.01002.2004>.
- Burke, T.A. *et al.* (2014) 'Homeostatic Actin Cytoskeleton Networks Are Regulated by Assembly Factor Competition for Monomers', *Current Biology*, 24(5), pp. 579–585. Available at: <https://doi.org/10.1016/j.cub.2014.01.072>.
- Burns, S. *et al.* (2004) 'Maturation of DC is associated with changes in motile characteristics and adherence', *Cell Motility and the Cytoskeleton*, 57(2), pp. 118–132. Available at: <https://doi.org/10.1002/cm.10163>.
- Callaghan, J. *et al.* (1999) 'Direct interaction of EEA1 with Rab5b', *European Journal of Biochemistry*, 265(1), pp. 361–366. Available at: <https://doi.org/10.1046/j.1432-1327.1999.00743.x>.
- Calle, Y. *et al.* (2004) 'WASp deficiency in mice results in failure to form osteoclast sealing zones and defects in bone resorption', *Blood*, 103(9), pp. 3552–3561. Available at: <https://doi.org/10.1182/blood-2003-04-1259>.
- Cannon, G.J. and Swanson, J.A. (1992) 'The macrophage capacity for phagocytosis', *Journal of Cell Science*, 101(4), pp. 907–913. Available at: <https://doi.org/10.1242/jcs.101.4.907>.
- Canton, J. (2014) 'Phagosome maturation in polarized macrophages', *Journal of Leukocyte Biology*, 96(5), pp. 729–738. Available at: <https://doi.org/10.1189/jlb.1MR0114-021R>.

## REFERENCES

- Carmona, G. *et al.* (2016) 'Lamellipodin promotes invasive 3D cancer cell migration via regulated interactions with Ena/VASP and SCAR/WAVE', *Oncogene*, 35(39), pp. 5155–5169. Available at: <https://doi.org/10.1038/onc.2016.47>.
- Caron, E. and Hall, A. (1998) 'Identification of Two Distinct Mechanisms of Phagocytosis Controlled by Different Rho GTPases', *Science*, 282(5394), pp. 1717–1721. Available at: <https://doi.org/10.1126/science.282.5394.1717>.
- Cervero, P. *et al.* (2012) 'Proteomic analysis of podosome fractions from macrophages reveals similarities to spreading initiation centres', *European Journal of Cell Biology*, 91(11–12), pp. 908–922. Available at: <https://doi.org/10.1016/j.ejcb.2012.05.005>.
- Cervero, P. *et al.* (2018) 'Lymphocyte-specific protein 1 regulates mechanosensory oscillation of podosomes and actin isoform-based actomyosin symmetry breaking', *Nature Communications*, 9(1), p. 515. Available at: <https://doi.org/10.1038/s41467-018-02904-x>.
- Chabadel, A. *et al.* (2007) 'CD44 and  $\beta 3$  Integrin Organize Two Functionally Distinct Actin-based Domains in Osteoclasts', *Molecular Biology of the Cell*. Edited by D. Drubin, 18(12), pp. 4899–4910. Available at: <https://doi.org/10.1091/mbc.e07-04-0378>.
- Chesarone, M.A., DuPage, A.G. and Goode, B.L. (2010) 'Unleashing formins to remodel the actin and microtubule cytoskeletons', *Nature Reviews Molecular Cell Biology*, 11(1), pp. 62–74. Available at: <https://doi.org/10.1038/nrm2816>.
- Chieriegatti, E. *et al.* (1998) 'Myr 7 is a novel myosin IX-RhoGAP expressed in rat brain', *Journal of Cell Science*, 111(24), pp. 3597–3608. Available at: <https://doi.org/10.1242/jcs.111.24.3597>.
- Christoforidis, S. *et al.* (1999) 'The Rab5 effector EEA1 is a core component of endosome docking', *Nature*, 397(6720), pp. 621–625. Available at: <https://doi.org/10.1038/17618>.
- Chugh, P. and Paluch, E.K. (2018) 'The actin cortex at a glance', *Journal of Cell Science*, 131(14), p. jcs186254. Available at: <https://doi.org/10.1242/jcs.186254>.
- Clerc, P. and Sansonetti, P.J. (1987) 'Entry of *Shigella flexneri* into HeLa cells: evidence for directed phagocytosis involving actin polymerization and myosin accumulation', *Infection and Immunity*, 55(11), pp. 2681–2688. Available at: <https://doi.org/10.1128/iai.55.11.2681-2688.1987>.
- Collin, O. *et al.* (2006) 'Spatiotemporal dynamics of actin-rich adhesion microdomains: influence of substrate flexibility', *Journal of Cell Science*, 119(9), pp. 1914–1925. Available at: <https://doi.org/10.1242/jcs.02838>.
- Collin, O. *et al.* (2008) 'Self-Organized Podosomes Are Dynamic Mechanosensors', *Current Biology*, 18(17), pp. 1288–1294. Available at: <https://doi.org/10.1016/j.cub.2008.07.046>.
- Colucci-Guyon, E. *et al.* (2005) 'A Role for Mammalian Diaphanous-Related Formins in Complement Receptor (CR3)-Mediated Phagocytosis in Macrophages', *Current Biology*, 15(22), pp. 2007–2012. Available at: <https://doi.org/10.1016/j.cub.2005.09.051>.
- Coppolino, M.G. *et al.* (2001) 'Evidence for a molecular complex consisting of Fyb/SLAP, SLP-76, Nck, VASP and WASP that links the actin cytoskeleton to Fc $\gamma$  receptor signalling during phagocytosis', *Journal of Cell Science*, 114(23), pp. 4307–4318. Available at: <https://doi.org/10.1242/jcs.114.23.4307>.

## REFERENCES

- Cortesio, C.L. *et al.* (2010) 'Impaired podosome formation and invasive migration of macrophages from patients with a PSTPIP1 mutation and PAPA syndrome', *Arthritis & Rheumatism*, 62(8), pp. 2556–2558. Available at: <https://doi.org/10.1002/art.27521>.
- Cox, D. *et al.* (1999) 'A Requirement for Phosphatidylinositol 3-Kinase in Pseudopod Extension', *Journal of Biological Chemistry*, 274(3), pp. 1240–1247. Available at: <https://doi.org/10.1074/jbc.274.3.1240>.
- Cox, D. *et al.* (2002) 'Myosin X is a downstream effector of PI(3)K during phagocytosis', *Nature Cell Biology*, 4(7), pp. 469–477. Available at: <https://doi.org/10.1038/ncb805>.
- Crimaldi, L., Courtneidge, S.A. and Gimona, M. (2009) 'Tks5 recruits AFAP-110, p190RhoGAP, and cortactin for podosome formation', *Experimental Cell Research*, 315(15), pp. 2581–2592. Available at: <https://doi.org/10.1016/j.yexcr.2009.06.012>.
- Daëron, M. and Lesourne, R. (2006) 'Negative Signaling in Fc Receptor Complexes', in *Advances in Immunology*. Elsevier, pp. 39–86. Available at: [https://doi.org/10.1016/S0065-2776\(05\)89002-9](https://doi.org/10.1016/S0065-2776(05)89002-9).
- David-Pfeuty, T. and Singer, S.J. (1980) 'Altered distributions of the cytoskeletal proteins vinculin and alpha-actinin in cultured fibroblasts transformed by Rous sarcoma virus.', *Proceedings of the National Academy of Sciences*, 77(11), pp. 6687–6691. Available at: <https://doi.org/10.1073/pnas.77.11.6687>.
- Dembo, M. and Wang, Y.-L. (1999) 'Stresses at the Cell-to-Substrate Interface during Locomotion of Fibroblasts', *Biophysical Journal*, 76(4), pp. 2307–2316. Available at: [https://doi.org/10.1016/S0006-3495\(99\)77386-8](https://doi.org/10.1016/S0006-3495(99)77386-8).
- Desai, J. (2018) 'Candida albicans Hyphae: From Growth Initiation to Invasion', *Journal of Fungi*, 4(1), p. 10. Available at: <https://doi.org/10.3390/jof4010010>.
- Deschamps, C., Echard, A. and Niedergang, F. (2013) 'Phagocytosis and Cytokinesis: Do Cells Use Common Tools to Cut and to Eat? Highlights on Common Themes and Differences: Phagocytosis and Cytokinesis', *Traffic*, 14(4), pp. 355–364. Available at: <https://doi.org/10.1111/tra.12045>.
- Desjardins, M. (1995) 'Biogenesis of phagolysosomes: the "kiss and run" hypothesis', *Trends in Cell Biology*, 5(5), pp. 183–186. Available at: [https://doi.org/10.1016/0962-8924\(95\)80001-W](https://doi.org/10.1016/0962-8924(95)80001-W).
- Di, A. *et al.* (2003) 'Dynamin Regulates Focal Exocytosis in Phagocytosing Macrophages', *Molecular Biology of the Cell*, 14(5), pp. 2016–2028. Available at: <https://doi.org/10.1091/mbc.e02-09-0626>.
- Diakonova, M., Bokoch, G. and Swanson, J.A. (2002) 'Dynamics of Cytoskeletal Proteins during Fcγ Receptor-mediated Phagocytosis in Macrophages', *Molecular Biology of the Cell*. Edited by T.D. Pollard, 13(2), pp. 402–411. Available at: <https://doi.org/10.1091/mbc.01-05-0273>.
- Diz-Muñoz, A., Fletcher, D.A. and Weiner, O.D. (2013) 'Use the force: membrane tension as an organizer of cell shape and motility', *Trends in Cell Biology*, 23(2), pp. 47–53. Available at: <https://doi.org/10.1016/j.tcb.2012.09.006>.
- Dovas, A. *et al.* (2009) 'Regulation of podosome dynamics by WASp phosphorylation: implication in matrix degradation and chemotaxis in macrophages', *Journal of Cell Science*, 122(21), pp. 3873–3882. Available at: <https://doi.org/10.1242/jcs.051755>.
- van den Dries, K. *et al.* (2012) 'Geometry sensing by dendritic cells dictates spatial organization and PGE2-induced dissolution of podosomes', *Cellular and Molecular Life Sciences*, 69(11), pp. 1889–1901. Available at: <https://doi.org/10.1007/s00018-011-0908-y>.

## REFERENCES

- van den Dries, K. *et al.* (2013) 'Dual-color superresolution microscopy reveals nanoscale organization of mechanosensory podosomes', *Molecular Biology of the Cell*. Edited by M.H. Ginsberg, 24(13), pp. 2112–2123. Available at: <https://doi.org/10.1091/mbc.e12-12-0856>.
- van den Dries, K., Nahidiazar, L., *et al.* (2019) 'Modular actin nano-architecture enables podosome protrusion and mechanosensing', *Nature Communications*, 10(1), p. 5171. Available at: <https://doi.org/10.1038/s41467-019-13123-3>.
- Dries, K. van den *et al.* (2019) 'Probing the mechanical landscape – new insights into podosome architecture and mechanics'. Available at: <https://doi.org/10.1242/jcs.236828>.
- van den Dries, K., Linder, S., *et al.* (2019) 'Probing the mechanical landscape – new insights into podosome architecture and mechanics', *Journal of Cell Science*, 132(24), p. jcs236828. Available at: <https://doi.org/10.1242/jcs.236828>.
- van den Dries, K., Bolomini-Vittori, M. and Cambi, A. (2014) 'Spatiotemporal organization and mechanosensory function of podosomes', *Cell Adhesion & Migration*, 8(3), pp. 268–272. Available at: <https://doi.org/10.4161/cam.28182>.
- Dunn, J.D. *et al.* (2018) 'Eat Prey, Live: Dictyostelium discoideum As a Model for Cell-Autonomous Defenses', *Frontiers in Immunology*, 8, p. 1906. Available at: <https://doi.org/10.3389/fimmu.2017.01906>.
- Dupré-Crochet, S., Erard, M. and Nüße, O. (2013) 'ROS production in phagocytes: why, when, and where?', *Journal of Leukocyte Biology*, 94(4), pp. 657–670. Available at: <https://doi.org/10.1189/jlb.1012544>.
- Dustin, M.L. (2016) 'Complement Receptors in Myeloid Cell Adhesion and Phagocytosis', *Microbiology Spectrum*. Edited by S. Gordon, 4(6), p. 4.6.04. Available at: <https://doi.org/10.1128/microbiolspec.MCHD-0034-2016>.
- El Azzouzi, K., Wiesner, C. and Linder, S. (2016) 'Metalloproteinase MT1-MMP islets act as memory devices for podosome reemergence', *Journal of Cell Biology*, 213(1), pp. 109–125. Available at: <https://doi.org/10.1083/jcb.201510043>.
- Erwig, L.P. and Gow, N.A.R. (2016) 'Interactions of fungal pathogens with phagocytes', *Nature Reviews Microbiology*, 14(3), pp. 163–176. Available at: <https://doi.org/10.1038/nrmicro.2015.21>.
- Evans, E., Leung, A. and Zhelev, D. (1993) 'Synchrony of cell spreading and contraction force as phagocytes engulf large pathogens', *Journal of Cell Biology*, 122(6), pp. 1295–1300. Available at: <https://doi.org/10.1083/jcb.122.6.1295>.
- Evans, E.A., Waugh, R. and Melnik, L. (1976) 'Elastic area compressibility modulus of red cell membrane', *Biophysical Journal*, 16(6), pp. 585–595. Available at: [https://doi.org/10.1016/S0006-3495\(76\)85713-X](https://doi.org/10.1016/S0006-3495(76)85713-X).
- Evans, J.G. *et al.* (2003) 'Macrophage podosomes assemble at the leading lamella by growth and fragmentation', *Journal of Cell Biology*, 161(4), pp. 697–705. Available at: <https://doi.org/10.1083/jcb.200212037>.
- Fairn, G.D. and Grinstein, S. (2012) 'How nascent phagosomes mature to become phagolysosomes', *Trends in Immunology*, 33(8), pp. 397–405. Available at: <https://doi.org/10.1016/j.it.2012.03.003>.

## REFERENCES

- Ferron, F. *et al.* (2007) 'Structural basis for the recruitment of profilin–actin complexes during filament elongation by Ena/VASP', *The EMBO Journal*, 26(21), pp. 4597–4606. Available at: <https://doi.org/10.1038/sj.emboj.7601874>.
- Finlay, B.B., Ruschkowski, S. and Dedhar, S. (1991) 'Cytoskeletal rearrangements accompanying salmonella entry into epithelial cells', *Journal of Cell Science*, 99(2), pp. 283–296. Available at: <https://doi.org/10.1242/jcs.99.2.283>.
- Flannagan, R.S. *et al.* (2010) 'Dynamic macrophage “probing” is required for the efficient capture of phagocytic targets', *Journal of Cell Biology*, 191(6), pp. 1205–1218. Available at: <https://doi.org/10.1083/jcb.201007056>.
- Flannagan, R.S., Jaumouillé, V. and Grinstein, S. (2012) 'The Cell Biology of Phagocytosis', *Annual Review of Pathology: Mechanisms of Disease*, 7(1), pp. 61–98. Available at: <https://doi.org/10.1146/annurev-pathol-011811-132445>.
- Fodor, S., Jakus, Z. and Mócsai, A. (2006) 'ITAM-based signaling beyond the adaptive immune response', *Immunology Letters*, 104(1–2), pp. 29–37. Available at: <https://doi.org/10.1016/j.imlet.2005.11.001>.
- Freeman, S. and Grinstein, S. (2014) 'Phagocytosis: receptors, signal integration, and the cytoskeleton'. Available at: <https://doi.org/10.1111/imr.12212>.
- Freeman, S.A. *et al.* (2016) 'Integrins Form an Expanding Diffusional Barrier that Coordinates Phagocytosis', *Cell*, 164(1–2), pp. 128–140. Available at: <https://doi.org/10.1016/j.cell.2015.11.048>.
- Fu, Y.L. and Harrison, R.E. (2021) 'Microbial Phagocytic Receptors and Their Potential Involvement in Cytokine Induction in Macrophages', *Frontiers in Immunology*, 12, p. 662063. Available at: <https://doi.org/10.3389/fimmu.2021.662063>.
- Galán, J.E., Ginocchio, C. and Costeas, P. (1992) 'Molecular and functional characterization of the Salmonella invasion gene invA: homology of InvA to members of a new protein family', *Journal of Bacteriology*, 174(13), pp. 4338–4349. Available at: <https://doi.org/10.1128/jb.174.13.4338-4349.1992>.
- Gawden-Bone, C. *et al.* (2010) 'Dendritic cell podosomes are protrusive and invade the extracellular matrix using metalloproteinase MMP-14', *Journal of Cell Science*, 123(9), pp. 1427–1437. Available at: <https://doi.org/10.1242/jcs.056515>.
- Geblinger, D., Geiger, B. and Addadi, L. (2009) 'Surface-Induced Regulation of Podosome Organization and Dynamics in Cultured Osteoclasts', *ChemBioChem*, 10(1), pp. 158–165. Available at: <https://doi.org/10.1002/cbic.200800549>.
- Geijtenbeek, T.B.H. *et al.* (2000) 'DC-SIGN, a Dendritic Cell–Specific HIV-1-Binding Protein that Enhances trans-Infection of T Cells', *Cell*, 100(5), pp. 587–597. Available at: [https://doi.org/10.1016/S0092-8674\(00\)80694-7](https://doi.org/10.1016/S0092-8674(00)80694-7).
- Geng, J. *et al.* (2021) 'TLR4 signalling via Piezo1 engages and enhances the macrophage mediated host response during bacterial infection', *Nature Communications*, 12(1), p. 3519. Available at: <https://doi.org/10.1038/s41467-021-23683-y>.

## REFERENCES

- Ghiran, I. *et al.* (2000) 'Complement Receptor 1/Cd35 Is a Receptor for Mannan-Binding Lectin', *Journal of Experimental Medicine*, 192(12), pp. 1797–1808. Available at: <https://doi.org/10.1084/jem.192.12.1797>.
- Gold, E.S. *et al.* (1999) 'Dynamin 2 Is Required for Phagocytosis in Macrophages', *Journal of Experimental Medicine*, 190(12), pp. 1849–1856. Available at: <https://doi.org/10.1084/jem.190.12.1849>.
- Goldschmidt-Clermont, P.J. *et al.* (1990) 'The Actin-Binding Protein Profilin Binds to PIP<sub>2</sub> and Inhibits Its Hydrolysis by Phospholipase C', *Science*, 247(4950), pp. 1575–1578. Available at: <https://doi.org/10.1126/science.2157283>.
- Goldschmidt-Clermont, P.J. *et al.* (1992) 'The control of actin nucleotide exchange by thymosin beta 4 and profilin. A potential regulatory mechanism for actin polymerization in cells.', *Molecular Biology of the Cell*, 3(9), pp. 1015–1024. Available at: <https://doi.org/10.1091/mbc.3.9.1015>.
- Gordon, S. and Martinez-Pomares, L. (2017) 'Physiological roles of macrophages', *Pflügers Archiv: European Journal of Physiology*, 469(3–4), pp. 365–374. Available at: <https://doi.org/10.1007/s00424-017-1945-7>.
- Gordon, S. and Taylor, P.R. (2005) 'Monocyte and macrophage heterogeneity', *Nature Reviews Immunology*, 5(12), pp. 953–964. Available at: <https://doi.org/10.1038/nri1733>.
- Griffin, F.M. *et al.* (1975) 'Studies on the mechanism of phagocytosis. I. Requirements for circumferential attachment of particle-bound ligands to specific receptors on the macrophage plasma membrane.', *Journal of Experimental Medicine*, 142(5), pp. 1263–1282. Available at: <https://doi.org/10.1084/jem.142.5.1263>.
- Griffin, F.M., Griffin, J.A. and Silverstein, S.C. (1976) 'Studies on the mechanism of phagocytosis. II. The interaction of macrophages with anti-immunoglobulin IgG-coated bone marrow-derived lymphocytes.', *Journal of Experimental Medicine*, 144(3), pp. 788–809. Available at: <https://doi.org/10.1084/jem.144.3.788>.
- Guilliams, M. *et al.* (2014) 'Dendritic cells, monocytes and macrophages: a unified nomenclature based on ontogeny', *Nature Reviews Immunology*, 14(8), pp. 571–578. Available at: <https://doi.org/10.1038/nri3712>.
- Gutierrez, M.G. (2013) 'Functional role(s) of phagosomal Rab GTPases', *Small GTPases*, 4(3), pp. 148–158. Available at: <https://doi.org/10.4161/sgtp.25604>.
- Hajjoul, H. *et al.* (2009) 'Lab-on-Chip for fast 3D particle tracking in living cells', *Lab on a Chip*, 9(21), p. 3054. Available at: <https://doi.org/10.1039/b909016a>.
- Hall, A.B. *et al.* (2006) 'Requirements for Vav Guanine Nucleotide Exchange Factors and Rho GTPases in FcγR- and Complement-Mediated Phagocytosis', *Immunity*, 24(3), pp. 305–316. Available at: <https://doi.org/10.1016/j.immuni.2006.02.005>.
- Harris, A.K., Wild, P. and Stopak, D. (1980) 'Silicone Rubber Substrata: A New Wrinkle in the Study of Cell Locomotion', *Science*, 208(4440), pp. 177–179. Available at: <https://doi.org/10.1126/science.6987736>.

## REFERENCES

- Heinrich, V. (2015) 'Controlled One-on-One Encounters between Immune Cells and Microbes Reveal Mechanisms of Phagocytosis', *Biophysical Journal*, 109(3), pp. 469–476. Available at: <https://doi.org/10.1016/j.bpj.2015.06.042>.
- Herant, M., Heinrich, V. and Dembo, M. (2005) 'Mechanics of neutrophil phagocytosis: behavior of the cortical tension', *Journal of Cell Science*, 118(9), pp. 1789–1797. Available at: <https://doi.org/10.1242/jcs.02275>.
- Herant, M., Heinrich, V. and Dembo, M. (2006) 'Mechanics of neutrophil phagocytosis: experiments and quantitative models', *Journal of Cell Science*, 119(9), pp. 1903–1913. Available at: <https://doi.org/10.1242/jcs.02876>.
- Herron, J.C. *et al.* (2022) 'Actin nano-architecture of phagocytic podosomes'. Available at: <https://doi.org/10.1038/s41467-022-32038-0>.
- Hochmuth, F.M. *et al.* (1996) 'Deformation and flow of membrane into tethers extracted from neuronal growth cones', *Biophysical Journal*, 70(1), pp. 358–369. Available at: [https://doi.org/10.1016/S0006-3495\(96\)79577-2](https://doi.org/10.1016/S0006-3495(96)79577-2).
- Hoppe, A.D. and Swanson, J.A. (2004) 'Cdc42, Rac1, and Rac2 Display Distinct Patterns of Activation during Phagocytosis', *Molecular Biology of the Cell*, 15(8), pp. 3509–3519. Available at: <https://doi.org/10.1091/mbc.e03-11-0847>.
- Horsthemke, M. *et al.* (2017) 'Multiple roles of filopodial dynamics in particle capture and phagocytosis and phenotypes of Cdc42 and Myo10 deletion', *Journal of Biological Chemistry*, 292(17), pp. 7258–7273. Available at: <https://doi.org/10.1074/jbc.M116.766923>.
- Hotulainen, P. and Lappalainen, P. (2006) 'Stress fibers are generated by two distinct actin assembly mechanisms in motile cells', *Journal of Cell Biology*, 173(3), pp. 383–394. Available at: <https://doi.org/10.1083/jcb.200511093>.
- Hur, S.S. *et al.* (2020) 'Traction Force Microscopy for Understanding Cellular Mechanotransduction', *BMB Reports*, 53(2), pp. 74–81. Available at: <https://doi.org/10.5483/BMBRep.2020.53.2.308>.
- Huynh, K.K. and Grinstein, S. (2008) 'Phagocytosis: Dynamin's Dual Role in Phagosome Biogenesis', *Current Biology*, 18(13), pp. R563–R565. Available at: <https://doi.org/10.1016/j.cub.2008.05.032>.
- Imbert, P.R.C. *et al.* (2021) 'An Acquired and Endogenous Glycocalyx Forms a Bidirectional "Don't Eat" and "Don't Eat Me" Barrier to Phagocytosis', *Current Biology*, 31(1), pp. 77–89.e5. Available at: <https://doi.org/10.1016/j.cub.2020.09.082>.
- Iqbal, Z. *et al.* (2010) 'Disruption of the Podosome Adaptor Protein TKS4 (SH3PXD2B) Causes the Skeletal Dysplasia, Eye, and Cardiac Abnormalities of Frank-Ter Haar Syndrome', *The American Journal of Human Genetics*, 86(2), pp. 254–261. Available at: <https://doi.org/10.1016/j.ajhg.2010.01.009>.
- Irmscher, M. *et al.* (2013) 'A method for time-resolved measurements of the mechanics of phagocytic cups', *Journal of The Royal Society Interface*, 10(82), p. 20121048. Available at: <https://doi.org/10.1098/rsif.2012.1048>.
- Ito, H. and Kaneko, M. (2020) 'On-chip cell manipulation and applications to deformability measurements', *ROBOMECH Journal*, 7(1), p. 3. Available at: <https://doi.org/10.1186/s40648-020-0154-x>.

## REFERENCES

- Jaumouillé, V., Cartagena-Rivera, A. and Waterman, C.M. (2019) 'Coupling of  $\beta 2$  integrins to actin by a mechanosensitive molecular clutch drives complement receptor-mediated phagocytosis'. Available at: <https://doi.org/10.1038/s41556-019-0414-2>.
- Jaumouillé, V. and Grinstein, S. (2011) 'Receptor mobility, the cytoskeleton, and particle binding during phagocytosis', *Current Opinion in Cell Biology*, 23(1), pp. 22–29. Available at: <https://doi.org/10.1016/j.ceb.2010.10.006>.
- Jaumouillé, V. and Waterman, C.M. (2020a) 'Physical Constraints and Forces Involved in Phagocytosis'. Available at: <https://doi.org/10.3389/fimmu.2020.01097>.
- Jaumouillé, V. and Waterman, C.M. (2020b) 'Physical Constraints and Forces Involved in Phagocytosis', *Frontiers in Immunology*, 11, p. 1097. Available at: <https://doi.org/10.3389/fimmu.2020.01097>.
- Kahr, W.H.A. *et al.* (2017) 'Loss of the Arp2/3 complex component ARPC1B causes platelet abnormalities and predisposes to inflammatory disease', *Nature Communications*, 8(1), p. 14816. Available at: <https://doi.org/10.1038/ncomms14816>.
- Kalashnikov, N. and Moraes, C. (2022) 'Engineering physical microenvironments to study innate immune cell biophysics', *APL Bioengineering*, 6(3), p. 031504. Available at: <https://doi.org/10.1063/5.0098578>.
- Kanchanawong, P. *et al.* (2010) 'Nanoscale architecture of integrin-based cell adhesions', *Nature*, 468(7323), pp. 580–584. Available at: <https://doi.org/10.1038/nature09621>.
- Kaplan, G. (1977) 'Differences in the Mode of Phagocytosis with Fc and C3 Receptors in Macrophages', *Scandinavian Journal of Immunology*, 6(8), pp. 797–807. Available at: <https://doi.org/10.1111/j.1365-3083.1977.tb02153.x>.
- Katoh, H. and Negishi, M. (2003) 'RhoG activates Rac1 by direct interaction with the Dock180-binding protein Elmo', *Nature*, 424(6947), pp. 461–464. Available at: <https://doi.org/10.1038/nature01817>.
- Kim, J.H. *et al.* (2015) 'Mechanical Tension Drives Cell Membrane Fusion', *Developmental Cell*, 32(5), pp. 561–573. Available at: <https://doi.org/10.1016/j.devcel.2015.01.005>.
- Kinchen, J.M. and Ravichandran, K.S. (2008) 'Phagosome maturation: going through the acid test', *Nature Reviews Molecular Cell Biology*, 9(10), pp. 781–795. Available at: <https://doi.org/10.1038/nrm2515>.
- Kitano, M. *et al.* (2008) 'Imaging of Rab5 activity identifies essential regulators for phagosome maturation', *Nature*, 453(7192), pp. 241–245. Available at: <https://doi.org/10.1038/nature06857>.
- Kopp, P. *et al.* (2006) 'The Kinesin KIF1C and Microtubule Plus Ends Regulate Podosome Dynamics in Macrophages', *Molecular Biology of the Cell*. Edited by P. Matsudaira, 17(6), pp. 2811–2823. Available at: <https://doi.org/10.1091/mbc.e05-11-1010>.
- Kovari, D.T. *et al.* (2016) 'Frustrated Phagocytic Spreading of J774A-1 Macrophages Ends in Myosin II-Dependent Contraction.' Available at: <https://doi.org/10.1016/j.bpj.2016.11.009>.
- Krause, M. *et al.* (2004) 'Lamellipodin, an Ena/VASP Ligand, Is Implicated in the Regulation of Lamellipodial Dynamics', *Developmental Cell*, 7(4), pp. 571–583. Available at: <https://doi.org/10.1016/j.devcel.2004.07.024>.

## REFERENCES

- Kress, H. *et al.* (2007) 'Filopodia act as phagocytic tentacles and pull with discrete steps and a load-dependent velocity', *Proceedings of the National Academy of Sciences*, 104(28), pp. 11633–11638. Available at: <https://doi.org/10.1073/pnas.0702449104>.
- Krieg, M. *et al.* (2018) 'Atomic force microscopy-based mechanobiology', *Nature Reviews Physics*, 1(1), pp. 41–57. Available at: <https://doi.org/10.1038/s42254-018-0001-7>.
- Kronenberg, N.M. *et al.* (2017) 'Long-term imaging of cellular forces with high precision by elastic resonator interference stress microscopy', *Nature Cell Biology*, 19(7), pp. 864–872. Available at: <https://doi.org/10.1038/ncb3561>.
- Labernadie, A. *et al.* (2010) 'Dynamics of podosome stiffness revealed by atomic force microscopy', *Proceedings of the National Academy of Sciences*, 107(49), pp. 21016–21021. Available at: <https://doi.org/10.1073/pnas.1007835107>.
- Labernadie, A. *et al.* (2014) 'Protrusion force microscopy reveals oscillatory force generation and mechanosensing activity of human macrophage podosomes', *Nature Communications*, 5(1), p. 5343. Available at: <https://doi.org/10.1038/ncomms6343>.
- Labrousse, A. (2011) 'Frustrated phagocytosis on micro-patterned immune complexes to characterize lysosome movements in live macrophages', *Frontiers in Immunology*, 2. Available at: <https://doi.org/10.3389/fimmu.2011.00051>.
- Lagarrigue, F., Kim, C. and Ginsberg, M.H. (2016) 'The Rap1-RIAM-talin axis of integrin activation and blood cell function', *Blood*, 128(4), pp. 479–487. Available at: <https://doi.org/10.1182/blood-2015-12-638700>.
- Leishman, W.B. (1902) 'NOTE ON A METHOD OF QUANTITATIVELY ESTIMATING THE PHAGOCYtic POWER OF THE LEUCOCYTES OF THE BLOOD', *BMJ*, 1(2141), pp. 73–75. Available at: <https://doi.org/10.1136/bmj.1.2141.73-a>.
- Levin, R., Grinstein, S. and Canton, J. (2016) 'The life cycle of phagosomes: formation, maturation, and resolution', *Immunological Reviews*, 273(1), pp. 156–179. Available at: <https://doi.org/10.1111/imr.12439>.
- Levin, R., Grinstein, S. and Schlam, D. (2015) 'Phosphoinositides in phagocytosis and macropinocytosis', *Biochimica et Biophysica Acta (BBA) - Molecular and Cell Biology of Lipids*, 1851(6), pp. 805–823. Available at: <https://doi.org/10.1016/j.bbailip.2014.09.005>.
- Lewkowicz, E. *et al.* (2008) 'The microtubule-binding protein CLIP-170 coordinates mDia1 and actin reorganization during CR3-mediated phagocytosis', *Journal of Cell Biology*, 183(7), pp. 1287–1298. Available at: <https://doi.org/10.1083/jcb.200807023>.
- Liebl, D. and Griffiths, G. (2009) 'Transient assembly of F-actin by phagosomes delays phagosome fusion with lysosomes in cargo-overloaded macrophages', *Journal of Cell Science*, 122(16), pp. 2935–2945. Available at: <https://doi.org/10.1242/jcs.048355>.
- Linder, S. *et al.* (1999) 'Wiskott-Aldrich syndrome protein regulates podosomes in primary human macrophages', *Proceedings of the National Academy of Sciences*, 96(17), pp. 9648–9653. Available at: <https://doi.org/10.1073/pnas.96.17.9648>.

## REFERENCES

- Linder, S. *et al.* (2000) 'The Polarization Defect of Wiskott-Aldrich Syndrome Macrophages Is Linked to Dislocalization of the Arp2/3 Complex', *The Journal of Immunology*, 165(1), pp. 221–225. Available at: <https://doi.org/10.4049/jimmunol.165.1.221>.
- Linder, S. (2007) 'The matrix corroded: podosomes and invadopodia in extracellular matrix degradation', *Trends in Cell Biology*, 17(3), pp. 107–117. Available at: <https://doi.org/10.1016/j.tcb.2007.01.002>.
- Linder, S. and Aepfelbacher, M. (2003) 'Podosomes: adhesion hot-spots of invasive cells', *Trends in Cell Biology*, 13(7), pp. 376–385. Available at: [https://doi.org/10.1016/S0962-8924\(03\)00128-4](https://doi.org/10.1016/S0962-8924(03)00128-4).
- Linder, S., Wiesner, C. and Himmel, M. (2011) 'Degrading Devices: Invadosomes in Proteolytic Cell Invasion', *Annual Review of Cell and Developmental Biology*, 27(1), pp. 185–211. Available at: <https://doi.org/10.1146/annurev-cellbio-092910-154216>.
- van Lookeren Campagne, M., Wiesmann, C. and Brown, E.J. (2007) 'Macrophage complement receptors and pathogen clearance', *Cellular Microbiology*, 9(9), pp. 2095–2102. Available at: <https://doi.org/10.1111/j.1462-5822.2007.00981.x>.
- Marchisio, P. *et al.* (1988) 'Vinculin, talin, and integrins are localized at specific adhesion sites of malignant B lymphocytes', *Blood*, 72(2), pp. 830–833. Available at: <https://doi.org/10.1182/blood.V72.2.830.830>.
- Marie-Anaïs, F. *et al.* (2016) 'Dynamin-Actin Cross Talk Contributes to Phagosome Formation and Closure: Role of Dynamin in Phagosome Formation and Closure', *Traffic*, 17(5), pp. 487–499. Available at: <https://doi.org/10.1111/tra.12386>.
- Marshansky, V. and Futai, M. (2008) 'The V-type H<sup>+</sup>-ATPase in vesicular trafficking: targeting, regulation and function', *Current Opinion in Cell Biology*, 20(4), pp. 415–426. Available at: <https://doi.org/10.1016/j.ceb.2008.03.015>.
- Masters, T.A. *et al.* (2013) 'Plasma membrane tension orchestrates membrane trafficking, cytoskeletal remodeling, and biochemical signaling during phagocytosis', *Proceedings of the National Academy of Sciences*, 110(29), pp. 11875–11880. Available at: <https://doi.org/10.1073/pnas.1301766110>.
- May, R.C. *et al.* (2000) 'Involvement of the Arp2/3 complex in phagocytosis mediated by FcγR or CR3', *Nature Cell Biology*, 2(4), pp. 246–248. Available at: <https://doi.org/10.1038/35008673>.
- Metchnikoff, E. (1905) 'Immunity in infective diseases', *Cambridge University Press*.
- Mills, C.D. *et al.* (2000) 'M-1/M-2 Macrophages and the Th1/Th2 Paradigm', *The Journal of Immunology*, 164(12), pp. 6166–6173. Available at: <https://doi.org/10.4049/jimmunol.164.12.6166>.
- Mohagheghian, E. *et al.* (2018) 'Quantifying compressive forces between living cell layers and within tissues using elastic round microgels', *Nature Communications*, 9(1), p. 1878. Available at: <https://doi.org/10.1038/s41467-018-04245-1>.
- Montaño-Rendón, F. *et al.* (2022) 'PtdIns(3,4)P<sub>2</sub>, Lamellipodin, and VASP coordinate actin dynamics during phagocytosis in macrophages', *Journal of Cell Biology*, 221(11), p. e202207042. Available at: <https://doi.org/10.1083/jcb.202207042>.

## REFERENCES

- Moreau, V. *et al.* (2003) 'Actin Can Reorganize into Podosomes in Aortic Endothelial Cells, a Process Controlled by Cdc42 and RhoA', *Molecular and Cellular Biology*, 23(19), pp. 6809–6822. Available at: <https://doi.org/10.1128/MCB.23.19.6809-6822.2003>.
- Morlot, S. and Roux, A. (2013) 'Mechanics of Dynamin-Mediated Membrane Fission', *Annual Review of Biophysics*, 42(1), pp. 629–649. Available at: <https://doi.org/10.1146/annurev-biophys-050511-102247>.
- Mosser, D.M. and Edwards, J.P. (2008) 'Exploring the full spectrum of macrophage activation', *Nature Reviews Immunology*, 8(12), pp. 958–969. Available at: <https://doi.org/10.1038/nri2448>.
- Mularski, A. *et al.* (2021) *Dynamin-2 controls complement receptor 3- mediated phagocytosis completion and closure.* preprint. Cell Biology. Available at: <https://doi.org/10.1101/2021.02.14.431164>.
- Murphy, J. *et al.* (2008) 'The Prolonged Life-Span of Alveolar Macrophages', *American Journal of Respiratory Cell and Molecular Biology*, 38(4), pp. 380–385. Available at: <https://doi.org/10.1165/rcmb.2007-0224RC>.
- Mustapha, F., Sengupta, K. and Puech, P.-H. (2022) 'May the force be with your (immune) cells: an introduction to traction force microscopy in Immunology', *Frontiers in Immunology*, 13, p. 898558. Available at: <https://doi.org/10.3389/fimmu.2022.898558>.
- Mylvaganam, S., Freeman, S. and Grinstein, S. (2021) 'The cytoskeleton in phagocytosis and macropinocytosis'. Available at: <https://doi.org/10.1016/j.cub.2021.01.036>.
- Nédélec, F., Surrey, T. and Karsenti, E. (2003) 'Self-organisation and forces in the microtubule cytoskeleton', *Current Opinion in Cell Biology*, 15(1), pp. 118–124. Available at: [https://doi.org/10.1016/S0955-0674\(02\)00014-5](https://doi.org/10.1016/S0955-0674(02)00014-5).
- Nelsen, E. *et al.* (2019) 'Combined Atomic Force Microscope and Volumetric Light Sheet System for Mechanobiology'. Available at: <https://doi.org/10.1101/812396>.
- Newman, S.L., Mikus, L.K. and Tucci, M.A. (1991) 'Differential requirements for cellular cytoskeleton in human macrophage complement receptor- and Fc receptor-mediated phagocytosis', *Journal of Immunology (Baltimore, Md.: 1950)*, 146(3), pp. 967–974.
- Nimmerjahn, F. and Ravetch, J.V. (2010) 'Antibody-mediated modulation of immune responses: IgG-mediated inhibition', *Immunological Reviews*, 236(1), pp. 265–275. Available at: <https://doi.org/10.1111/j.1600-065X.2010.00910.x>.
- Nourse, J.L. and Pathak, M.M. (2017) 'How cells channel their stress: Interplay between Piezo1 and the cytoskeleton', *Seminars in Cell & Developmental Biology*, 71, pp. 3–12. Available at: <https://doi.org/10.1016/j.semcdb.2017.06.018>.
- Nüsse, O. (2011) 'Biochemistry of the Phagosome: The Challenge to Study a Transient Organelle', *The Scientific World JOURNAL*, 11, pp. 2364–2381. Available at: <https://doi.org/10.1100/2011/741046>.
- Nussenzveig, H.M. (2018) 'Cell membrane biophysics with optical tweezers', *European Biophysics Journal*, 47(5), pp. 499–514. Available at: <https://doi.org/10.1007/s00249-017-1268-9>.

## REFERENCES

- Oikawa, T. *et al.* (2012) 'Tks5-dependent formation of circumferential podosomes/invadopodia mediates cell–cell fusion', *Journal of Cell Biology*, 197(4), pp. 553–568. Available at: <https://doi.org/10.1083/jcb.201111116>.
- Olazabal, I.M. *et al.* (2002) 'Rho-Kinase and Myosin-II Control Phagocytic Cup Formation during CR, but Not Fc $\gamma$ R, Phagocytosis', *Current Biology*, 12(16), pp. 1413–1418. Available at: [https://doi.org/10.1016/S0960-9822\(02\)01069-2](https://doi.org/10.1016/S0960-9822(02)01069-2).
- Ortiz-Stern, A. and Rosales, C. (2005) 'Fc $\gamma$ RIIIB stimulation promotes  $\beta$ 1 integrin activation in human neutrophils', *Journal of Leukocyte Biology*, 77(5), pp. 787–799. Available at: <https://doi.org/10.1189/jlb.0504310>.
- Osiak, A.-E., Zenner, G. and Linder, S. (2005) 'Subconfluent endothelial cells form podosomes downstream of cytokine and RhoGTPase signaling', *Experimental Cell Research*, 307(2), pp. 342–353. Available at: <https://doi.org/10.1016/j.yexcr.2005.03.035>.
- Ostrowski, P.P. *et al.* (2019) 'Dynamic Podosome-Like Structures in Nascent Phagosomes Are Coordinated by Phosphoinositides.' Available at: <https://doi.org/10.1016/j.devcel.2019.05.028>.
- Ostrowski, P.P., Grinstein, S. and Freeman, S.A. (2016) 'Diffusion Barriers, Mechanical Forces, and the Biophysics of Phagocytosis', *Developmental Cell*, 38(2), pp. 135–146. Available at: <https://doi.org/10.1016/j.devcel.2016.06.023>.
- Pacheco, P., White, D. and Sulchek, T. (2013) 'Effects of Microparticle Size and Fc Density on Macrophage Phagocytosis', *PLoS ONE*. Edited by Y. Wang, 8(4), p. e60989. Available at: <https://doi.org/10.1371/journal.pone.0060989>.
- Pal, K. *et al.* (2021) 'Ubiquitous membrane-bound DNase activity in podosomes and invadopodia', *Journal of Cell Biology*, 220(7), p. e202008079. Available at: <https://doi.org/10.1083/jcb.202008079>.
- Panzer, L. *et al.* (2015) 'The formins FHOD1 and INF2 regulate inter- and intra-structural contractility of podosomes', *Journal of Cell Science*, p. jcs.177691. Available at: <https://doi.org/10.1242/jcs.177691>.
- Paterson, E.K. and Courtneidge, S.A. (2018) 'Invadosomes are coming: new insights into function and disease relevance', *The FEBS Journal*, 285(1), pp. 8–27. Available at: <https://doi.org/10.1111/febs.14123>.
- Paterson, N. and Lämmermann, T. (2022) 'Macrophage network dynamics depend on haptokinesis for optimal local surveillance', *eLife*, 11, p. e75354. Available at: <https://doi.org/10.7554/eLife.75354>.
- Poirier, M.B. *et al.* (2020) 'F-actin flashes on phagosomes mechanically deform contents for efficient digestion in macrophages', *Journal of Cell Science*, p. jcs.239384. Available at: <https://doi.org/10.1242/jcs.239384>.
- Pollard, J.W. (2009) 'Trophic macrophages in development and disease', *Nature Reviews Immunology*, 9(4), pp. 259–270. Available at: <https://doi.org/10.1038/nri2528>.
- Pollard, T.D. and Borisy, G.G. (2003) 'Cellular Motility Driven by Assembly and Disassembly of Actin Filaments', *Cell*, 112(4), pp. 453–465. Available at: [https://doi.org/10.1016/S0092-8674\(03\)00120-X](https://doi.org/10.1016/S0092-8674(03)00120-X).
- Proag, A. *et al.* (2015) 'Working Together: Spatial Synchrony in the Force and Actin Dynamics of Podosome First Neighbors', *ACS Nano*, 9(4), pp. 3800–3813. Available at: <https://doi.org/10.1021/nn506745r>.

## REFERENCES

- Proag, A. *et al.* (2016) 'Evaluation of the force and spatial dynamics of macrophage podosomes by multi-particle tracking', *Methods*, 94, pp. 75–84. Available at: <https://doi.org/10.1016/j.ymeth.2015.09.002>.
- Rabinovitch, M. (1995) 'Professional and non-professional phagocytes: an introduction', *Trends in Cell Biology*, 5(3), pp. 85–87. Available at: [https://doi.org/10.1016/S0962-8924\(00\)88955-2](https://doi.org/10.1016/S0962-8924(00)88955-2).
- Ravetch, J.V. and Bolland, S. (2001) 'IgG Fc Receptors', *Annual Review of Immunology*, 19(1), pp. 275–290. Available at: <https://doi.org/10.1146/annurev.immunol.19.1.275>.
- Raza, Y., Salman, H. and Luberto, C. (2021) 'Sphingolipids in Hematopoiesis: Exploring Their Role in Lineage Commitment', *Cells*, 10(10), p. 2507. Available at: <https://doi.org/10.3390/cells10102507>.
- del Rio, A. *et al.* (2009) 'Stretching Single Talin Rod Molecules Activates Vinculin Binding', *Science*, 323(5914), pp. 638–641. Available at: <https://doi.org/10.1126/science.1162912>.
- Roberts, J. and Quastel, J. (1963) 'PARTICLE UPTAKE BY POLYMORPHONUCLEAR LEUCOCYTES AND EHRLICH ASCITES-CARCINOMA CELLS', *Biochemical Journal*, 89(1), pp. 150–156. Available at: <https://doi.org/10.1042/bj0890150>.
- Ros, M. *et al.* (2020) 'ER-resident oxidoreductases are glycosylated and trafficked to the cell surface to promote matrix degradation by tumour cells', *Nature Cell Biology*, 22(11), pp. 1371–1381. Available at: <https://doi.org/10.1038/s41556-020-00590-w>.
- Rosales, C. (2007) 'Fc receptor and integrin signaling in phagocytes', *Signal Transduction*, 7(5–6), pp. 386–401. Available at: <https://doi.org/10.1002/sita.200700141>.
- Rosales, C. and Uribe-Querol, E. (2013a) 'Antibody - Fc Receptor Interactions in Antimicrobial Functions', *Current Immunology Reviews*, 9(1), pp. 44–55. Available at: <https://doi.org/10.2174/1573395511309010006>.
- Rosales, C. and Uribe-Querol, E. (2013b) 'Fc receptors: Cell activators of antibody functions', *Advances in Bioscience and Biotechnology*, 04(04), pp. 21–33. Available at: <https://doi.org/10.4236/abb.2013.44A004>.
- Ross, G.D. *et al.* (1992) 'Macrophage cytoskeleton association with CR3 and CR4 regulates receptor mobility and phagocytosis of iC3b-opsonized erythrocytes', *Journal of Leukocyte Biology*, 51(2), pp. 109–117. Available at: <https://doi.org/10.1002/jlb.51.2.109>.
- Rotty, J.D. *et al.* (2015) 'Profilin-1 Serves as a Gatekeeper for Actin Assembly by Arp2/3-Dependent and -Independent Pathways', *Developmental Cell*, 32(1), pp. 54–67. Available at: <https://doi.org/10.1016/j.devcel.2014.10.026>.
- Rotty, J.D. *et al.* (2017) 'Arp2/3 Complex Is Required for Macrophage Integrin Functions but Is Dispensable for FcR Phagocytosis and In Vivo Motility', *Developmental Cell*, 42(5), pp. 498–513.e6. Available at: <https://doi.org/10.1016/j.devcel.2017.08.003>.
- Rougerie, P. and Cox, D. (2020) 'Spatio-temporal mapping of mechanical force generated by macrophages during FcγR-dependent phagocytosis reveals adaptation to target stiffness'. Available at: <https://doi.org/10.1101/2020.04.14.041335>.

## REFERENCES

- Rougerie, P., Miskolci, V. and Cox, D. (2013) 'Generation of membrane structures during phagocytosis and chemotaxis of macrophages: role and regulation of the actin cytoskeleton', *Immunological Reviews*, 256(1), pp. 222–239. Available at: <https://doi.org/10.1111/imr.12118>.
- Sánchez-Mejorada, G. and Rosales, C. (1998) 'Signal transduction by immunoglobulin Fc receptors', *Journal of Leukocyte Biology*, 63(5), pp. 521–533. Available at: <https://doi.org/10.1002/jlb.63.5.521>.
- Sarkar, R. and Rybenkov, V.V. (2016) 'A Guide to Magnetic Tweezers and Their Applications', *Frontiers in Physics*, 4. Available at: <https://doi.org/10.3389/fphy.2016.00048>.
- Schoen, I. *et al.* (2010) 'Probing Cellular Traction Forces by Micropillar Arrays: Contribution of Substrate Warping to Pillar Deflection', *Nano Letters*, 10(5), pp. 1823–1830. Available at: <https://doi.org/10.1021/nl100533c>.
- Schuerle, S. *et al.* (2017) 'Robotically controlled microprey to resolve initial attack modes preceding phagocytosis', *Science Robotics*, 2(2), p. eaah6094. Available at: <https://doi.org/10.1126/scirobotics.aah6094>.
- Schwarz, U.S. and Soiné, J.R.D. (2015) 'Traction force microscopy on soft elastic substrates: A guide to recent computational advances', *Biochimica et Biophysica Acta (BBA) - Molecular Cell Research*, 1853(11), pp. 3095–3104. Available at: <https://doi.org/10.1016/j.bbamcr.2015.05.028>.
- Scott, C.C. *et al.* (2005) 'Phosphatidylinositol-4,5-bisphosphate hydrolysis directs actin remodeling during phagocytosis', *Journal of Cell Biology*, 169(1), pp. 139–149. Available at: <https://doi.org/10.1083/jcb.200412162>.
- Seals, D.F. *et al.* (2005) 'The adaptor protein Tks5/Fish is required for podosome formation and function, and for the protease-driven invasion of cancer cells', *Cancer Cell*, 7(2), pp. 155–165. Available at: <https://doi.org/10.1016/j.ccr.2005.01.006>.
- Sens, K.L. *et al.* (2010) 'An invasive podosome-like structure promotes fusion pore formation during myoblast fusion', *Journal of Cell Biology*, 191(5), pp. 1013–1027. Available at: <https://doi.org/10.1083/jcb.201006006>.
- Sens, P. and Plastino, J. (2015) 'Membrane tension and cytoskeleton organization in cell motility', *Journal of Physics: Condensed Matter*, 27(27), p. 273103. Available at: <https://doi.org/10.1088/0953-8984/27/27/273103>.
- Sheetz, M.P. (2001) 'Cell control by membrane–cytoskeleton adhesion', *Nature Reviews Molecular Cell Biology*, 2(5), pp. 392–396. Available at: <https://doi.org/10.1038/35073095>.
- Shibata, H., Heo, Y.J. and Takeuchi, S. (2011) 'Simple molding fabrication for poly acrylamide hydrogel', in *2011 IEEE 24th International Conference on Micro Electro Mechanical Systems. 2011 IEEE 24th International Conference on Micro Electro Mechanical Systems (MEMS)*, Cancun, Mexico: IEEE, pp. 885–888. Available at: <https://doi.org/10.1109/MEMSYS.2011.5734567>.
- Simon, S.I. and Schmid-Schönbein, G.W. (1988) 'Biophysical aspects of microsphere engulfment by human neutrophils', *Biophysical Journal*, 53(2), pp. 163–173. Available at: [https://doi.org/10.1016/S0006-3495\(88\)83078-9](https://doi.org/10.1016/S0006-3495(88)83078-9).
- Springer, T.A. (1990) 'Adhesion receptors of the immune system', *Nature*, 346(6283), pp. 425–434. Available at: <https://doi.org/10.1038/346425a0>.

## REFERENCES

- Starnes, T.W. *et al.* (2014) 'The F-BAR protein PSTPIP1 controls extracellular matrix degradation and filopodia formation in macrophages', *Blood*, 123(17), pp. 2703–2714. Available at: <https://doi.org/10.1182/blood-2013-07-516948>.
- Staszowska, A.D. *et al.* (2017) 'Investigation of podosome ring protein arrangement using localization microscopy images', *Methods*, 115, pp. 9–16. Available at: <https://doi.org/10.1016/j.ymeth.2016.11.005>.
- Steffen, A. *et al.* (2006) 'Filopodia Formation in the Absence of Functional WAVE- and Arp2/3-Complexes', *Molecular Biology of the Cell*. Edited by M. Ginsberg, 17(6), pp. 2581–2591. Available at: <https://doi.org/10.1091/mbc.e05-11-1088>.
- Stellwagen, N.C. (1998) 'Apparent pore size of polyacrylamide gels: Comparison of gels cast and run in Tris-acetate-EDTA and Tris-borate-EDTA buffers', *Electrophoresis*, 19(10), pp. 1542–1547. Available at: <https://doi.org/10.1002/elps.1150191004>.
- Stow, J.L. and Condon, N.D. (2016) 'The cell surface environment for pathogen recognition and entry', *Clinical & Translational Immunology*, 5(4), p. e71. Available at: <https://doi.org/10.1038/cti.2016.15>.
- Strick, T.R. *et al.* (1996) 'The Elasticity of a Single Supercoiled DNA Molecule', *Science*, 271(5257), pp. 1835–1837. Available at: <https://doi.org/10.1126/science.271.5257.1835>.
- Suarez, C. *et al.* (2015) 'Profilin Regulates F-Actin Network Homeostasis by Favoring Formin over Arp2/3 Complex', *Developmental Cell*, 32(1), pp. 43–53. Available at: <https://doi.org/10.1016/j.devcel.2014.10.027>.
- Subramani, R. *et al.* (2020) 'The Influence of Swelling on Elastic Properties of Polyacrylamide Hydrogels', *Frontiers in Materials*, 7, p. 212. Available at: <https://doi.org/10.3389/fmats.2020.00212>.
- Suraneni, P. *et al.* (2012) 'The Arp2/3 complex is required for lamellipodia extension and directional fibroblast cell migration', *Journal of Cell Biology*, 197(2), pp. 239–251. Available at: <https://doi.org/10.1083/jcb.201112113>.
- Swanson, J.A. *et al.* (1999) 'A contractile activity that closes phagosomes in macrophages', *Journal of Cell Science*, 112(3), pp. 307–316. Available at: <https://doi.org/10.1242/jcs.112.3.307>.
- Swanson, J.A. and Baer, S.C. (1995) 'Phagocytosis by zippers and triggers', *Trends in Cell Biology*, 5(3), pp. 89–93. Available at: [https://doi.org/10.1016/S0962-8924\(00\)88956-4](https://doi.org/10.1016/S0962-8924(00)88956-4).
- Tabb, J.S. *et al.* (1998) 'Transport of ER vesicles on actin filaments in neurons by myosin V', *Journal of Cell Science*, 111(21), pp. 3221–3234. Available at: <https://doi.org/10.1242/jcs.111.21.3221>.
- Tan, J.L. *et al.* (2003) 'Cells lying on a bed of microneedles: An approach to isolate mechanical force', *Proceedings of the National Academy of Sciences*, 100(4), pp. 1484–1489. Available at: <https://doi.org/10.1073/pnas.0235407100>.
- Tarone, G. *et al.* (1985) 'Rous sarcoma virus-transformed fibroblasts adhere primarily at discrete protrusions of the ventral membrane called podosomes', *Experimental Cell Research*, 159(1), pp. 141–157. Available at: [https://doi.org/10.1016/S0014-4827\(85\)80044-6](https://doi.org/10.1016/S0014-4827(85)80044-6).
- Tatin, F. *et al.* (2006) 'A signalling cascade involving PKC, Src and Cdc42 regulates podosome assembly in cultured endothelial cells in response to phorbol ester', *Journal of Cell Science*, 119(4), pp. 769–781. Available at: <https://doi.org/10.1242/jcs.02787>.

## REFERENCES

- Taylor, P.R. *et al.* (2005) 'MACROPHAGE RECEPTORS AND IMMUNE RECOGNITION', *Annual Review of Immunology*, 23(1), pp. 901–944. Available at: <https://doi.org/10.1146/annurev.immunol.23.021704.115816>.
- Tehrani, S. *et al.* (2006) 'Cortactin Has an Essential and Specific Role in Osteoclast Actin Assembly', *Molecular Biology of the Cell*. Edited by T. Pollard, 17(7), pp. 2882–2895. Available at: <https://doi.org/10.1091/mbc.e06-03-0187>.
- Tertrais, M. *et al.* (2021) 'Phagocytosis is coupled to the formation of phagosome-associated podosomes and a transient disruption of podosomes in human macrophages', *European Journal of Cell Biology*, 100(4), p. 151161. Available at: <https://doi.org/10.1016/j.ejcb.2021.151161>.
- Thatcher, S. and *et al.* (2017) 'Matrix Metalloproteinases-14, -9 and -2 are Localized to the Podosome and Involved in Podosome Development in the A7r5 Smooth Muscle Cell', *Journal of Cardiobiology*, 5(1), pp. 1–10. Available at: <https://doi.org/10.13188/2332-3671.1000020>.
- Thrasher, A.J. and Burns, S.O. (2010) 'WASP: a key immunological multitasker', *Nature Reviews Immunology*, 10(3), pp. 182–192. Available at: <https://doi.org/10.1038/nri2724>.
- Tohyama, Y. and Yamamura, H. (2006) 'Complement-mediated phagocytosis – the role of Syk', *IUBMB Life (International Union of Biochemistry and Molecular Biology: Life)*, 58(5–6), pp. 304–308. Available at: <https://doi.org/10.1080/15216540600746377>.
- Träber, N. *et al.* (2019) 'Polyacrylamide Bead Sensors for in vivo Quantification of Cell-Scale Stress in Zebrafish Development', *Scientific Reports*, 9(1), p. 17031. Available at: <https://doi.org/10.1038/s41598-019-53425-6>.
- Tridandapani, S. *et al.* (2002) 'Regulated Expression and Inhibitory Function of FcγRIIb in Human Monocytic Cells', *Journal of Biological Chemistry*, 277(7), pp. 5082–5089. Available at: <https://doi.org/10.1074/jbc.M110277200>.
- Tsai, R.K. and Discher, D.E. (2008) 'Inhibition of "self" engulfment through deactivation of myosin-II at the phagocytic synapse between human cells', *Journal of Cell Biology*, 180(5), pp. 989–1003. Available at: <https://doi.org/10.1083/jcb.200708043>.
- Tse, S.M.L. *et al.* (2003) 'Differential Role of Actin, Clathrin, and Dynamin in Fcγ Receptor-mediated Endocytosis and Phagocytosis', *Journal of Biological Chemistry*, 278(5), pp. 3331–3338. Available at: <https://doi.org/10.1074/jbc.M207966200>.
- Tusan, C.G. *et al.* (2018) 'Collective Cell Behavior in Mechanosensing of Substrate Thickness', *Biophysical Journal*, 114(11), pp. 2743–2755. Available at: <https://doi.org/10.1016/j.bpj.2018.03.037>.
- Underhill, D.M. and Goodridge, H.S. (2007) 'The many faces of ITAMs', *Trends in Immunology*, 28(2), pp. 66–73. Available at: <https://doi.org/10.1016/j.it.2006.12.004>.
- Underhill, D.M. and Goodridge, H.S. (2012) 'Information processing during phagocytosis', *Nature Reviews Immunology*, 12(7), pp. 492–502. Available at: <https://doi.org/10.1038/nri3244>.
- Uribe-Querol, E. and Rosales, C. (2017) 'Control of Phagocytosis by Microbial Pathogens', *Frontiers in Immunology*, 8, p. 1368. Available at: <https://doi.org/10.3389/fimmu.2017.01368>.
- Uribe-Querol, E. and Rosales, C. (2020) 'Phagocytosis: Our Current Understanding of a Universal Biological Process'. Available at: <https://doi.org/10.3389/fimmu.2020.01066>.

## REFERENCES

- Van Goethem, E. *et al.* (2010) 'Matrix architecture dictates three-dimensional migration modes of human macrophages: differential involvement of proteases and podosome-like structures', *Journal of Immunology (Baltimore, Md.: 1950)*, 184(2), pp. 1049–1061. Available at: <https://doi.org/10.4049/jimmunol.0902223>.
- Van Goethem, E. *et al.* (2011) 'Macrophage podosomes go 3D', *European Journal of Cell Biology*, 90(2–3), pp. 224–236. Available at: <https://doi.org/10.1016/j.ejcb.2010.07.011>.
- Vicente-Manzanares, M. and Sánchez-Madrid, F. (2004) 'Role of the cytoskeleton during leukocyte responses', *Nature Reviews Immunology*, 4(2), pp. 110–122. Available at: <https://doi.org/10.1038/nri1268>.
- Vieira, O.V. *et al.* (2003) 'Modulation of Rab5 and Rab7 Recruitment to Phagosomes by Phosphatidylinositol 3-Kinase', *Molecular and Cellular Biology*, 23(7), pp. 2501–2514. Available at: <https://doi.org/10.1128/MCB.23.7.2501-2514.2003>.
- Vonna, L. *et al.* (2003) 'Local force induced conical protrusions of phagocytic cells', *Journal of Cell Science*, 116(5), pp. 785–790. Available at: <https://doi.org/10.1242/jcs.00230>.
- Vonna, L. *et al.* (2007) 'Micromechanics of filopodia mediated capture of pathogens by macrophages', *European Biophysics Journal*, 36(2), pp. 145–151. Available at: <https://doi.org/10.1007/s00249-006-0118-y>.
- Vorselen, D. *et al.* (2020) 'Microparticle traction force microscopy reveals subcellular force exertion patterns in immune cell–target interactions', *Nature Communications*, 11(1), p. 20. Available at: <https://doi.org/10.1038/s41467-019-13804-z>.
- Vorselen, D. *et al.* (2021) *Phagocytic “teeth” and myosin-II “jaw” power target constriction during phagocytosis*. preprint. Cell Biology. Available at: <https://doi.org/10.1101/2021.03.14.435346>.
- Vorselen, D. *et al.* (2022) *Cell surface receptors TREM2, CD14 and integrin  $\alpha_M \beta_2$  drive sinking engulfment in phosphatidylserine-mediated phagocytosis*. preprint. Cell Biology. Available at: <https://doi.org/10.1101/2022.07.30.502145>.
- Vorselen, D., Labitigan, R.L.D. and Theriot, J.A. (2020) 'A mechanical perspective on phagocytic cup formation', *Current Opinion in Cell Biology*, 66, pp. 112–122. Available at: <https://doi.org/10.1016/j.ceb.2020.05.011>.
- West, M.A. *et al.* (2004) 'Enhanced Dendritic Cell Antigen Capture via Toll-Like Receptor-Induced Actin Remodeling', *Science*, 305(5687), pp. 1153–1157. Available at: <https://doi.org/10.1126/science.1099153>.
- Wiesner, C. *et al.* (2010) 'KIF5B and KIF3A/KIF3B kinesins drive MT1-MMP surface exposure, CD44 shedding, and extracellular matrix degradation in primary macrophages', *Blood*, 116(9), pp. 1559–1569. Available at: <https://doi.org/10.1182/blood-2009-12-257089>.
- Wiesner, C., Azzouzi, K. el and Linder, S. (2013) 'A specific subset of RabGTPases controls cell surface exposure of MT1-MMP, extracellular matrix degradation and 3D invasion of macrophages', *Journal of Cell Science*, p. jcs.122358. Available at: <https://doi.org/10.1242/jcs.122358>.
- Wright, S.D. and Silverstein, S.C. (1984) 'Phagocytosing macrophages exclude proteins from the zones of contact with opsonized targets', *Nature*, 309(5966), pp. 359–361. Available at: <https://doi.org/10.1038/309359a0>.

## REFERENCES

- Wu, C. *et al.* (2012) 'Arp2/3 Is Critical for Lamellipodia and Response to Extracellular Matrix Cues but Is Dispensable for Chemotaxis', *Cell*, 148(5), pp. 973–987. Available at: <https://doi.org/10.1016/j.cell.2011.12.034>.
- Xiao, H. and Liu, M. (2013) 'Atypical protein kinase C in cell motility', *Cellular and Molecular Life Sciences*, 70(17), pp. 3057–3066. Available at: <https://doi.org/10.1007/s00018-012-1192-1>.
- Yam, P.T. and Theriot, J.A. (2004) 'Repeated Cycles of Rapid Actin Assembly and Disassembly on Epithelial Cell Phagosomes', *Molecular Biology of the Cell*, 15(12), pp. 5647–5658. Available at: <https://doi.org/10.1091/mbc.e04-06-0509>.
- Yamauchi, S., Kawauchi, K. and Sawada, Y. (2012) 'Myosin II-dependent exclusion of CD45 from the site of Fcγ receptor activation during phagocytosis', *FEBS Letters*, 586(19), pp. 3229–3235. Available at: <https://doi.org/10.1016/j.febslet.2012.06.041>.
- Zak, A. *et al.* (2019) *Single-cell immuno-mechanics: rapid viscoelastic changes are a hall-mark of early leukocyte activation*. preprint. Biophysics. Available at: <https://doi.org/10.1101/851634>.
- Zallone, A.Z. *et al.* (1983) 'Osteoclasts and monocytes have similar cytoskeletal structures and adhesion property in vitro', *Journal of Anatomy*, 137 (Pt 1)(Pt 1), pp. 57–70.
- van Zon, J.S. *et al.* (2009) 'A mechanical bottleneck explains the variation in cup growth during FcγR phagocytosis', *Molecular Systems Biology*, 5(1), p. 298. Available at: <https://doi.org/10.1038/msb.2009.59>.

Cover pages image credit

**LITTERATURE REVIEW**

CHAPTER I

*Murine macrophage phagocytosing polystyrene beads coated with IgG.*

C.Bigot, P.Verdys, R.Poincloux

CHAPTER II

*Unroofed human macrophage on PDMS micropillar.*

C.Bigot, J.Rey-Barroso, R.Poincloux

CHAPTER III

*Human macrophage phagocytosing polystyrene beads coated with IgG.*

M.Tertrais, R.Poincloux

CHAPTER IV

*Array of PDMS micropillars of various diameter size.*

C.Bigot, R.Poincloux

CHAPTER V

*Murine macrophage phagocytosing polystyrene beads coated with IgG.*

M.Tertrais, R.Poincloux

**RESULTS**

*Human macrophage phagocytosing polystyrene beads coated with IgG.*

M.Tertrais, R.Poincloux

CHAPTER I

*Advancing phagocytic cup on murine macrophage targeting polystyrene bead.*

C.Bigot, P.Verdys, R.Poincloux

CHAPTER II

*Human macrophages phagocytosing PDMS micropillars.*

C.Bigot, R.Poincloux

## ANNEXES

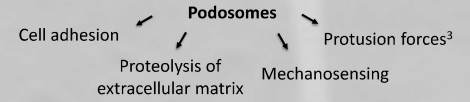
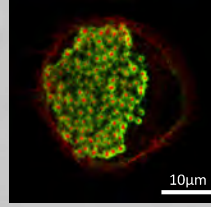
- Poster presented in *Microphysiological systems*, April 2022
- Poster presented in *Invadosome consortium*, September 2022
- Protocol of micropillar fabrication

## Introduction

Macrophages are professional phagocytes of the immune system. One of their key roles is to ingest and digest large particles, a process called phagocytosis, which involves dynamic actin reorganization and generation of contraction forces<sup>1</sup>.



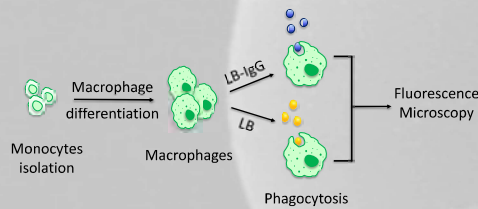
During the first steps of phagocytosis, actin filaments organize as a dense meshwork underlying the plasma membrane in a structure called the phagocytic cup. Following the formation of this cup, actin re-organizes progressively all around the particle until closure of the phagosome membrane<sup>2</sup>. Phagosomes then fuse with endosomes and lysosomes, to form a phagolysosome in which the engulfed particle will be degraded.



Podosome-like structures have been observed at the phagocytic cup and are thought to be not only involved in the early stages of phagocytosis but also play a role all along phagosome maturation. However, it is still unknown whether podosome-like structures are present after phagosome closure.

## Experimental model

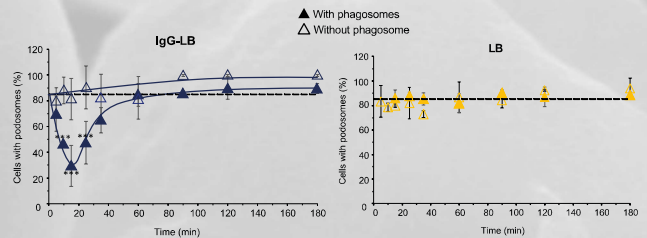
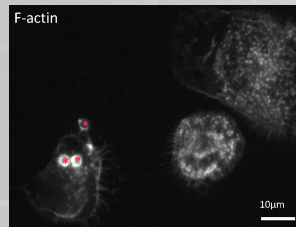
Our model consists in placing latex beads (LB), previously coated with either ovalbumin or immunoglobulin G (IgG) to trigger Fcγ-mediated phagocytosis, with human monocyte-derived macrophages. After 5 to 180 min, the phagocytic activity is quantified by fluorescence microscopy.



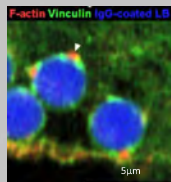
## Disruption of podosomes during phagocytosis

Podosomes remain in cells that do not ingest beads while they disappear in the neighbor cell with phagosomes (materialized by red stars)

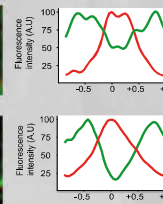
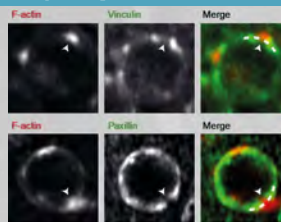
Phagocytosis of IgG-LB, but not LB, induces a transient disruption of podosomes at the ventral face of macrophages<sup>4</sup>



## Podosomes-like structures are present at the membrane of nascent and closed phagosomes



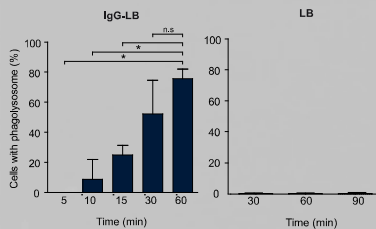
F-actin foci form on phagocytic cups and closed phagosomes containing IgG-LB, they did not form on phagosomes containing LB.



Components belonging to the adhesion complex (integrins, vinculin, paxillin, talin) that are present in the ring of podosomes, also localized in close proximity of actin foci on phagosomes. Analysis of fluorescence intensity profiles revealed that, similarly to podosomes, vinculin and paxillin accumulated around the peak of F-actin.

Thus, we call these actin foci **PAPs**, for phagosomes associated podosomes<sup>4</sup>.

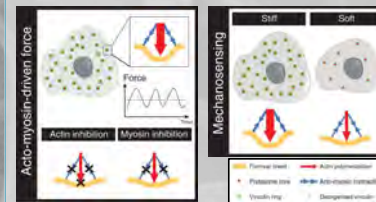
## PAPs correlates with phagolysosome formation



The formation of phagolysosomes was examined by monitoring the transfer of lysosome-associated membrane protein 1 (LAMP-1) to the membrane of phagosomes.

Phagocytic particles that do not trigger the formation of PAPs do not end up in phagolysosomes<sup>4</sup>.

## Forces applied by podosomes



From Labernadie et al. 2014

Podosomes exert a mechanosensing activity by applying a force protruding perpendicularly to the substratum and depending on the substrate stiffness<sup>3</sup>.

Are PAPs involved in force generation on phagosome and for what purpose?

## Conclusion and perspectives

- Phagocytosis of IgG-LB, but not LB, is concomitant with the apparition of PAPs.
- Formation of PAPs leads to phagosome maturation and to podosome disruption in a synchronized manner.
- The disruption of podosomes when PAPs are present could help at redirecting vesicles containing proteases to phagosomes to digest microorganisms.
- Protrusion force generated by podosomes to sense the environment may also operate in podosome-like structures at the phagocytic cup and closed phagosome

## Bibliography

- Vorselen et al., 2021
- Jaumouillé et al., 2020
- Labernadie et al. 2014
- Tertrais, Bigot et al. 2021

## Aknowledgments



# MECHANOBIOLOGY OF PHAGOCYTOSIS IN MACROPHAGES

C. Bigot<sup>1,2</sup>, M. Tertrais<sup>1</sup>, J. Rey-Barroso<sup>1</sup>, M. Malgeri<sup>2</sup>, M. Verdier<sup>1</sup>, A. Labrousse<sup>1</sup>, A. Laborde<sup>2</sup>, I. Maridonneau-Parini<sup>1</sup>, L. Malaquin<sup>2</sup>, R. Poincloux<sup>1</sup>

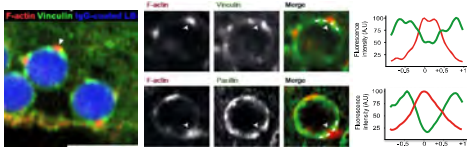


claire.bigot@laas.fr

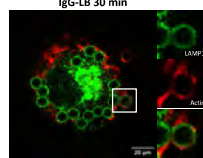
1. Institut de Pharmacologie et de Biologie Structurale, Université de Toulouse, CNRS, UPS, Toulouse 31077, France; LAAS-CNRS, Université de Toulouse, CNRS, INSA, Toulouse 31031, France

## « Deformable micropillars as force probes of frustrated-phagocytosis »

### Podosome-like structures are involved in phagocytosis



Presence of podosome-like structure at the phagosome membrane



Correlation of these structures with phagosome maturation

Are podosomes involved in force generation on phagosome?  
How the forces applied by the cell to phagocyte are distributed?

Tertrais, Bigot et al., *EJC* 2020  
Ostrowski et al., *Dev Cell*, 2019

### Existing methods to investigate the forces exerted on the target of phagocytosis

Traction forces



Atomic Force Microscopy (AFM)

Compression forces



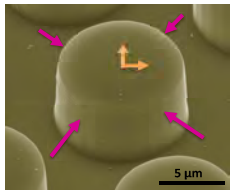
MicroParticles Traction Force Microscopy (MP-TFM)

Adapted from Vorselen et al., *COCB* 2020

Need for a new method to facilitate the exploration of forces

### New method to investigate both traction and compression forces

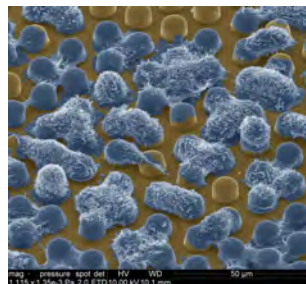
#### Microfabrication of IgG-coated elastic pillars



SEM observation of micropillar

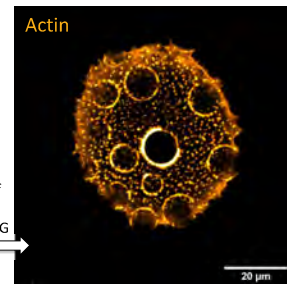
- Controlled size ( $\mu\text{m}$  range)
  - Controlled stiffness (polyacrylamide 3-40 kPa)
  - Frustrated phagocytosis: easier imaging on long time-scales (hour range)
- Compressive force: precision  $\approx 20\text{nm}$   
Traction force: precision  $\approx 100\text{nm}$

#### Frustrated phagocytosis of anchored pillars by macrophages



hMDM on  $9\mu\text{m}$  diameter pillars coated with IgG (SEM)

hMDM on 2kPa polyacrylamide pillars of various diameters (3 to  $9\mu\text{m}$ ) coated with IgG (Epifluorescence)

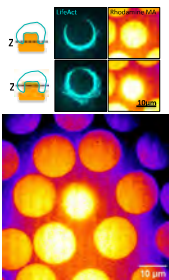


Ring of podosome-like structures around the pillar

hMDM: Human monocyte-derived macrophages

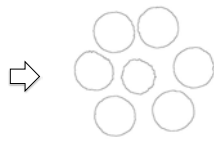
#### Evaluation of the compressive forces

##### Confocal imaging



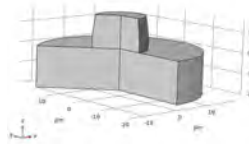
HoxB8 macrophage on 3kPa pillars coated with IgG

##### Analysis of geometry and deformation



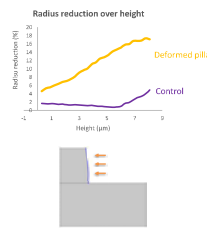
Height and radius of pillar of interest compared to surrounding pillars considered as control (no deformation)

##### Reconstitution of 3D geometry (no deformed)



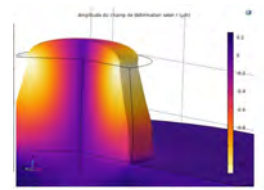
2D axisymmetric model  
Comsol Multiphysics®  
Young modulus  $E=3\text{kPa}$   
Density  $\rho=1$   
Poisson's ratio  $\nu=0.48$

##### Application of deformation curve



Equation of deformation curve applied on the edge of the pillar

##### Simulation of pressure necessary to obtain the deformation



Geometry of deformed pillar

Pressure  $P = 100$  to  $900\text{Pa}$   
Elastic energy  $E = 0,12\text{pJ}$

### Conclusions and perspectives

- Presence of podosome-like structure at the phagosome correlates with its maturation
- Podosome can apply protusive forces and therefore might be involved in force generation at the phagocytic cup
- Both traction and compression forces during phagocytosis can be evaluated experimentally thanks to deformable micropillars
- Numerical simulation can be used to analyse pressure distribution along the pillar
- Next step: exploration of the effect of the pillar stiffness, cell type and various inhibitors on deformation

### Aknowledgments



## Protocole préparation gel polyacrylamide

*D'après Anna Labernadie (optimisé pour IF)  
Adaptation pour micropiliers PAA et process au LAAS : Claire*

### I. Activation des lamelles de verre (IPBS, min 2h)

Permet de faire tenir le gel de polyacrylamide à la lamelle

Matériel (pour 15 lamelles) – pour les localisations, voir page 4 du protocole

- Grande boîte de Petri en verre
- Parafilm
- Lamelles de verre (nettoyées ou neuves)
- Solution de NaOH 0.1M
- Glutaraldéhyde 0.5% dans H<sub>2</sub>Odi (Gluta stock 25%) (40µl pour 2ml)
- APTMS
- H<sub>2</sub>O di
- Pipette pasteur

Protocole : tout faire **sous sorbonne !!**

#### 1- Installation lamelles

- a. Mettre une feuille de parafilm dans la boîte de Petri
- b. Déposer les lamelles de verre sur le parafilm sans qu'elles se touchent

#### 2- Nettoyage lamelles

- a. Recouvrir chaque lamelle d'une goutte NaOH 0.1M (à la pipette pasteur) **3min**
- b. Aspirer la goutte le plus possible avec aspiration robinet, maintenir lamelle avec aiguille pour éviter qu'elle soit aspirée aussi

#### 3- Fonctionnalisation APTMS

- a. Recouvrir chaque lamelle d'une goutte d'APTMS pur **3min**
- b. Bien aspirer la goutte

#### 4- Rinçage

- a. Remplir la boîte Petri de H<sub>2</sub>Odi pour rincer grossièrement les lamelles, laisser **2min**
- b. Préparer une nouvelle boîte de Petri avec parafilm
- c. Reprendre chaque lamelle et les plonger plusieurs fois dans un cristalliseur contenant H<sub>2</sub>Odi
- d. Puis les déposer dans la boîte propre
- e. Redéposer en goutte H<sub>2</sub>O di sur chaque lamelles x2 **env 2min** chaque
- f. Bien aspirer la goutte

#### 5- Fonctionnalisation Gluta : déposer en goutte la Gluta 0.5% **30 min**

#### 6- Rinçage comme étape 4-

#### 7- Séchage : sécher chaque lamelle (préalablement déposé sur un papier filtre scotché sur la paillasse) une par une à l'azote doucement

#### 8- Stockage

- a. Déposer les lamelles dans une nouvelle boîte Petri+parafilm et entourer de parafilm
- b. Mettre à l'abri de la lumière et au sec

*Les lamelles peuvent se conserver actives jusqu'à plusieurs semaines*

#### Note importante :

- Ne pas utiliser l'APTMS directement en contact avec du plastique, il le dissout !!
- Les étapes de rinçage des lamelles à l'H<sub>2</sub>O sont très importantes sinon, l'APTMS réagit avec la Gluta et forme un film jaune qui empêchera le gel de s'accrocher sur la lamelle.

## II. Préparation des gels de polyacrylamide (LAAS, salle blanche)

### Matériel :

- Lamelles de verre préalablement activées
- Moule silicium
- Solution d'acrylamide 30%
- Solution de Bis Acrylamide 1%
- Rhodamine méthacrylate (2.5mg/ml)
- Solution de TEMED (initiateur)
- Solution d'APS 10% (catalyseur)
- H<sub>2</sub>O<sub>di</sub>
- Boîtes de culture

Protocole : Préparer pour chaque gel (chaque rigidité désirée) un Eppendorf de 500µl

### 1- Fonctionnalisation du moule

Passer le moule 15min à l'UV-Ozone cleaner (*penser à réserver sur LIMS avant*)

### 2- Préparation des mix

- a. Mélanger selon le tableau suivant: Acryl, Bisacryl, H<sub>2</sub>O<sub>di</sub>, rhodamine méthacrylate en commençant par 3kPa (plus c'est mou plus c'est long à polymériser)

*Gamme avec concentration constante d'acryl*

Rigidité (kPa)	Acryl (%)	Bisacryl (%)	Acryl 30% (µl)	Bis 1% (µl)	H <sub>2</sub> O <sub>di</sub> (µl)	Rhodamine MA (µl)	TEMED (µl)	APS (µl)	Vol total (µl)
35	10	0,3	167	150	177	5	0.75	5	504.75
10	10	0.1	167	50	278	5	0.75	5	505.75
3	10	0.03	167	15	313	5	0.75	5	505.75

- b. Faire ensuite l'ajout du TEMED, vortexer ou mélanger avec pipette
- c. Ajouter ensuite rapidement l'APS, vortexer

### 3- Moulage

Déposer rapidement le mélange sur les moules silicium en commençant par 100kPa

<b>Dimensions</b>	12mm (24puits)	18mm (12 puits)	25mm (pour confocal)
<b>Volume</b>	5µl	7µl	10µl

### 4- Aplanissement surface

- a. Recouvrir rapidement chaque goutte avec une lamelle activée
- b. Laisser polymériser quelques minutes (40min pour le plus mou, 15min pour 25kPa)
- c. Vérifier la prise dans le reste du mélange dans le tube Eppendorf (le gel a bien pris quand un anneau se devine sur les bords de la lamelle)
- d. Réhydrater l'ensemble moule + lamelle dans un bain de PBS
- e. (Laisser incubé overnight dans le PBS) *pas obligatoire*
- f. Déposer une goutte d'eau sur le bord du système (lamelle)

### 5- Démoulage

- a. Passer une lame de scalpel entre lamelle et moule et faire levier doucement
- b. Retirer la lamelle avec le gel transféré dessus (si tout va bien)
- c. Déposer les lamelles gels dans des boîtes de cultures contenant H<sub>2</sub>O<sub>di</sub>

**Note :** pour faciliter le démoulage, laisser une partie de la lamelle dépasser du moule (il est possible pour cela de casser le moule)

### III. Fonctionnalisation des gels de polyacrylamide (LAAS, salle blanche)

#### Matériel:

- Boite de culture
- Grande boîte de Petri
- Tampon HEPES 50mM pH = 8.4\*
- Solution de SULFO-SANPAH 1mg/ml en tampon HEPES pH= 8.4\* solution à faire extemporanément
- Solution de protéine pour coating (voir selon manip) [final] de 100µg/ml (collagen, fibrinogen, gélatine) à 10 µg/ml (fibronectin, laminin) ou OVA (1mg/ml) selon la protéine en tampon HEPES pH = 8.4 (verif solubilité de la prot à ce pH)
- Lampe UV (365nm)
  - o les timings sont pour lampe UV salle blanche (365-405nm, 30W/m2)
  - o pour lampe vieille lampe UV IPBS (365nm, 0.5W/m2) → faire 2x10min (et pas 2x30sec)

#### Protocole :

##### 1- Lavage

- a. Laver les gels H<sub>2</sub>Odi x2 pour **1min** aspirer à l'évier, ne surtout pas toucher le gel !!

##### 2- Tampon

- a. Incuber en tampon HEPES pH = 8.4 50mM x2 **5min**

##### 3- Préparation Sulfosanpah

- a. Peser le Sulfosanpah pour avoir au final une solution à 1mg/ml
- b. Solubiliser dans HEPES 50mM pH8.4, vortexer (protéger de la lumière !)

##### 4- Fonctionnalisation UV

- a. Une fois devant la lampe UV : déposer les gels dans la boîte de Petri (gels vers le haut) *ou parafilm sur couvercle boîte 24*
- b. Déposer environs 60µl de Sulfo sur chaque gel (pour gel 24puits)
- c. Placer sous la lampe UV **30sec** (sans le couvercle de la boîte de Petri)
- d. Sortir la boîte : la solution de Sulfo a bruni (sulfo activé)
- e. Aspirer doucement à la pipette pasteur l'excès de Sulfo, le jeter
- f. Refaire un run de **30sec** en remettant 60 µl de Sulfo sur les gels
- g. Aspirer l'excédent
- h. Remettre les gels dans la plaque de culture en tampon HEPES 50mM pH 8.4

##### 5- Lavages

- a. Lavages HEPES x3 de **3min** chaque (ne pas trop attendre avant coating)

##### 6- Protéine coating

- a. Préparer la solution de protéine avec tampon HEPES
- b. Déposer des gouttes de la solution de protéine (70µl) directement sur les piliers
- c. Couvrir et protéger de la lumière
- d. Laisser OverNight à 4°C ou 30min RT
- e. Pour coating IgG : Laver HEPES, incubation 30min RT avec IgG à 100µg/ml
- f. Lavages HEPES x2\_3 minutes

#### IV. Culture cellulaire (C211 ou grande culture)

Si manip au LAAS : penser à amener les cellules de l'IPBS la veille pour qu'elles s'équilibrent à l'incubateur)

##### Sous PSM

- 1- Transférer les lamelles avec piliers fonctionnalisés dans une boîte de culture stérile P6
- 2- Laver en PBS **5min** 2 fois
- 3- Passer en milieu de culture (RPMI sans SVF) et mettre à 37°C le temps de décoller les cellules\*
- 4- Quand les cellules sont dans la centri : laver les piliers en milieu RPMI chaud (sans SVF) 2 fois rapidement
- 5- Remettre en RPMI
- 6- Aspirer le RPMI puis déposer les cellules ( $\geq 200.000$  cell/ml, 1ml/puits)
- 7- Laisser les cellules adhérer pendant 30min (macrophages humains) ou 45min (murins) à l'incubateur
- 8- Fixer pour IF ou **observation live**
  - a. Attraper la lamelle au fond du puits et la monter sur un anneau métallique (bien visser pour étanchéité)
  - b. Aspirer le milieu qui reste dans le puit et le déposer dans l'anneau (en vérifiant qu'il n'y a pas de fuites en déposant le système sur un Kimtech
  - c. Nettoyer dessous lamelle avec Kimtech + Ethanol, mettre sur microscope inversé

**Note** : pas de SVF pour que 1. Les cellules adhèrent plus vite 2. Pas de protéines en plus de celles qu'on a coatées en III.6

##### \*Décoller cellules :

Mettre au bain marie 15min avant : PBS, RPMI (sans SVF), RPMI+SVF, Trypsine 0,05% pour hMDM ou PBS-EDTA (10mM) pour HoxB8

	<b>hMDM</b>	<b>HoxB8</b>
1. Lavage	Aspirer milieu, lavage 1xPBS chaud	
2. Décollage	<b>Trypsine 0,05%</b> 10min à 37°C 0,5ml pour 1puits P6	<b>PBS-EDTA 10mM</b> 10min à 37°C 0,5ml pour 1puits P6
3. Neutralisation	Neutraliser avec 0,5ml RPMI+SVF10%	
4. Flushage	Flusher x10	
5. Tranfert	Transférer dans tube 15ml, compléter à 5ml avec RPMI	
6. Centrifugation	<b>10min</b> , rpm 1300	<b>5min</b> , rpm 1300
7. Resuspension	Resuspendre dans volume nécessaire pour avoir <b><math>2 \cdot 10^5</math> cell/ml</b> x nb puits nécessaires	Resuspendre dans volume nécessaire pour avoir <b><math>4 \cdot 10^5</math> cell/ml</b> x nb puits nécessaires

<b>Références et localisations produits</b>
---

Produit	Fournisseur	Réf	Conditionnement	Localisation
Acrylamide	Sigma	A-9099	25g	F1 bac à légumes
Bisacrylamide	Sigma	146072	100g	F1 bac à légumes
APTMS (3-aminopropyl triméthoxysilane)	Sigma	281778	100ml	Placard chimie
Rhodamine B	Sigma			
XLINKER Sulfo-SANPAH	VWR	GENOBC 38	100mg	F3 Reno
HEPES	Sigma	H3375	25g	Etagère chimie
Prot coating (FN, FG, Coll)				C5.3.N8
TEMED	Sigma	T9281		Placard chimie
Glutaraldéhyde (stock 25%)				F1 boîte PFA/Glut
APS (peroxydisulfate d'ammonium ) (stock 10%)			alicots	C2.2
OVA				
Anti-OVA (rabbit polyclonal)	Millipore	AB1225	100µl	C1.bte Margot
Fibrinogen				

<b>Solutions stock</b>
------------------------

<b>Acrylamide 30%</b>	15g acrylamide poudre (CMR TOXIQUE) + 35ml H2O di
<b>Bis Acrylamide 1%</b>	0.5g Bis acryl poudre (CMR TOXIQUE) + 49.5ml H2O di
<b>Tampon HEPES</b> pH = 8.4 2,38g qsp 200ml (PM=238.3g/mol)	<ol style="list-style-type: none"> <li>1. Diluer 2,38g poudre dans 150ml H2O di</li> <li>2. Ajuster pH avec NaOH 1M et papier pH - besoin de beaucoup de NaOH, prévoir pour ajuster le volume à 200ml</li> <li>3. Finir remplir les 50ml qui restent</li> </ol>